

Fermilab Library



0 1160 0000336 2



KEK - 88-15
KEK Report 88-15
March 1989
M

Workshop on Cooling of X-Ray Monochromators on High Power Beamlines

KEK, Tsukuba, Japan
August 31, 1988

Edited by

T. MATSUSHITA and T. ISHIKAWA

NATIONAL LABORATORY FOR
HIGH ENERGY PHYSICS

FERMI
QC467
.W67
1989

WORKSHOP ON X-RAY MONOCHROMATORS COOLING

T. MATSUSHITA et al.

Workshop on Cooling of X-Ray Monochromators
on High Power Beamlines

Preface

This is a report of a Workshop on Cooling of X-ray Monochromators on High Power Beamlines held on August 31, 1988 at the Photon Factory during the Third International Conference on Synchrotron Radiation Instrumentation (SRI88).

On high power beamlines, especially on insertion device beamlines, heating of crystal monochromators is becoming a serious problem: Researchers observe that the intensity of the X-ray beam on the sample is not proportional to the source intensity because of thermal distortion of the monochromator crystal. This problem will be even more serious on beamlines for the next generation X-ray rings.

In the very tight program of the SRI88 conference, only 2 speakers were able to give invited talks closely related to this problem in the session of OPTICAL COMPONENTS FOR HIGH POWER BEAMLINES on Wednesday morning of August 31, 1988. We held this workshop in the afternoon of the same day with the intention of offering further opportunities to exchange information on efforts underway at various laboratories and to discuss ideas how to solve this problem. We also intended that the workshop would be a 'follow-up' to the X-ray optics workshop held at ESRF, Grenoble in September 1987, where the importance of crystal cooling was strongly pointed out.

There were 32 participants from 7 countries. 12 people represented their experiences and ideas for reducing thermal distortion of crystal monochromators. Following those presentations, there were discussions on collaborations for solving this important problem. The attendees agreed that exchange of information should be continued by holding such meetings at reasonable intervals.

This report includes materials offered by speakers in this workshop and by some speakers in the session on OPTICAL COMPONENTS ON HIGH POWER BEAMLINES of SRI88.

We would like to express our thanks to speakers and participants of the workshop for their invaluable contributions.

T. Matsushita and T. Ishikawa

Table of Contents

V. Saile	Investigations of Heat Load Problems at HASYLAB	1
E. Ziegler	Damage of Multilayers in a Wiggler Beam	17
T. W. Barbee, Jr.	Multilayers for High Power Beamlines	43
J. B. Kortright	Multilayer Mirrors as Power Filters in Insertion Device Beamlines	58
T. Oversluizen	Design and Performance of a Directly Water-cooled Silicon Crystal for Use in High-power Synchrotron Radiation Applications	69
R. K. Smither	Liquid Gallium Cooling of Silicon Crystals in High Intensity Photon Beams	91
R. K. Smither	Variable Focus Crystal Diffraction Lens	117
P. van Zuylen	Cooling Geometry for a Crystal Monochromator in a High Power Beamline	132
P. Pattison	Design and Testing of Water-cooled Monochromators on the SRS Wiggler Beam-line	148
U. Bonse	Direct-watercooled Double Monochromator for Quantitative Microtomography at a Synchrotron-radiation Source	163
J. Arthur	Micro-channel Water Cooling of Silicon Monochromator Crystals	172
D. Bilderback	Cooling of Silicon Monochromator Optics - Present Test Results and Future Needs -	178

W. Graeff	A Thin Laue Crystal as a Monochromator in a Wiggler Beam	182
J. Hastings	Cooling not so Perfect Crystals	186
T. Ishikawa	Heating Problems of Crystal Monochromators at the Photon Factory	190
A. K. Freund	Research and Development of X-ray Optics at the ESRF Present and Planned Activities	195
List of Participants		206

Investigations of Heat Load Problems at HASYLAB*

V. Saile

Hamburger Synchrotronstrahlungslabor HASYLAB at DESY,
D-2000 Hamburg 52, FRG

The high synchrotron radiation power emitted by the 5.3 GeV DORIS II storage ring causes severe problems for optical elements like mirrors, gratings, and crystals. This is especially true for wigglers and undulators operated in this ring. In view of future even more powerful light sources we initiated a program on heat load effects. The goals are to measure quantitatively reversible deformations of surfaces and to compare these results with theory, to test various materials which might be used for mirrors, to characterize crystals and multilayers exposed to intense beams, and to check experimentally the performance of cooling systems. The main diagnostic tools are an infrared camera for monitoring the temperature distribution over the surface and a Michelson interferometer for measuring distortions. The first experiments concentrated on a systematic study of mirrors. It was found that SiC is by far the best material withstanding power densities of more than 2 W/mm^2 without a significant deformation. Results on various single crystals and multilayers have been obtained as well. However, more experimental data are needed in order to allow for general conclusions.

* This work is based on a collaboration between the Fritz-Haber-Institut (Berlin), BESSY (Berlin), and HASYLAB (Hamburg).

Heat Load / Radiation Damage

History :

- ~ 1976 : Problems at DESY and DORIS
- ~ 1979 : Tests for HASYLAB →
Metal Mirrors
AlMg₅ } Kanigen
OHFC-Cu }

No Damage for $P'' \leq 0.5 \text{ W/mm}^2$

- ~ 1979 - 1986 ESRF Instrum. Subgroup
ESRP (Warning)
- ~ 1986 Wiggler / Undulator W1

Reversible Deformation at
 $P'' \sim 0.5 \text{ W/mm}^2$



Experimental Program: DORIS-Bypass (1991)
ESRF (1993/94)
BESSY II

An Effort to study Radiation Effects

Fritz - Haber - Inst. : E.E. Koch (BESSY)
S. Mourikis
W. Jark

HASYLAB

V. Saile

+ Kollaborations : PF : S. Sato
ESRF : E. Ziegler
Trieste : C. Lenardi

Goals:

- Heating and Distortion of Mirror, Crystals, ...
- Cooling Configurations
- New Materials
- Calculations

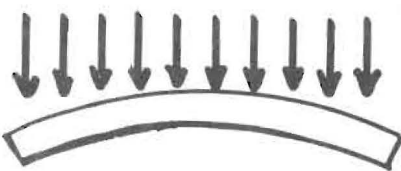
Avoid Overdesign

Experiment reversible effects

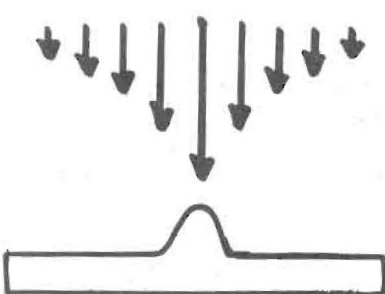
Other Projects: CHESS (D. Bilderback), LBL, LLNL
APS (R.K. Smither), PF (S. Sato),
Trieste (C. Lenardi), ESRF (E. Ziegler),
TNO (P. van Zuylen),

Relevant SR - Properties:

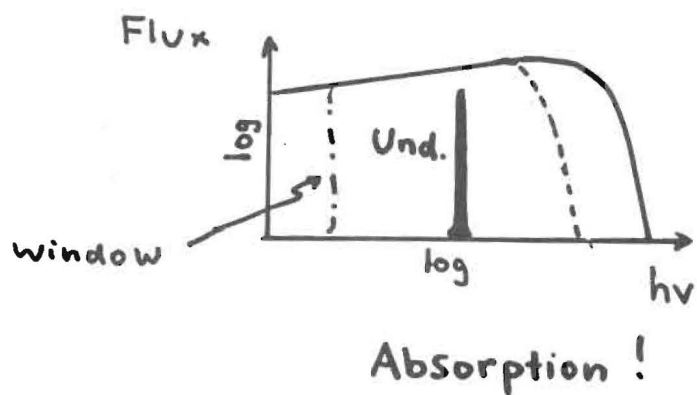
Total Power : $P_T \sim E^2 \langle B^2 \rangle$
 [W]



Surface Power Density : $P_S'' \sim E^4$ ⚡
 [W/mm²]



Spectral Distribution : $\mathcal{E}_c \sim E^2 \cdot B$



Maximum Thermal Loads:

For a sinusoidal wiggler / undulator and "negligible" electron beam size and divergence ($\gamma^{-1} \cdot z > \sigma_z$; $\gamma^{-1} > \sigma_z'$)

(G. Brown, K. Halbach, J. Harris, H. Winick, NIMPR 208 (1983) 65):

Total Power

$$P[\text{W}] = 1.27 E^2 \langle B^2 \rangle \cdot L \cdot I$$

⚡ ⚡ ⚡ ⚡
[GeV] [T] [mm] [A]

Power per horizontal angle:

$$P'[\text{W/mrad}] = 4.33 E^3 B_{\text{max}} I \cdot N$$

No. of Poles

Power per unit solid angle:

$$P''[\text{W/mrad}^2] = 5.38 E^4 B_{\text{max}} I \cdot N$$

Linear power density at distance z [m]:

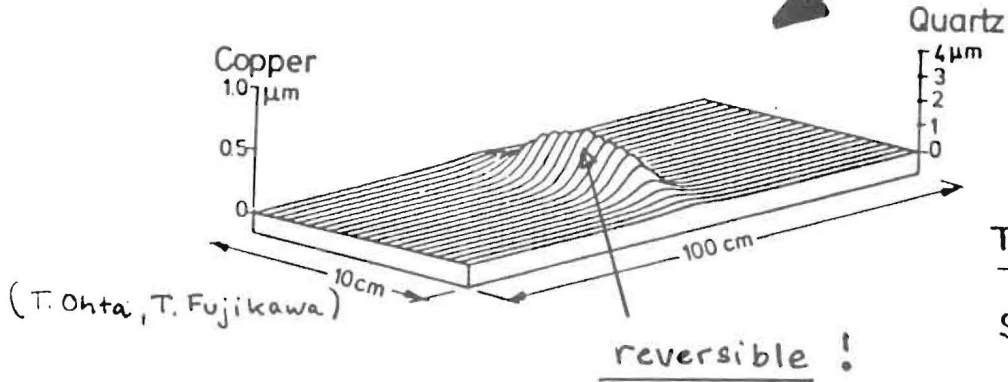
$$W'[\text{W/mm}] = P'/z \sim E^3 B_{\text{max}} I N$$

Surface power density:

$$W''[\text{W/mm}^2] = P''/z^2 \sim E^4 B_{\text{max}} I N$$

Thermal Load: rather Flux than Brilliance

Heat Load :



SR

$$P_H'' \text{ [W/mrad}^2\text{]}$$

$$\sim (E^4) \text{ BIN}$$

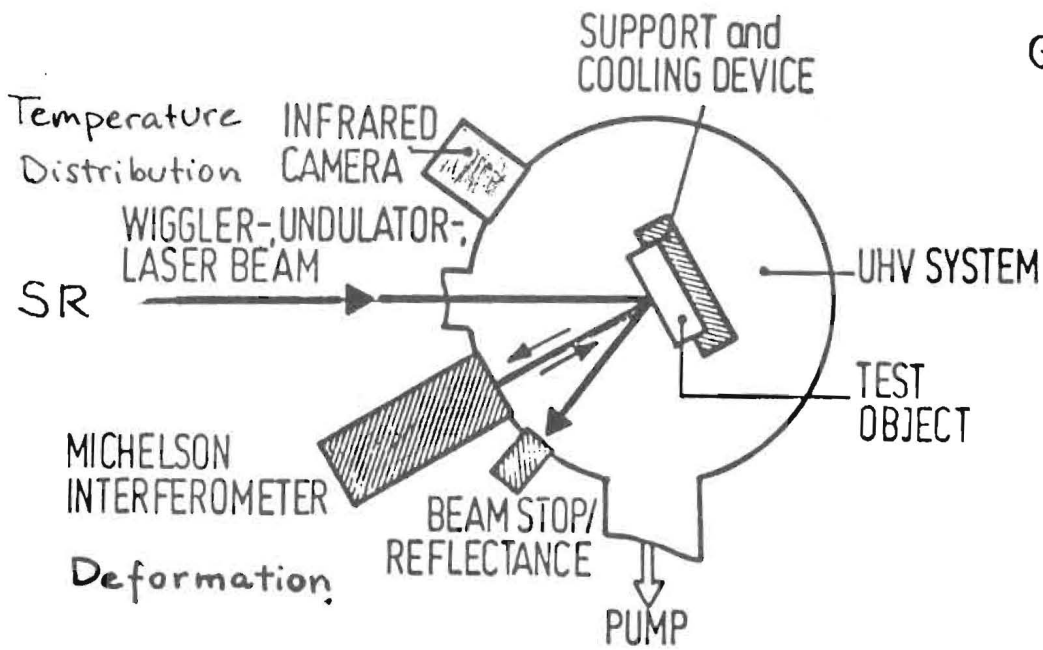
HASYLAB:

Today : 4000

Soon : > 10000

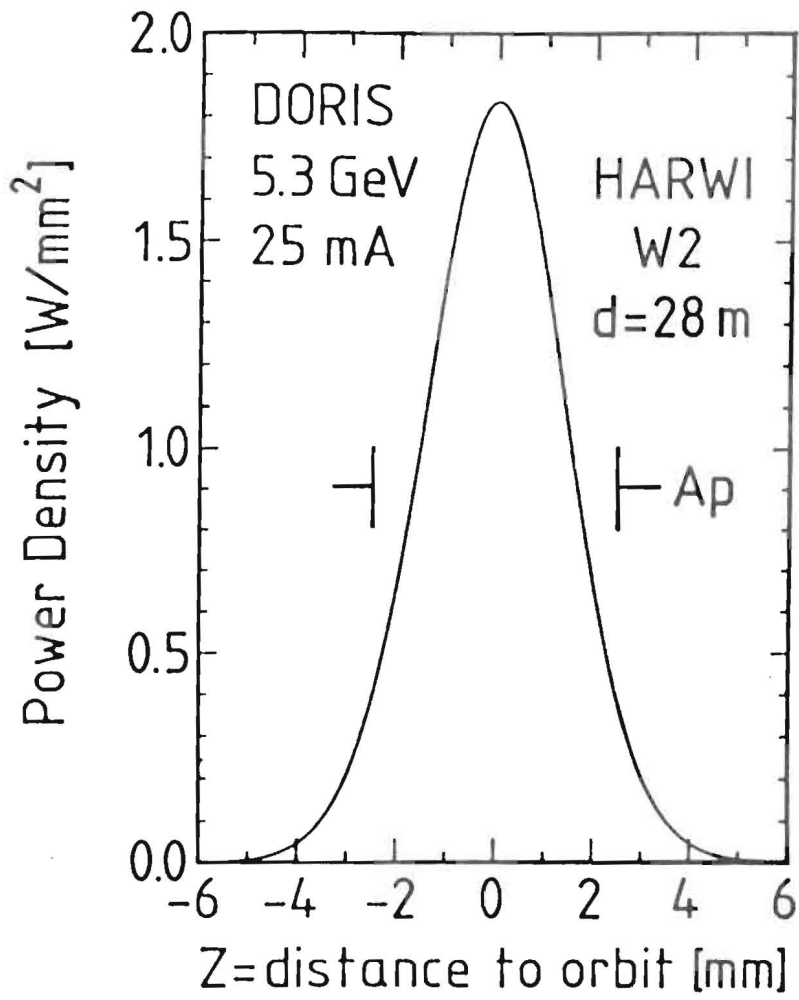
W/mrad²

Geometry

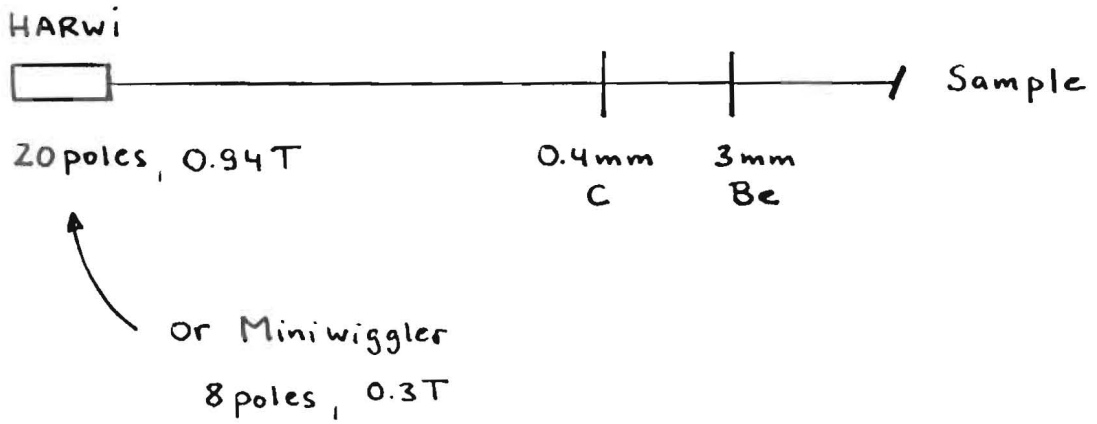


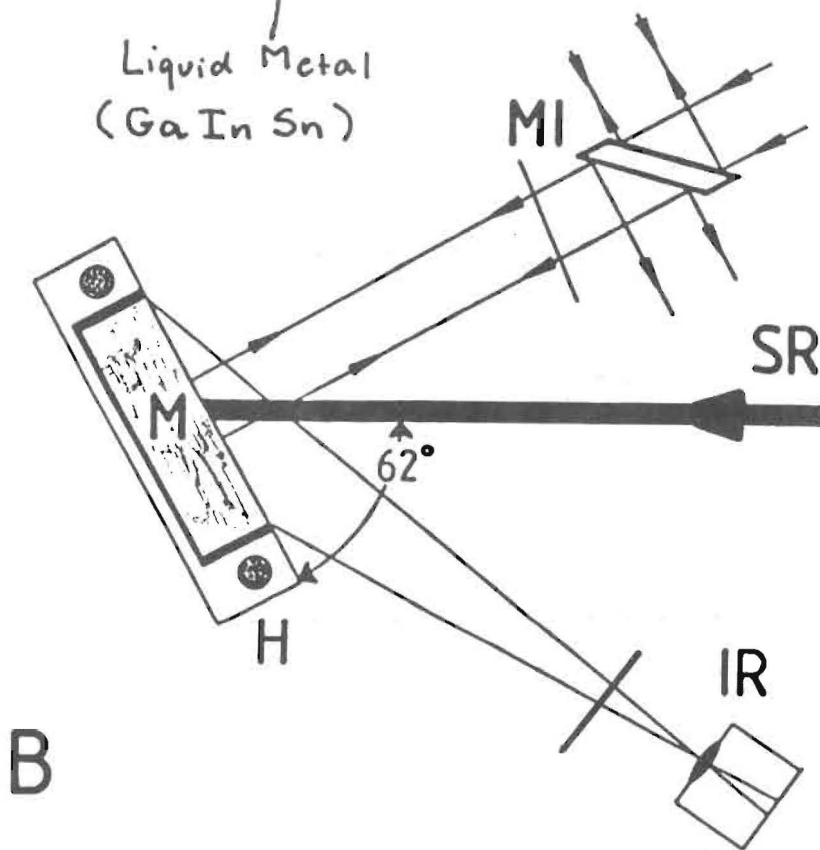
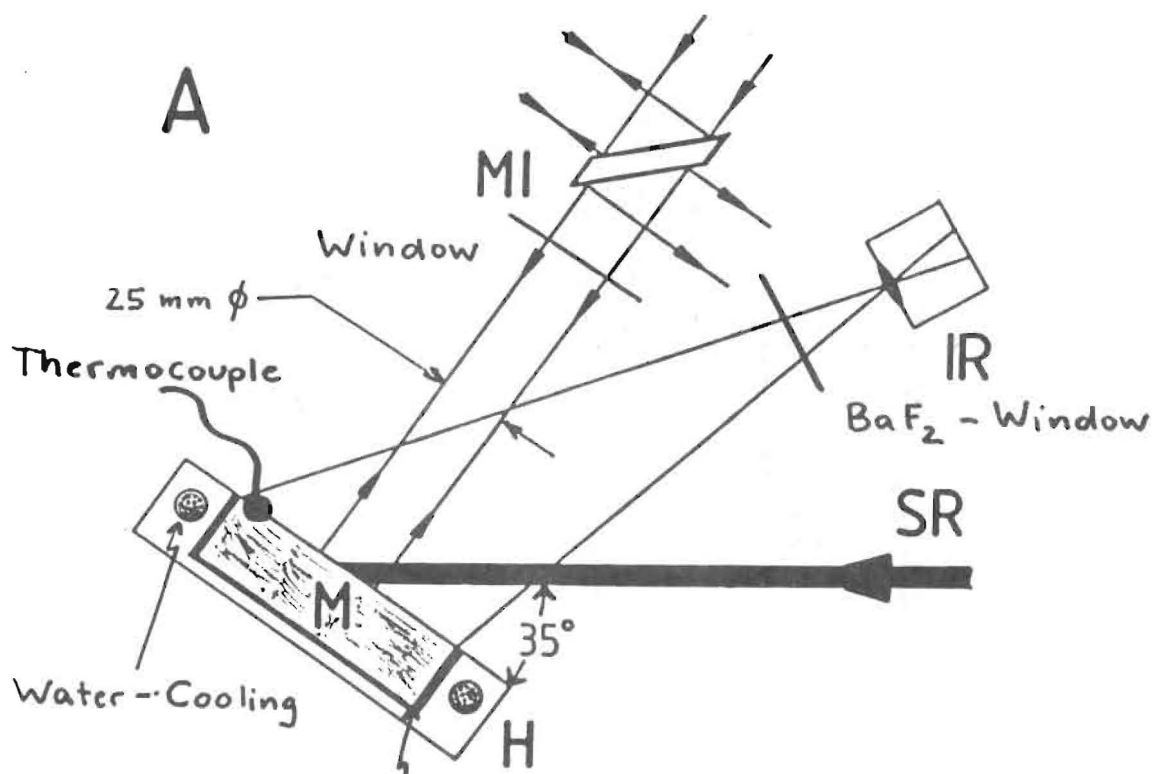
Experimental Set-Up

Vertical Plane:

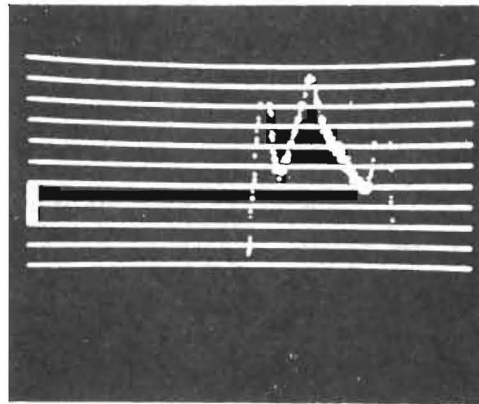
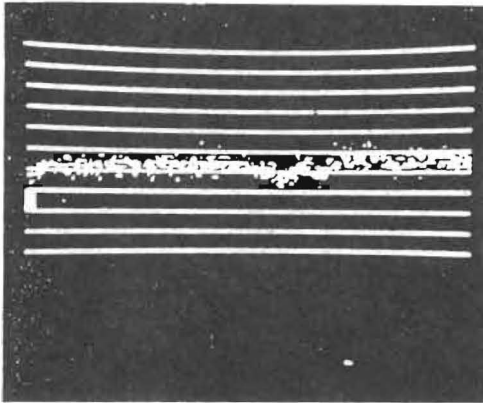
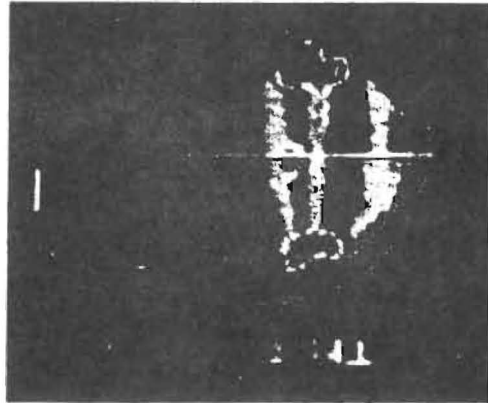
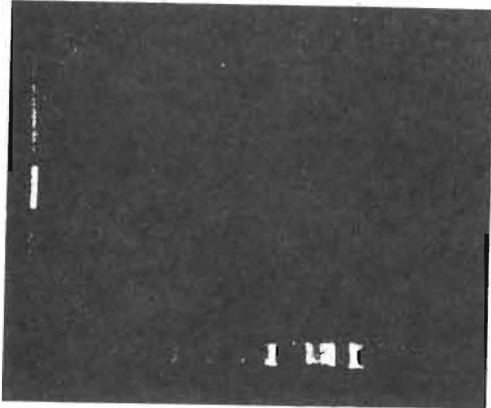
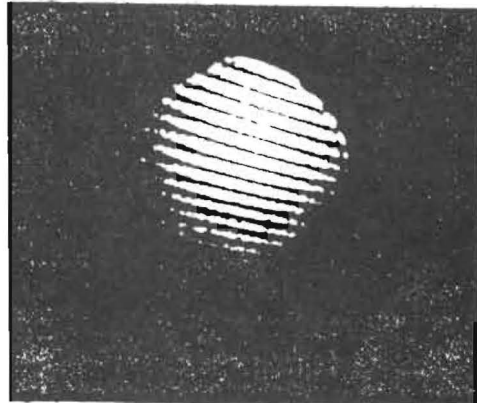
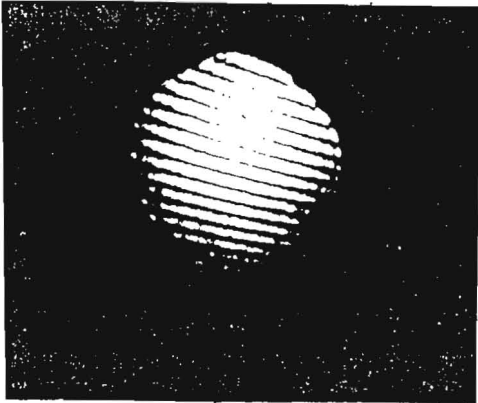


Horizontal: Line





Vacuum Graphite Coating IR-Emittance

SiCErgebnisse:Temperaturerhöhung zu $T = 10^4$ °C nach 25 Min.kaltheiß $\Delta T = 4$  $\Delta H = 0$

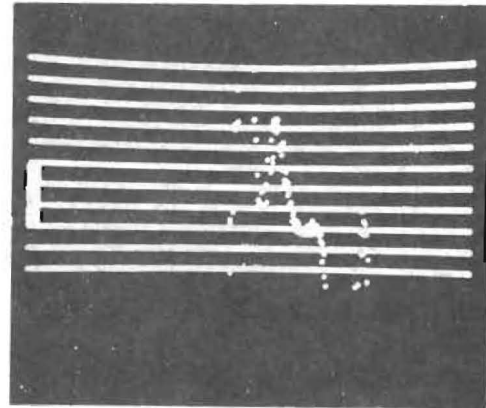
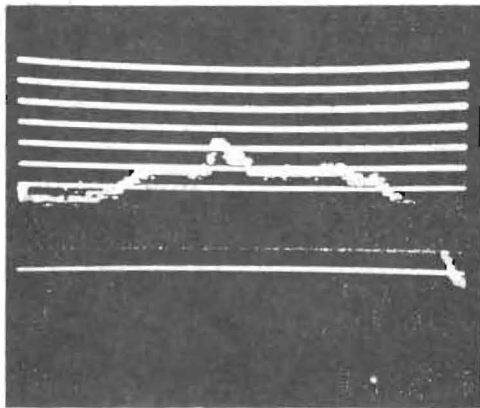
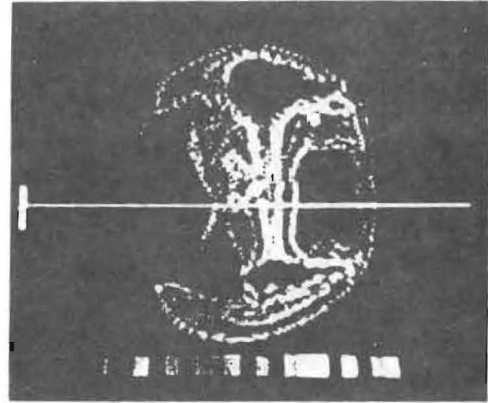
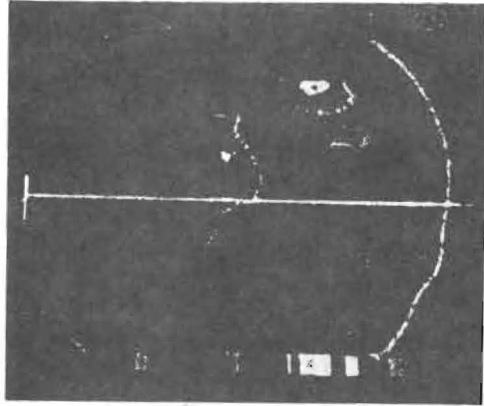
AIN + Kanigen

Ergebnisse:

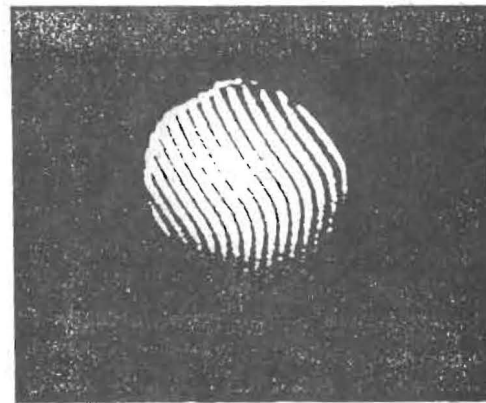
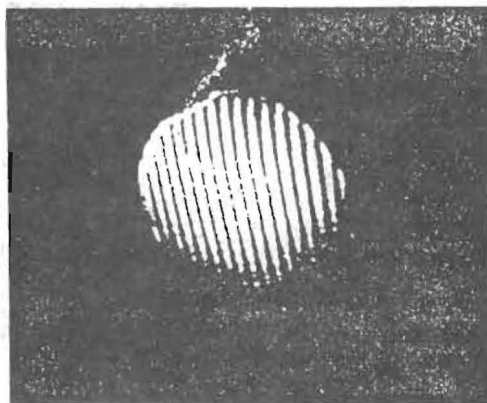
Temperaturerhöhung zu $T = 157^{\circ}\text{C}$ nach 10 Min.

kalt

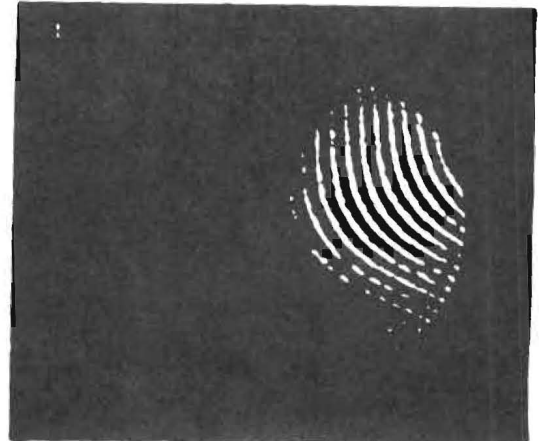
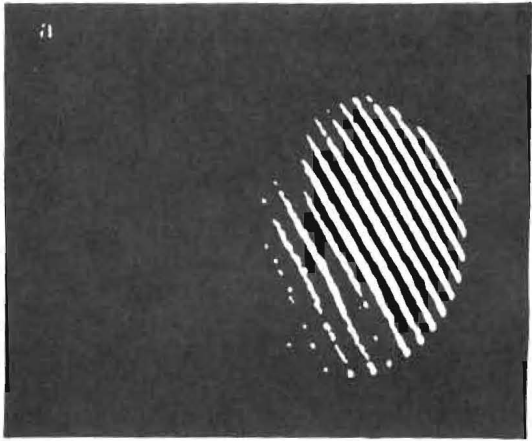
heiß



$\Delta T = 18^{\circ}$



$\Delta H = 55\%$



Ge (220) : 5mm thick



157 W, 1.95 W/mm²

Tension free Support

Water-Cooling, Liquid Metal ϵ \rightarrow 1 Fringe



Irreversible Damage

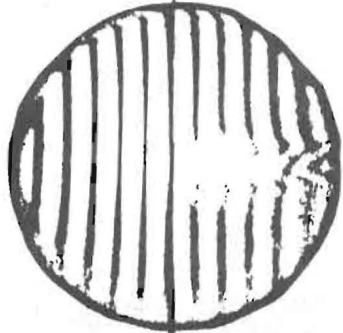


CVD SiC



Suprasil I
uncoated

depth of valley: $\sim 0.6 \mu\text{m}$



Suprasil I
+ 300 Å Pt

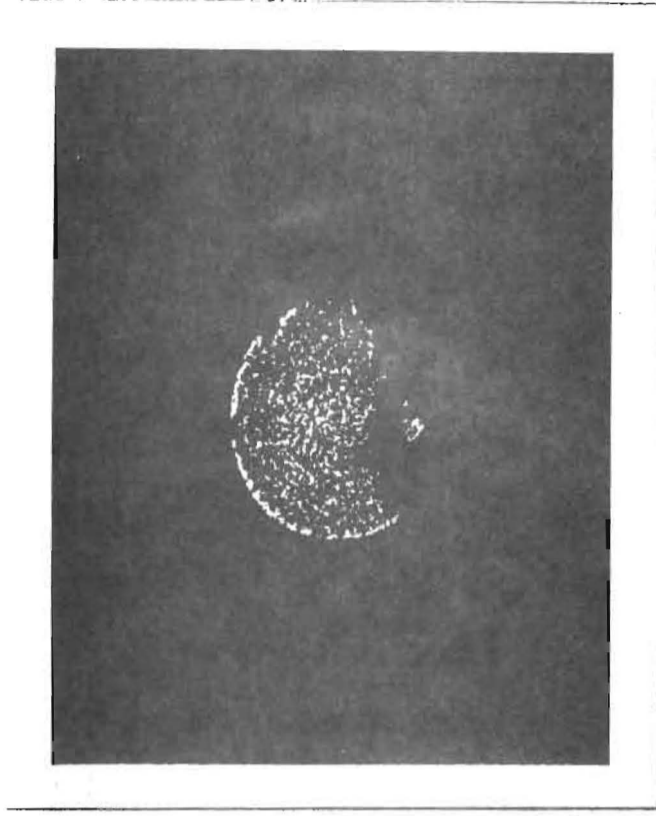
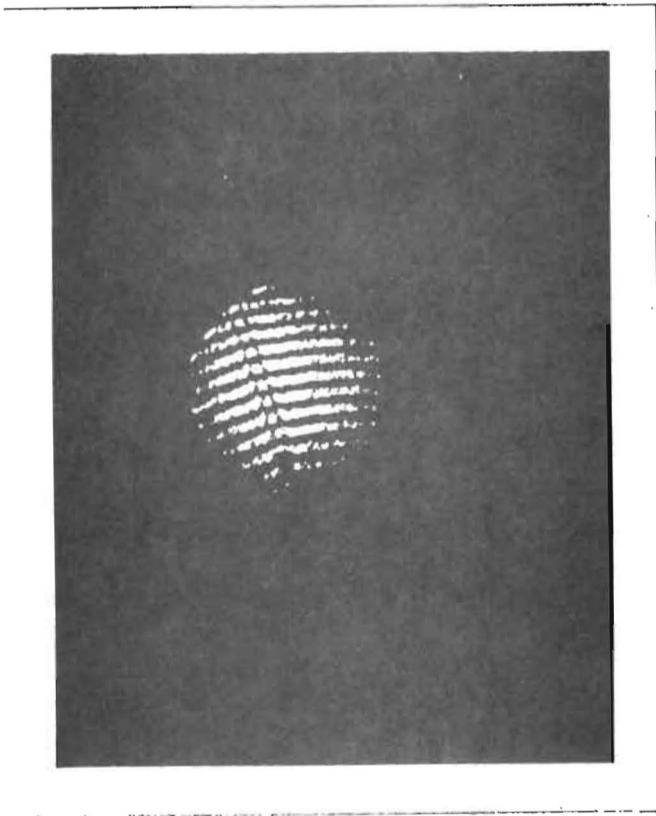
shielded | irradiated (3 and 5 GeV,
40 and 15 mA)

5m from source

near normal incidence

Interference fringes

S. Bernstorff, Staatsexamensarb., Uni. Hamburg
1980
R. Zietz, V. Saile, R.-P. Haelbich,
Proc. VUV VI, p. III 42 (1980)



Radiation damage in a Cu/canigen mirror (left photo) and AlN (right photo).
For AlN, the canigen coating is split away.

Results and Conclusions

1. Deformation is reversible and instantaneous
(timescale ~ 1 sec)
2. Cooling: reduces average Temperature, T .
Liquid metal \rightarrow Equilibrium T is reached
within ~ 30 sec (compared to ~ 30 min.)
However cooling samples from the sides and
the back does not reduce Temp. gradient $\Delta T/x$
" " " high ob bump ΔH

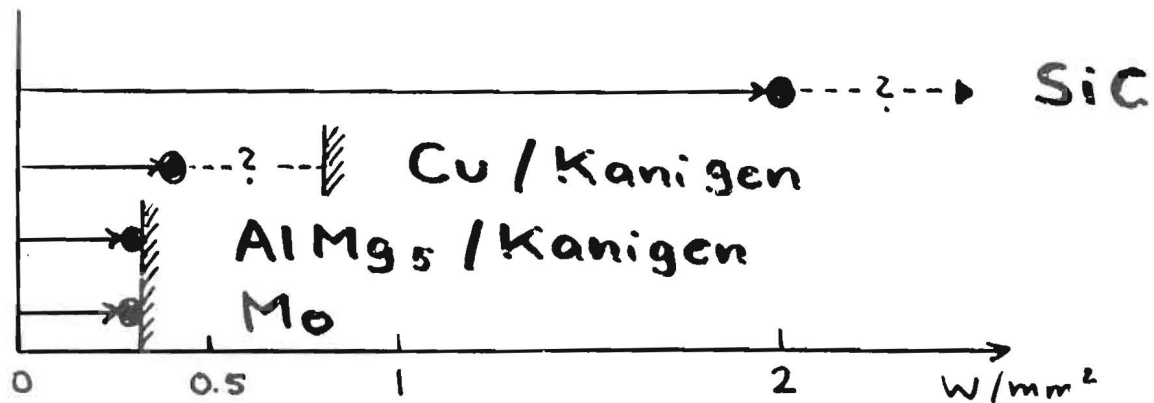
 \rightarrow Cooling channels very close to the
Surface: R. DiGennaro (Mirrors)
D. Bilderback } (Crystals)
U. Bonse }
T. Oversluisen }

Liquid Ga: R.K. Smither
3. Coating Mirror Substrates with Kanigen:
($\sim 50\mu\text{m}$) has no significant effect on $\Delta T, \Delta H$

4. Experimental Resolution for $\Delta H: 50 \text{ nm}$
 $\Delta \alpha: 2 \text{ arcsec}$

5. Within that resolution:

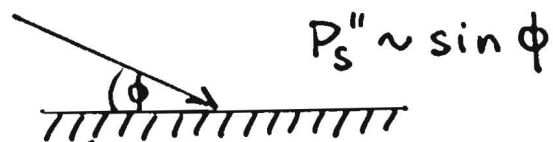
SiC withstands $P_s'' > 2 \text{ W/mm}^2$



6. Applications of SiC for

Soft X-rays $\longrightarrow P_s'' > 100 \text{ W/mm}^2$

X-rays $\longrightarrow P_s'' > 250 \text{ W/mm}^2$



7. Other Results: Crystals, Optics for High Power Lasers
 Windows, Multi layers

Next Experiments: Very thin crystals, mirrors

Goals:

- Surface Deformation vs. Power Density ✓
- Surface Deformation of Crystals: Systematic Investigation: Started
- Threshold for irreversible damage ?

What else ?

DAMAGE OF MULTILAYERS IN A WIGGLER BEAM

E. Ziegler

European Synchrotron Radiation Facility, B.P. 220,
38043 Grenoble Cedex, France

Y. Lepêtre

Université d'Aix-Marseille III, Faculté de Saint-Jérôme,
13397 Marseille Cedex, France

St. Jochsch, V. Saile

Hasylab, Desy, Notkestrasse 85, D-2000 Hamburg 52, FRG

S. Mourikis

Surface Physics Department, Fritz-Haber-Institut
der Max-Planck Gesellschaft, 1000 Berlin 33, FRG

P. J. Viccaro

Argonne National Laboratory, Argonne IL 60439, USA

B. Blanchart, G. Rolland, F. Laugier

CEN-G, 85X, 38041 Grenoble Cedex, France

S. Heald

Brookhaven National Laboratory, Upton,
Long Island NY 11973, USA

ABSTRACT

The use of multilayer reflectors under intense synchrotron X-ray beams requires to develop a new generation of multilayered materials that can withstand a high power load in excess of 100 W/mm^2 . Multilayers with the high-Z layer consisting either of a pure element or of compounds such as carbides have been produced and exposed to a wiggler beam with a power density of about 1 W/mm^2 . The resulting damage ranges from the total destruction of the layering to a reduction of the reflectivity by typically 40-60%. In some cases an only 1-15% loss in reflectivity has been observed. A more detailed presentation is the subject of poster A-094 presented during the SRI 88 Conference held in Tsukuba.

SHORT-PERIOD MULTILAYERS

FOR

SYNCHROTRON BEAM LINES

(5-25 keV) \longrightarrow 1.5-2.5 nm period

REFOCUSING MIRROR

after mono. X-als

size reduction/ grazing mirrors

FIRST OPTICAL ELEMENT

before high res. X-als

protection/ high flux beam
large & adjustable band-pass

SHORT-PERIOD MULTILAYERS

COMPROMISE : 1.5-2.5 nm

- { reflectivity
- { Bragg angle

MORE INTERFACES INVOLVED /soft X-ray

- { to produce
- { to keep under intense flux

SMALLER ROCKING-CURVE

/soft X-ray case

- { long range slope errors
- { substrate microfacetting

FIRST "White beam" EXPOSURE

(W/C) 10 bi-layers

6.8 - nm period

top layer : C

mounted on water-cooled Cu block

with contact agent : Apiezon M grease

10^{-5} Torr vacuum

Brookhaven

$I = 100$ mA

after Be window

before monochromator

15 days exposure

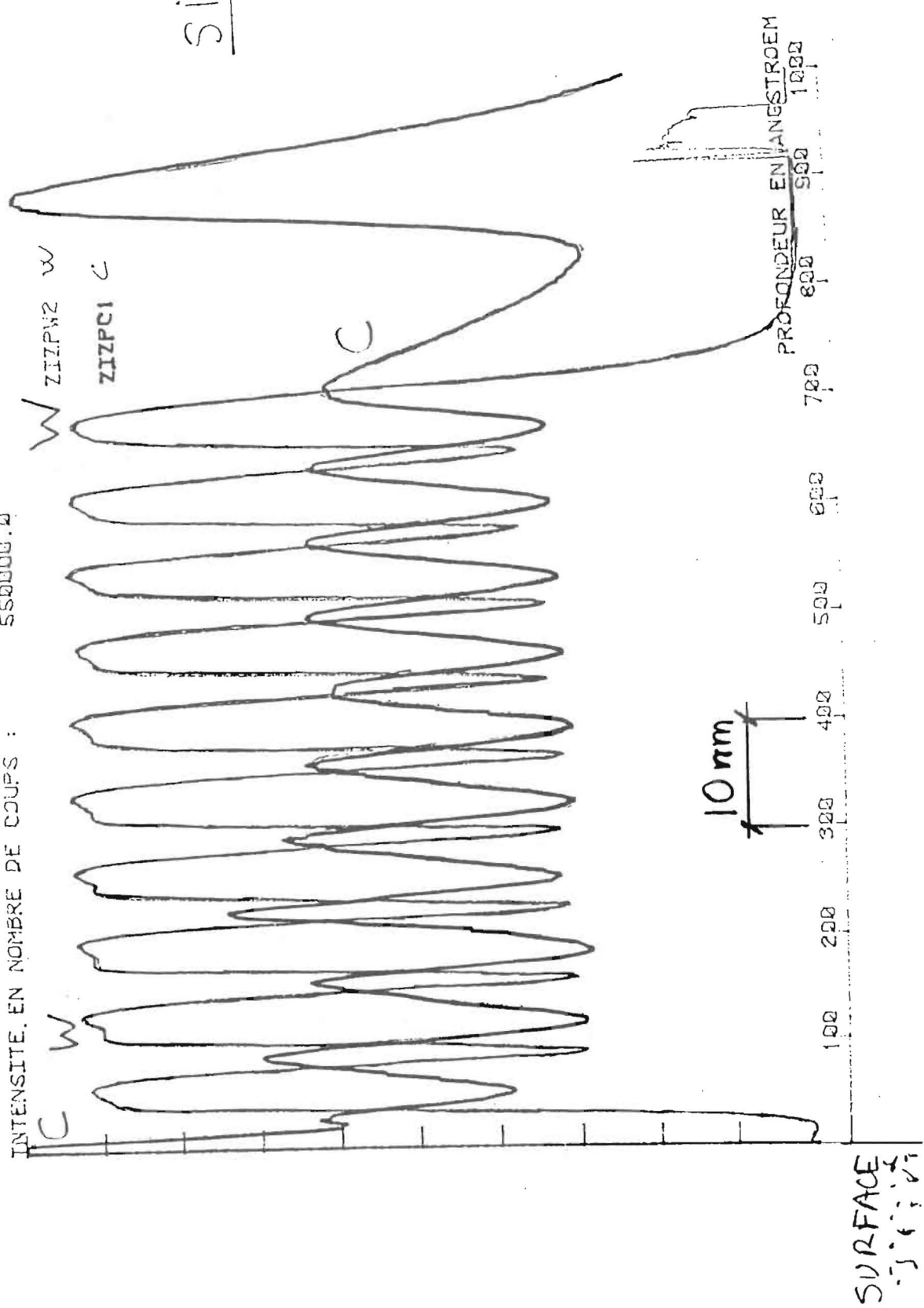
} 6 W/mrad

or

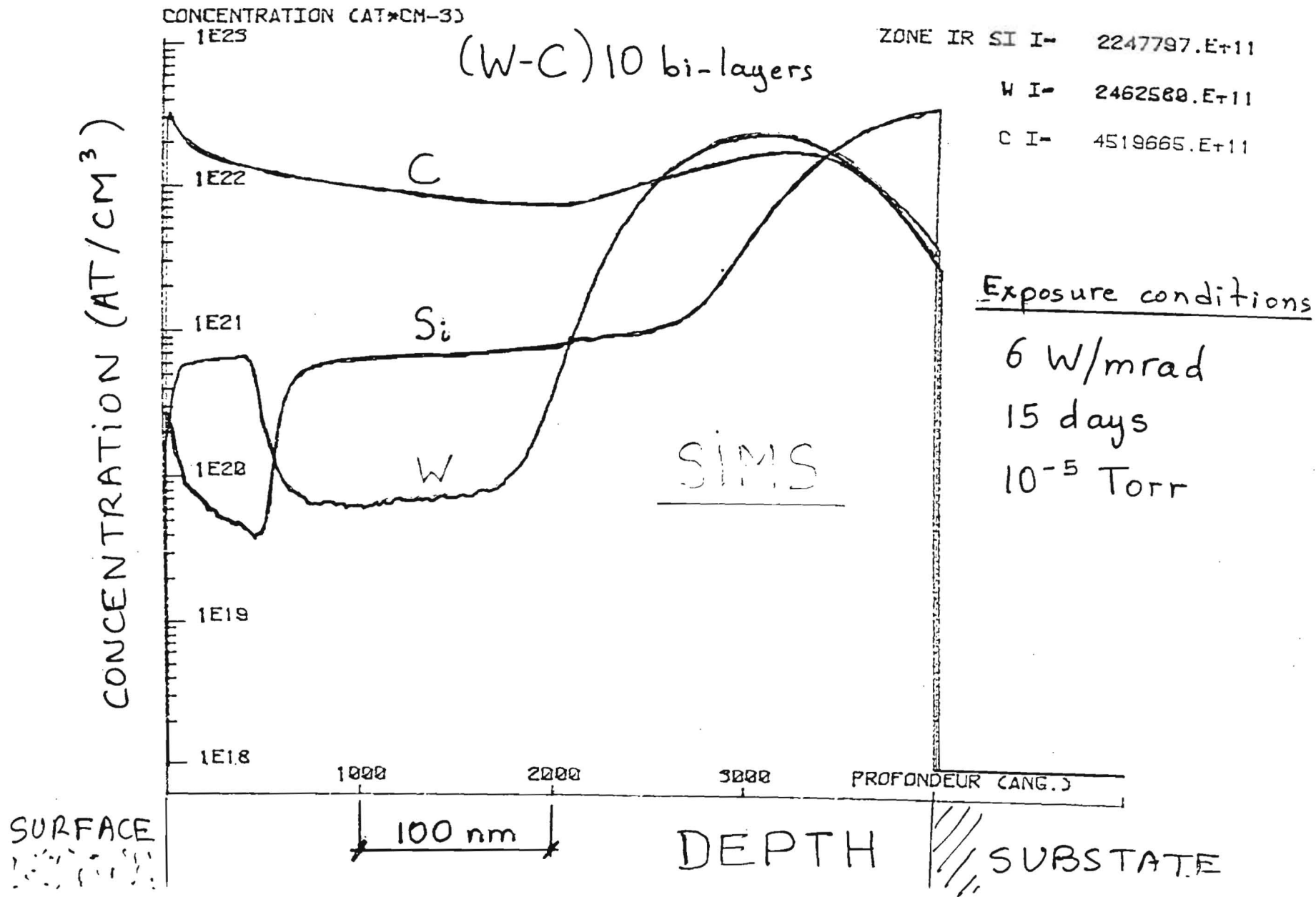
5 W/cm beam

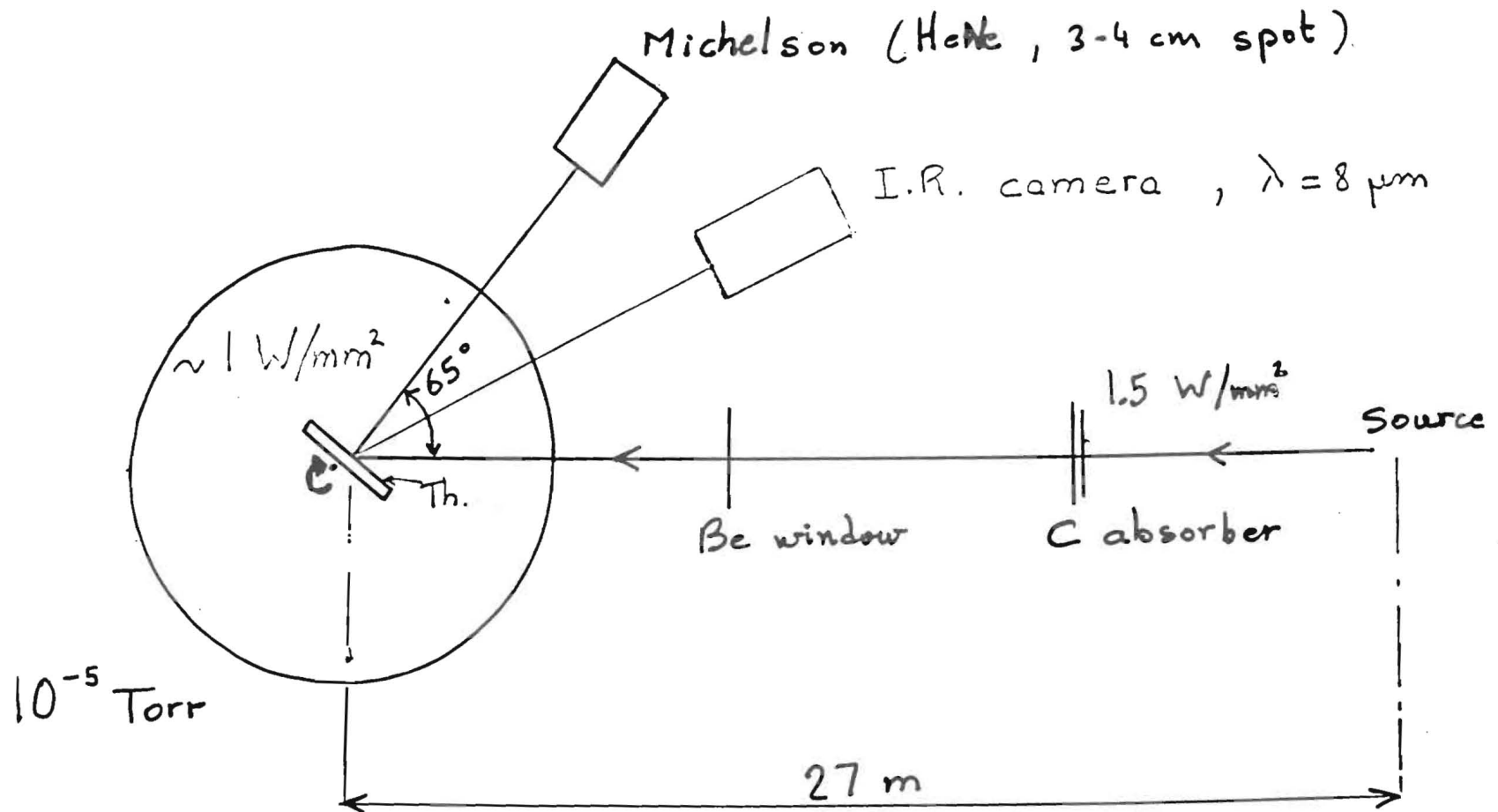
(WC) 10 bi-layers , 6.8-nm period , NOT EXPOSED

INTENSITE. EN NOMBRE DE COUPS : 550000.0



SIMS





— 24 —

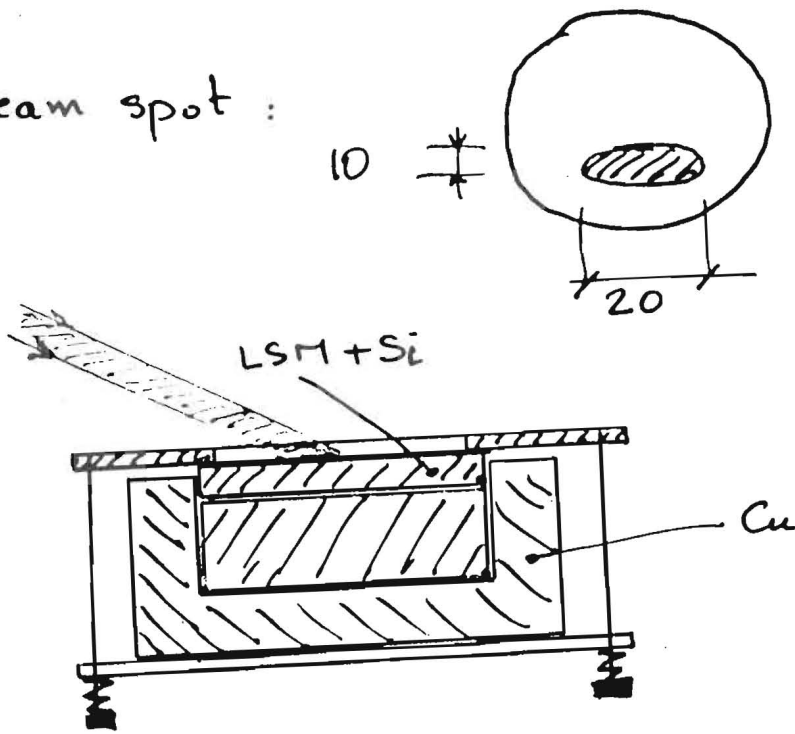
HARWI WIGGLER "White beam" exposure

- * see W. Graeff et al. (IV-4)
- * see S. Mourikis et al. (V-1)

THIS IS A SURVIVAL TEST

- poor cooling contact
(only to protect rotating feedthrough)
- vacuum : $10^{-3} - 10^{-5}$ Torr

- beam spot : 10×20 mm²
gaussian shape



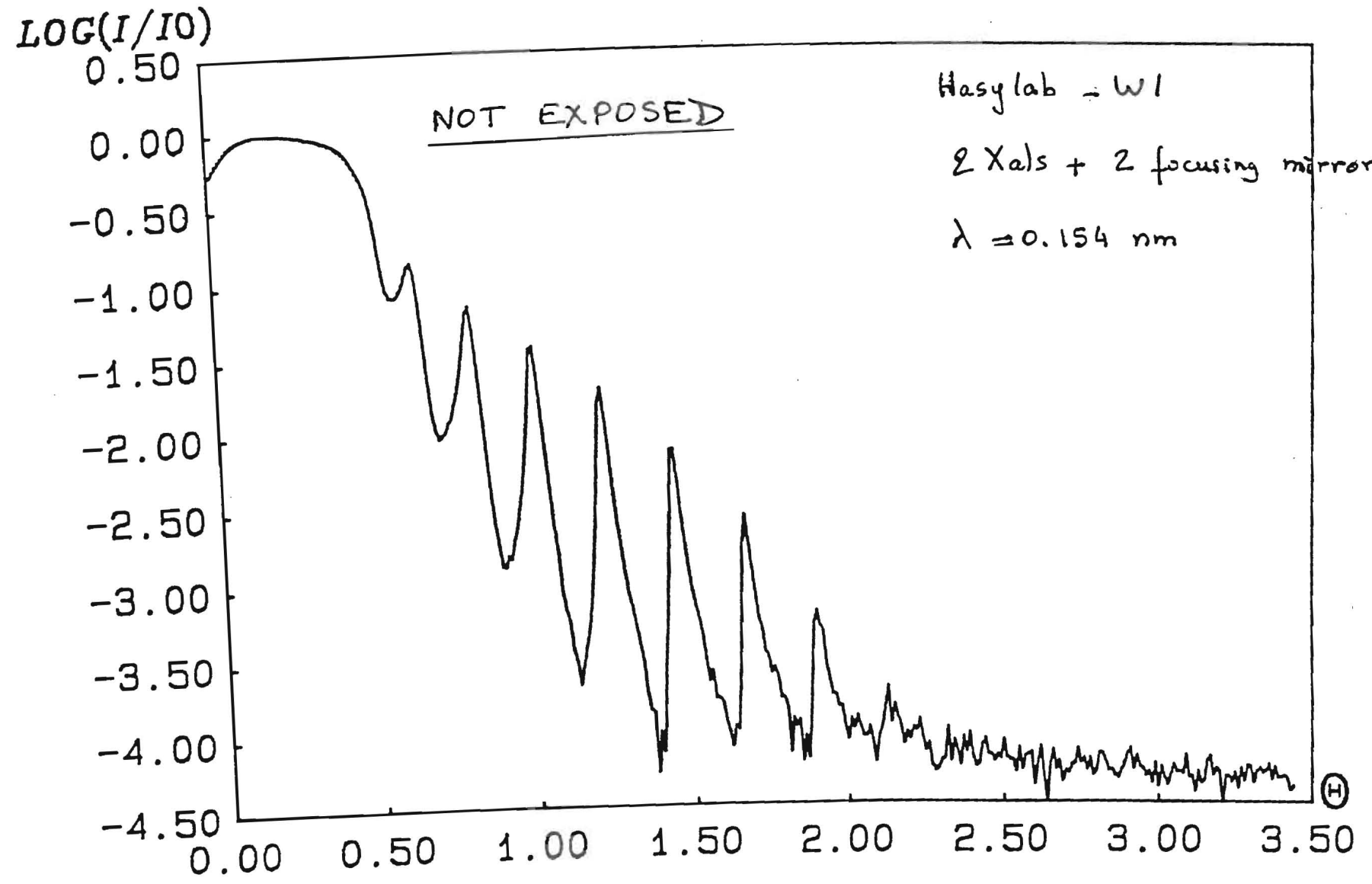
- shutter closed if temp. ≥ 500 °C

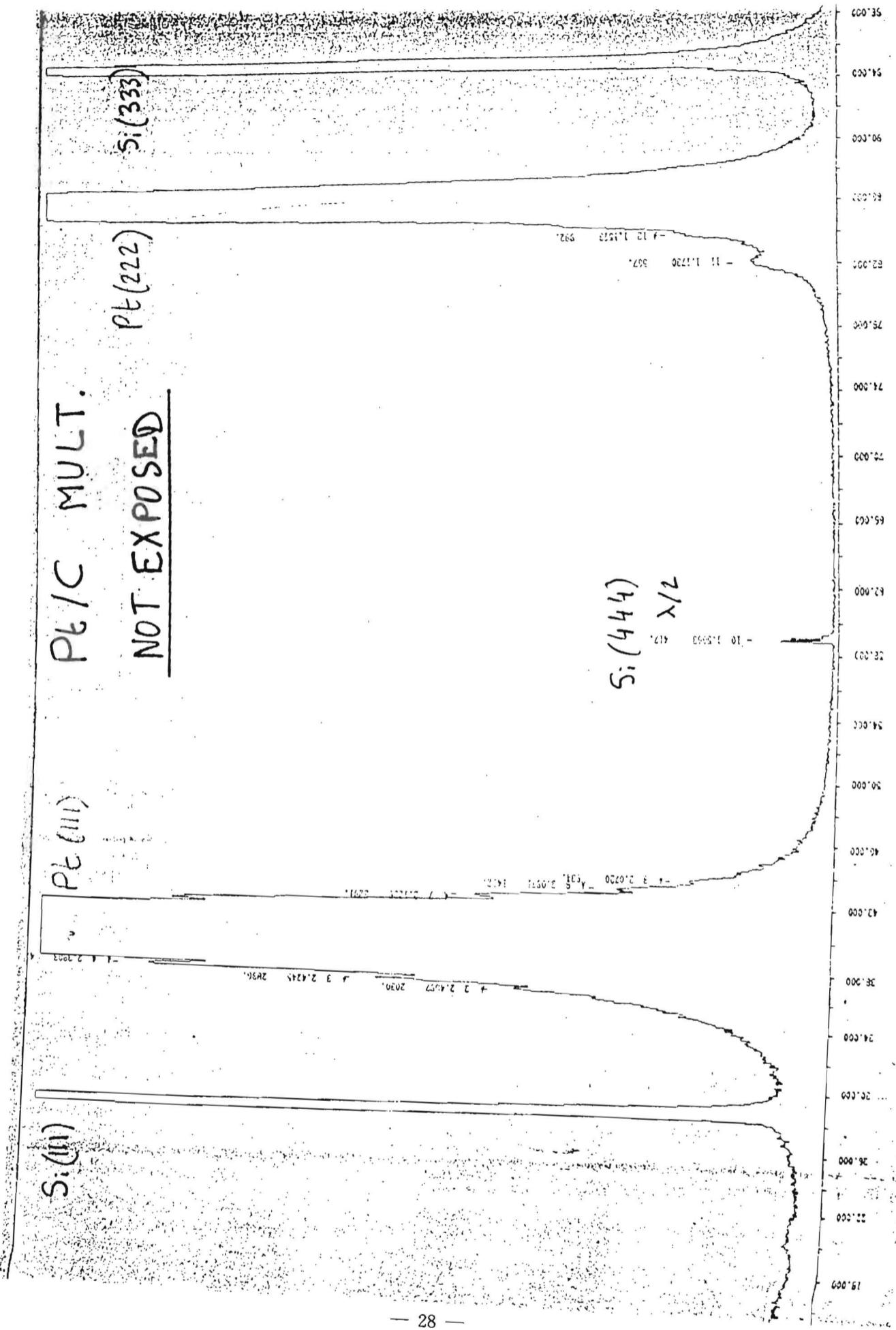
- 1 W/mm^2 at $\begin{cases} 5.2 \text{ GeV} \\ I \leq 40 \text{ mA} \end{cases}$

Ref.	Multilayer ^{layers}	Sputtering	Period (nm)	Max. temp (°C)
4-21-87 #1	Pt/C 50	R.F.	21.0	500
4-12-88 #4	W/Si 50	DC biased-Reactive (<u>C₂H₂</u>)	11.5	450
6-28-88 #126	W-Si/C 90	Triode	3.4	350
4-14-88 #2	W/C 20	Reactive (<u>N₂</u>)	10.6	350-400
8-01-88	W/C 300	R.F.	1.5	400
4-14-88 #3	W/C 50	Reactive (<u>C₂H₂</u>)	11.6	750 (furnace)

Silicon substrate (3mm thick)

PT-C (21-4-87)#1

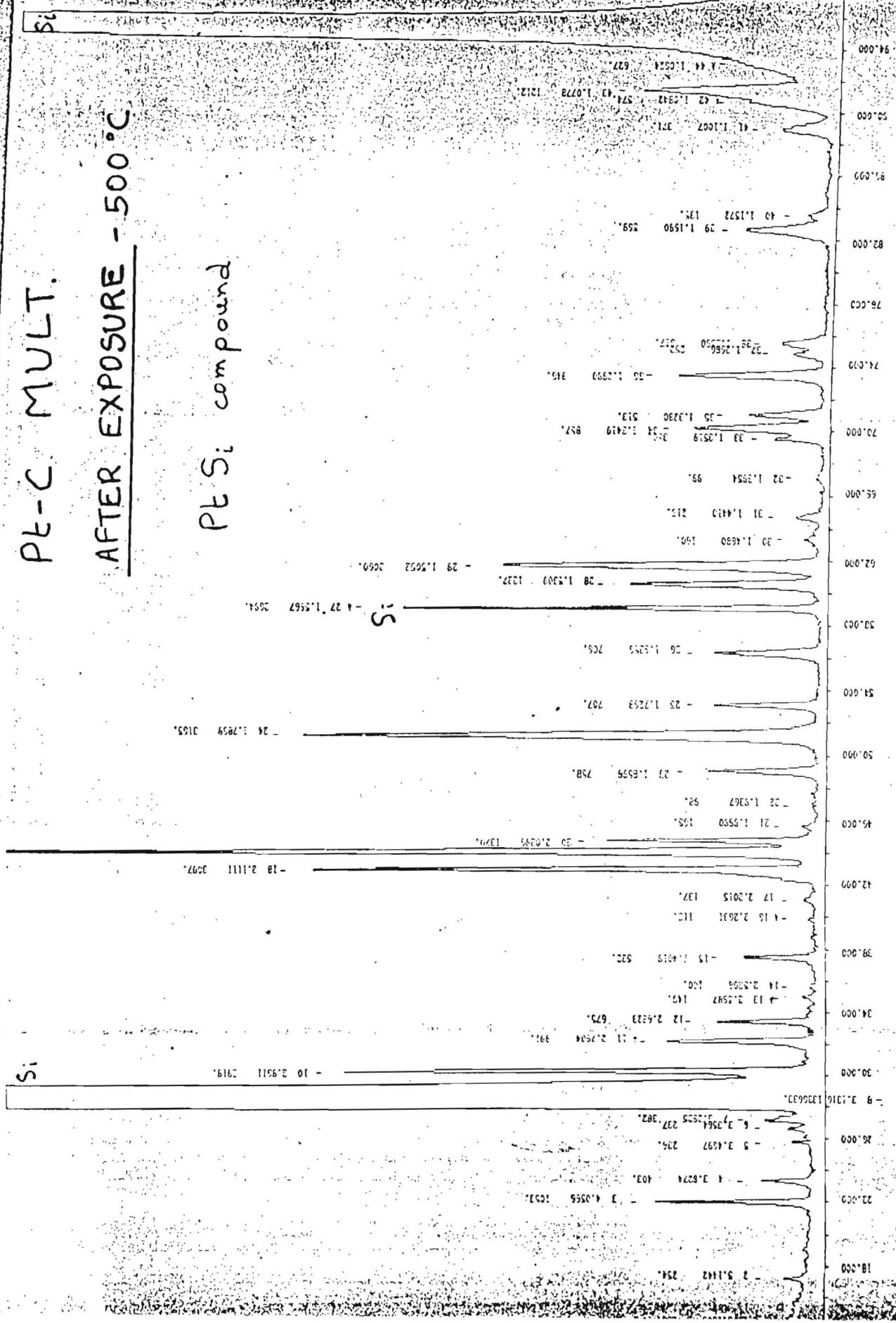




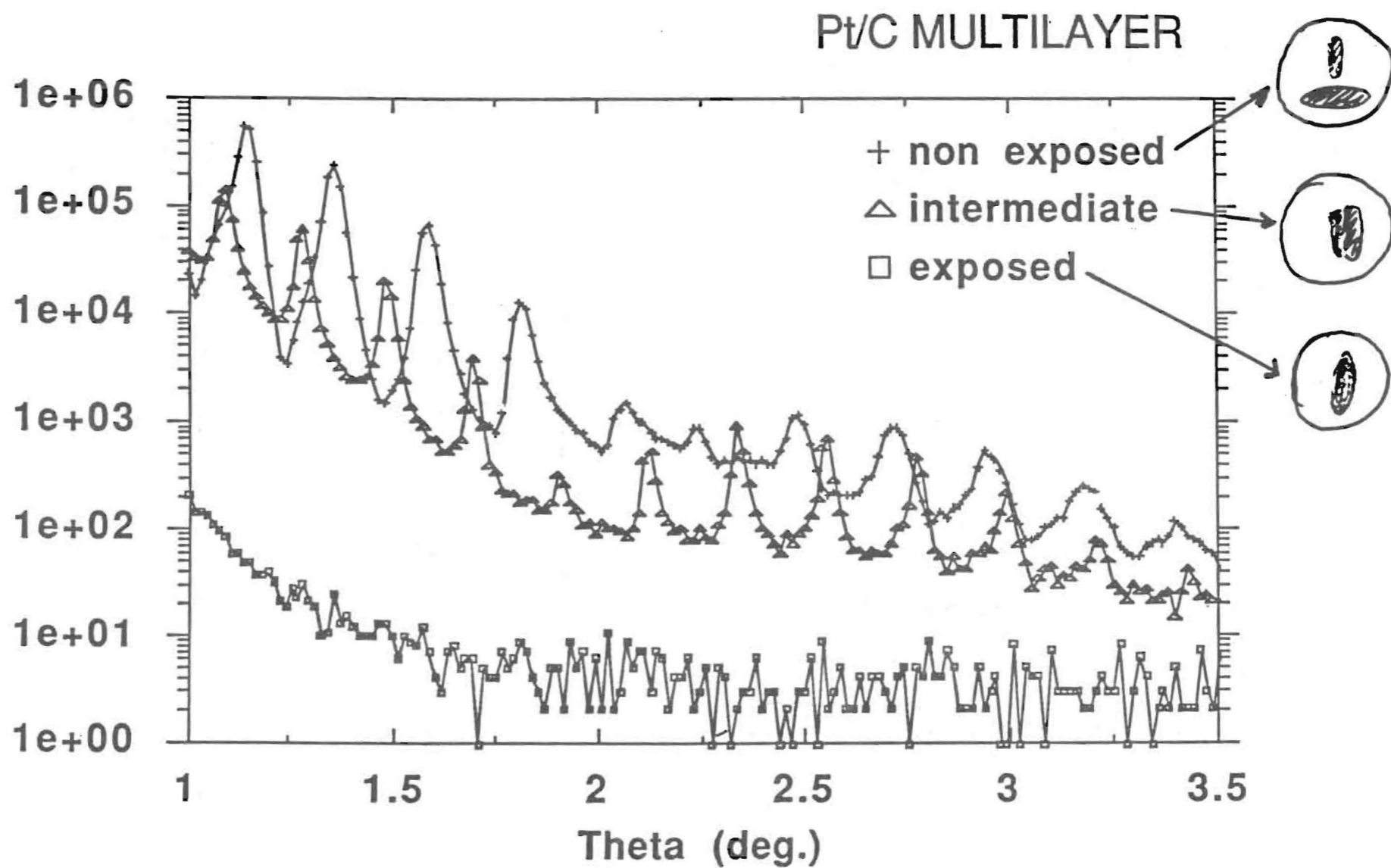
PE-C MULT.

AFTER EXPOSURE - 500 °C

Pt Si compound



X-ray tube / Slits (0.1°) / Sample / Slits (0.1° - 0.018°) / Curved X-ai / Detector

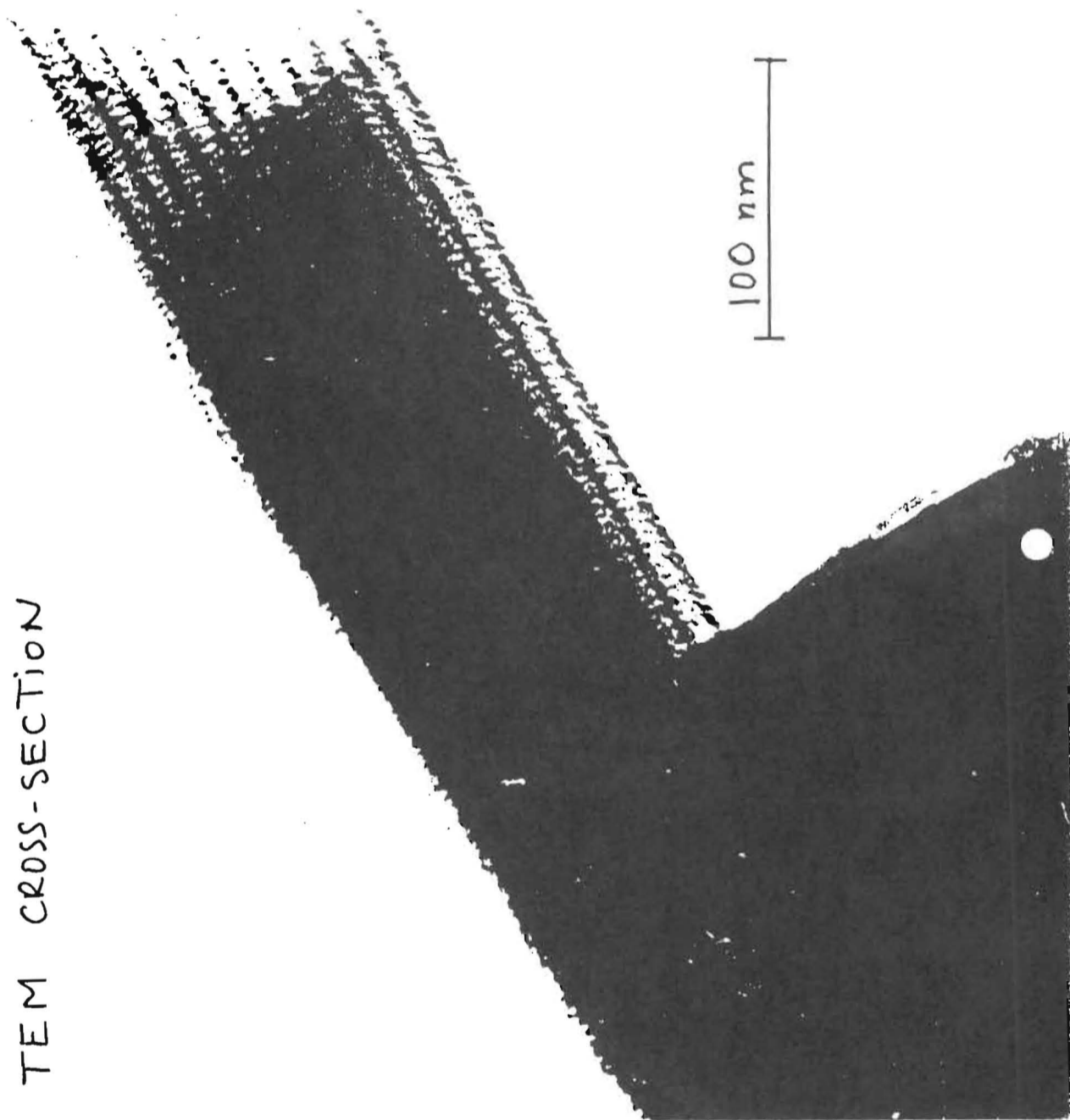


TEM CROSS-SECTION

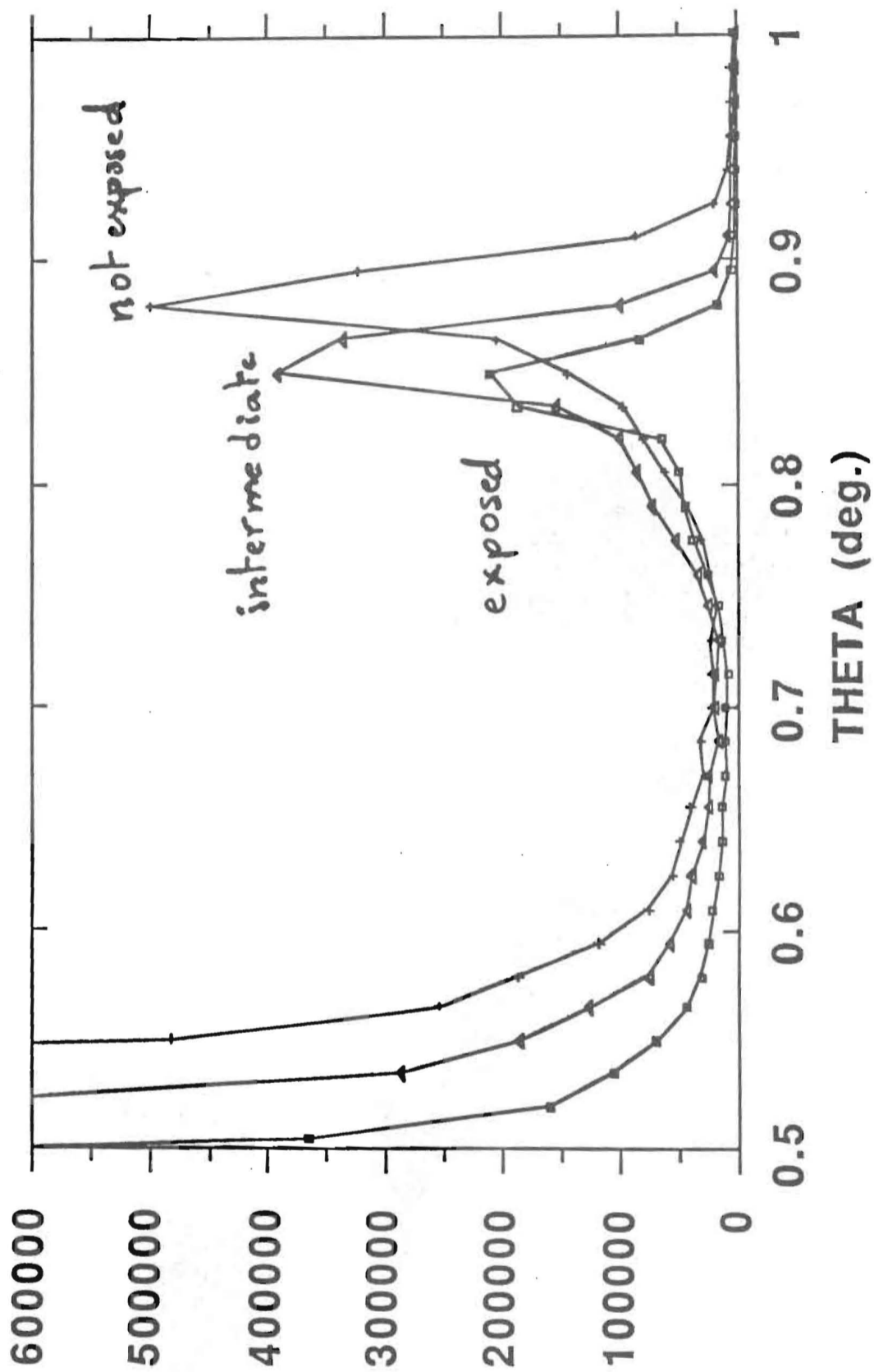
(W-Si) 4-12-88 #4

Reactive (C_2H_2)

BEFORE EXPOS.

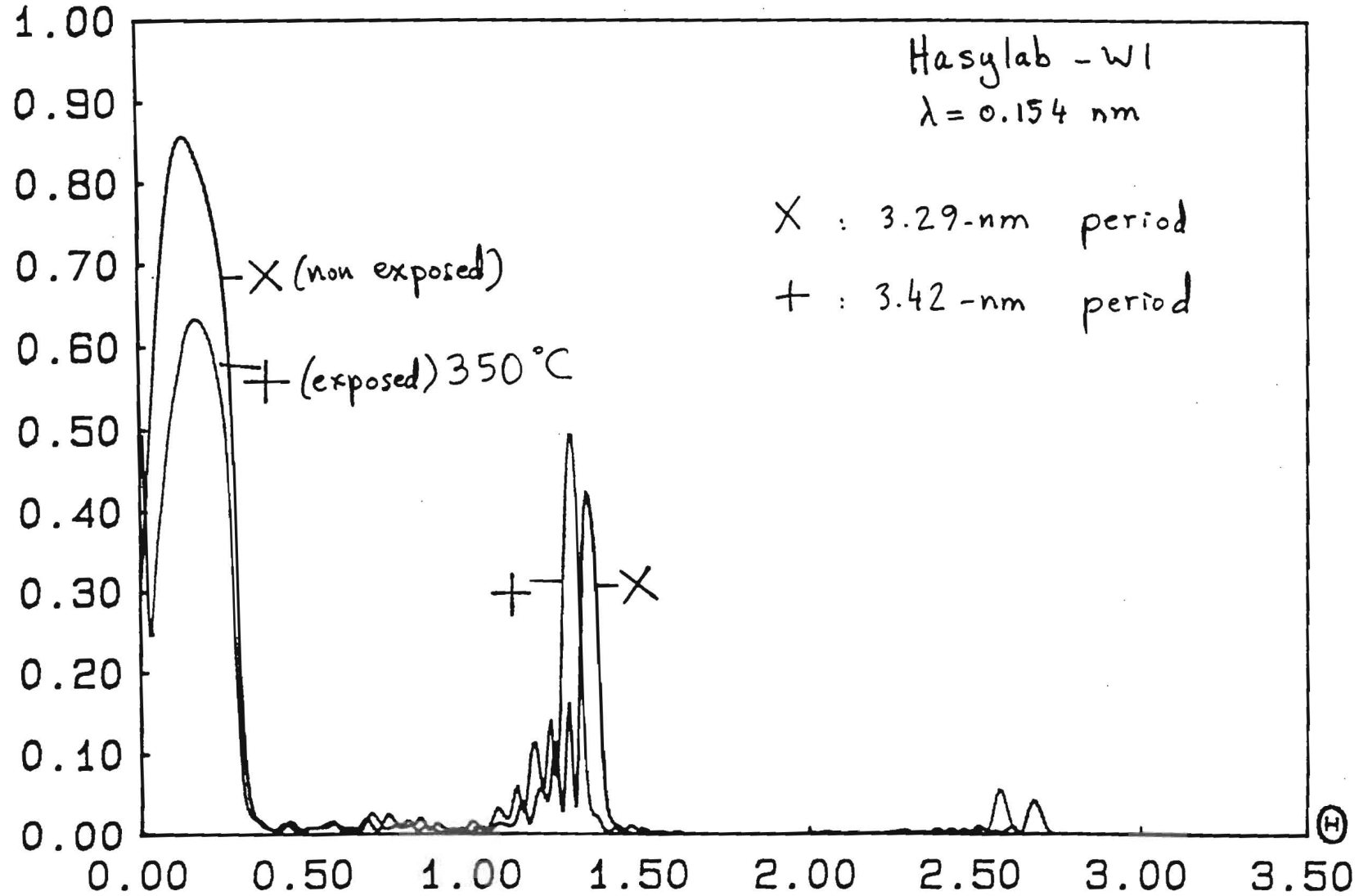


W/Si (4-12-88) #4



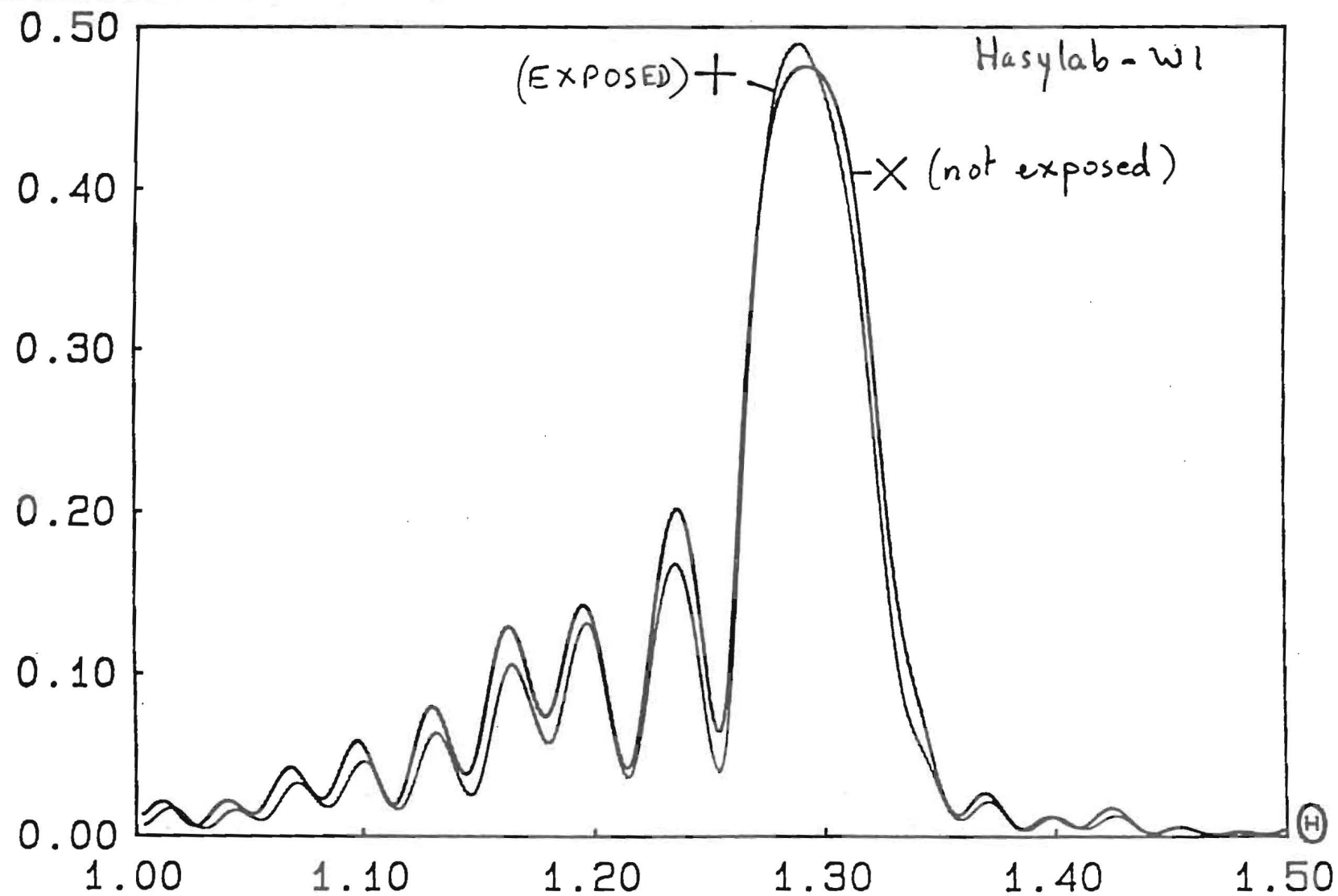
C-W-SI126;+EX.,xREF.

REFLECTIVITY



C-W-SI126;+IN,xOUT

REFLECTIVITY

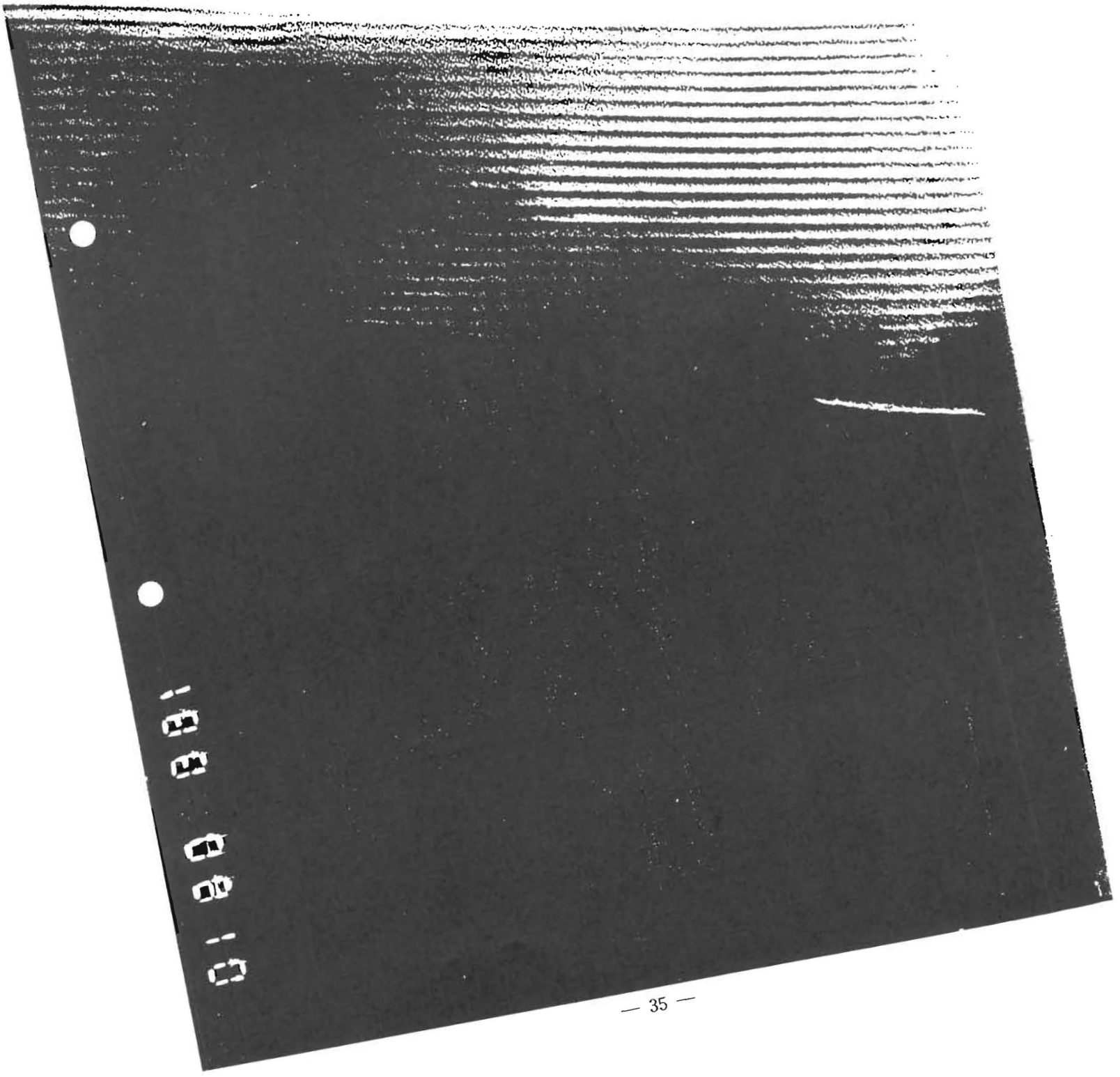


(W/C) 4-14-88 #2

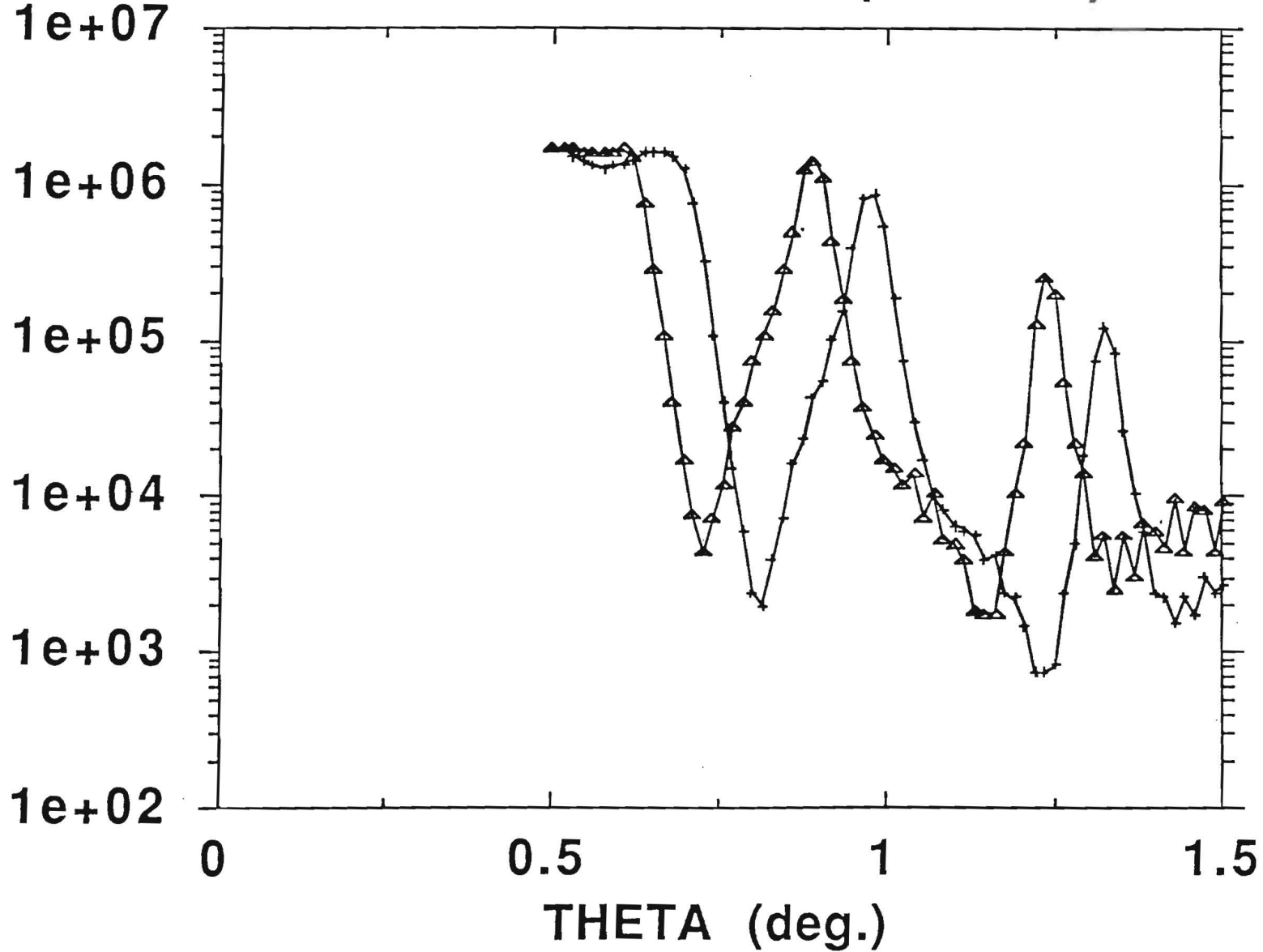
Reactive (N₂)

NOT EXPOSED

100 nm

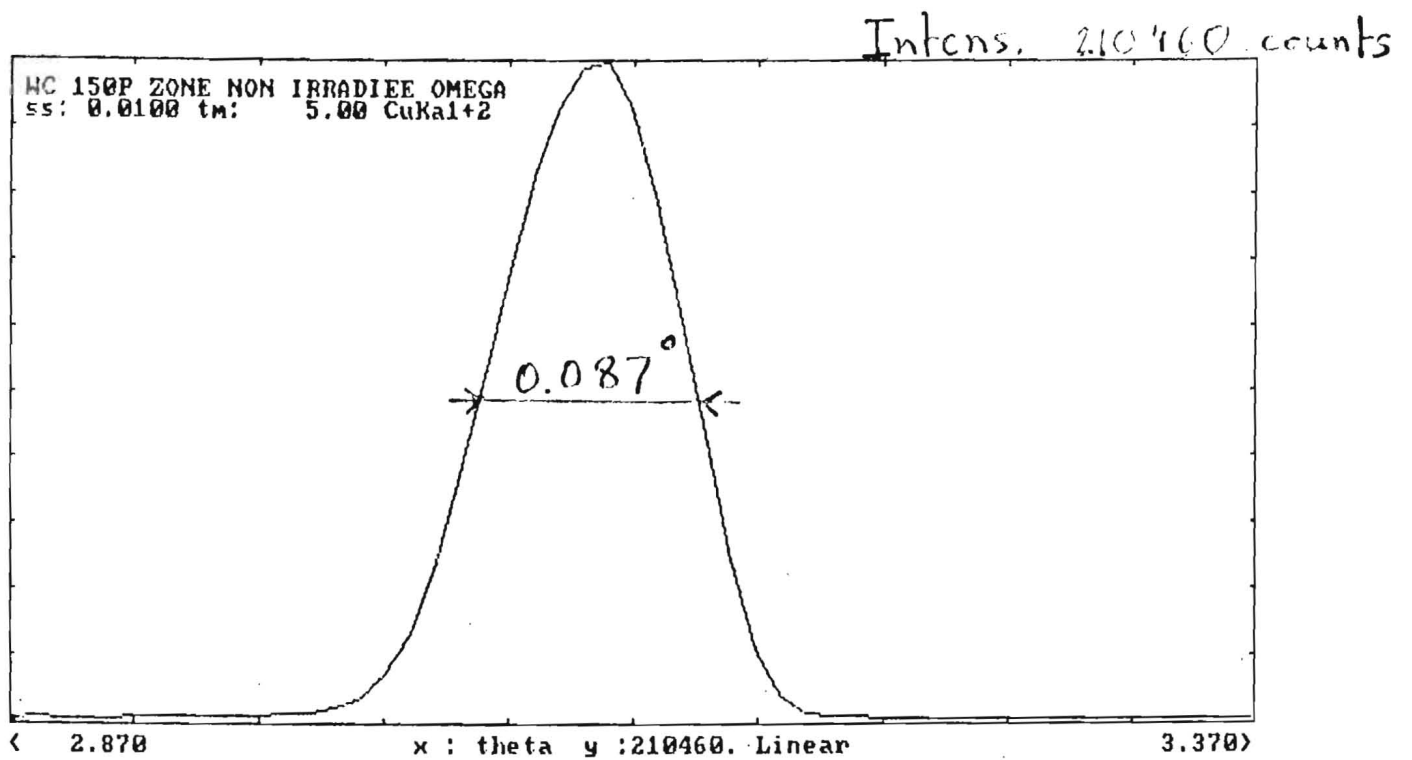
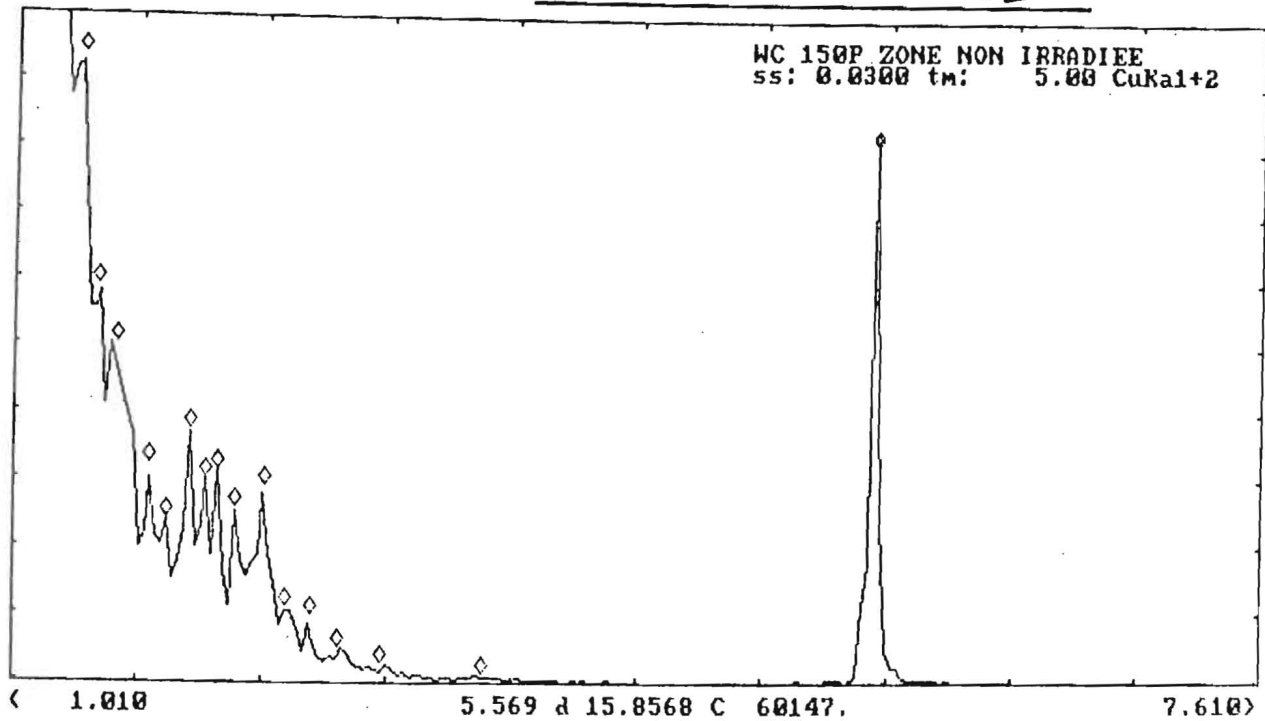


W/C (4-14-88)#2

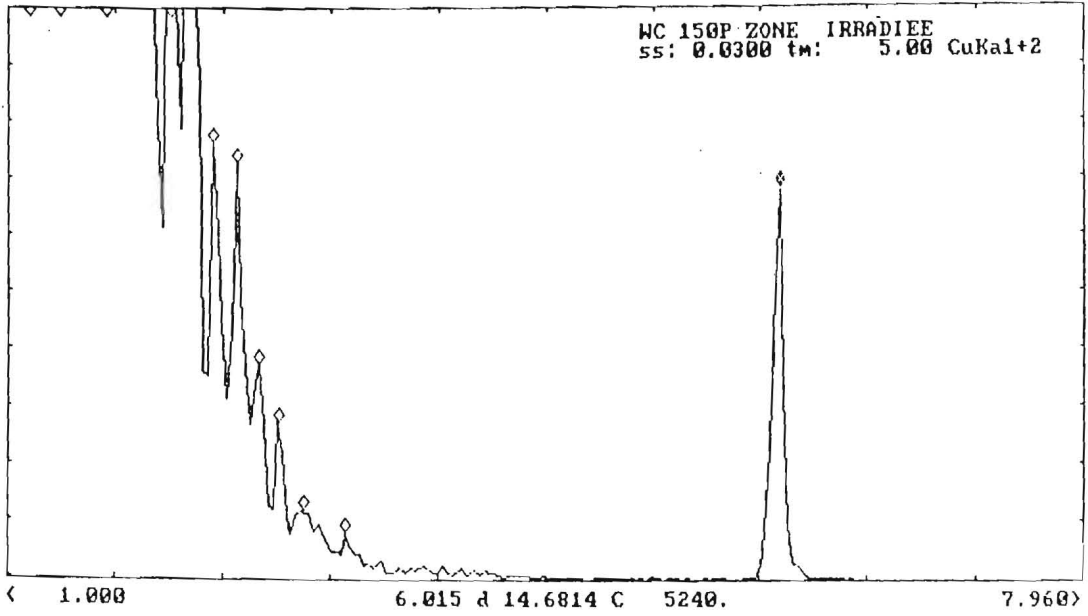


(WC) 150 μ , 1.58-mm period

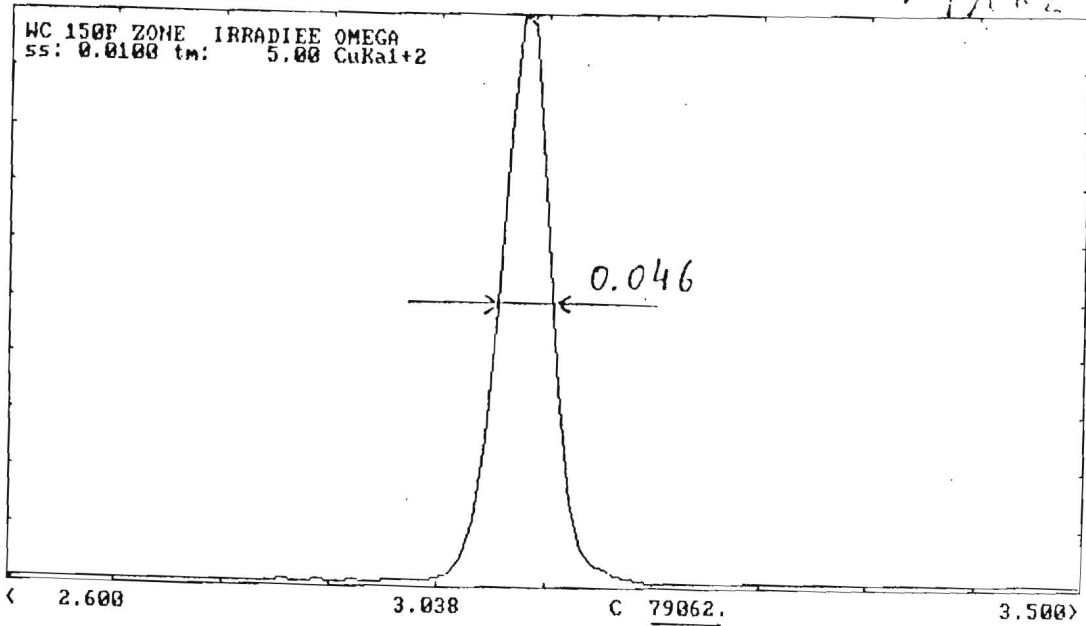
NOT EXPOSED



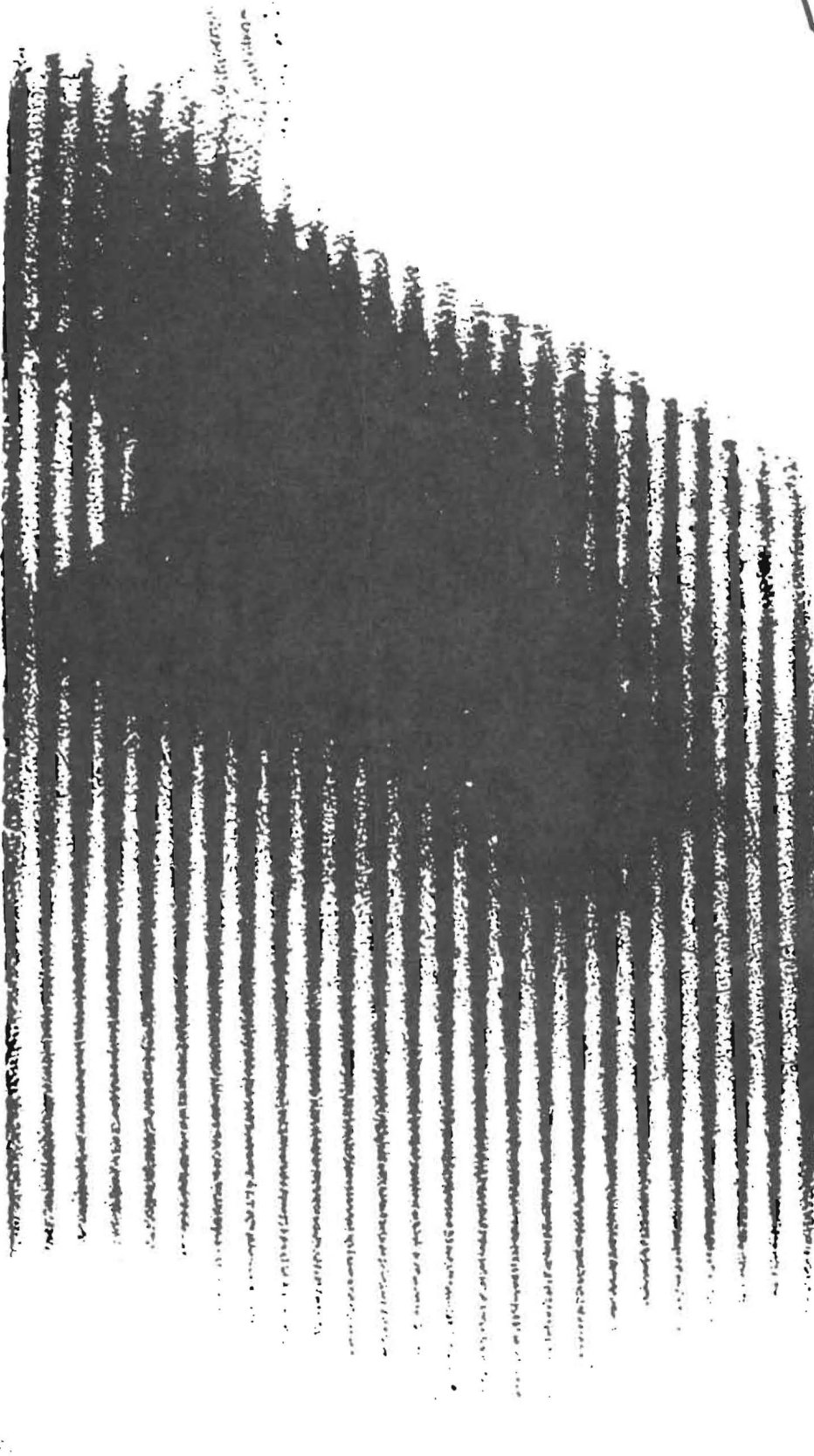
(W/C) 150 p, 1.5 nm period
 EXPOSED - 400 °C



Intens. { 38% decrease
 12062 counts



(w/c)50, Reactive (C_2H_2)



100 nm

Reflectivity

(W/C) 50 layers

SCAN E41488.3B 4mA F=286p t=10s FL=2.45mm Reactive (C₂H₂)

I = 50000

After 750°C, 8 hours
(10⁻⁵ - 10⁻⁶ Torr)

0.47

0

ECH X 2.1mrad \ 120 pas

21mrad

SUMMARY - CONCLUSION

High exposure tests :

PT/C	500°C	destroyed
W/Si (C ₂ H ₂ reactive)	450°C	: 40% decrease Refl.
W-Si/C	350°C	no change in reflectivity * (WSi ₂ ?)
W/C (N ₂ reactive)	350°C	: period shift * few Refl. changes
W/C	400°C	$\frac{1}{2} \times \text{FWHM}$, 40% decrease Refl.
W/C (C ₂ H ₂ reactive)	650°C TEM 750°C furnace	: no change *

At the expenses of reflectivity
some heat load capability has been shown

Work in progress :

rapid laser annealing
(Lab. CNRS - St Gobain, F) pulsed laser heating

reactive sputtering and co-sputtering

Production Facility at ESRF

plasma-assisted CVD (next year) : carbides - silicides

laser evaporation (F. Comin, S. Ferrer)

ACKNOWLEDGEMENTS

A. FREUND / ESRF

J. P. SIMON, C. BERNARD / LTPCM, St Martin d'Hères, France

G. FENSKE / Argonne National Laboratory

R. RIVOIRA / Université d'Aix-Marseille III, France

W. JARK / Fritz-Haber-Institut, Berlin

Th. WROBLEWSKI / Hasylab - DESY, Hamburg

MULTILAYERS FOR HIGH POWER BEAMLINES

T. W. Barbee, Jr.

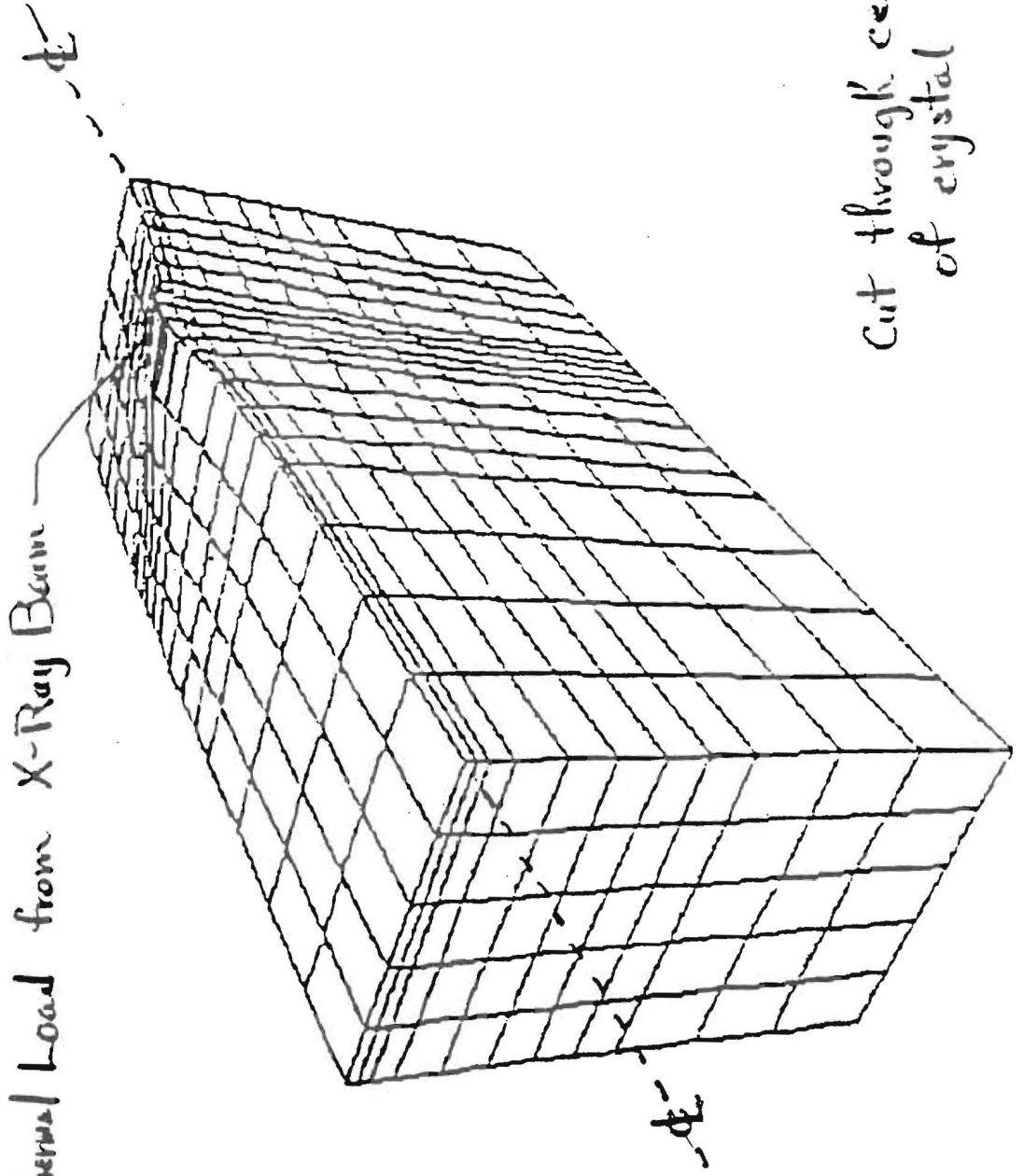
Lawrence Livermore National Laboratory
Livermore, CA 94550, USA

Multilayers for High Power Beam Lines

- I. Introduction
 - 1. Substrate
 - 2. M.L. Stability
 - 3. MATERIALS Selection
- II. Stability of Substrate
- III. Is the Effort worth it?
- IV. MATERIALS:
 - 1. Compounds
 - 2. Refractory Amorphous M.L.s
 - 3. Crystalline Refractory
 - 4. Single Crystal !!
 - Intermetallics
 - Refractory Oxides
- V. Yes - It is important!

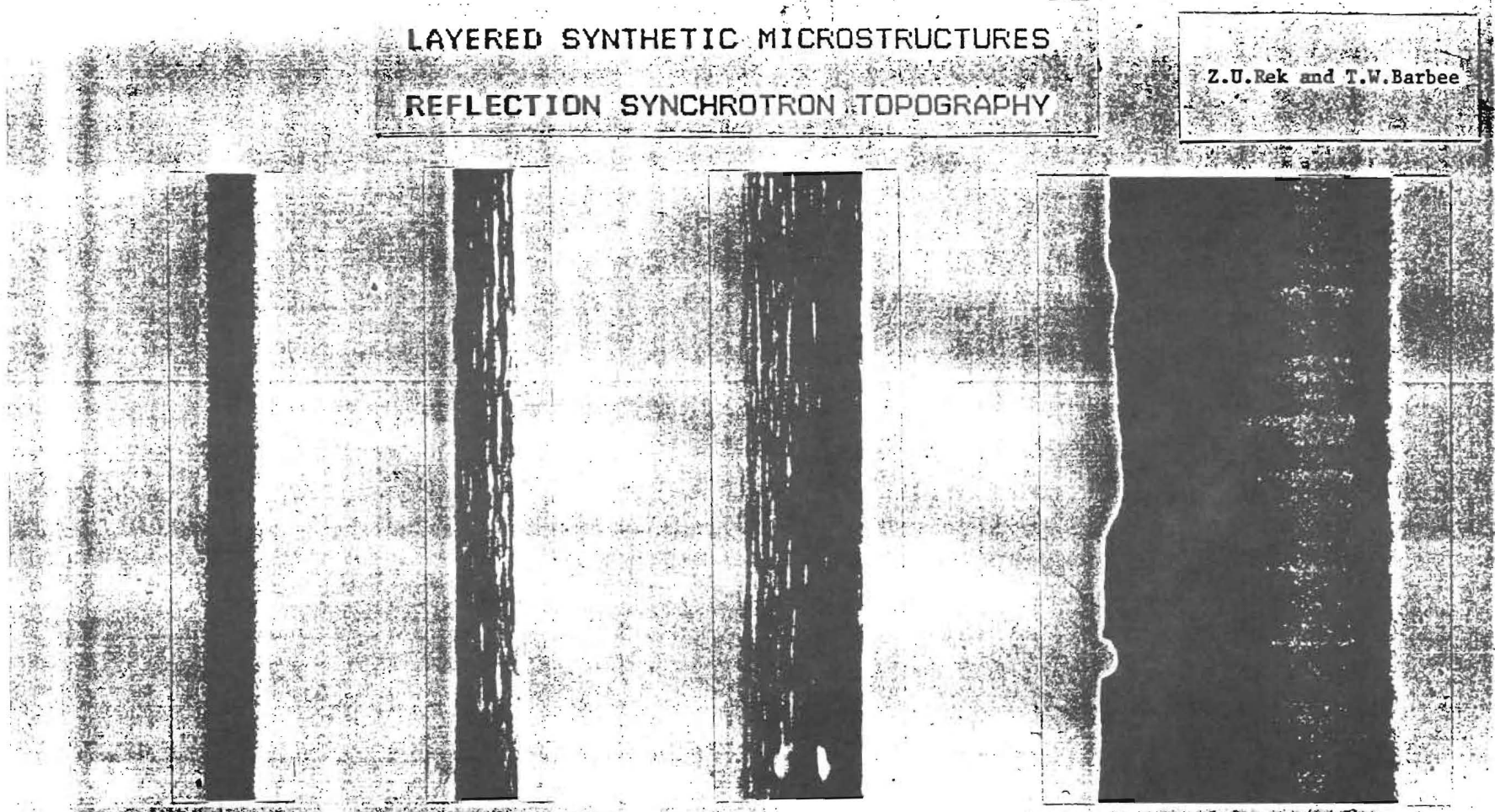
Thermal Loading Distorts Crystal

- reduced output flux
- output flux and energy change as stored current decreases



LAYERED SYNTHETIC MICROSTRUCTURES
REFLECTION SYNCHROTRON TOPOGRAPHY

Z.U.Rek and T.W.Barbee



DIRECT BEAM

SI(111) SUBSTRATE

SI(100) SUBSTRATE

HOYA GLASS SUBSTRATE

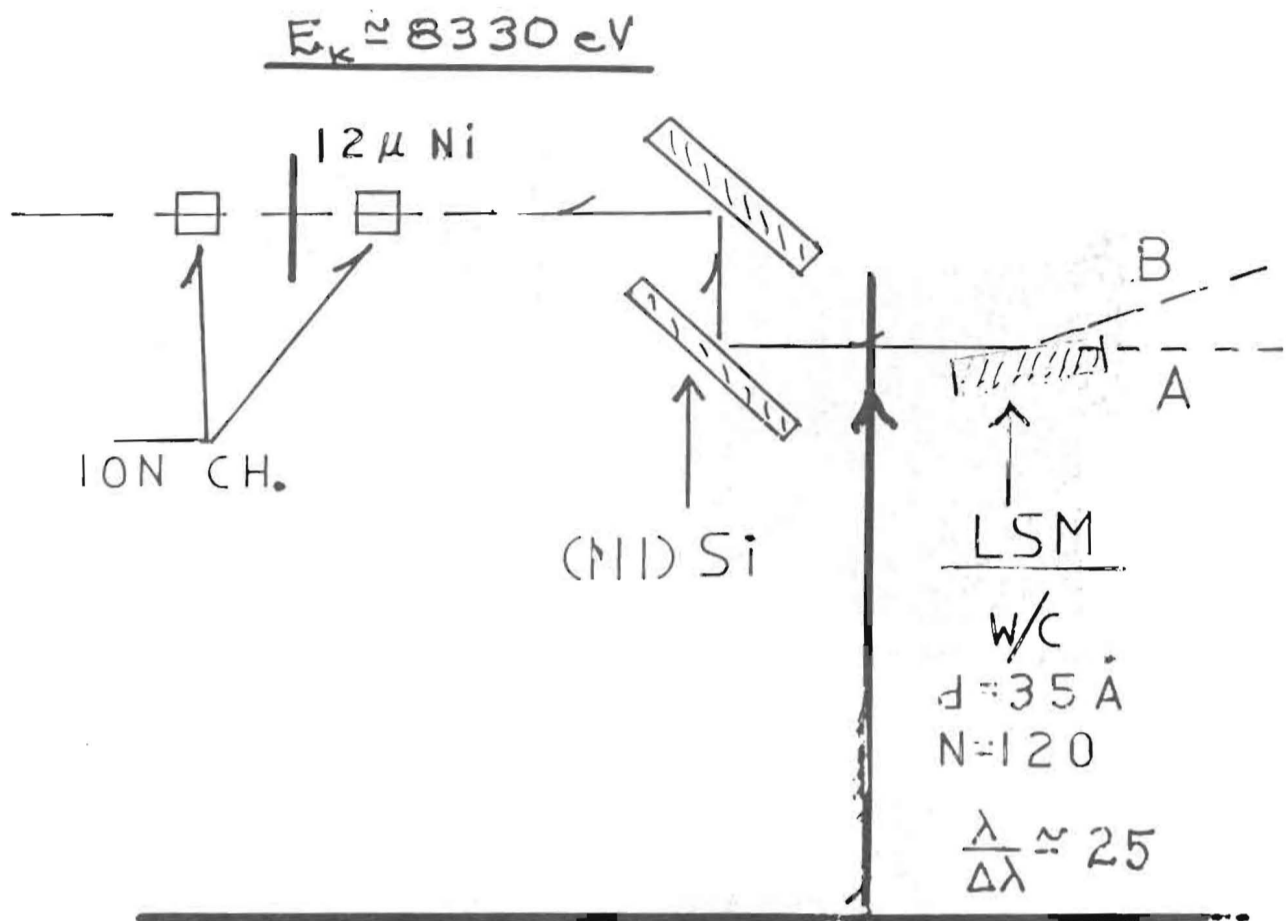
1.5 KeV



CERVIT
Pd/C
D=43 Å
N=120

100 X





Si: $\Delta\theta = \Omega$ (Ω - Div. of incident BEAM)

$$\frac{\Delta\lambda}{\lambda} = (\Omega + W_{si}) \cot\theta_B$$

\therefore If Ω increased by LSM
Energy resolution is decreased

10 1.10
(44)

EE

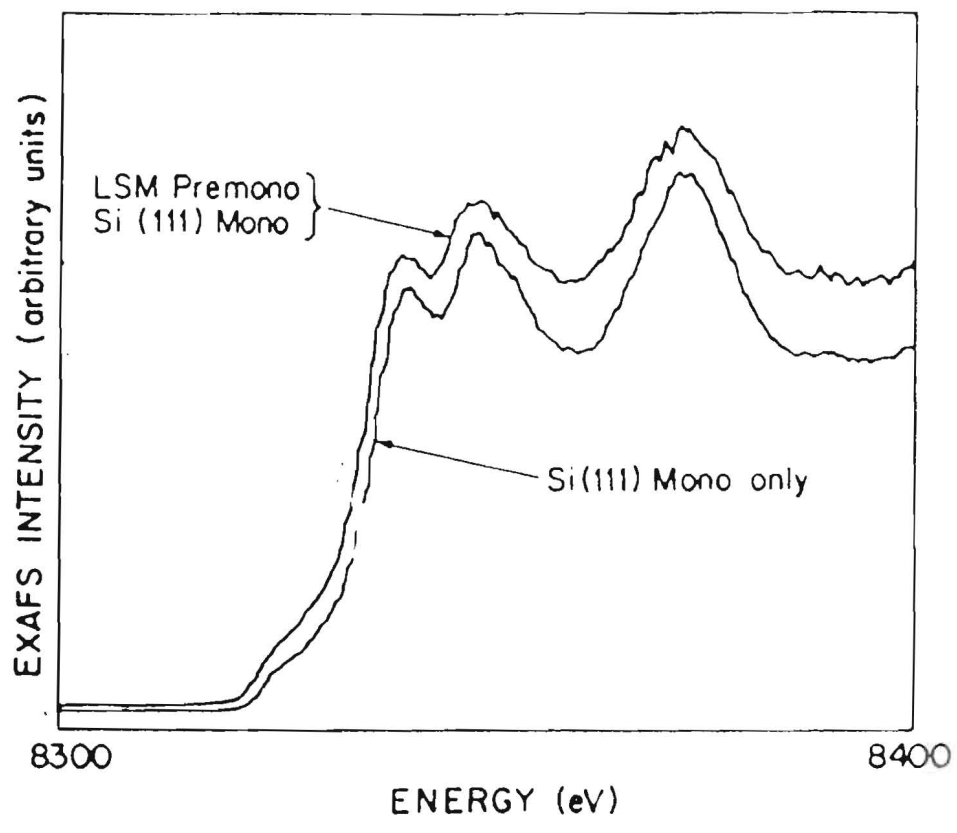
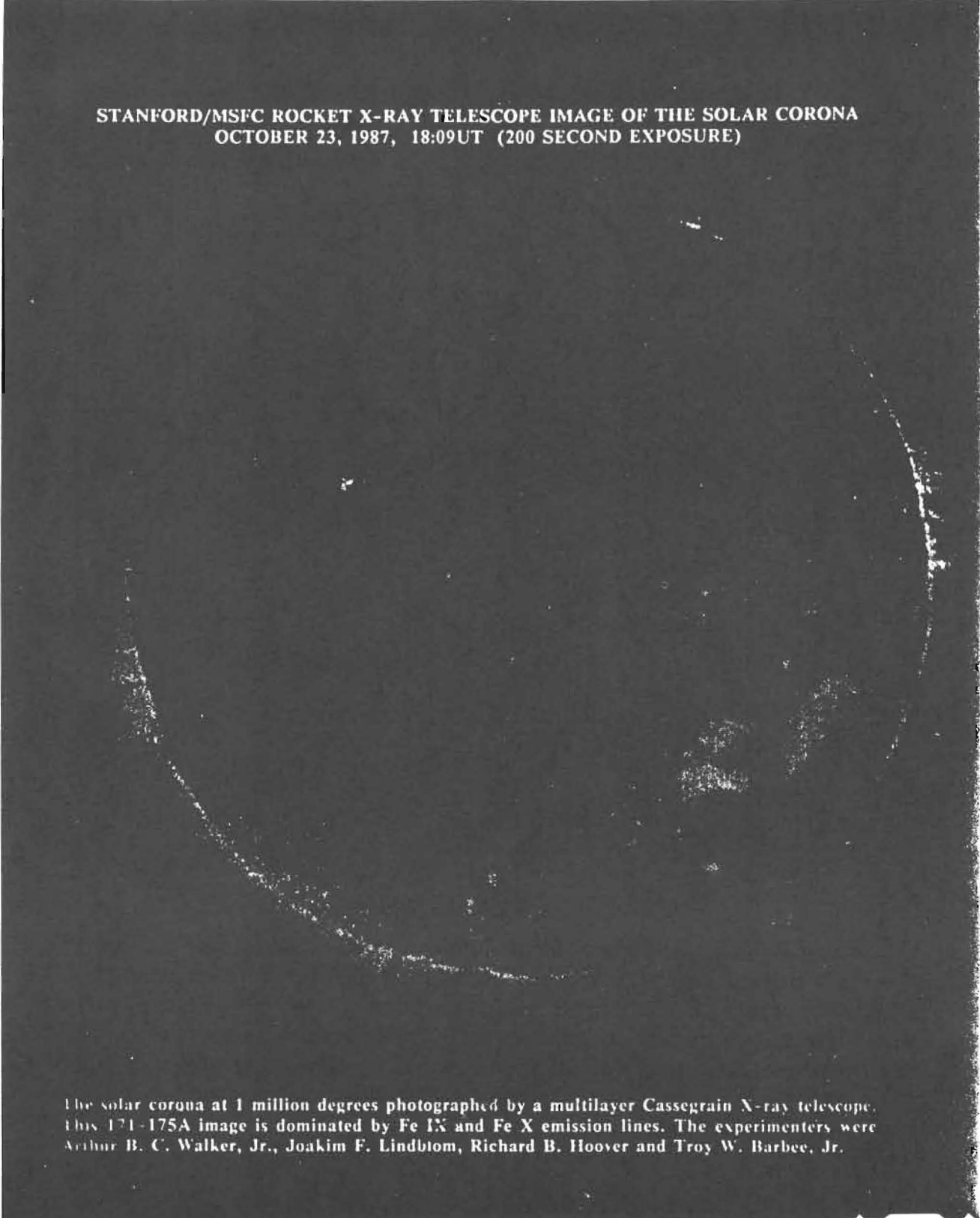


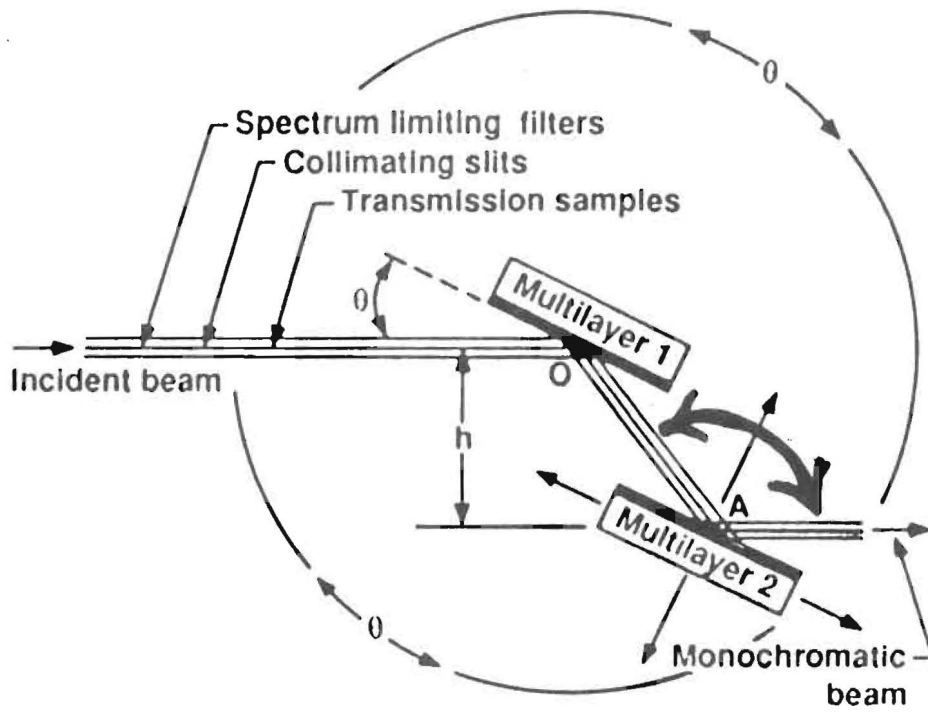
Fig. 13. EXAFS spectrum of a 12 μm thick nickel foil⁸⁴ over the energy range 8300 to 8400 eV obtained using a two-crystal (111) silicon crystal monochromator, compared to an EXAFS spectrum from the same nickel foil taken using the same two-crystal (111) silicon crystal monochromator preceded by a tungsten-carbon LSM premonochromator. The LSM structural parameters are $t_w = 13.2 \text{ \AA}$, $t_c = 19.8 \text{ \AA}$, $N(W/C) = 100$.

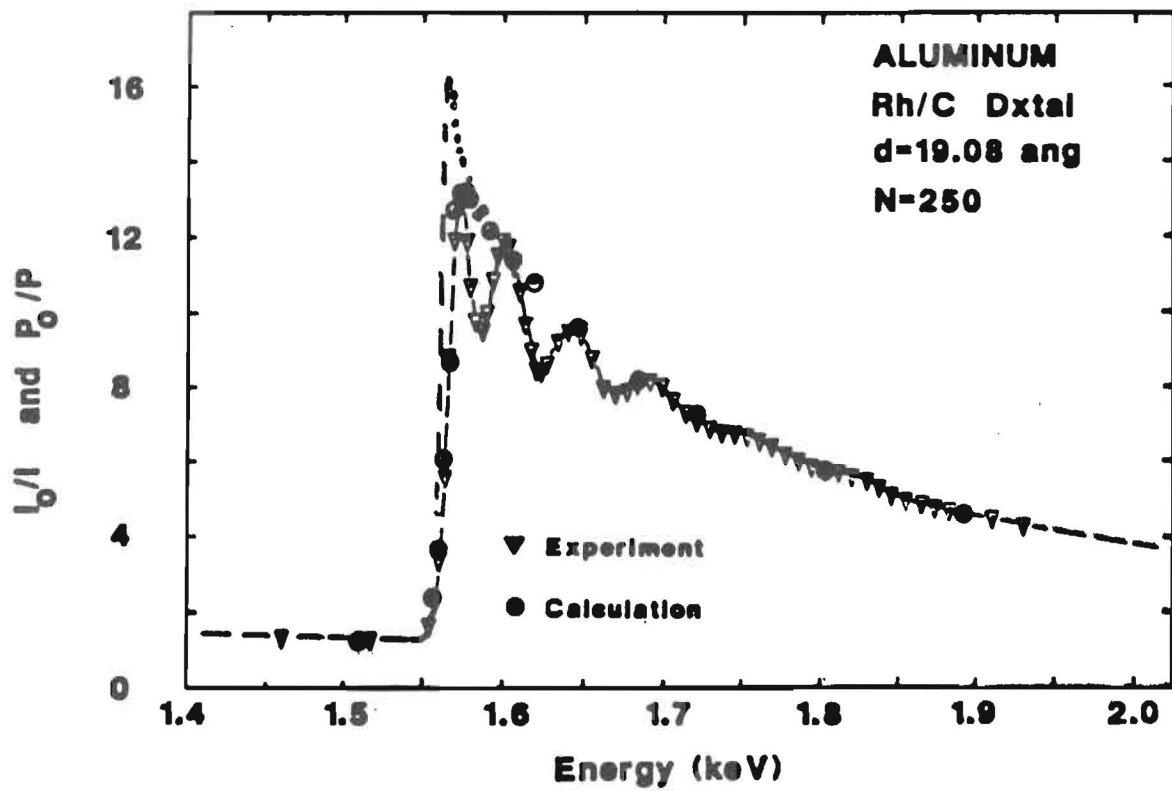
STANFORD/MSFC ROCKET X-RAY TELESCOPE IMAGE OF THE SOLAR CORONA
OCTOBER 23, 1987, 18:09UT (200 SECOND EXPOSURE)



The solar corona at 1 million degrees photographed by a multilayer Cassegrain X-ray telescope. This 171-175A image is dominated by Fe IX and Fe X emission lines. The experimenters were Arthur B. C. Walker, Jr., Joakim E. Lindbom, Richard B. Hoover and Troy W. Barbee, Jr.

8952-05

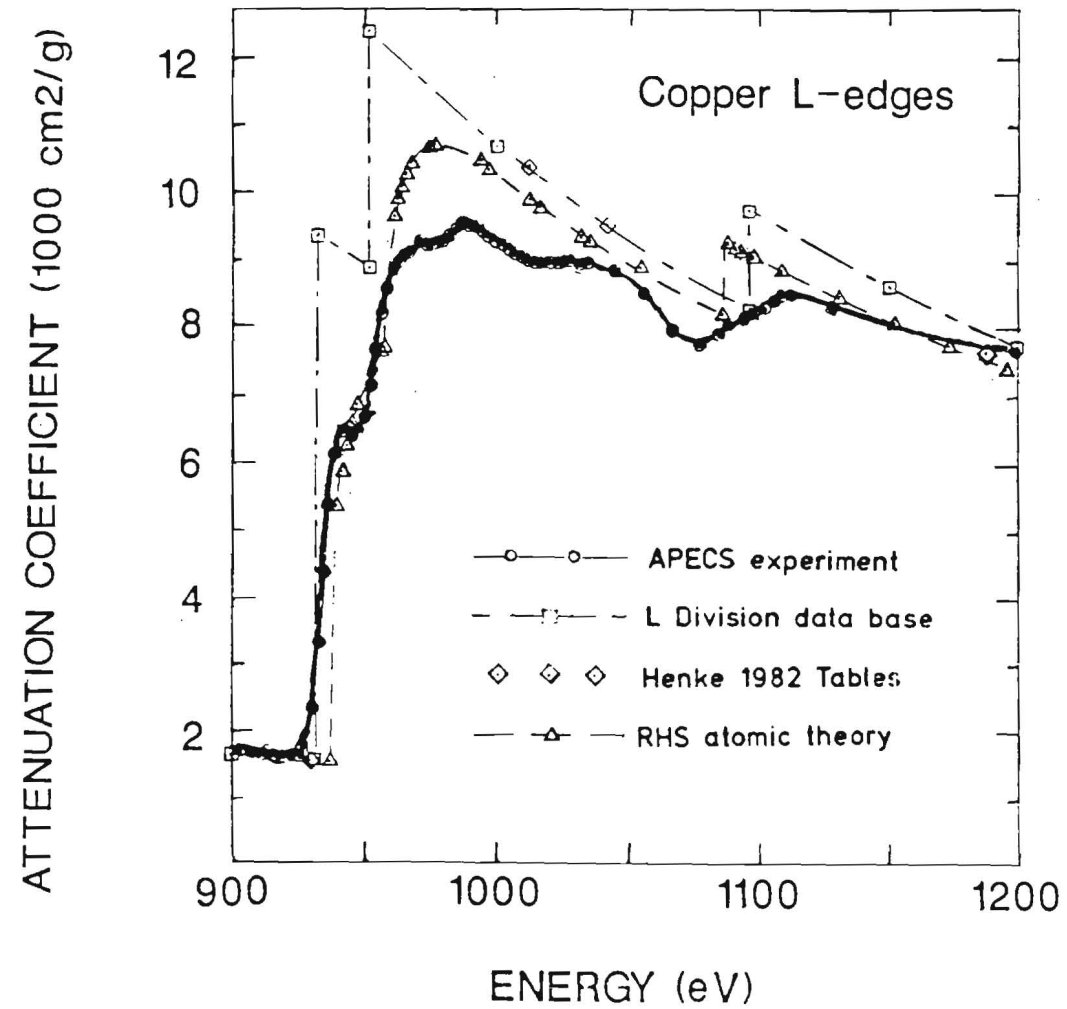




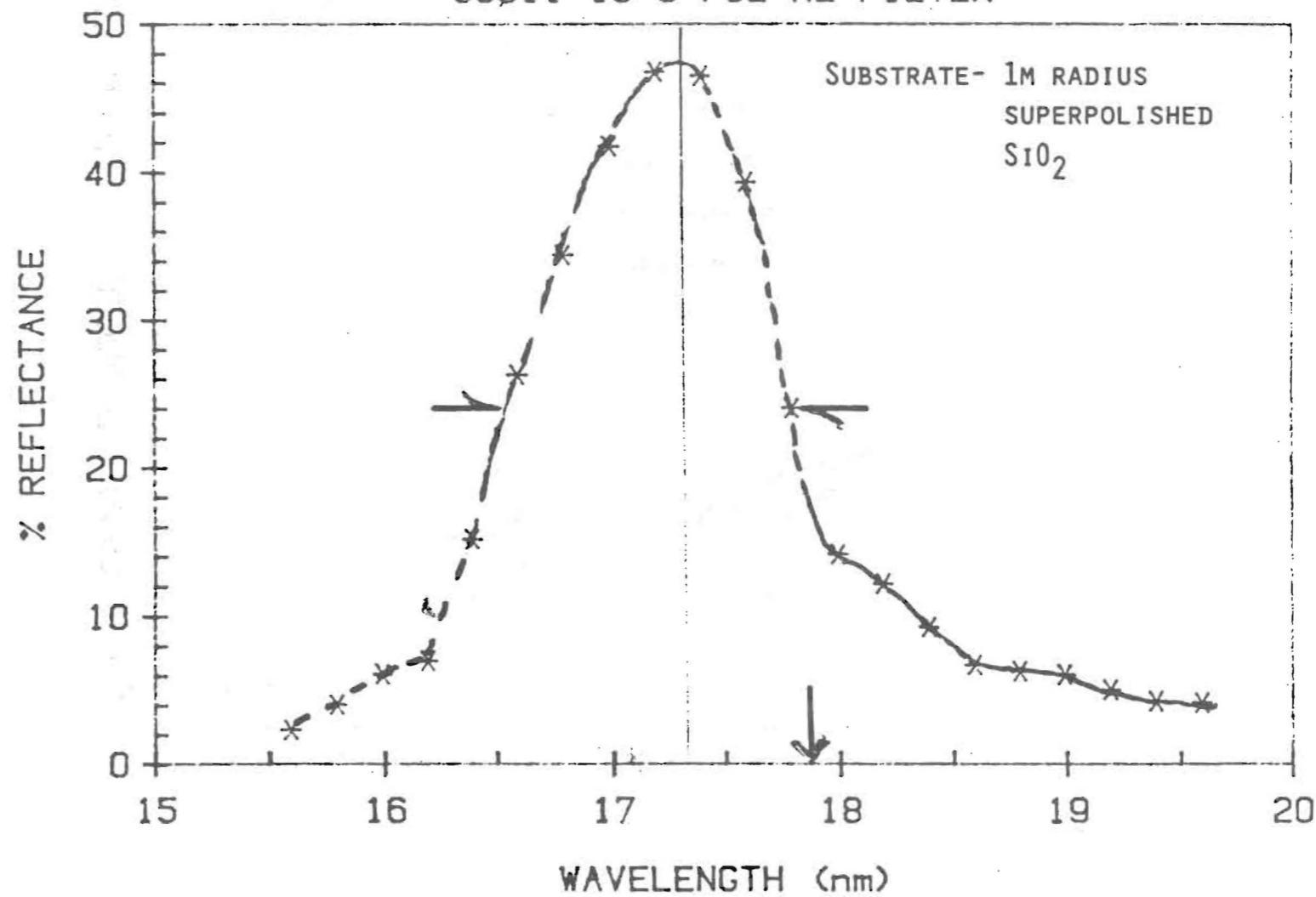
Aluminum K edge 1558 eV

- calculation 2.05 micron Al
- no EXAFS or NEXAFS

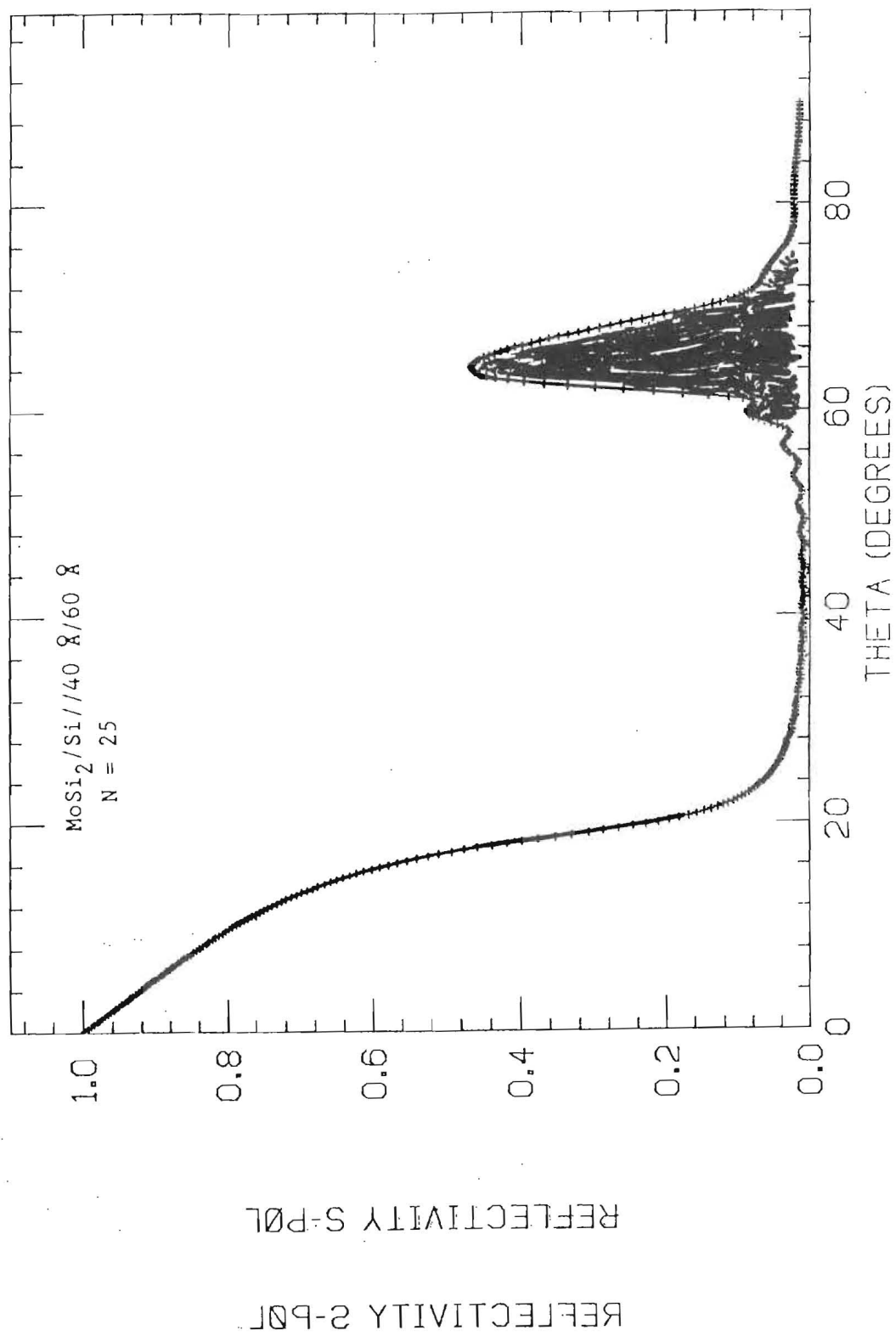
ABSOLUTE PHOTOABSORPTION EXPERIMENTAL CROSS SECTIONS (APECS)



DATA TAKEN BY RITA KESKI-KUHA AT NBS-SURF FACILITY
85011 15 S-POL AL FILTER



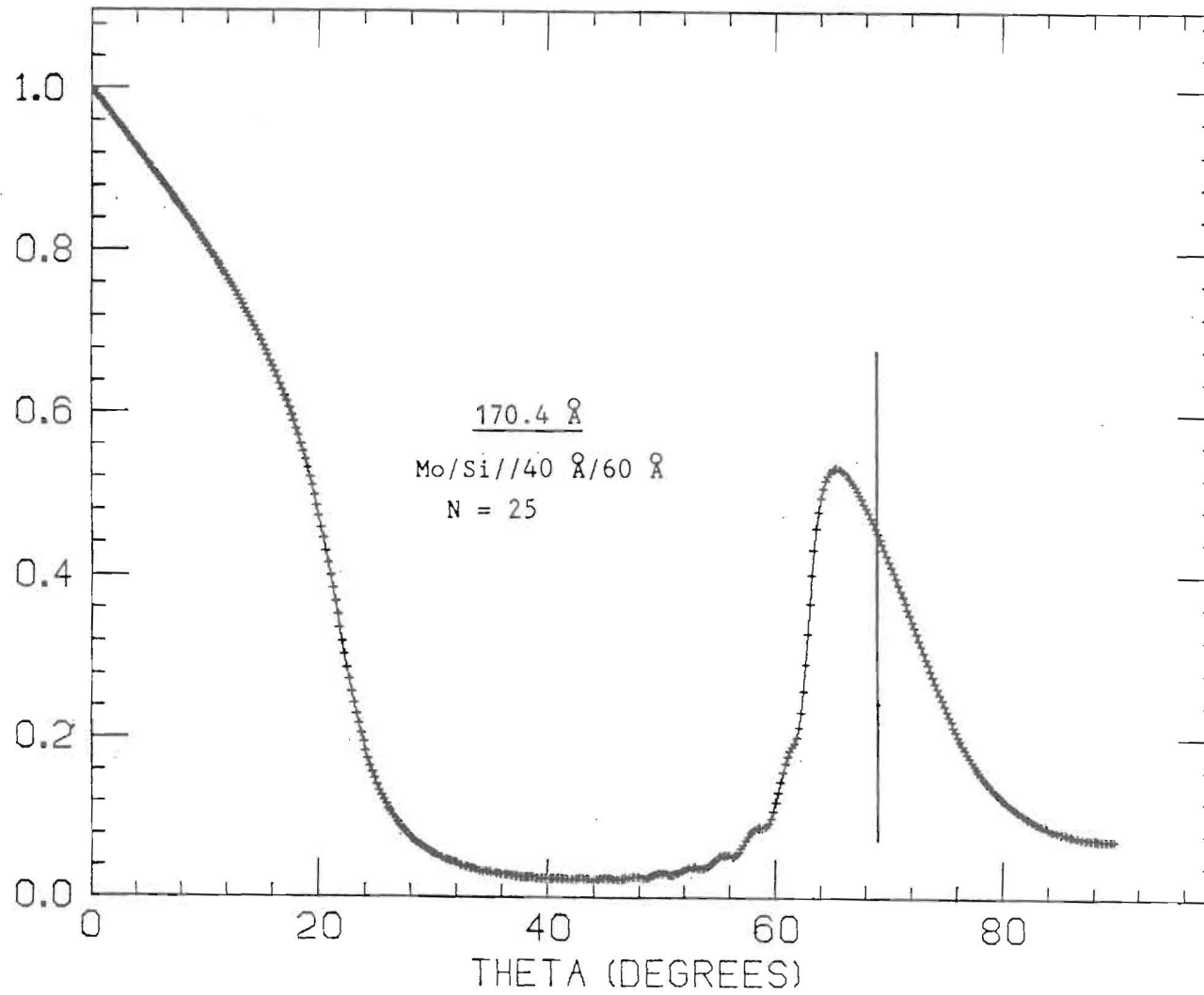
2255 PLOTTED



REFLECTIVITY 2-POL

REFLECTIVITY S-POL

2231 PLOTTED



MATERIALS:

A. WC/C ($\rho_{WC} = 15 \text{ g/cc}$) ★

B. HfC/C

C. MoSi₂/Si ★

D. SiC/C ★

E. Be/NiBe (To be attempted)

Abrupt

F. W/C

G. Mo/C

H. MoSi₂/C

I. WSiC/C

Graded Interface

Multilayer Mirrors as Power Filters in Insertion Device Beamlines

J.B. Kortright and R.S. DiGennaro
Center for X-ray Optics
Lawrence Berkeley Laboratory
Berkeley, California 94720 USA

Radiated power incident on thermally sensitive optics can be reduced by placing mirrors in front these optics in high power synchrotron radiation beamlines. Multilayer mirrors act as bandpass filters and hence reflect less power down beamlines than total reflection mirrors, which act as low-pass filters. Calculations of the power reduction obtained by multilayer mirrors relative to total reflection mirrors in wiggler beamlines on the upcoming generation of 1-2 and 6-7 GeV synchrotron radiation sources indicate that multilayer mirrors provide roughly an order of magnitude greater power reduction compared to total reflection mirrors, when each mirror is optimized for the same photon energy. The increases in absorbed power by the multilayer over the total reflection mirrors are only incremental. The maximum calculated absorbed power densities are within the range of those for which water-cooled metal mirror substrates have already been designed. Thus it appears that cooling multilayers in these situations should present no fundamental difficulties. Even so, questions of mirror distortion and multilayer radiation stability need to be carefully studied. Multilayer premirrors appear to be more generally useful as power filters in wiggler beamlines than in undulator beamlines because the broad spectral distribution from wigglers can be effectively filtered by multilayer bandpass reflectors. Multilayers in undulator beamlines can be effective as power filters in certain instances.

Reference

J.B. Kortright and R.S. DiGennaro, to be published in Proc. of SRI '88, Rev. Sci. Inst.

**MULTILAYER MIRRORS AS POWER
FILTERS IN INSERTION DEVICE
BEAMLINES**

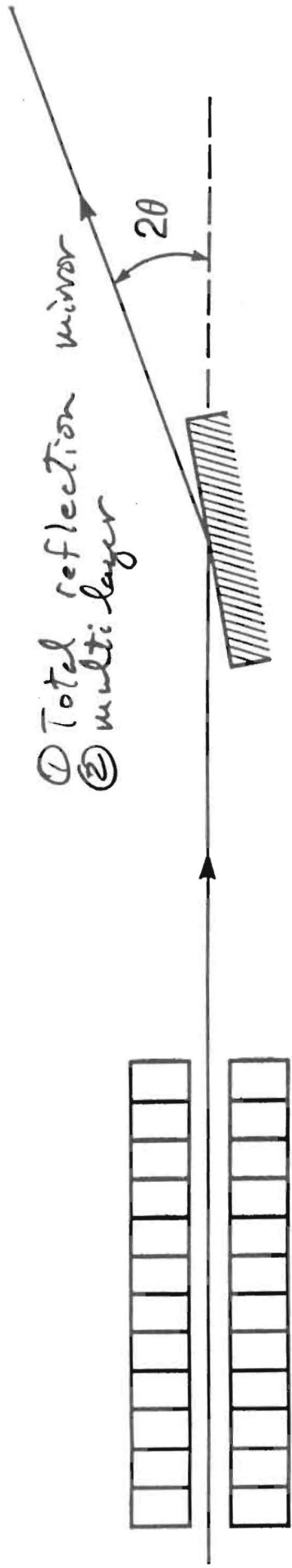
**J.B. Kortright and R.S. DiGennaro
Center for X-ray Optics
Lawrence Berkeley Laboratory
University of California
Berkeley, California 94720 USA**

Table 1. Wiggler parameters used to generate flux and power spectra for 1.5 GeV and 7.0 GeV synchrotron radiation sources. Values for some other quantities are included.

	<u>ALS</u>	<u>APS</u>
electron energy, E [GeV]	1.5	7.0
peak magnetic field, B_0 [T]	2.07	1.0
number of wiggler poles, N	32	20
wiggler period, λ_w [cm]	13.6	15.0
ring current, I [A]	0.4	0.1
max. critical photon energy, $\epsilon_{c,max}$ [keV]	3.1	32.6
total radiated power, P_T [kW]	1.87*	4.71
peak power density, [kW/mrad ²]	0.73	26.
distance to first optic [m]	12.0	32.0

*Calculations are based on accepting the central 5 mrad horizontal fan from the wiggler. The total radiated power into the entire horizontal fan is 5.36 kW.

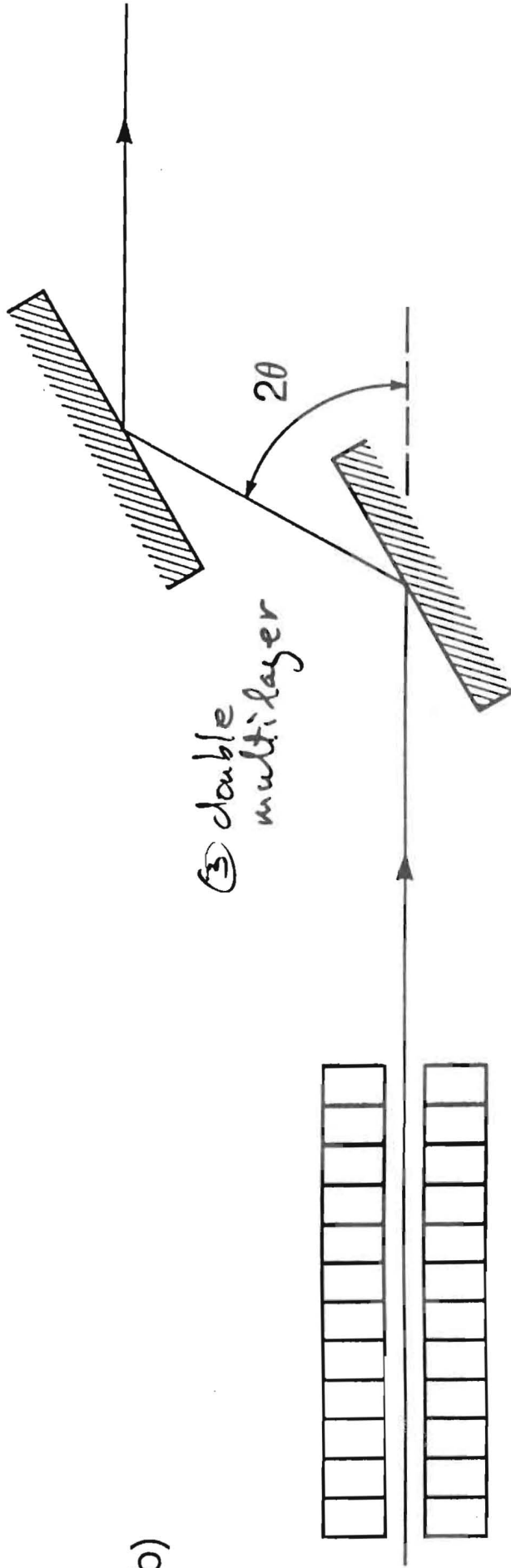
a)



- ① Total reflection mirror
- ② multi layer

Wiggler

b)



- ③ double multi layer

Figure 1

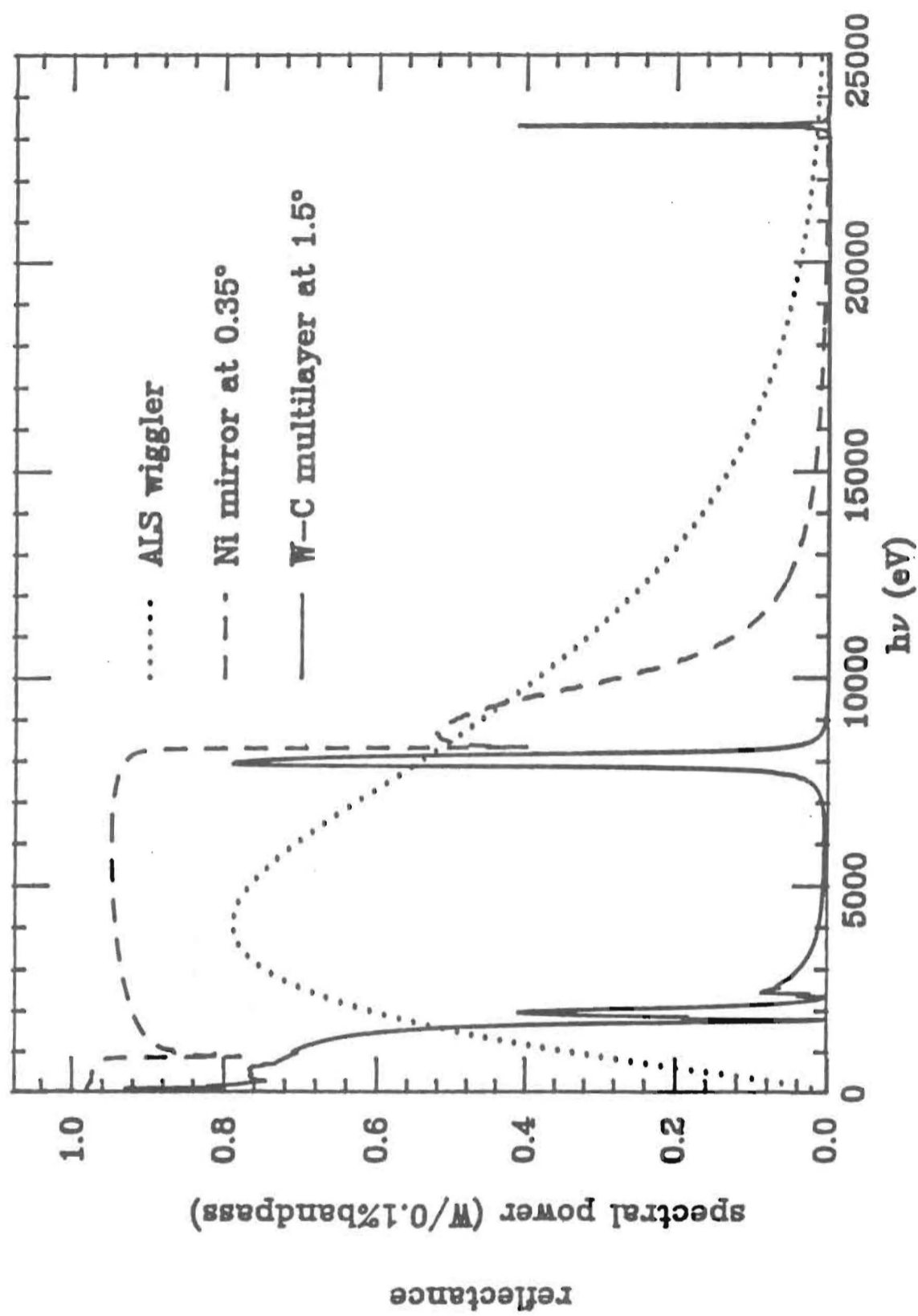


Figure 2

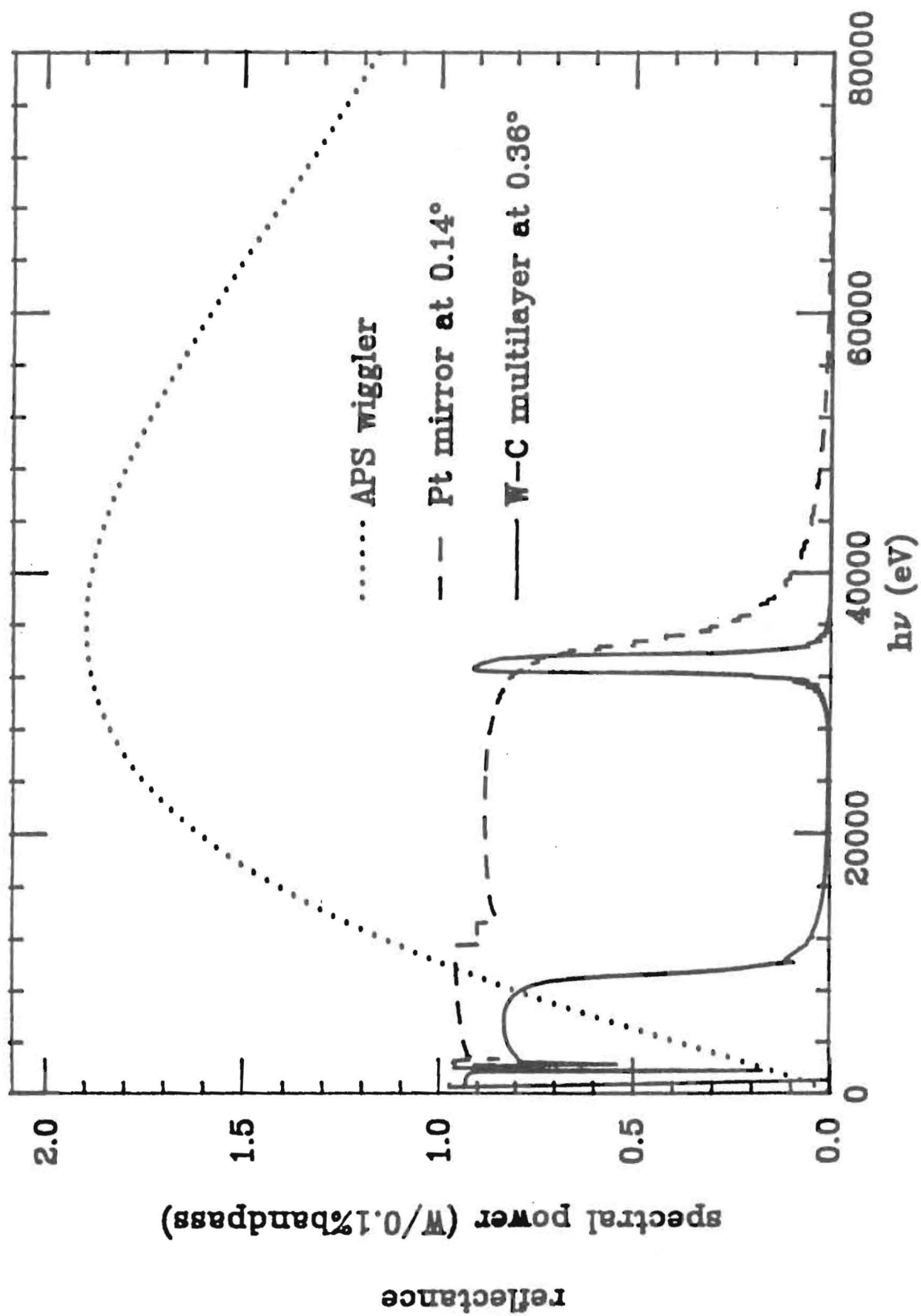


Figure 3

Table 2. Power filtering results for various cases considered.

	P_R	P_A	P_{den}	Flux
<u>ALS wiggler (1.87 kW incident power)</u>				
$h\nu = 1.5 \text{ keV}$				
Ni mirror at 1.5°	0.49	1.38	13.	1.2×10^{15}
W/C multilayer at 7.9°	0.025	1.86	69.	8.2×10^{14}
double multilayer	0.005			3.3×10^{14}
$h\nu = 3.1 \text{ keV}$				
Ni mirror at 1.0°	0.80	1.07	9.	9.9×10^{14}
W/C multilayer at 3.8°	0.12	1.75	34.	5.8×10^{14}
double multilayer	0.04			2.2×10^{14}
$h\nu = 8.0 \text{ keV}$				
Ni mirror at 0.35°	1.58	0.29	3.	3.9×10^{14}
W/C multilayer at 1.5°	0.44	1.43	13.	3.2×10^{14}
double multilayer	0.28			2.5×10^{14}
<u>APS wiggler (4.71 kW incident power)</u>				
$h\nu = 8.0 \text{ keV}$				
Pt mirror at 0.45°	0.80	3.91	20.	5.0×10^{14}
W/C multilayer at 1.5°	0.11	4.61	66.	4.8×10^{14}
double multilayer	0.06			3.6×10^{14}
$h\nu = 20.0 \text{ keV}$				
Pt mirror at 0.2°	1.89	2.82	9.	3.9×10^{14}
W/C multilayer at 0.6°	0.42	4.29	27.	4.0×10^{14}
double multilayer	0.27			3.2×10^{14}
$h\nu = 32.6 \text{ keV}$				
Pt mirror at 0.14°	2.59	2.12	6.	2.8×10^{14}
W/C multilayer at 0.36°	0.82	3.89	16.	3.3×10^{14}
double multilayer	0.62			3.0×10^{14}
$h\nu = 45.0 \text{ keV}$				
Pt mirror at 0.11°	3.07	1.64	5.	8.4×10^{13}
W/C multilayer at 0.26°	1.13	3.58	12.	2.4×10^{14}
double multilayer	0.88			2.2×10^{14}

— P_R is total reflected power [kW]

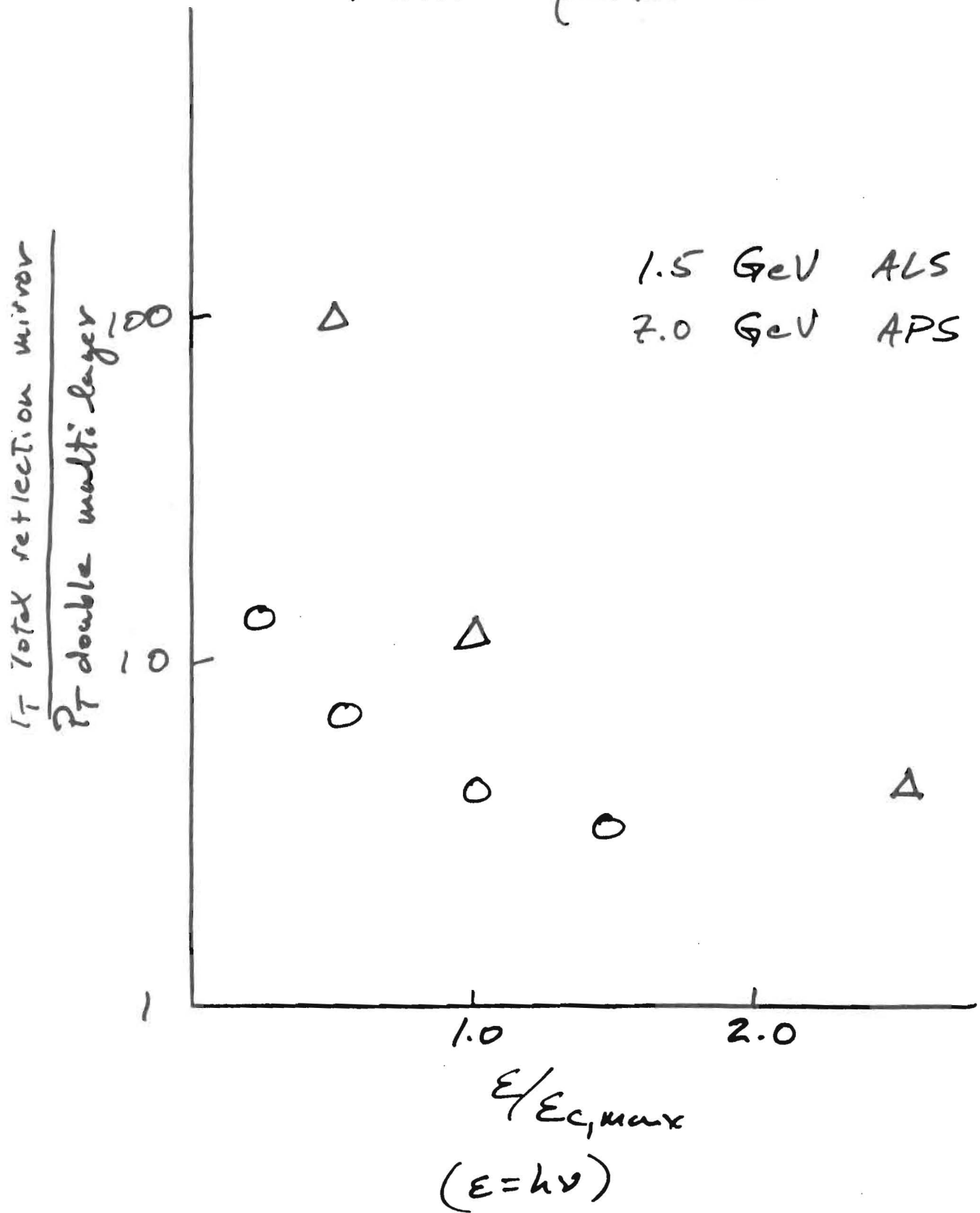
— P_A is total absorbed power in first optic [kW]

— P_{den} is peak absorbed power density at first optic [W/cm^2]

— Flux reflected by optical system [$\#/\text{sec} \cdot 0.1\% \text{ bandwidth}$]*

*Flux numbers are based on calculations assuming ideal wiggler sources and ideal reflectors.

Multilayer vs. Total Reflection mirror performance



Thermal Loads and Performance Requirements

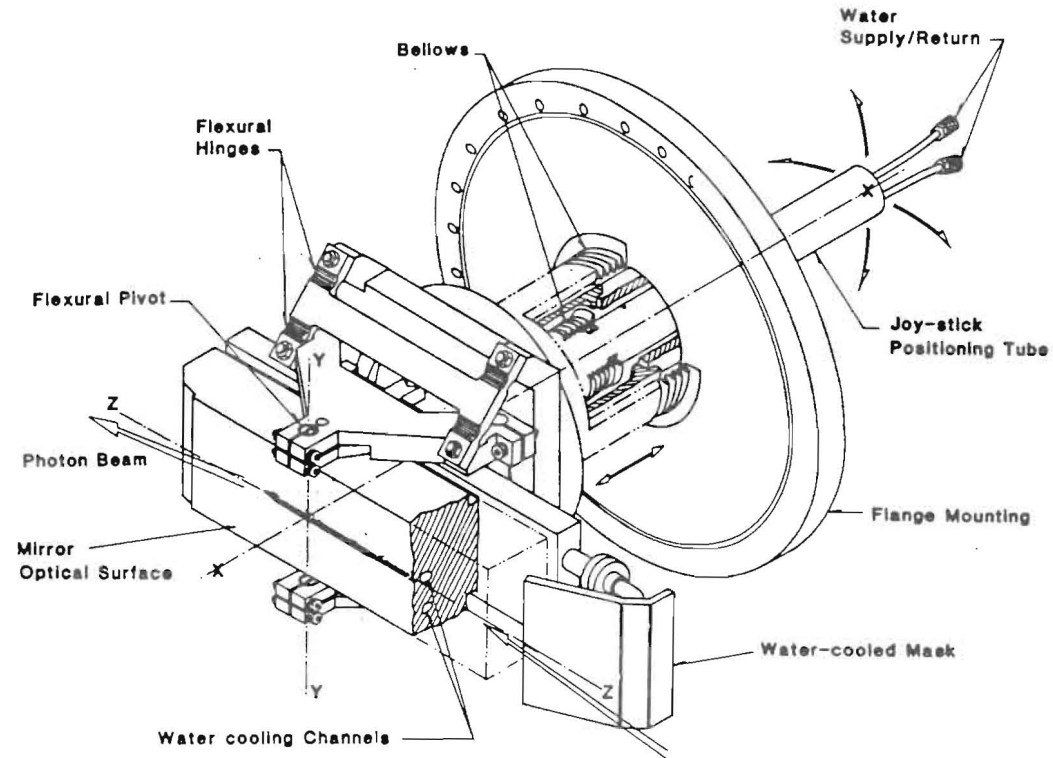
	<u>NSLS X-1 Beam Line</u>	<u>SSRL Beam Line VI - VUV Branch</u>
Deflection Angle	4.5°	5.6°
Max. Total Absorbed Power	700 W	2400 W
Peak Power Density	70 W/cm ²	520 W/cm ²
Source Distance	14 m	8.7 m
Source Size:		
Horiz. $2\sigma_H$	1 mm	8 mm
Vertical $2\sigma_V$	0.2 mm	0.6 mm
Surface Figure Tolerances:		
Tangential (horiz.) Δ_t	8 arcsec	100 arcsec
Sagittal (vert.) Δ_s	40 arcsec	150 arcsec



LBL has developed a
water-cooled x-ray mirror



- For VUV branchline on
LBL/Exxon/SSRL Beamline VI
- For X1 Beamline at NSLS



SUMMARY

- Total power reflected by multilayers $\sim 10^4$ less than total reflection mirrors.
 - Absorbed power densities within manageable limits.
 - Flux through multilayers is good.
- \therefore Multilayers should be further investigated as power filters

DESIGN AND PERFORMANCE OF A DIRECTLY WATER-COOLED
SILICON CRYSTAL FOR USE IN HIGH-POWER SYNCHROTRON
RADIATION APPLICATIONS

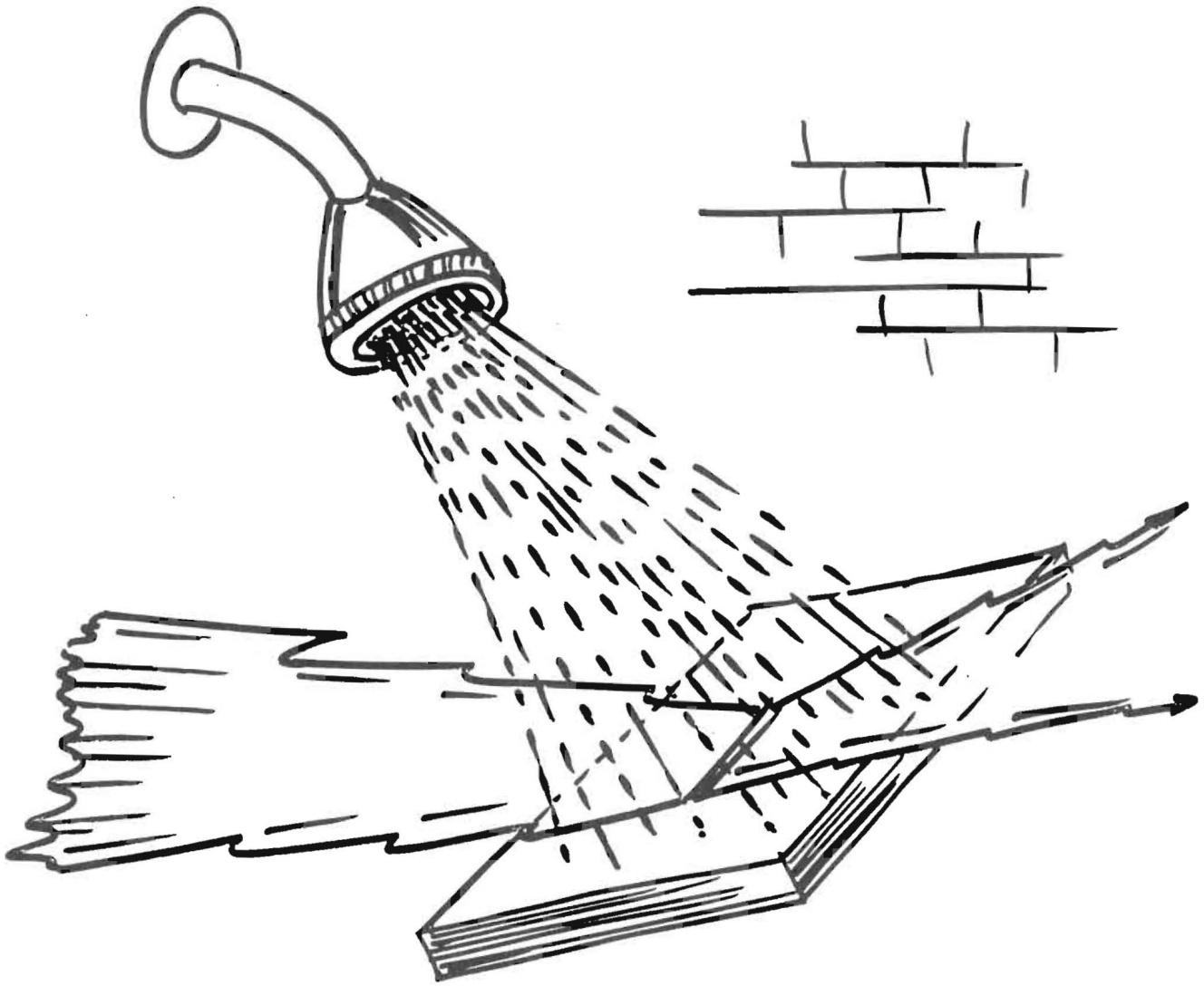
T. Oversluizen

National Synchrotron Light Source
Brookhaven National Laboratory
Upton, Ny 11973, USA

DESIGN AND PERFORMANCE OF A
DIRECTLY WATER-COOLED SILICON
CRYSTAL FOR USE IN HIGH-POWER
SYNCHROTRON RADIATION
APPLICATIONS

~

T. ISHIKAWA	}	PHOTON FACTORY.
T. MATSUSHITA		
A. MIKUNI		
T. OVERSLUIZEN	}	NSLS.
S. SHARMA		
P. STEFAN		



"CRYSTAL ~ COOLING"

WHAT'S THE PROBLEM?

- 1 Si CRYSTALS ARE USED EXTENSIVELY AT SR FACILITIES FOR MONOCHROMATORS
- 2 PRACTICALLY ALL BEAM POWER IS ABSORBED IN THE FIRST CRYSTAL
- 3 LOCAL HEATING RESULTS, BECAUSE OF THE SMALL AREA OF THE BEAM FOOTPRINT
- 4 RESULTING DISTORSION OF THE CRYSTAL COMPROMISES THE AVAILABLE BEAM PARAMETERS SUCH AS:
OUTPUT FLUX, BRIGHTNESS,
BANDWIDTH

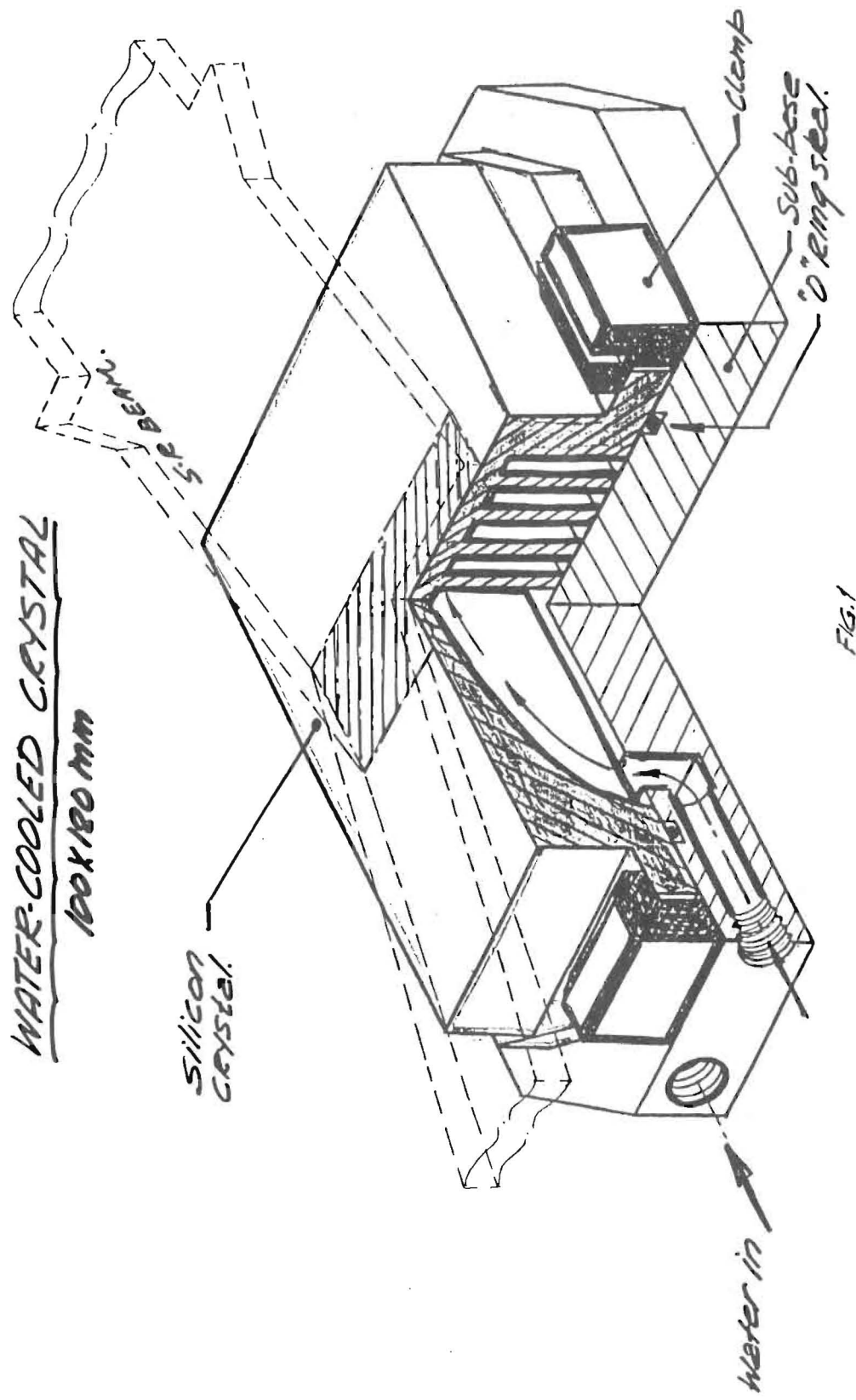
STATEMENT

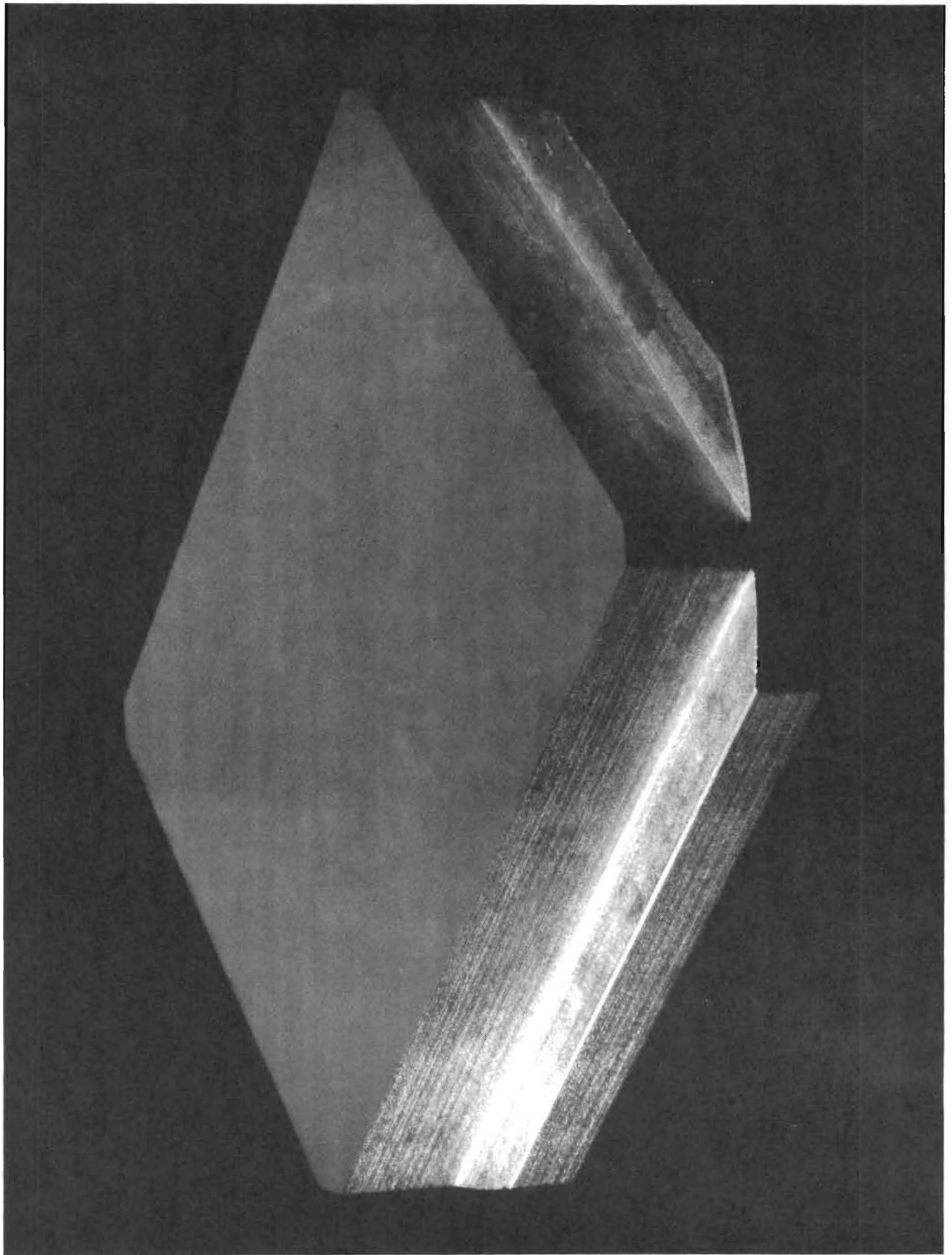
WITHOUT THE DEVELOPMENT OF NEW COOLING TECHNIQUES THE FULL POTENTIAL OF THIS GENERATION AND THE NEXT GENERATION OF INSERTION DEVICES WILL NOT BE REALISED!

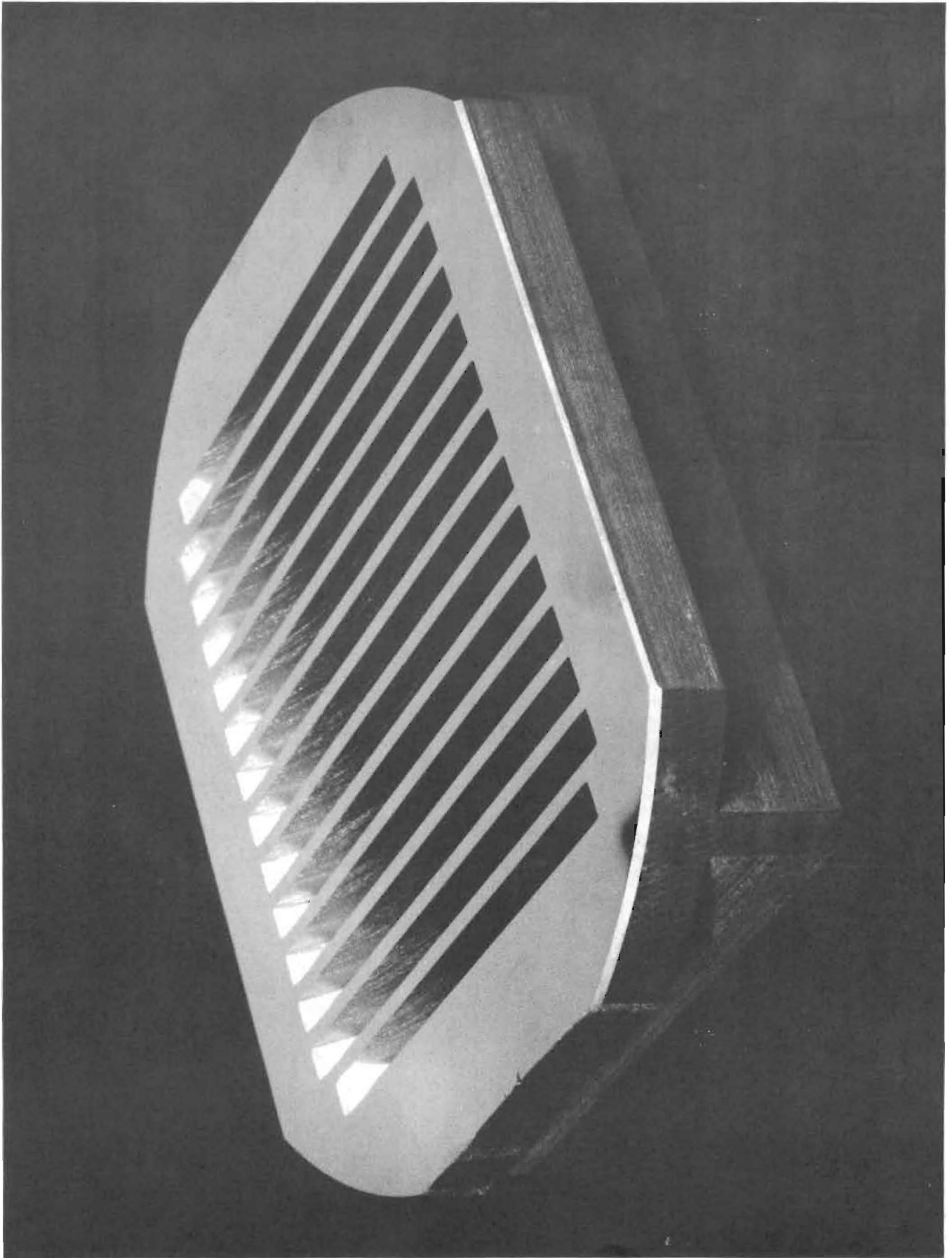
DEVICE	λ_0 (cm)	K_{max}	N	E (GeV)	I ring (mA)	d (m)	Pd_{Ave} (W/mm ²)
PF Multipole Wiggler	12.0	16.8	26	2.5	350	25.5	3.6
NSLS Hybrid Wiggler	12.0	12.3	15	2.5	250	16.0	2.8
CHESS Wiggler	34.0	49.5	3	5.4	70	14.5	5.9
SSRL 54 Pole Wiggler	7.0	10.7	27	3.0	100	22.8	3.1
PEP Undulator	7.7	1.59	26	15.0	30	56.0	12.3
ESRF Undulator	5.0	2.10	40	6.0	100	30.0	11.5
APS Undulator "A"	3.3	2.37	156	7.0	100	30.0	142

This case: measured total power 1.5 kW
 (BL16 PF) POWER DENSITY 0.7 W/mm²

2







TESTING THE SYSTEM.

WHAT TO MEASURE?

- A. ROCKING CURVES.
 - B. OUTPUT PHOTON FLUX PROPORTIONAL TO THE RING CURRENT.
 - C. UNIFORM OUTPUT BEAM (TOPOGRAPHY).
-

ALL MEASUREMENTS SHOULD BE DONE AT:

- 1. FULL BEAM POWER.
(SMALLEST GAP ON WIGGLER)
 - 2. SAME ANGLE OF INCIDENCE ON FIRST CRYSTAL.
($14^\circ \sim 8.3 \text{ keV}$)
-

EXPERIMENTAL SETUP

PHOTON FACTORY - BL16

WIGGLER → FILTERS → WINDOWS → MONO → HUTCH.
IR₁

WIGGLER: 53 POLE, 1.5 T, 19 mm GAP.

FILTERS: 6 ea, CARBON, 0.13 mm

WINDOWS: 2 ea, Be. 0.2 mm

MONOCHROMATOR: KOH2U MODEL KMA-15
0.1 ARC-SEC θ /ST.

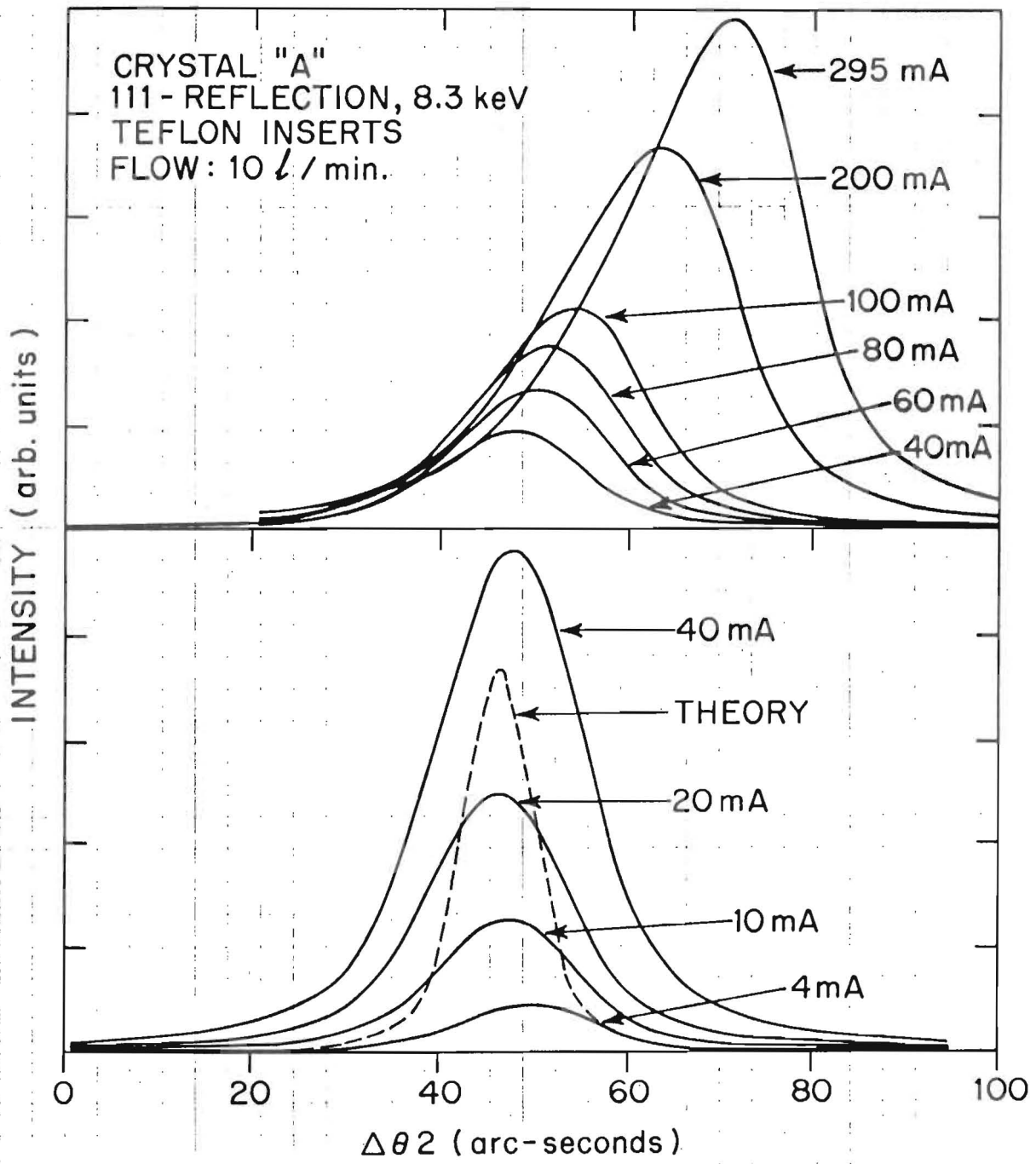
IR-TV CAMERA: - AVID

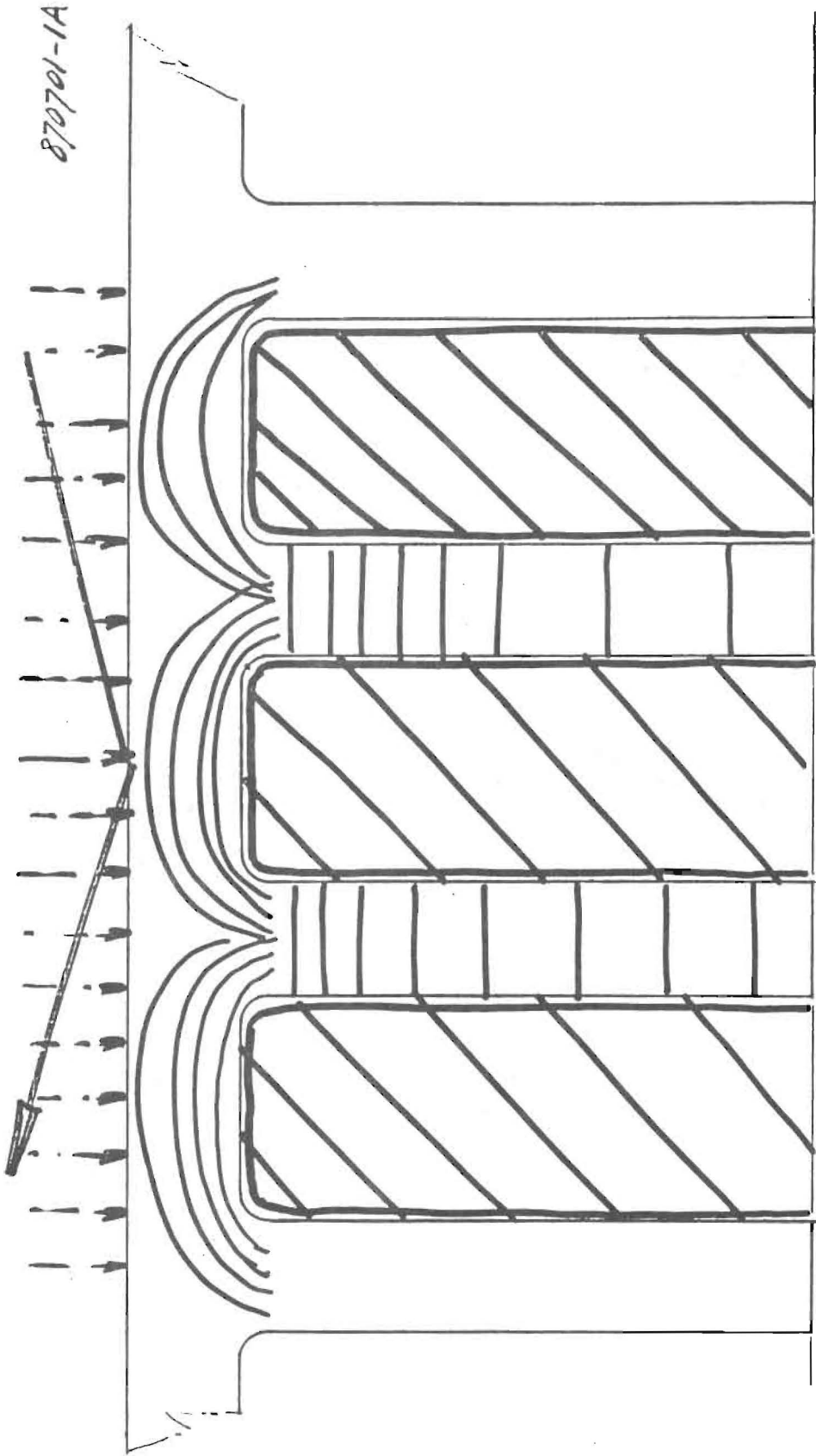
HUTCH: 10N CHAMBER(S)

WATER COOLING: 10-20 l/min CLOSED LOOP.



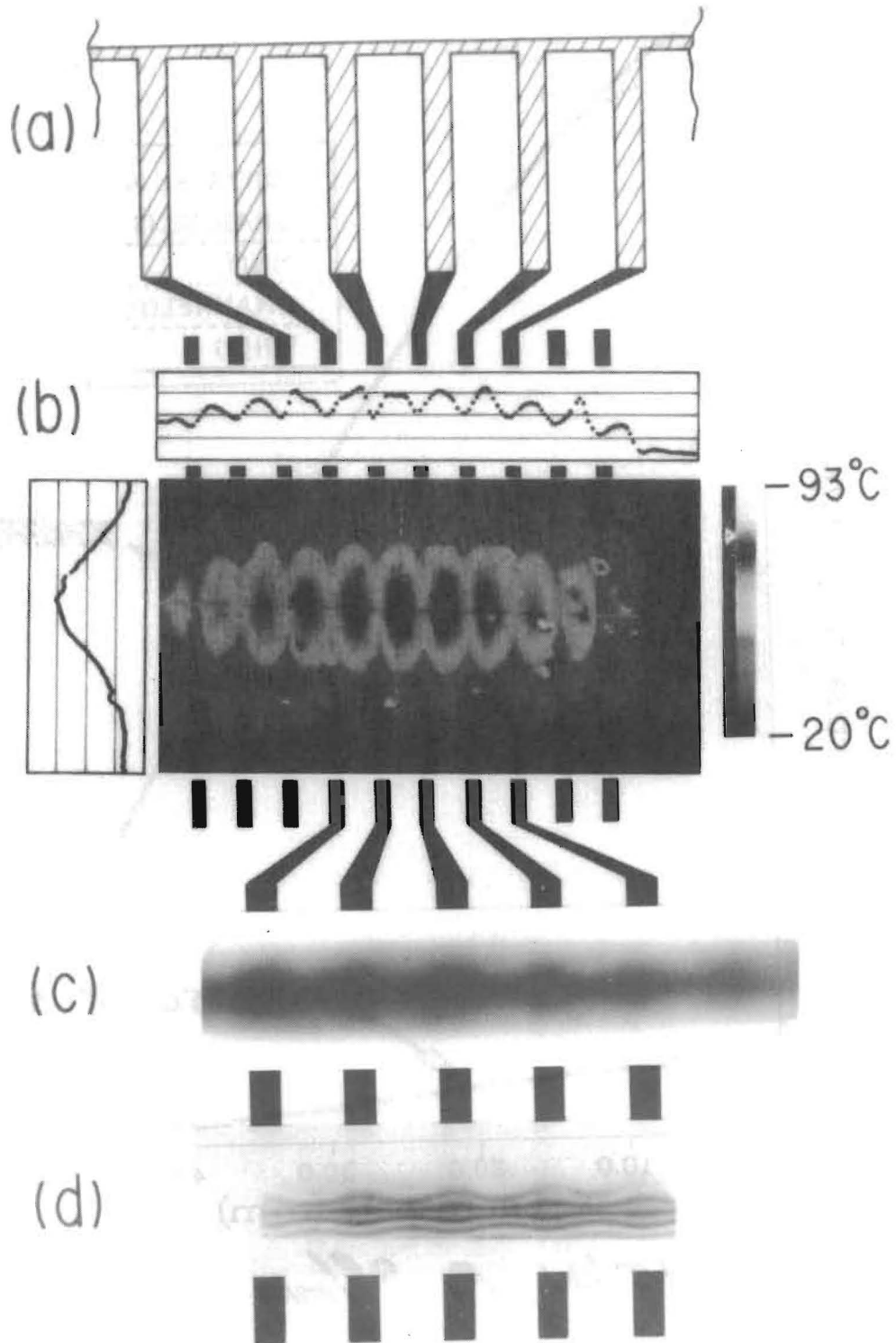
RESULTS →



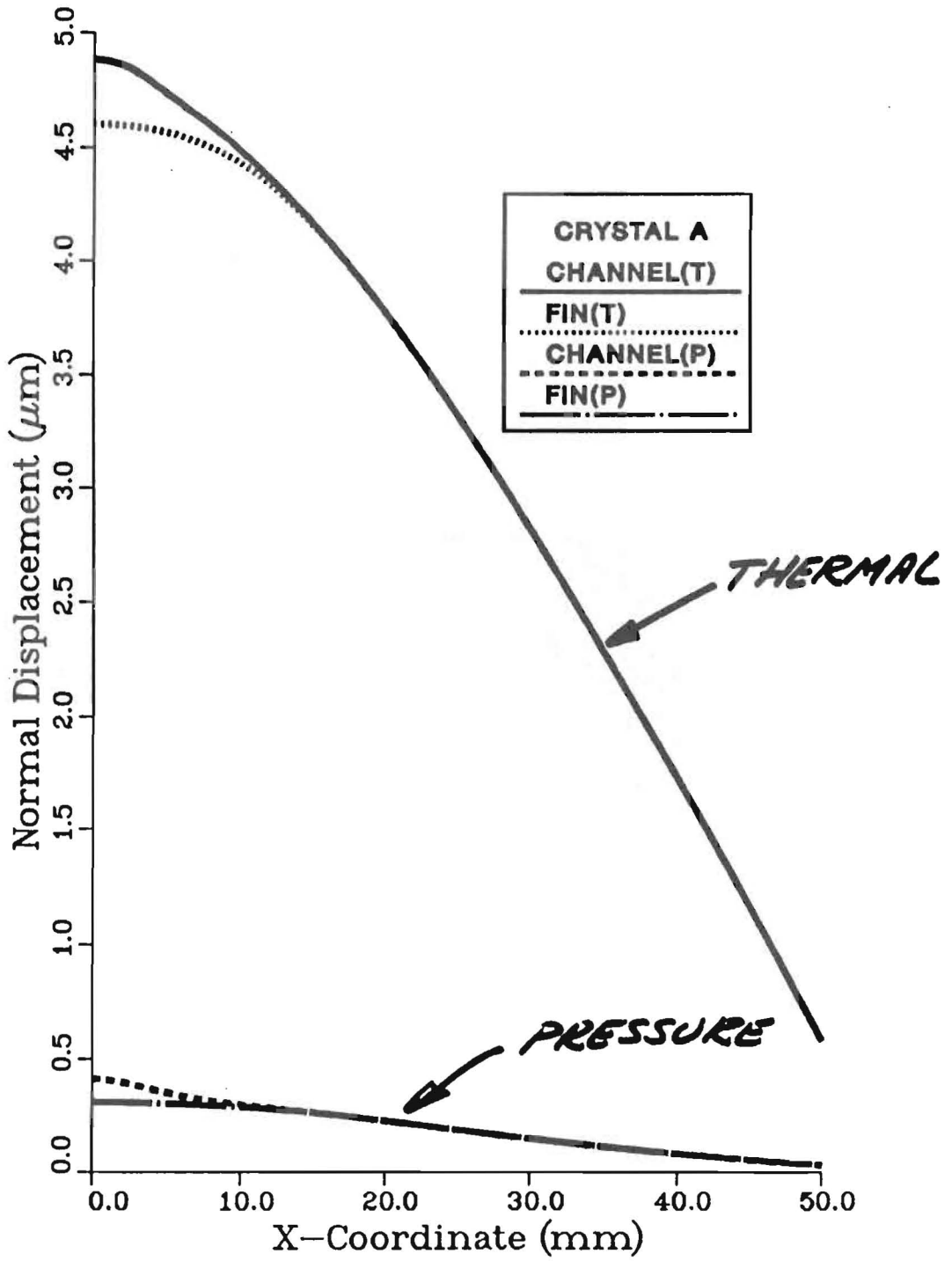


TYPICAL AXIAL SECTION

CRYSTAL "A"

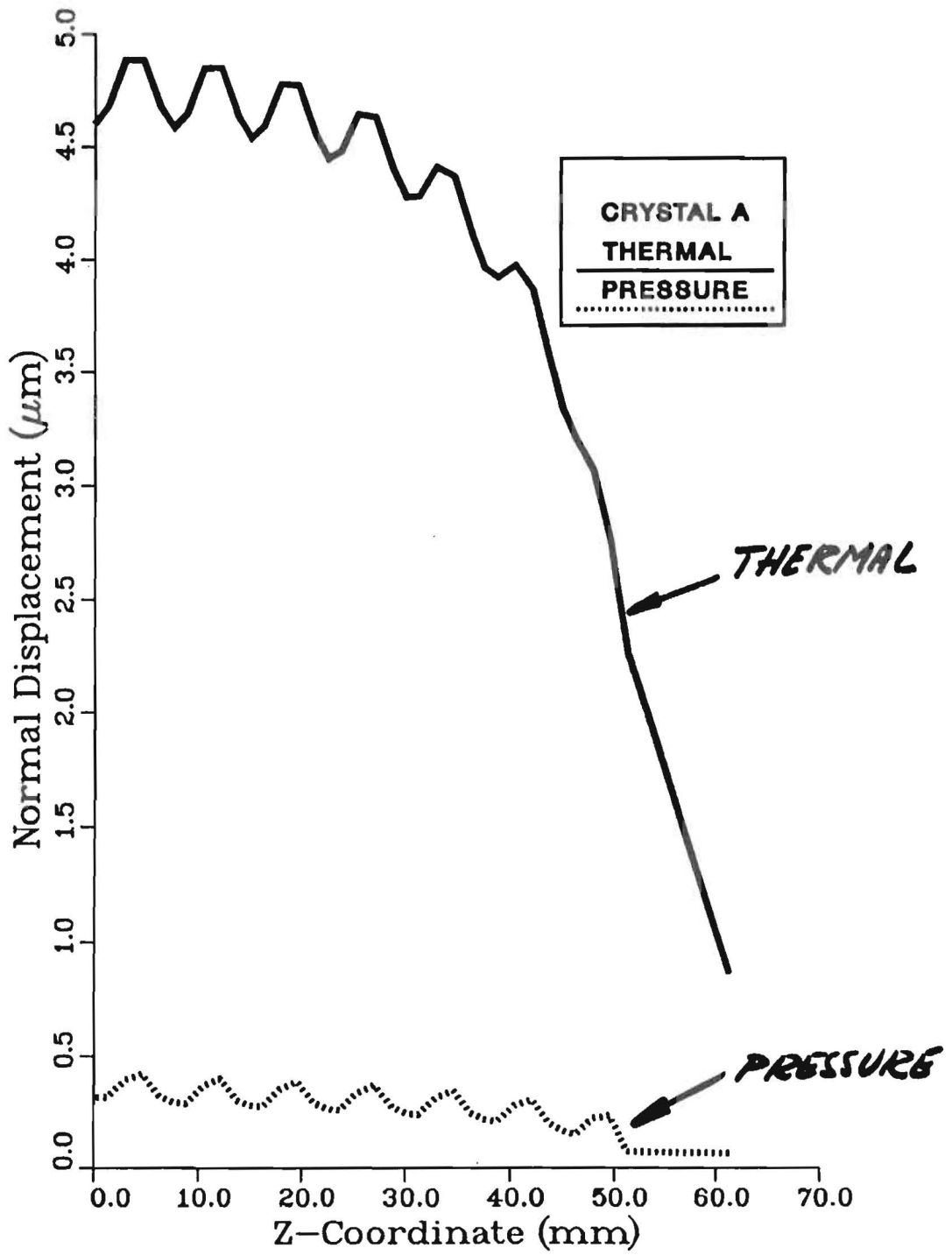


DEFORMATIONS – CRYSTAL A

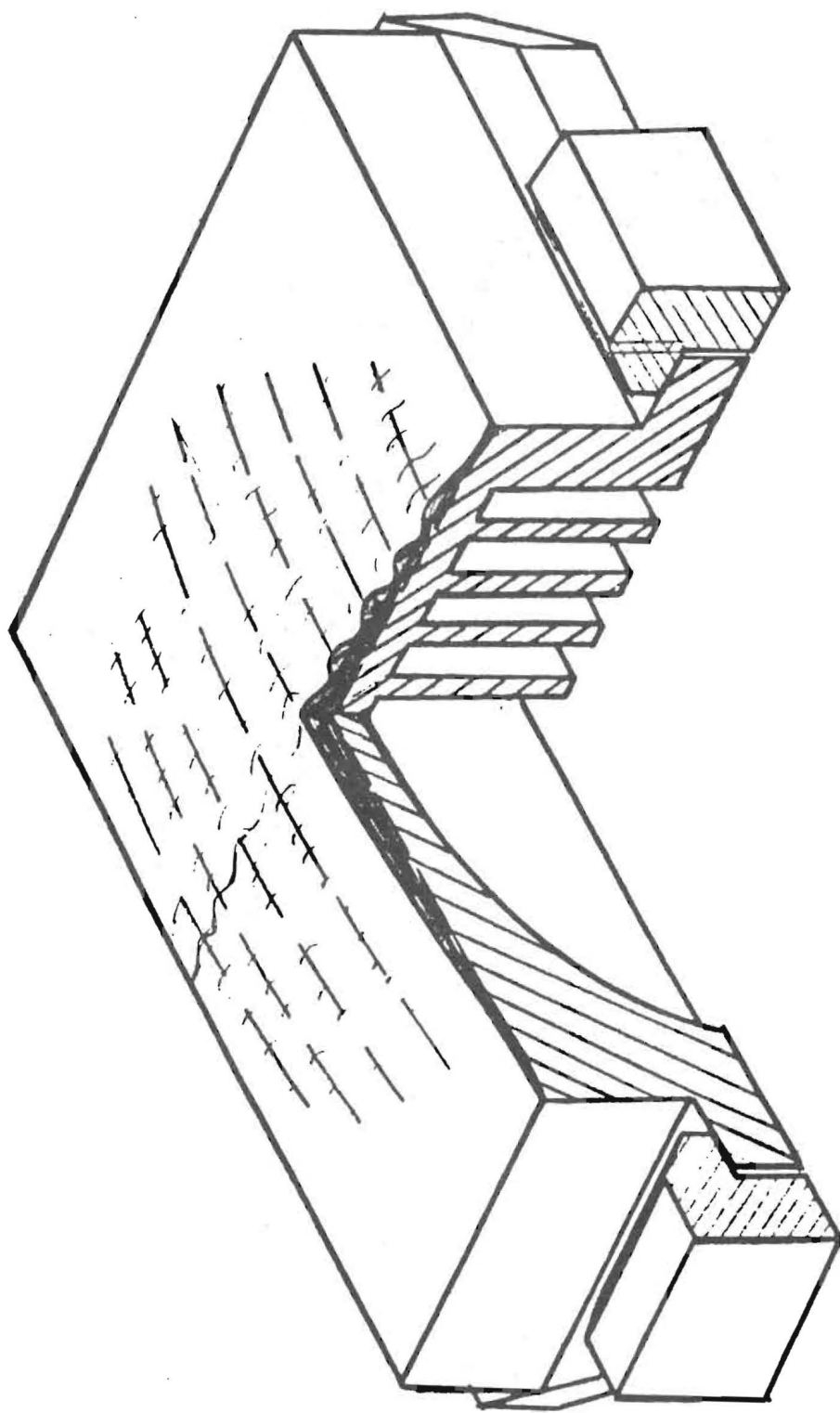


*t = 0.5 mm, P = 1.5 kW, F = 8°/min, p = 3.3 ATM.
 l = 30 mm*

DEFORMATIONS — CRYSTAL A

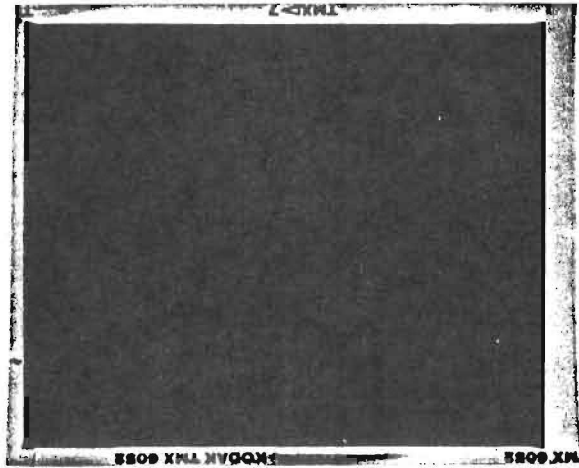
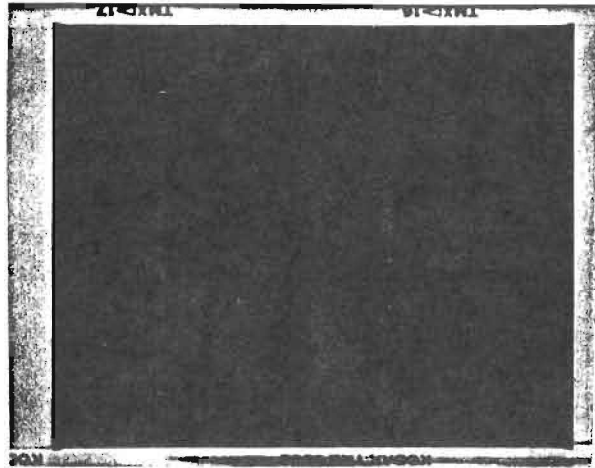


$t = 0.5 \text{ mm}$ $P = 1.5 \text{ kN}$ $F = 8 \text{ e/min}$ $p = 3.3 \text{ ATM}$ $e = 30 \text{ mm}$



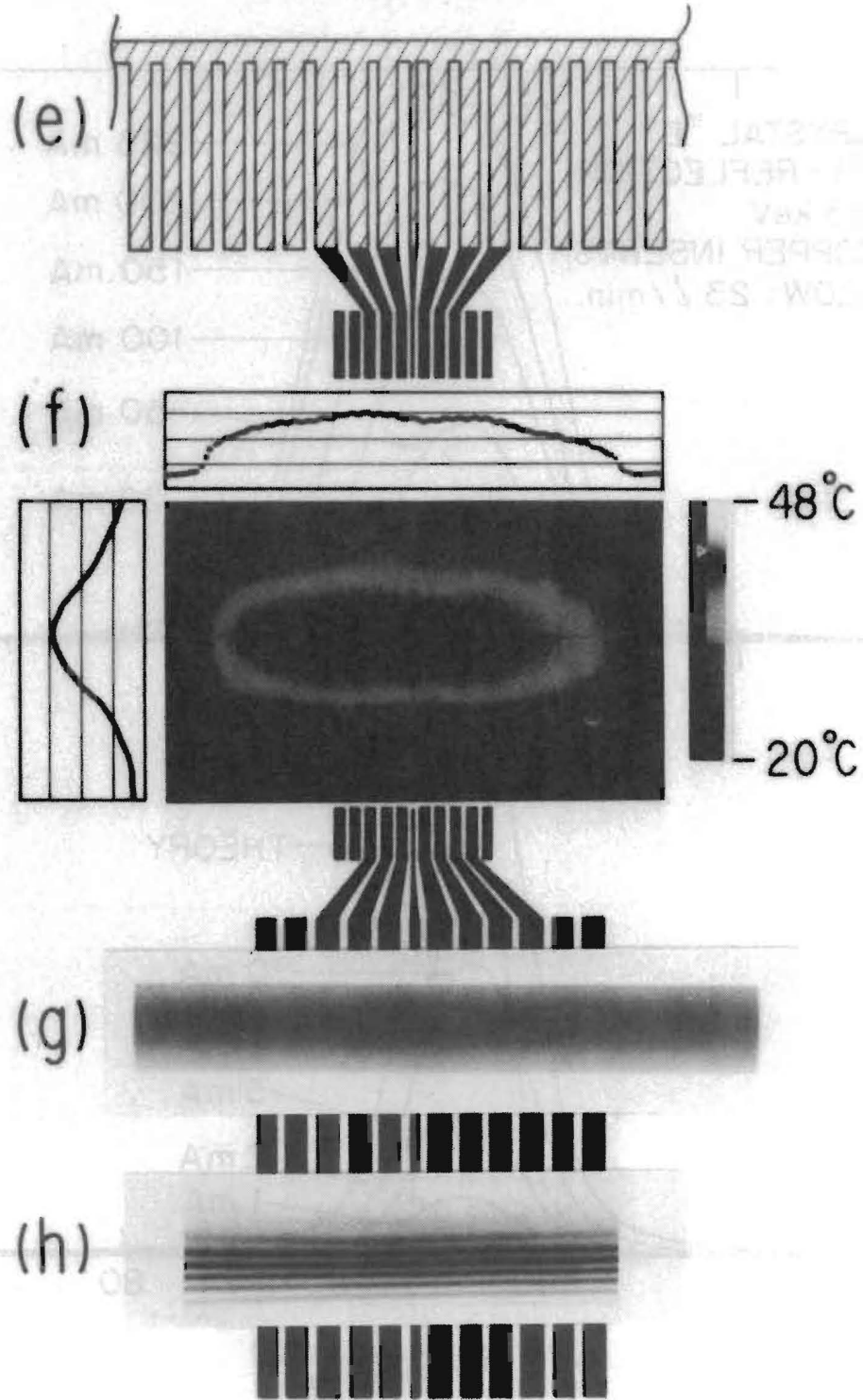
DEFORMED CRYSTAL SURFACE

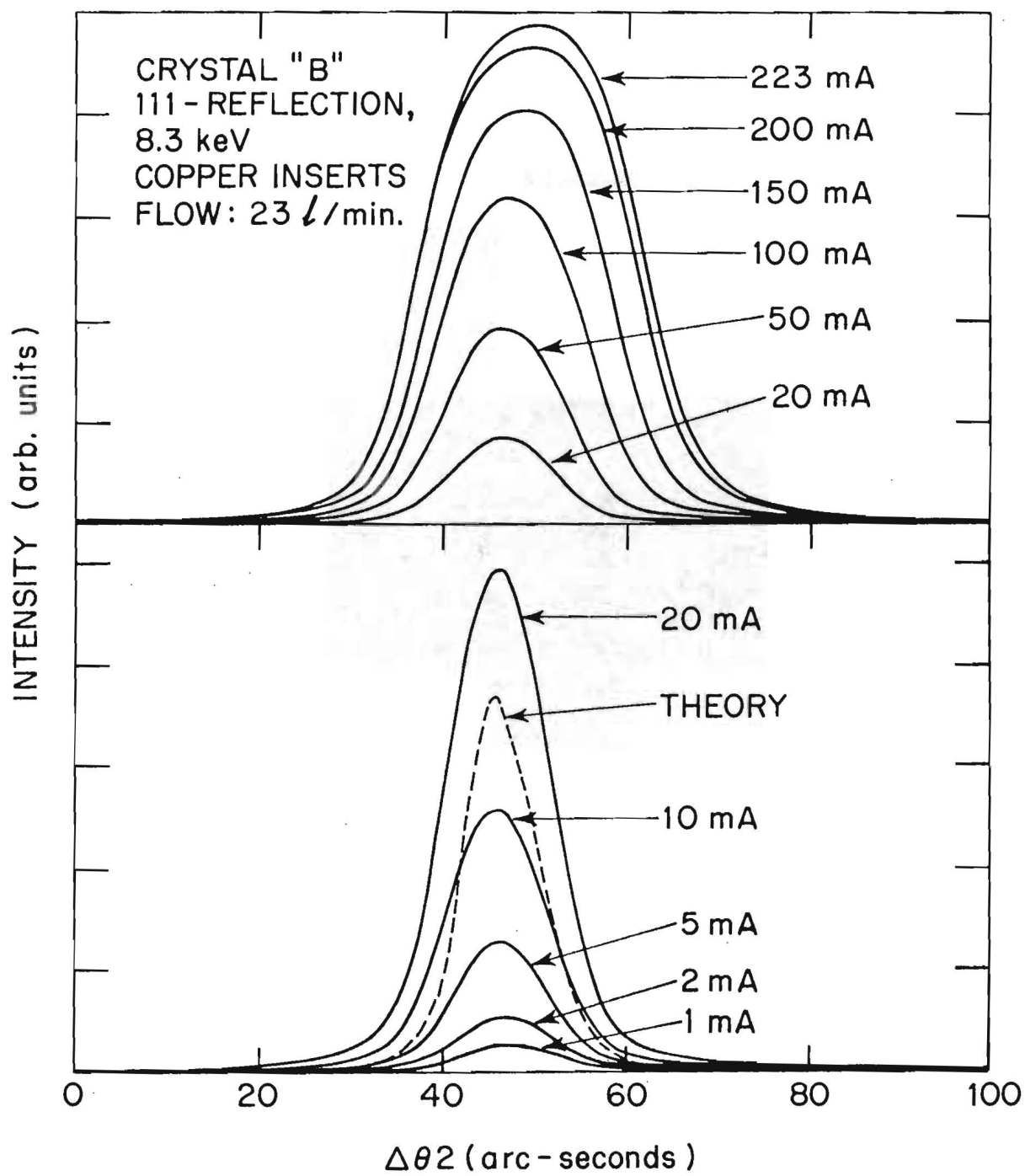
"KUSHI DANGO"

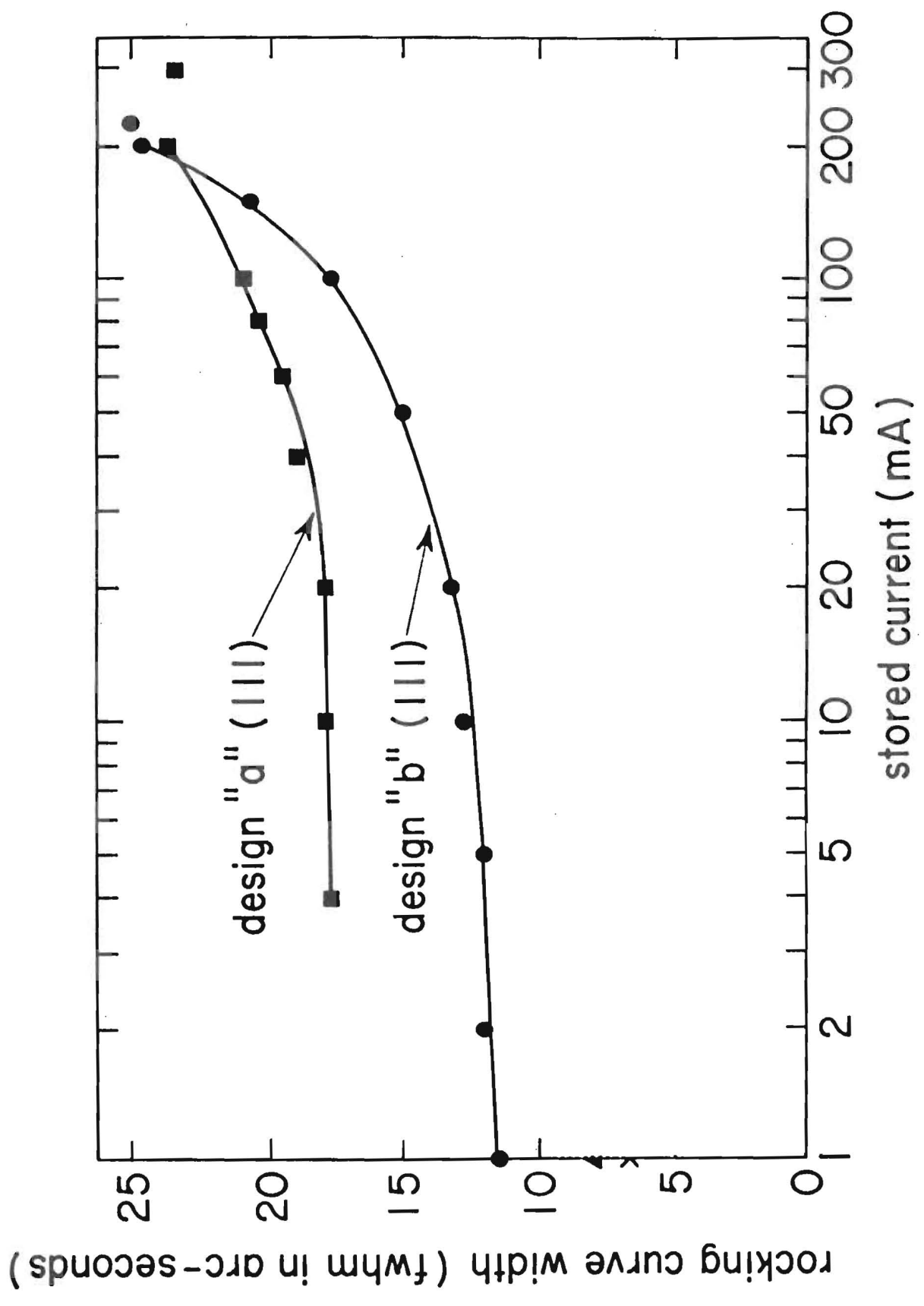


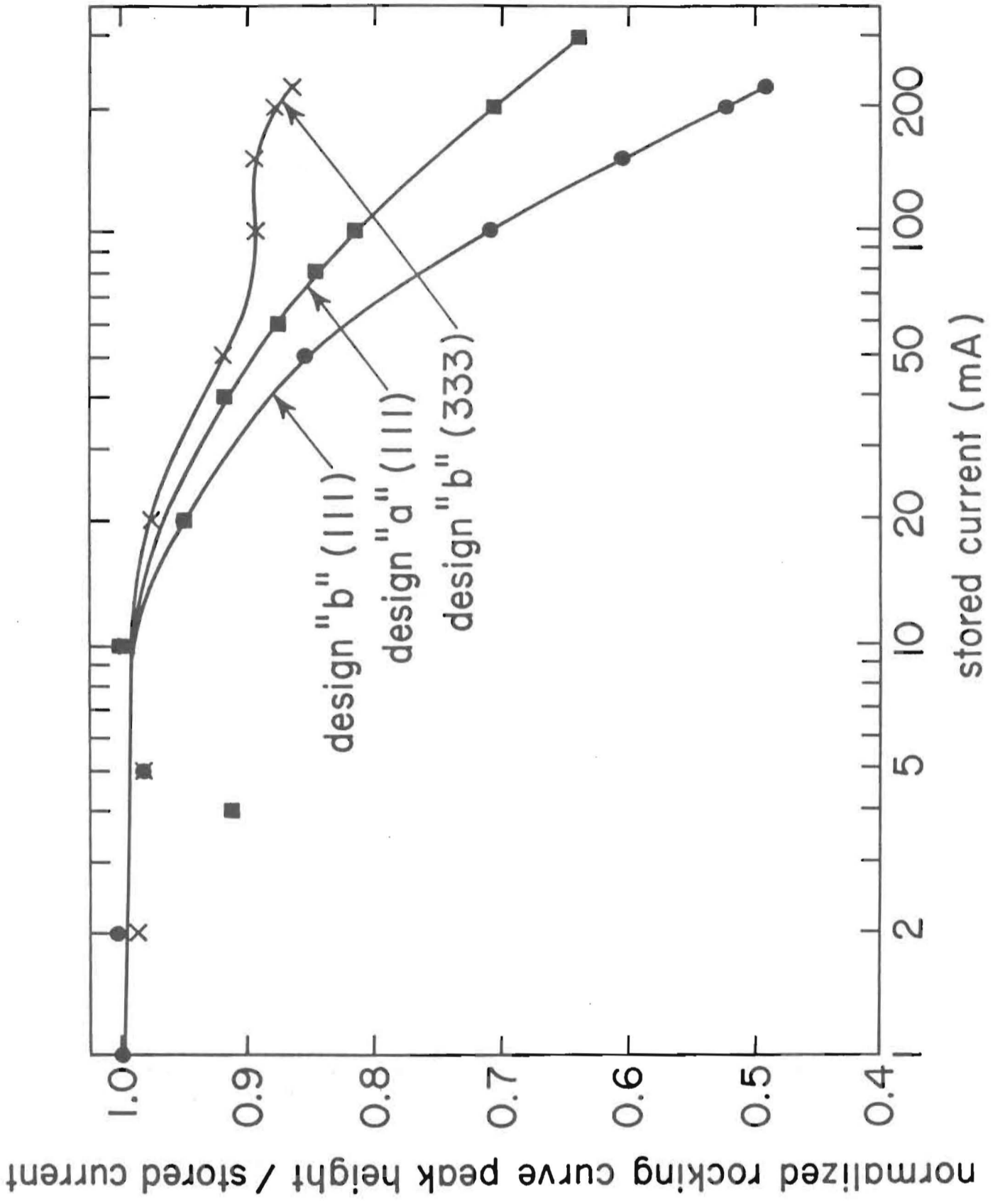
DESIGN	MINIMUM THICKNESS (mm)	FIN WIDTH (mm)	CHANNEL WIDTH (mm)	CHANNEL DIAMETER (mm)	NUMBER OF CHANNELS	OVERALL THICKNESS (mm)
"A"	1.0	2.5	5.0	101.6	14	30.0
"B"	1.5	0.8	0.8	100.0	30	21.7

CRYSTAL "B"









Invited paper, III-3, at the 3rd International Conference on Synchrotron Radiation Instrumentation, SRI-88, in Tsukuba, Japan, Aug. 29 - Sept. 2, 1988.

LIQUID GALLIUM COOLING OF SILICON CRYSTALS IN HIGH INTENSITY PHOTON BEAMS

11-11-88

R.K. Smither and G.A. Forster

Argonne National Laboratory, Argonne, IL 60439

D.H. Bilderback, M. Bedzyk, K. Finkelstein, C. Henderson, and J. White

Cornell University, Ithaca, NY 14853

L.E. Berman, P. Stephen, and T. Oversluizen

Brookhaven National Laboratory, Upton, NY 11973

Abstract

The high-brilliance, insertion-device-based, photon beams of the next generation of synchrotron sources (Argonne's APS and Grenoble's ESRF) will deliver large thermal loads (1 kW to 10 kW) to the first optical elements. Considering the problems that present synchrotron users are experiencing with beams from recently installed insertion devices, new and improved methods of cooling these first optical elements, particularly when they are diffraction crystals, are clearly needed. A series of finite element calculations were performed to test the efficiency of new cooling geometries and new cooling fluids. The best results were obtained with liquid Ga metal flowing in channels just below the surface of the crystal. Ga was selected because of its good thermal conductivity and thermal capacity, low melting point, high boiling point, low kinetic viscosity, and very low vapor pressure. Its very low vapor pressure, even at elevated temperatures, makes it especially attractive in UHV conditions. A series of experiments were conducted at CHESS in February of 1988 that compared liquid gallium cooled silicon diffraction crystals with water cooled crystals. The six pole wiggler beam was used to perform these tests on three different Si crystals, two new cooling geometries and the one presently in use. A special high pressure electromagnetic induction pump, recently developed at Argonne, was used to circulate the liquid gallium through the silicon crystals. In all experiments, the specially cooled crystal was used as the first crystal in a two crystal monochromator. An infrared camera was used to monitor the thermal profiles and correlated them with rocking curve measurements. A second set of cooling experiments were conducted in June of 1988 that used the intense, well collimated beam from the newly installed ANL/CHESS undulator. Tests were performed on two new Ga cooled Si crystals and compared with the standard CHESS water-cooled Si crystal. One of the crystals had cooling channels at two levels in the crystal that allowed one to actively control the the shape of the crystal surface. Both crystals showed major improvements over the standard water-cooled CHESS crystal.

INTRODUCTION

The high-brilliance, insertion-device-based, X-ray beams of the next generation of synchrotron sources, Argonne's Advanced Photon Source (APS), the European Synchrotron Radiation Facility (ESRF), and the Japanese Synchrotron Project will deliver large thermal loads to various components in the beam lines. The first optical element will often absorb the full heat of these intense X-ray beams which will range in power from 1 kW to 20 kW. The increased collimation of the next generation sources will increase the seriousness of these problems still further. Hence, improved methods of cooling the first optical elements, particularly when they are diffraction-crystals, are clearly needed.

Liquid metal cooling has worked well in other high heat load applications, particularly in high temperature reactors, and appeared to be a good solution in this case as well. After consulting the large bank of information on liquid metals available at ANL, liquid gallium was chosen as the most promising cooling fluid.¹ Liquid gallium has good thermal conductivity and thermal capacity, a low melting point, and a high boiling point. Its very low vapor pressure, even at elevated temperatures, makes it especially attractive in UHV conditions. This turned out to be a good choice because in the first tests of the use of liquid gallium as a cooling fluid for cooling diffraction crystals in a synchrotron beam, the new approach increased the usable flux from the first monochromator by factors of three to five and made it possible to use the full beam intensity for the first time.

PRESENT COOLING PROBLEMS

An example of the heat load problems encountered at operating synchrotron facilities is the two crystal monochromator used on the A2 beamline at CHESS. This monochromator intercepts one third of the beam (about 350 W for 70 mA storage ring current) from the six pole electromagnetic wiggler. The out put of this monochromator increased with increasing beam current until the current approaches 10 mA and then leveled off giving no further improvement as the beam was increased to 70 mA. A plot of the out put of the monochromator verses electron beam current is shown in figure 1. Thus a factor of seven in intensity was lost due to the distortion of the crystal by the heat load. When this problem was analyzed in detail it was found that the distortion of the first crystal spreads the diffracted beam in both angle and energy so that only some of the beam had the right incident angle and energy to be diffracted by the second crystal of the monochromator (see figure 2). The observed rocking curves, taken by rotating the second crystal in figure 2, are given in figure 3. The different curves are labeled with the corresponding current (electrons) in the storage ring. High temperatures and large distortions occur at small values of the ring current because of the long path that the heat must travel to exit the crystal.

SURFACE TEMPERATURES AND CRYSTAL DISTORTIONS

The temperature of the surface of the diffraction crystal (T_1) relative to the initial temperature of the cooling fluid (T_f) is given by equation (1)

$$T_1 = \Delta T_{12} + \Delta T_{23} + \Delta T_3 + T_f \quad (1)$$

where " ΔT_{12} " is the temperature difference across the crystal, " ΔT_{23} " is the temperature difference between the crystal surface adjacent to the cooling fluid, and the cooling fluid, and " ΔT_3 ", is the change in temperature of the cooling fluid relative to it's initial input temperature, " T_f ".

These temperature distributions generate three different kinds of distortions in the diffraction crystal. The first two are illustrated in figure 4. First, there is the over all bending or bowing of the crystal caused by the thermal gradients in the crystal, second, there is the thermal bump (shaded area) that is caused by the expansion of the crystal perpendicular to the surface and third, there is the change in the crystal lattice spacing through thermal expansion caused by the increase in the surface temperature of the crystal. These effects

vary over the surface of the crystal, following the variation in thermal loading of the surface. In the case of a crystal of uniform thickness, heated uniformly on the top surface and cooled uniformly on the bottom surface, the bowing of the surface is given by equations (2-4),

$$R = D / \alpha \Delta T_{12} = k / \alpha Q \quad (2)$$

$$\Delta T_{12} = T_1 - T_2 = Q D / k \quad (3)$$

$$\Delta \theta_b = \Delta x k / \alpha Q \quad (4)$$

where "D" is the thickness of the crystal, "R" is the radius of curvature of the crystal generated by "Q", the heat load per unit area, "α" is the thermal coefficient of expansion, "k" is the thermal conductivity, "ΔT₁₂" is the temperature difference between the top (T₁) and bottom surface (T₂) and "Δθ_b" is the change in angle or angular error that occurs as one moves a distance "Δx" along the surface of the bowed crystal. The value of "R" is independent of the thickness of the crystal "D" and depends only on the parameters, "k" and "α", of the crystal material and the heat flow, "Q", through the crystal. If "ΔT₁₂" is 50 °C and "D" is 1.5 cm and "α" is 3 x 10⁻⁶ per degree C (for silicon), then "R" = 100 m. This corresponds to heat flow through the crystal of Q = 50 watts per cm², from equation (2), where "k" = 1.5 watts per cm per °C (for silicon). In this example a distance of 1 cm along the face of the bowed crystal corresponds to a change in angle, and thus an angular error, of 20.4 arc sec.

If heat is added non-uniformly to the front face of the crystal, varying from zero to "Q" at the center of the beam, then the height (H) of the thermal bump is given to first order by equation (5).

$$H = \alpha \Delta T_{12} D / 2 \cong \alpha Q D^2 / 2k \quad (5)$$

where "Q" is now the heat load at the center of the thermal bump. Note that the value of "H" is proportional to "D²" and thus very sensitive to the thickness of the crystal. If the shape of the thermal bump is Gaussian with a FWHM of "2X", then the maximum slope and thus maximum angular error, "Δθ_{max}", is given by equation (6)

$$\Delta \theta_{\max} = 1.43 (H / 2X) = 1.43 (H / \text{FWHM}) \quad (6)$$

Using the above parameters and a "2X" = 2 cm, "Δθ_{max}" = 16.4 arc sec. This is similar to the angular error "Δθ_b" = 20.4 arcsec obtained by moving 1cm along the surface of the bowed crystal mentioned above. This thermal-bump angular error increases the incident angle of the photon beam on the upstream side of the thermal bump and decreases it on the down side of the bump,

giving a maximum spread of angular errors of 32.8 arc sec.

The third type of distortion produced by the photon beam is the change in the spacing between crystalline planes with the increase in the surface temperature of the crystal. For a given wavelength this change in spacing is equivalent to a change in the diffraction angle, " $\Delta\Theta_d$ ", given by equation (7),

$$\Delta\Theta_d = -\alpha \Delta T \tan\Theta \cong -\alpha \Delta T \Theta \quad (\text{small angle approx.}) \quad (7)$$

where " ΔT " is the variation in the temperature of the crystal surface. A 50 °C temperature rise will change the lattice spacing by " $\alpha \Delta T$ " = 1.5×10^{-4} and give an equivalent angular error of " $\Delta\Theta_d$ " = 3.0 arc sec for a 20 keV photon beam diffracted by (111) Si planes and " $\Delta\Theta_d$ " = 7.5 arc sec for an 8 keV photon beam. The d-spacing errors, " $\Delta\Theta_d$ ", are all in one direction so they cause an asymmetry in the overall angular error relative to the center of the photon beam. The " $\Delta\Theta_d$ " errors are 5 to 10 times less than the other two mentioned above and are comparable to the Darwin widths for these cases so they result in only a modest increase in the angular errors. These estimates of the relative importance of the different distortions are in agreement with the measurements of W. Edwards, et al.²

HEAT TRANSFER TO THE COOLING FLUID

The temperature difference, " ΔT_{13} ", between the surface of the crystal and the cooling fluid (see figure 4) is made up of two parts as shown in equation (8).

$$\Delta T_{13} = \Delta T_{12} + \Delta T_{23} \quad (8)$$

The first part, " ΔT_{12} ", is the same temperature difference that was discussed above and corresponds to the temperature difference across the crystal in figure 4. The second part, " ΔT_{23} ", is the temperature difference between the inner wall of the crystal (T_2) and the cooling fluid (T_3). This is given by equations (9,10)³

$$\Delta T_{23} = Q / h \quad (9)$$

$$h = A_1 k/d + A_2 (k^{0.6} C_v^{0.4} / d^{0.2} \nu^{0.8}) \nu^{0.8} \quad (10)$$

where " Q " is the heat load per unit area and " h " is the heat transfer coefficient at the solid-liquid interface. " h " consists of two parts, the first of which involves the thermal conductivity, " k ", divided by " d ", the effective hydraulic diameter, which reflects the size and shape of the cooling channels. The second term includes the ratio of " k " and " d " and in addition, " C_v " is the specific heat per unit volume, V is the velocity and ν is the kinetic viscosity of the cooling fluid. " A_1 " and " A_2 " are constants. The second term contains the

velocity of the cooling fluid and therefore, becomes the dominate term at high flow rates while the first term dominates at low flow rates.

FINITE ELEMENT ANALYSIS

A series of "finite element " calculations were made to determine the best cooling geometry for use with the first diffraction crystal of a two crystal monochromator¹. The first set of calculations obtained the distribution of temperatures through out the crystal when a heat load was applied. The second set, based on the first set, determined the resulting distortion of the crystal surface. The best results (least distortion) were obtained when the cooling fluid was circulated through channels just below the surface of a thick crystal. This reduced the effective value of "D", the distance between the diffraction surface of the crystal and the cooling fluid surface, to a minimum value and thus the angular errors generated by both the thermal bump and those from the change in crystal lattice spacing, to a minimum (see equations 5, 6 and 7). The angular errors from the bowing distortion are reduced by using a crystal that has considerable depth, "L", below the cooling channels. When the dimensions of the cooling channels are small compared to the thickness of the crystal and "L" is large compared to "D", the reduction in the bowing errors is roughly proportional to $(D / L)^2$.

The equations for the different distortions given in the previous section are only approximations for the more complicated crystal geometries with cooling channels in the crystal. The effective value of "D" is different for equation (2) than it is for equation (4). In equation (2) the effective value of "D" is less than the minimum distance between the surface and the cooling channel because of the fin cooling effect and in equation (4) the effective value of "D" is greater than because the thermal gradient extends down into the fin area between channels, increasing the depth over which the crystal expands. The finite element analysis is most useful for the calculations for these cases with complex geometries.

CHOICE OF GALLIUM AS THE COOLING FLUID

The finite element analysis was also used to compare different cooling fluids¹ and made it quite clear that liquid metals were more efficient cooling fluids than water under almost all conditions. Ga was the most attractive of the liquid metals for synchrotron applications¹. Table I compares the physical properties of liquid gallium with water.

These physical properties directly effect the value of "h" used to calculate " ΔT_{23} " in equations (9,10). The biggest difference between the two cooling fluids comes in the values for "k" their thermal conductivity. The high value of "k" for gallium makes both terms in equation (10) important while the very low value of "k" for water makes the first term very small and the second term small as well until the fluid velocity (V) becomes large. A plot of "h" verses flow rates for liquid gallium (upper curve) and water (lower curve) in 0.5 cm diameter channels, is given in figure 5. One can see immediately from this plot why gallium is the preferred cooling fluid. The value of "h" for gallium starts out much higher than that for water because of gallium's much larger thermal conductivity (k) and remains higher at all flow rates because the coefficient on the second term is also larger for gallium than for water.

ELECTROMAGNETIC INDUCTION PUMP

The liquid gallium is pumped through channels just below the surface of the silicon crystal with an electromagnetic induction pump developed at the Argonne National Laboratory for this purpose¹. The heart of the pump is a modified 5 hp, 3 - phase, induction motor, where the central rotor has been machined down to make room for the spiral stainless steel tube that fits into the widened gap between the now fixed rotor and the stator. The rotating magnetic field in the 3-phase motor induces a current to flow down one side of the coil and up the other side. The interaction of the moving magnetic field and the current generates a continuous, non-pulsating force on the liquid gallium that produces the pumping action. The pump develops a static head pressure of 45 psi and can pump 3 gpm through a typical cooling system with silicon crystal a mounted a few feet away from the pump. The essential features and the new developments in this pump are its high head pressure and its smooth, non-pulsating flow. Most liquid metal pumps are low pressure devices. The high pressure is needed to push the liquid gallium through the crystal cooling system at the high flow rates (1-3 gpm) needed to obtain optimum cooling of the crystals.

COOLING EXPERIMENTS WITH WIGGLER BEAMS

Water is used as the cooling fluid in most present day synchrotron facilities but as mentioned above, is not efficient enough to cool some of the more recently developed beams for newly installed wigglers and undulators and will encounter even more difficulties when trying to cool the insertion device beams at the next generation of synchrotrons (APS, ESRF, etc.)¹. This makes it very important to start investigating new cooling fluids and new cooling geometries.

A set of experiments were performed in February 1988, using the radiation from the six-pole wiggler at CHESS, the synchrotron facility at Cornell. A comparison was made between the performance of three silicon crystals as x-ray monochromators cooled with either liquid gallium or water. The two gallium cooled Si crystals had 5 mm dia. cooling channels drilled through them just below the diffraction surface (111). One measured 7.5 cm x 7.5 cm (diffraction area) by 1.5 cm thick and had five cooling channels whose center lines were 5 mm below the surface. The second channel-cooled crystal measured 10 cm long in the direction of the beam, 3.8 cm wide and 2.5 cm thick, with three 5mm dia. cooling channels with centers 5mm below the surface. The third crystal used in these tests was the Si crystal that is normally used in the CHESS monochromator on beamline A2. This crystal has the same dimensions as the crystal with three cooling channels describe above but was cooled on three sides with water cooled copper blocks thermally coupled to the crystal with an indium-gallium eutectic interface. Tests were also run on the three channel crystal with water cooling. The cross sections of these three crystals is shown in figure 6.

In all tests, the specially cooled crystal was used as the first crystal in a two crystal monochromator and received the full power (640 watts for 70 mA running at 5.4 GeV) of from the wiggler source. The wiggler is 14.0 m from the first crystal in the double crystal monochromator. The second crystal, located a few cm away, diffracts the beam a second time, returning it to the horizontal direction. The doubly diffracted beam is then analyzed in a hutch located 7.5 m farther down stream. An infrared camera was used to monitor the thermal profile of the photon beam on the crystals. This made it possible to measure the

height and shape of the thermal profile with different stored ring currents in the synchrotron and when carbon absorbers of different thickness were placed in the photon beam. Fig. 7 shows the thermal profile obtained with the three different crystals with 46 mA in the storage ring and compares the thermal profiles of one of the crystals when cooled with both gallium and water. The highest profile is that for the standard CHESS crystal with side cooling. The next three are for the 3-channel crystal. Water was used as the cooling fluid for the higher of the three and gallium for the next lower two. The lowest thermal profile is for the 5-channel crystal with gallium cooling. The improved cooling of this last case comes from a better cooling geometry. These measurements were correlated with rocking curve measurements at 8 and 20 keV, made by rotating the second crystal in the monochromator and with scanning slit measurements of the beam profile. At low photon beam intensities corresponding to low electron beam currents in the storage ring, almost all of the photons that are diffracted by the first crystal are also diffracted by the second crystal.

A comparison of the rocking curves obtained for the different crystals with different cooling fluids is shown in figure 8. The lower dashed curve corresponds to the Standard CHESS side-cooled crystal that was discussed in the section on "Present Cooling Problems". The use of water cooling near the surface in the 3-channel crystal reduced the distortion in the crystal by about 36 percent, with a corresponding increase in the peak intensity. This case is shown in figure 8 as the higher dashed curve. When Ga was used for the cooling fluid in this crystal, the rocking curve becomes narrower and higher (lower solid line). When the Ga flow rate in the crystal was increased to 1.33 gpm, the distortion was reduced by 30 percent. The best results were obtained with the Ga-cooled 5-channel crystal (upper solid curve) which increased the peak intensity by a factor of 3 to 5 (depending on the energy and cooling fluid flow rate) over that obtained with the side-cooled crystal. Figure 9 shows the rocking curve for the 5-channel crystal when different carbon absorbers are put into the photon beam. The observed intensity with the full beam (46 mA) is 5 percent less the predicted value, so the loss of intensity with the full beam is almost within our experimental error. This suggests that the intensity of the beam could be appreciable higher before major distortion occurs that would limit the intensity of the beam diffracted by the second crystal. The 5-channel crystal is known to have a small mosaic structure and this may account for some of its better diffraction efficiency and lower sensitivity to thermal loads. A detailed analysis of the thermal profiles observed for the 5-channel crystal and comparison with the calculated results suggests that the channels could be closer to the surface by a factor of 2.5 if the channels were made smaller. This would reduce the height of the thermal profile and the amount of distortion of the crystal surface by a similar factor of 2.5 for the bowing errors and a factor of 6.25 for the thermal bump errors. This would allow one to increase the intensity of the primary beam by a similar factor of 2.5 without serious losses in the final diffracted beam.

COOLING EXPERIMENTS WITH UNDULATOR BEAMS

A second set of experiments were performed at CHESS in June of 1988. They used the intense photon beams generated by the newly installed ANL/CHESS undulator.^{4,5} The experimental setup was the same as that used in the previous cooling experiments with a distance from the undulator to the first crystal of 18.5 m and the detector station located 7.5 m farther down stream. As before, an electromagnetic induction pump was used to circulate liquid gallium through channels in the first crystal. Two new silicon crystals with new cooling geometries were tested and compared to the performance of the standard CHESS

side-cooled crystal. The cross section and thermal foot print of the first crystal is shown in figure 10. It has a very thin top layer, 0.76 mm, cooled by slots 2.33 mm wide and supported by fins or ribs 0.80 mm wide. This upper structure was fabricated as a single piece and glued onto a 19.05 mm thick base crystal.⁶ It was designed to test the dependence of the crystal distortions on the thickness of the top layer. (see equations 4 and 6) The peak thermal load at the center of the photon beam was $29 \text{ W} / \text{mm}^2 / \text{mA}$ of beam in the storage ring. A plot of the peak temperature of the thermal bump versus flow rate of the liquid gallium for different synchrotron beam currents is given in figure 11. At first, the peak temperatures drop rapidly as the flow changes from laminar to turbulent and the distribution of the flow in the channels becomes more uniform. In this region equation (9) is not a good approximation for " ΔT_{23} ", the temperature difference at the solid-liquid interface. This is also the region where the thermal gradients extend down into the fin structure. This gives rise to an increase in the effective value of " D ", and thus an increase in both the bowing and the thermal bump. Part of the strong variation in peak temperature of the thermal profile will come from these effects. For flow rates of 0.6 gpm and above, the flow pattern stabilizes and equation (9) is a good approximation for " ΔT_{23} ". In this region the peak of the thermal profile shows an almost linear dependence on flow rate and agrees well with the " $v^{0.8}$ " dependence for the value of " h " given in equation (9), which leads to a similar dependence for the peak temperature of the thermal profile. All curves in figure 11 are decreasing with increasing flow rates so considerable improvement can be made by further increase in the flow rate. The peak temperature will approach a constant temperature given by equation 3, at high flow rates. This corresponds to the temperature difference across the top layer of the crystal, " ΔT_{12} ". This lower limit for the 70 mA curve is about 18°C and for the lowest curve at 30 mA is about 8°C . Doubling the flow rate to 3.2 gpm would reduce the maximum temperature for the 70 mA curve from 68°C to 43°C and for the 30 mA curve from 25°C to 16°C .

The second gallium cooled crystal tested was 7.7 cm wide, 7.7 long and 2 cm thick, with 2 sets of 5 cooling channels, 5mm in dia. The center line of the first set of channels were 5 mm below the surface giving a minimum distance to the surface of the crystal of 2.5 mm. The second set were 15 mm below the surface. The cross section and thermal foot print for this crystal are shown in figure 12. The energy of the diffracted beam is 8 keV and the incident angle about 13 degrees. The thermal profile is narrower than it was for the slotted crystal as would be expected because the lower energy beam strikes the crystal more perpendicular to the surface. The thicker top layer of the silicon crystal and the smaller thermal footprint will generate a larger " ΔT_{12} ". This will be reduced by some 10 to 20 percent by the more efficient fin-cooling of the much thicker rib structure but the " ΔT_{12} " will still be much larger for this crystal as compared to the slotted crystal. The larger " ΔT_{12} " will generate larger distortions of the crystal and thus wider rocking curves. Figure 13 compares the width of the rocking curves of the two gallium cooled crystals as a function beam current and gallium flow rate. The upper two curves are for the 10-hole dual level cooling-channel crystal. The upper curve is the case for 8 keV diffraction with a gallium flow of 0.62 gpm and the lower curve for 13 keV diffraction with 1.22 gpm flow. The lower slope of the second curve reflects both the larger thermal footprint and thus lower heat load per unit area of the more spread out beam of the 13 keV diffraction case and the more efficient cooling of the higher gallium flow rate. Higher flow rates will lower both of these

curves. The lower four curves are for the slotted crystal with the very thin top layer, with gallium flow rates that vary from 0.26 gpm to 1.62 gpm. Again, further improvement is possible with increased flow rates. The almost linear dependence of these curves on electron beam current makes it possible to extrapolate these curves to higher beam currents that will be available in the future. The curves for the 10-channel crystal start out higher than those for the slotted crystal. This is a result of the slightly mosaic structure of the virgin material from which the 10-channel crystal was fabricated.

Figure 14 is a plot of the count rate of the photon beam after it is diffracted by the second crystal in the two crystal monochromator as a function of the electron beam current in the synchrotron storage ring and gallium flow rate. If there were no distortion in the diffraction crystals these curves would be straight lines (see dashed curve). Again we see consider improvement with increased gallium flow and the better results for the slotted crystal with its much thinner top layer. It is interesting to note that at low flow rates, 0.26 gpm, the performance of the slotted crystal is very similar to the high flow case of the 10-hole crystal with its much thicker top layer. This is believed to be due to the poorer heat transfer in the slotted crystal at low flow rates that comes from the poorer flow pattern, less flow at the ends of the narrow slots. This poorer cooling of the fins, extends the thermal gradient down into the fin structure and increases the effective thickness of the top layer, "D". The height of the thermal bump is proportion to the square of the thickness of the top layer so modest penetrations of the thermal gradient into the fin structure will generate large changes in the height of this distortion. This is the same effect that one sees in dependence of the peak values for the thermal profile on flow rate in figure 12.

No matter how high the value of "h" is made through good cooling of the silicon crystal there will always be some bowing of the crystal and some height to the thermal bump unless an active way is found to correct the shape of the surface. The 10-channel crystal with its two levels of cooling channels is designed to accomplish this type of active control of the diffraction surface of the crystal⁷. By raising the temperature of the cooling fluid in the lower channels above that flowing in the upper channels, one can make the upper surface concave and actively compensate for the bowing and for the thermal bump. This effect is illustrated in figure 15. This effect was demonstrated with the 10-channel crystal during the ANL/CHESS undulator run⁷. Figure 16 compares the counting rate observed for the 10-channel crystal with and without a difference in temperature, " ΔT ", between the two sets of cooling channels as a function of storage ring current. The temperature difference must be adjusted at each value of the beam current to obtain the maximum counting rate. More details of this experiment are given in the poster session paper No. A111 of this conference⁷.

Although considerable progress has been made and much has been learned about the art of cooling silicon crystals with liquid metals, much more needs to be done before the next generation of synchrotrons comes on line. Further experiments need to be performed to see just how thin the top layer of the crystal can be made before the crystalline planes become distorted and to demonstrated how much improvement is possible with increased flow of the cooling fluid. Experiments with the two levels of cooling channels will also be most interesting. The latest version of this experiment uses film resistors on the back surface of the crystal to apply heat to the back of the crystal in place of the second level of cooling channels. This opens up the possibility of much greater control of the diffraction surface of the crystal than can be obtained with the two sets of cooling channels.

ACKNOWLEDGMENTS

The authors wish to thank J. Viccaro and D. Mills of ANL for many helpful discussions. This work was supported by the U.S. Department of Energy, BES-Materials Science, under contract no. W-31-109-ENG-38.

References:

- ¹ R. K. Smither, G.A. Forster, C.A. Kot, T.M. Kuzay, Nucl. Instr. & Meth., A266, 517(1988)
- ² W.R. Edwards, E.H. Hoyer and A.C. Thompson, SPIE, 582, 281(1985)
- ³ "Heat, Mass, and Momentum Transfer", Chapters 5-11, W. M. Rohsenow and H. Y. Choi, Prentice-Hall, Inc., Englewood Cliffs, NJ., 1961. "Heat Transfer", A.J. Chapman", Macmillan Publishing Co., New York, NY, Chapters 5-13, 1974.
- ⁴ B. Batterman, et al., "The performance of a Hard X-ray Undulator at CHESS", paper III-3, Proceedings of the 3rd International Conference on Synchrotron Radiation Instrumentation, edited by M. Ando, Rev. Sci. Instrum. __, __, (1989).
References cont.
- ⁵ D. Bilderback, C. Henderson, J. White, R. K. Smither and G.A. Forster, paper A088, "Undulator Heat Loading on X-ray Monochromators Cooled with Liquid Gallium", Proceedings of the 3rd International Conference on Synchrotron Radiation Instrumentation, edited by M. Ando, Rev. Sci. Instrum. __, __, (1989).
- ⁶ D. Bilderback, "Fabricating Rectangular Internal Cooling Channels in Silicon X-ray Monochromator Optics", paper A089, Proceedings of the 3rd International Conference on Synchrotron Radiation Instrumentation, edited by M. Ando, Rev. Sci. Instrum. __, __, (1989).
- ⁷ R. Smither, "Variable Focus Crystal Diffraction Lens", paper A111, Proceedings of the 3rd International Conference on Synchrotron Radiation Instrumentation, edited by M. Ando, Rev. Sci. Instrum., __, __ (1989).

Table I Comparison of fluid properties of Ga and H₂O. Figure of merit = $C_v \times v$.

	Gallium	H ₂ O
Density (g/cc) (40°C)	6.1	1.0
Melting Point (°C)	29.8	0.0
Boiling Point (°C)	2205.	100.
Vapor Pressure (mmHg) (100°C)	10 ⁻¹⁰	760.
Thermal Conductivity (W / cm, °C)	0.41	0.0068
Vol. Heat Capacity (Joules/cc, °C)	2.2	4.2
Viscosity (cp) (40°C)	1.6	1.0
Kinetic Viscosity (cp / g/cc)	0.27	4.2
Figure of Merit (Vol. Heat Cap. x Kin. Viscosity)	0.90	0.029

Figure Captions:

Figure 1. Plot of the count rate in the photon beam diffracted by the second crystal in the two crystal monochromator when one uses the standard CHESS side-cooled crystal with the full beam of the 6-pole wiggler versus the electron beam current in the storage ring.

Figure 2. Schematic drawing of the 2-crystal monochromator showing the effects of the photon beam heating of the first crystal.

Figure 3. A comparison of the rocking curves for the second crystal in the 2-crystal monochromator when the first crystal in the monochromator is the standard CHESS side-cooled crystal, for different electron beam currents in the storage ring.

Figure 4. Schematic drawing of the different thermal distortions of a diffraction crystal subject to high heat loads from synchrotron beams.

Figure 5. Plot of "h", the transfer coefficient, for liquid Ga (upper curve) and for water (lower curve) as a function of cooling fluid flow rate in a 0.5 dia. channel.

Figure 6. Drawings of the cross sections of the three cooled silicon crystals used in the wiggler experiments.

Figure captions cont.

Figure 7. Plot of the surface temperature profile in the direction of the beam for the three different cooled silicon crystals used in the wiggler experiments.

Figure 8. Plot of the rocking curves obtained with the three different silicon crystals in the wiggler experiments (photon energy of 20 keV, electron current of 46mA).

Figure 9. Plots of rocking curves for the 5 channel crystal for different thicknesses of the stepped carbon filter in the photon beam.

Figure 10. The thermal profile of the undulator beam superimposed on the cross section of the the slotted silicon crystal with the thin top layer. The side view and front view are crossed by lines at heights that correspond to the thermal isomers shown in the top view.

Figure 11. Plot of the peak temperature of the thermal profile as a function of the rate of flow of the cooling fluid for the slotted crystal.

Figure 12. The thermal profile of the undulator beam superimposed on the cross section of the the 10-channel crystal. The side view and front view are crossed by lines at heights that correspond to the thermal isomers shown in the top view.

Figure 13. Plot of the FWHM of the rocking curves of the 10-channel crystal (circles) and the slotted crystal (triangles) for different diffraction energies and flow rates for the cooling fluid (Ga), as a function of the electron beam current in the storage ring.

Figure 14. Plot of the counting rate in the photon beam from the monochromator verses the electron beam current, for the slotted crystal (triangles), the 10-channel crystal (circles) and the standard CHESS side-cooled crystal (squares), withr different flow rates for the cooling fluid.

Figure 15. Schematic drawing of the10-channel crystal with two different temperatures of cooling fluids flowing in the two different sets of cooling channels, with $T_2 > T_1$. This generates a concave surface on the top of the crystal.

Figure 16. A comparison of the count rate in the photon beam from monochromator verses electron beam current, for the 10-channel crystal with and without i a temperature difference (ΔT) between the upper and lower cooling channels.

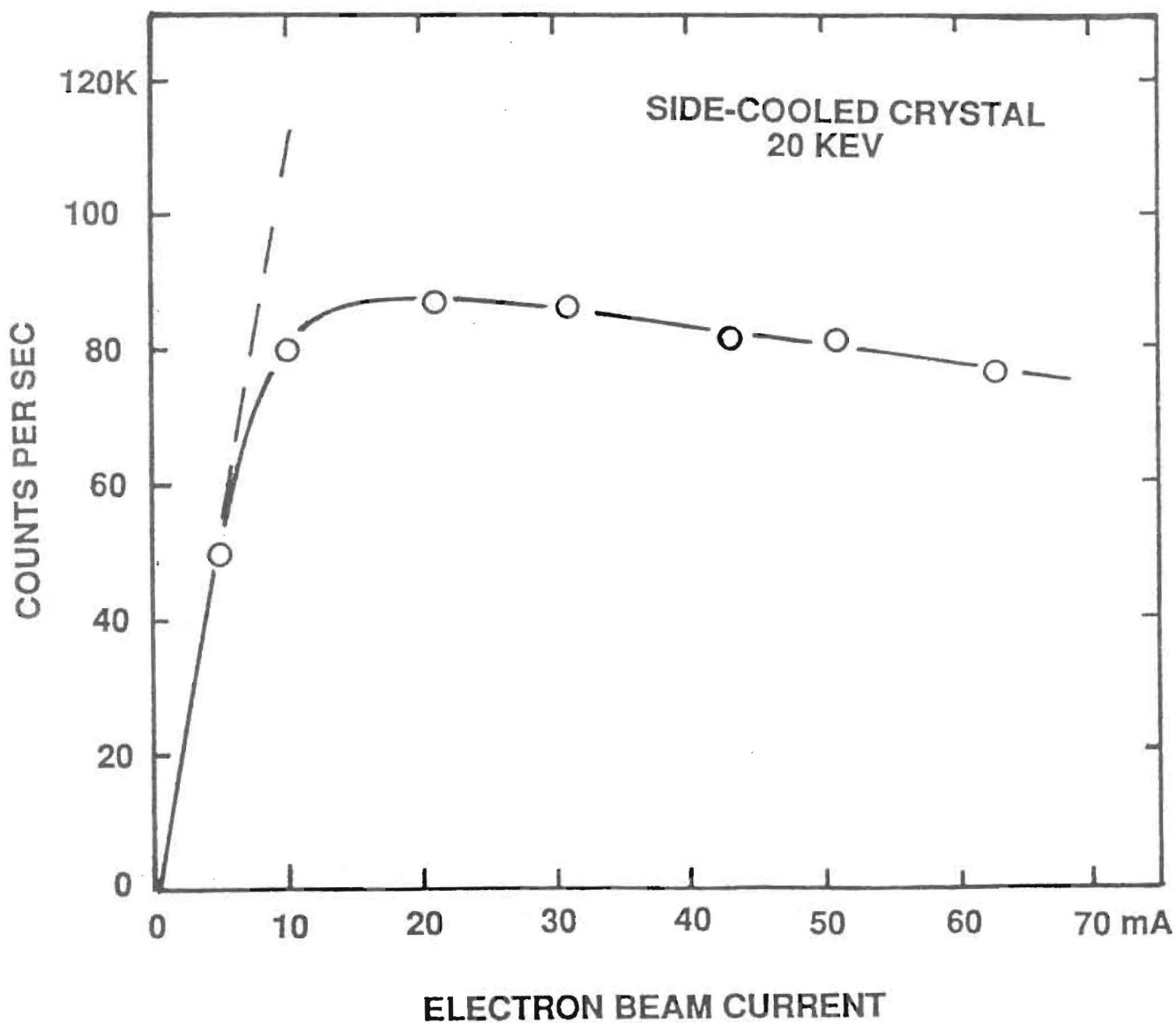


Figure 1. Plot of the count rate in the photon beam diffracted by the second crystal in the two crystal monochromator when one uses the standard CHESS side-cooled crystal with the full beam of the 6-pole wiggler versus the electron beam current in the storage ring.

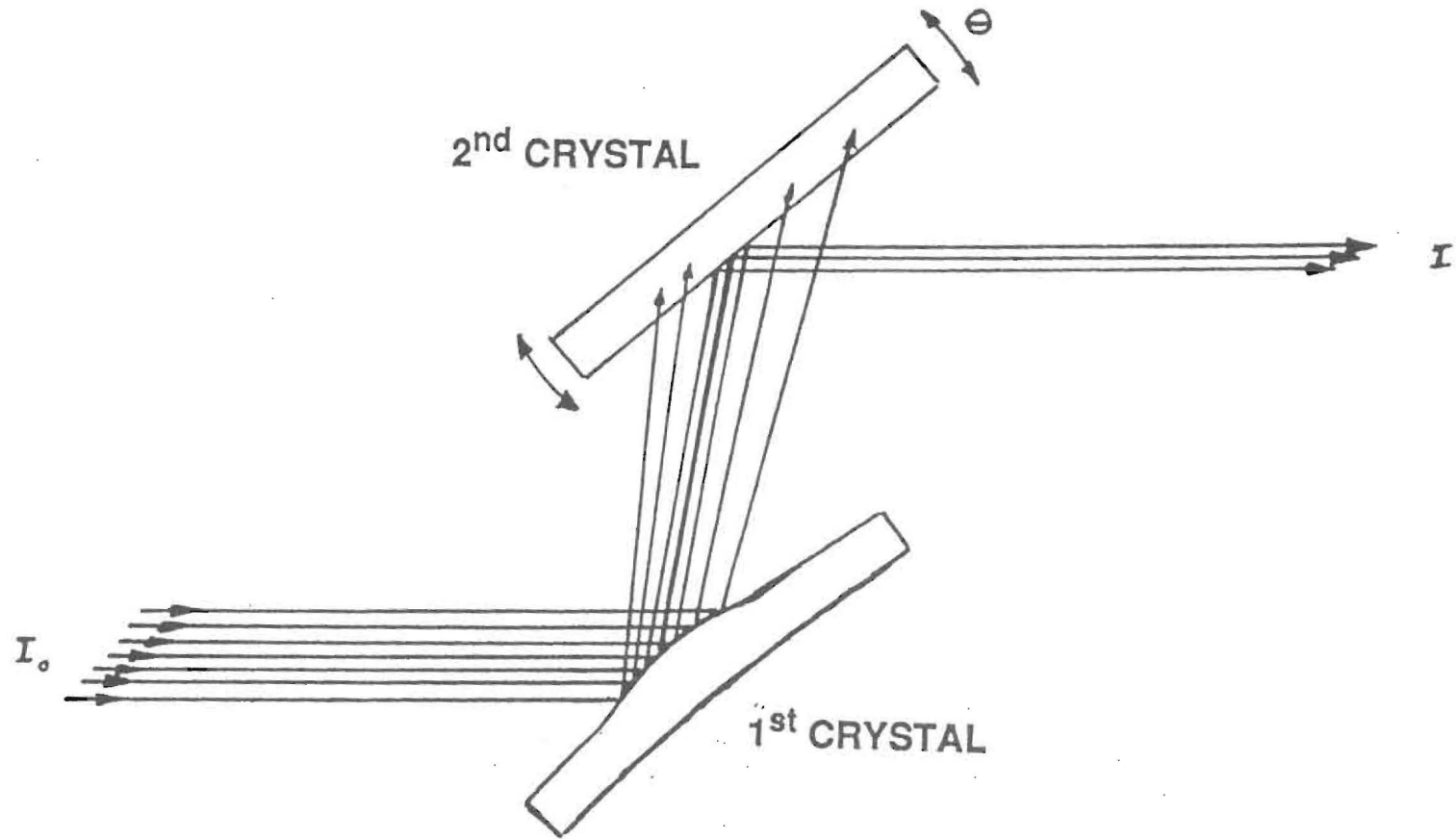


Fig 2

Figure 2. Schematic drawing of the 2-crystal monochromator showing the effects of the photon beam heating of the first crystal.

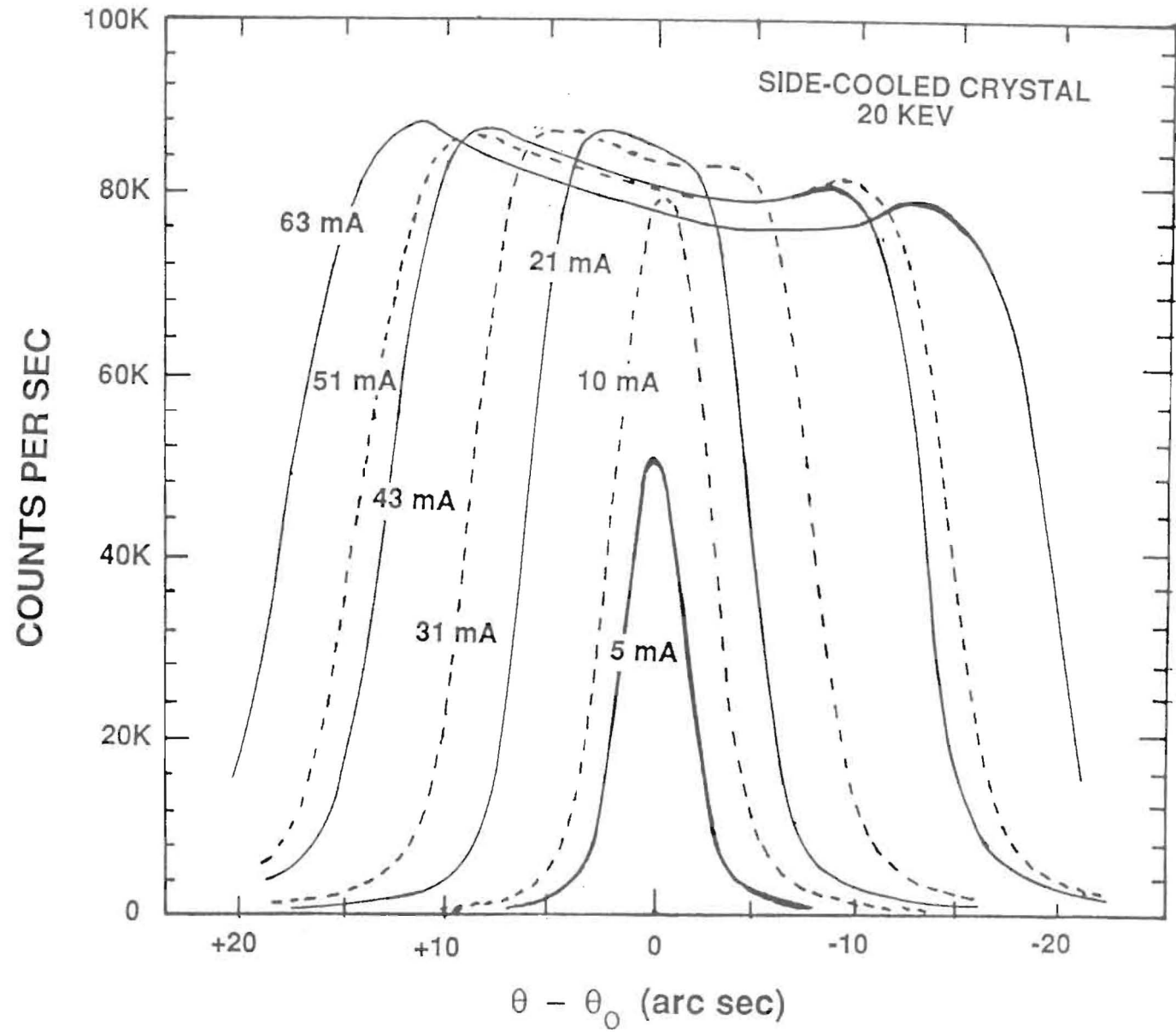


Figure 3. A comparison of the rocking curves for the second crystal in the 2-crystal monochromator when the first crystal in the monochromator is the standard CHSS side-cooled crystal, for different electron beam currents in the storage ring.

193

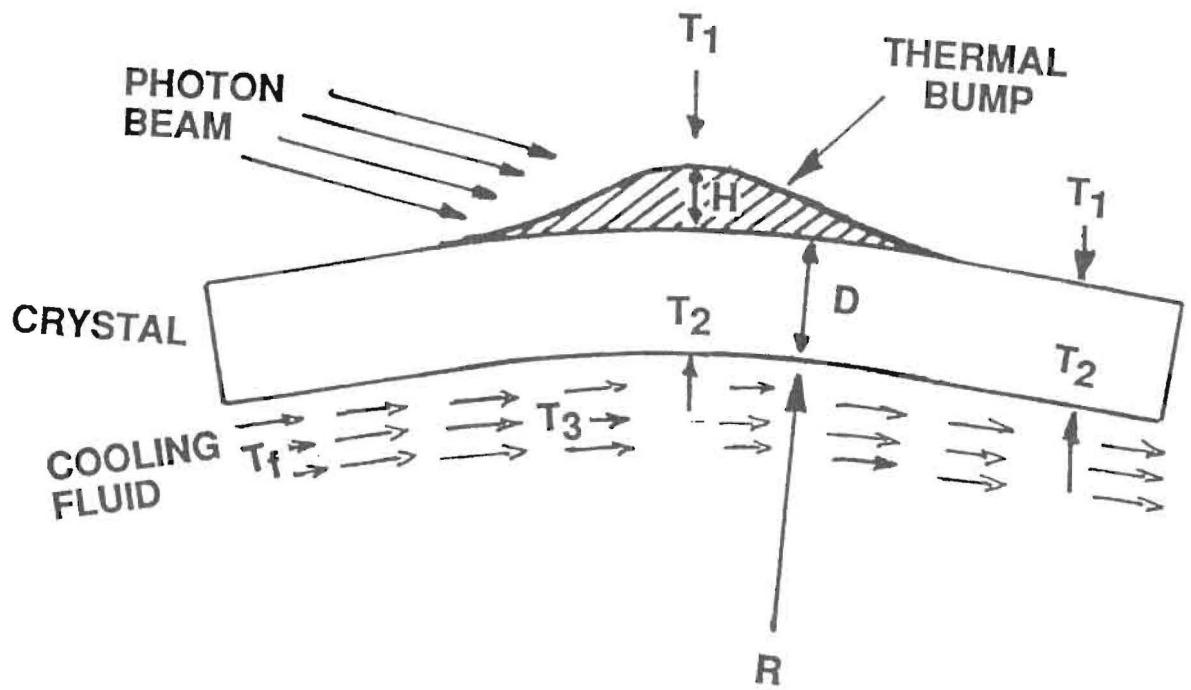


Figure 4. Schematic drawing of the different thermal distortions of a diffraction crystal subject to high heat loads from synchrotron beams.

Fig 4

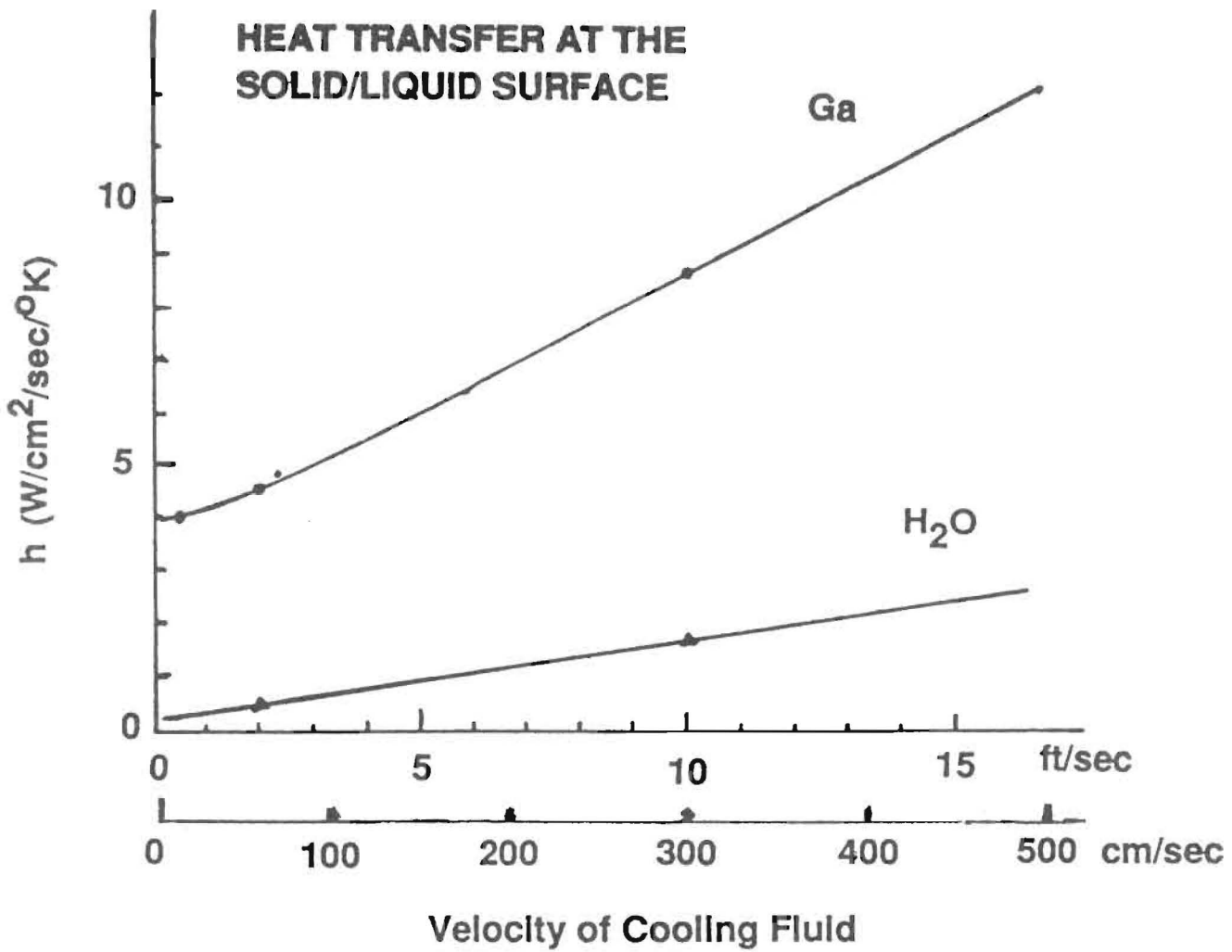


Figure 5. Plot of "h", the transfer coefficient, for liquid Ga (upper curve) and for water (lower curve) as a function of cooling fluid flow rate in a 0.5 dia. channel.

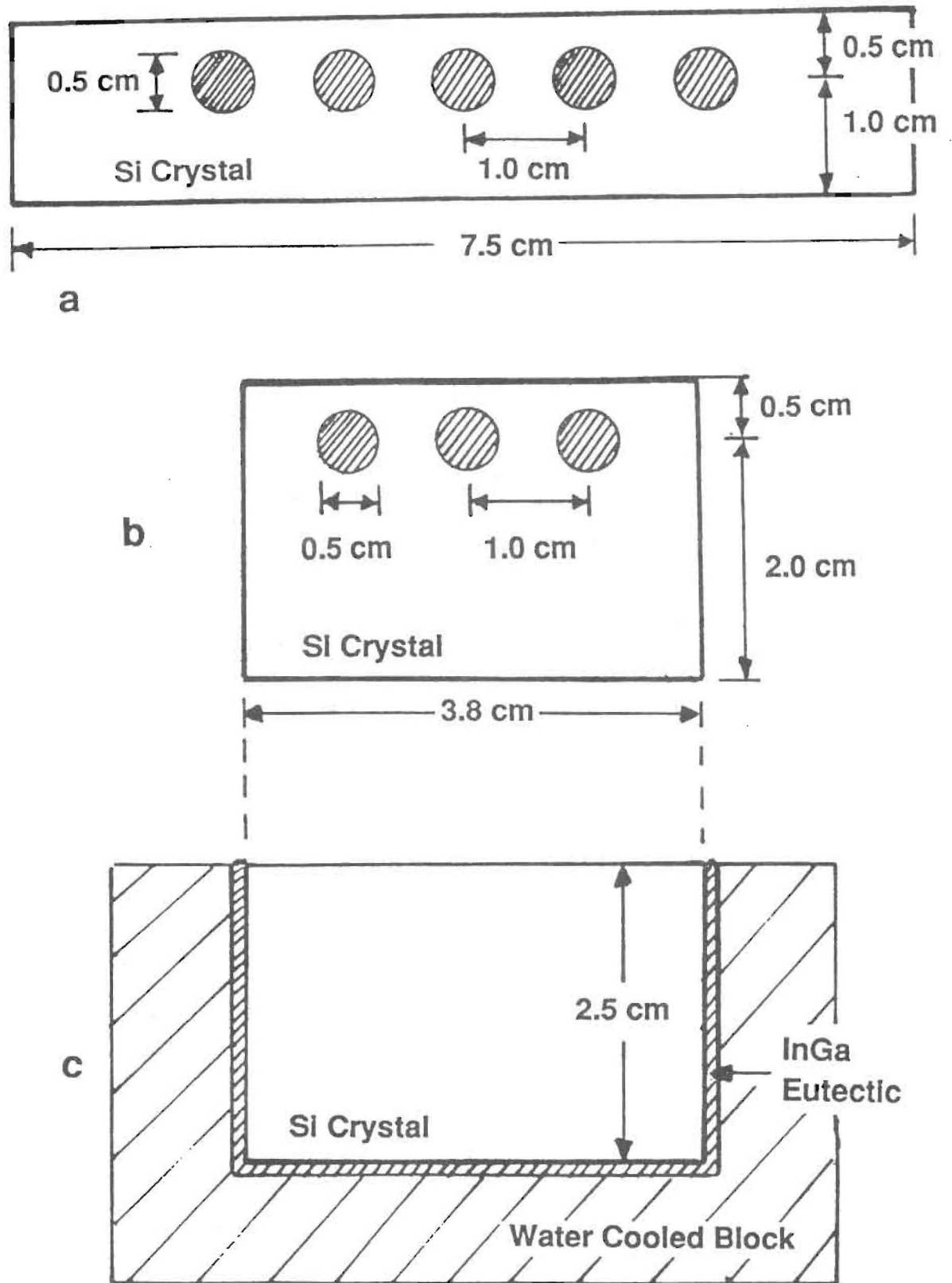


Figure 6. Drawings of the cross sections of the three cooled silicon crystals used in the wiggler experiments.

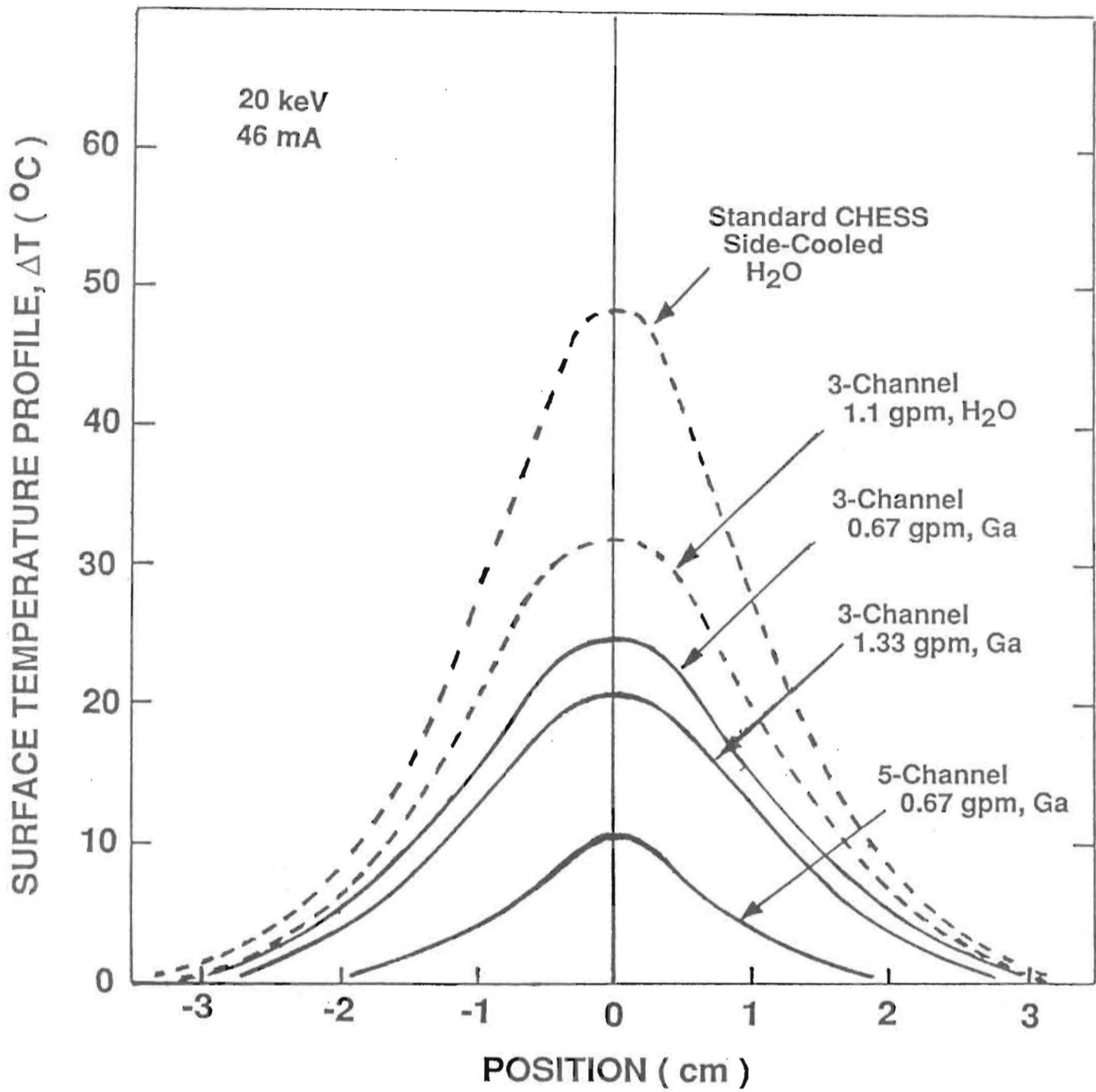


Figure 7. Plot of the surface temperature profile in the direction of the beam for the three different cooled silicon crystals used in the wiggler experiments.

Fig 7

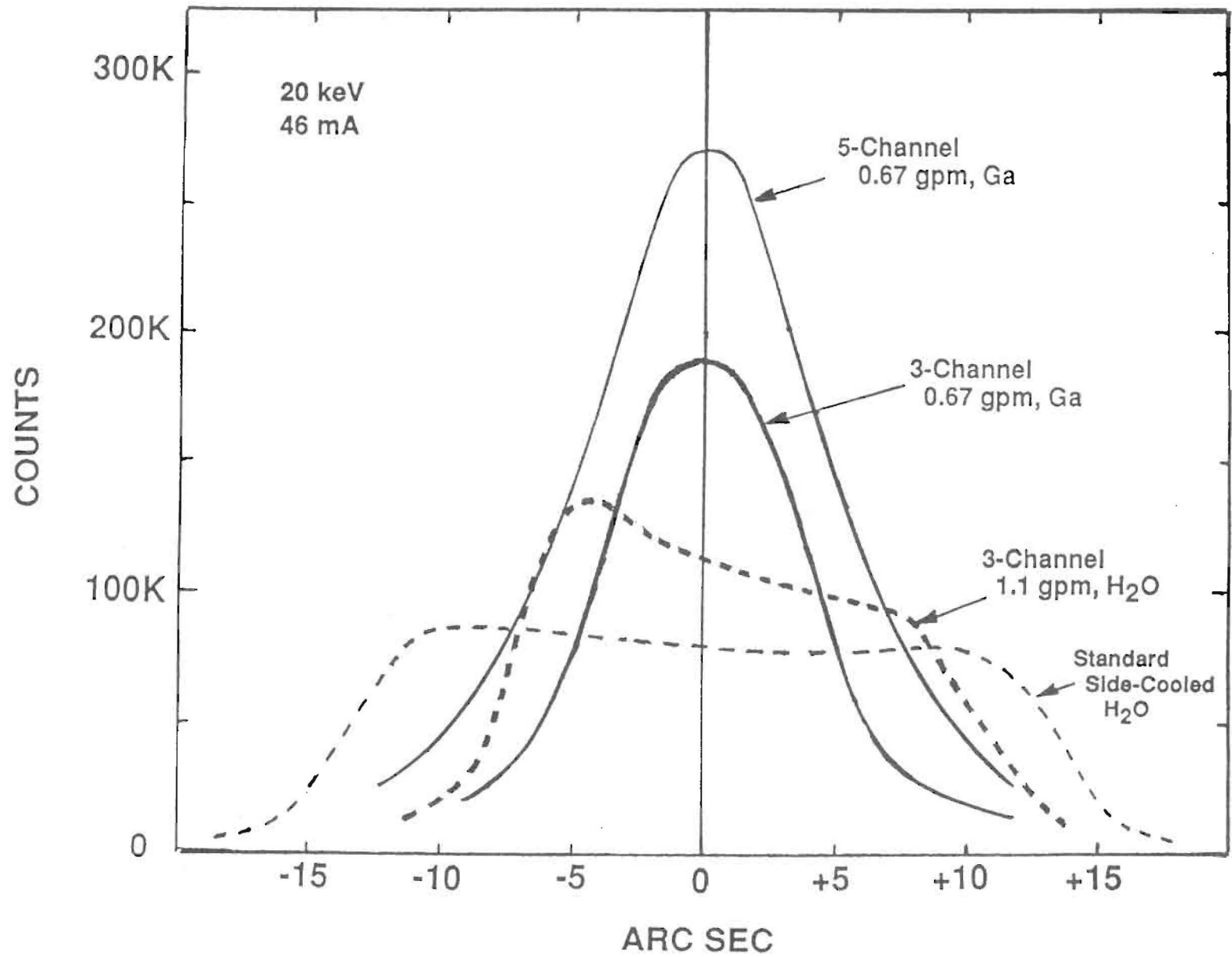


Fig. 8

Figure 8. Plot of the rocking curves obtained with the three different silicon crystals in the wiggler experiments (photon energy of 20 keV, electron current of 46mA).

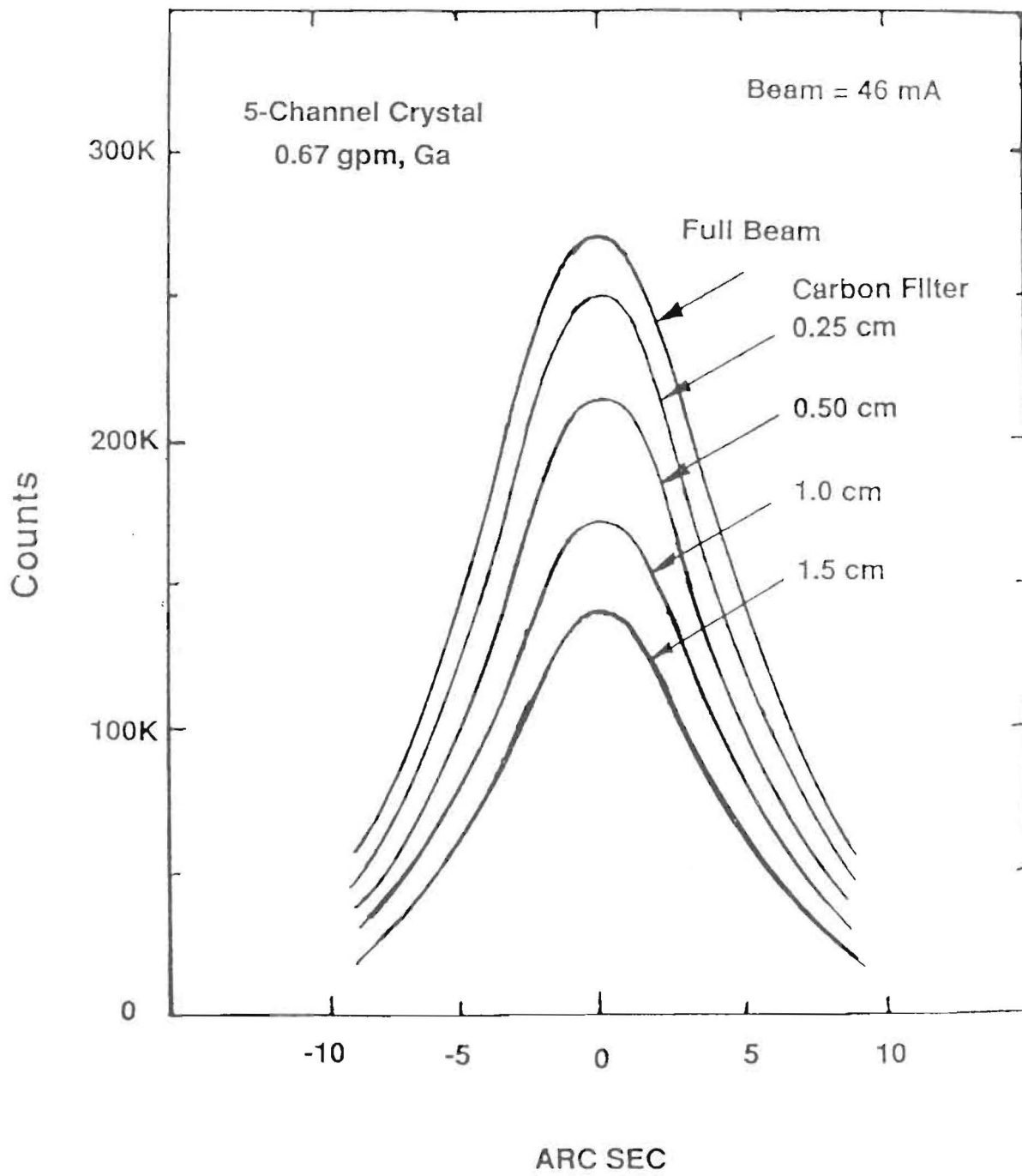
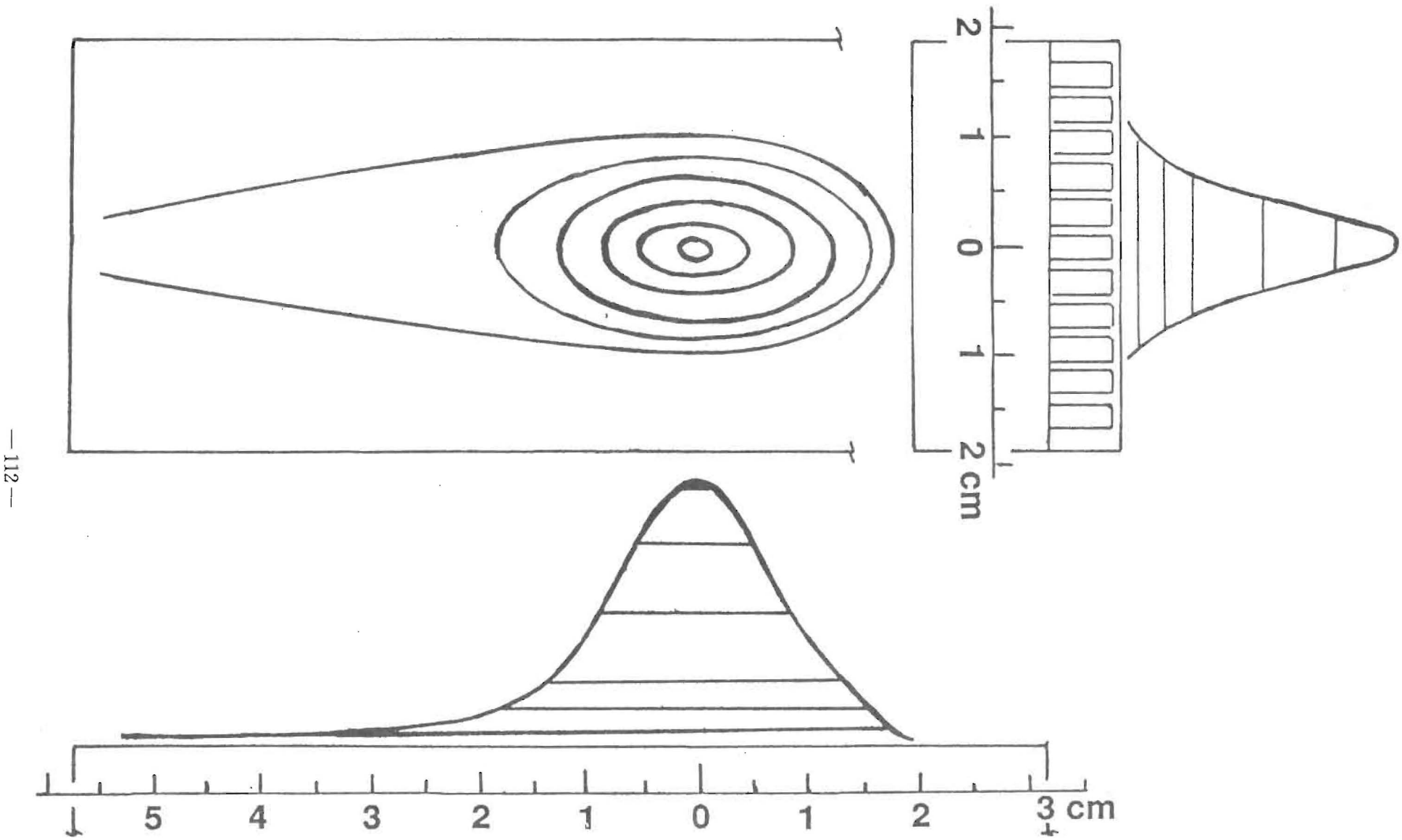


Figure 9. Plots of rocking curves for the 5 channel crystal for different thicknesses of the stepped carbon filter in the photon beam.

Fig. 9



—112—

Fig. 10

Figure 10. The thermal profile of the undulator beam superimposed on the cross section of the the slotted silicon crystal with the thin top layer. The side view and front view are crossed by lines at heights that correspond to the thermal isomers shown in the top view.

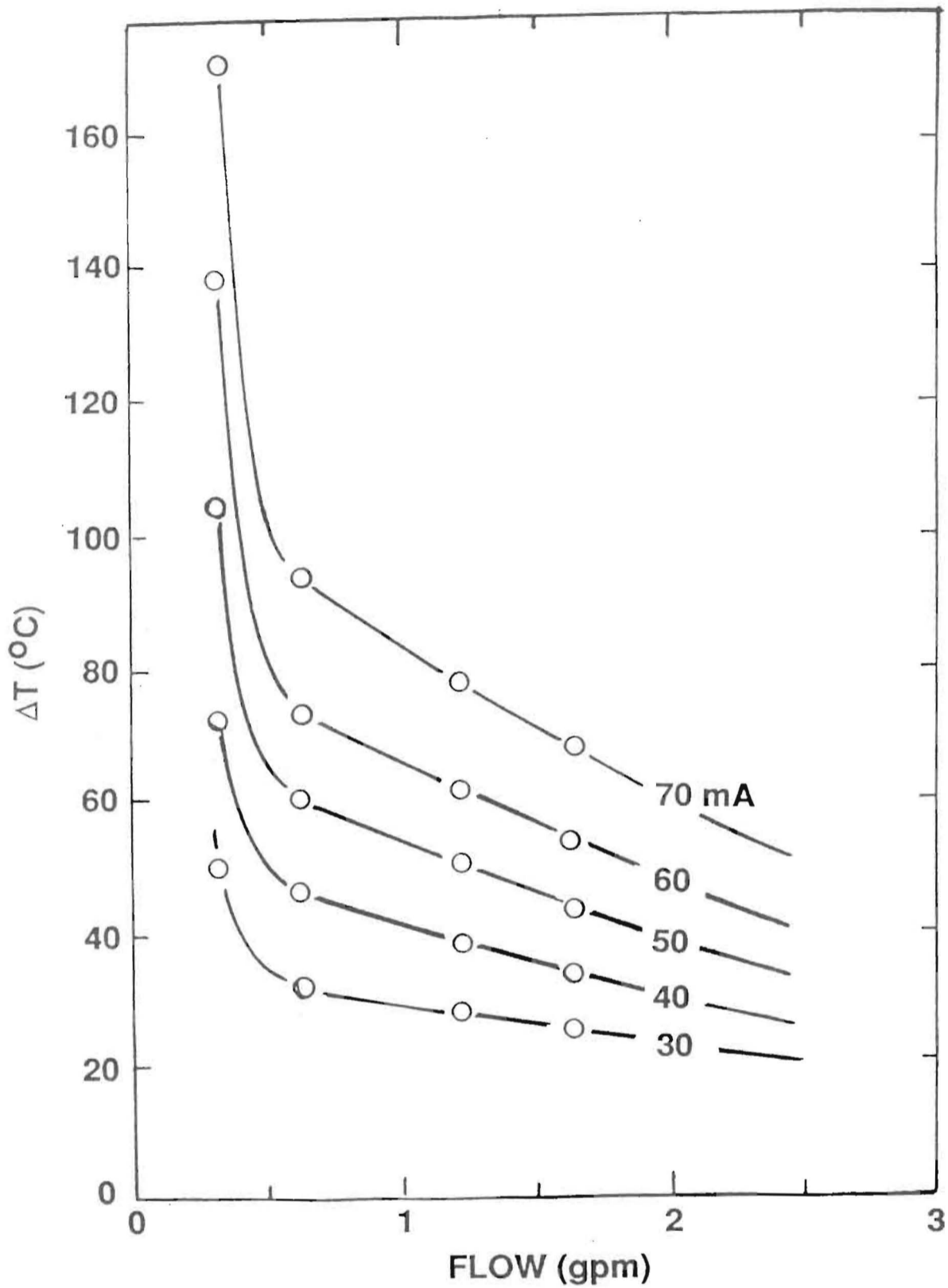


Figure 11. Plot of the peak temperature of the thermal profile as a function of the rate of flow of the cooling fluid for the slotted crystal.

1911

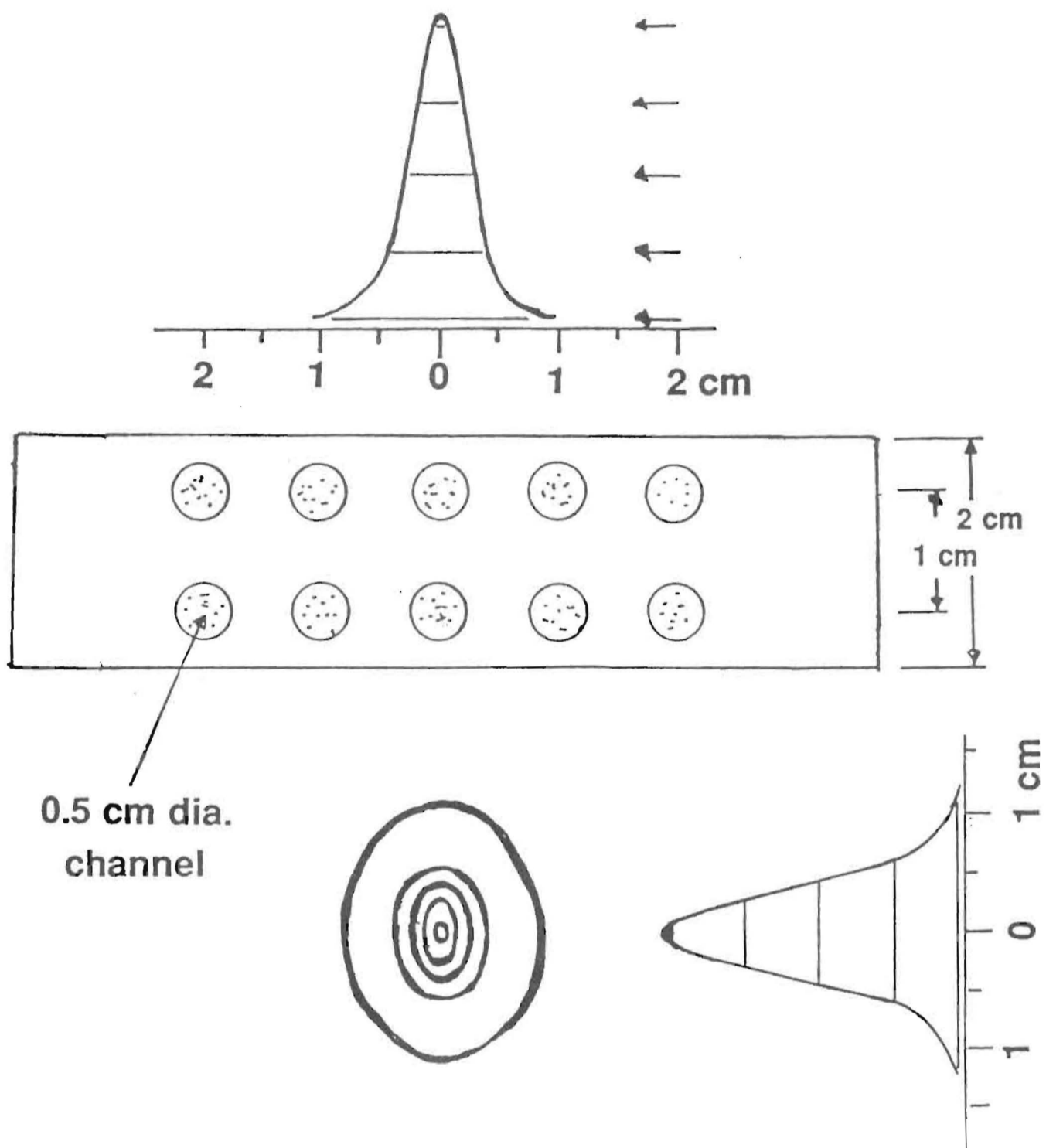


Figure 12. The thermal profile of the undulator beam superimposed on the cross section of the the 10-channel crystal. The side view and front view are crossed by lines at heights that correspond to the thermal isomers shown in the top view.

Fig 12

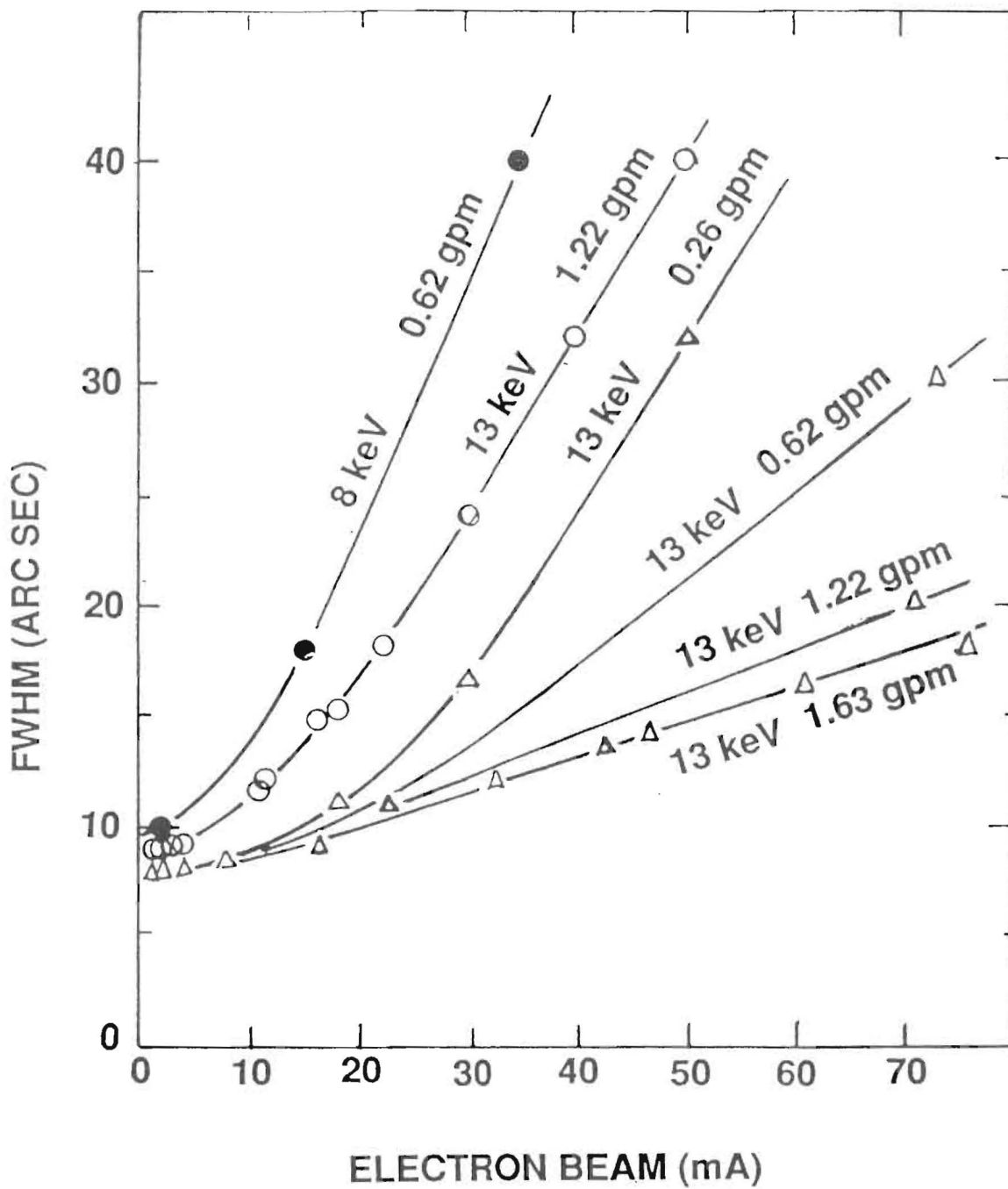


Figure 13. Plot of the FWHM of the rocking curves of the 10-channel crystal (circles) and the slotted crystal (triangles) for different diffraction energies and flow rates for the cooling fluid (Ga), as a function of the electron beam current in the storage ring.

11515

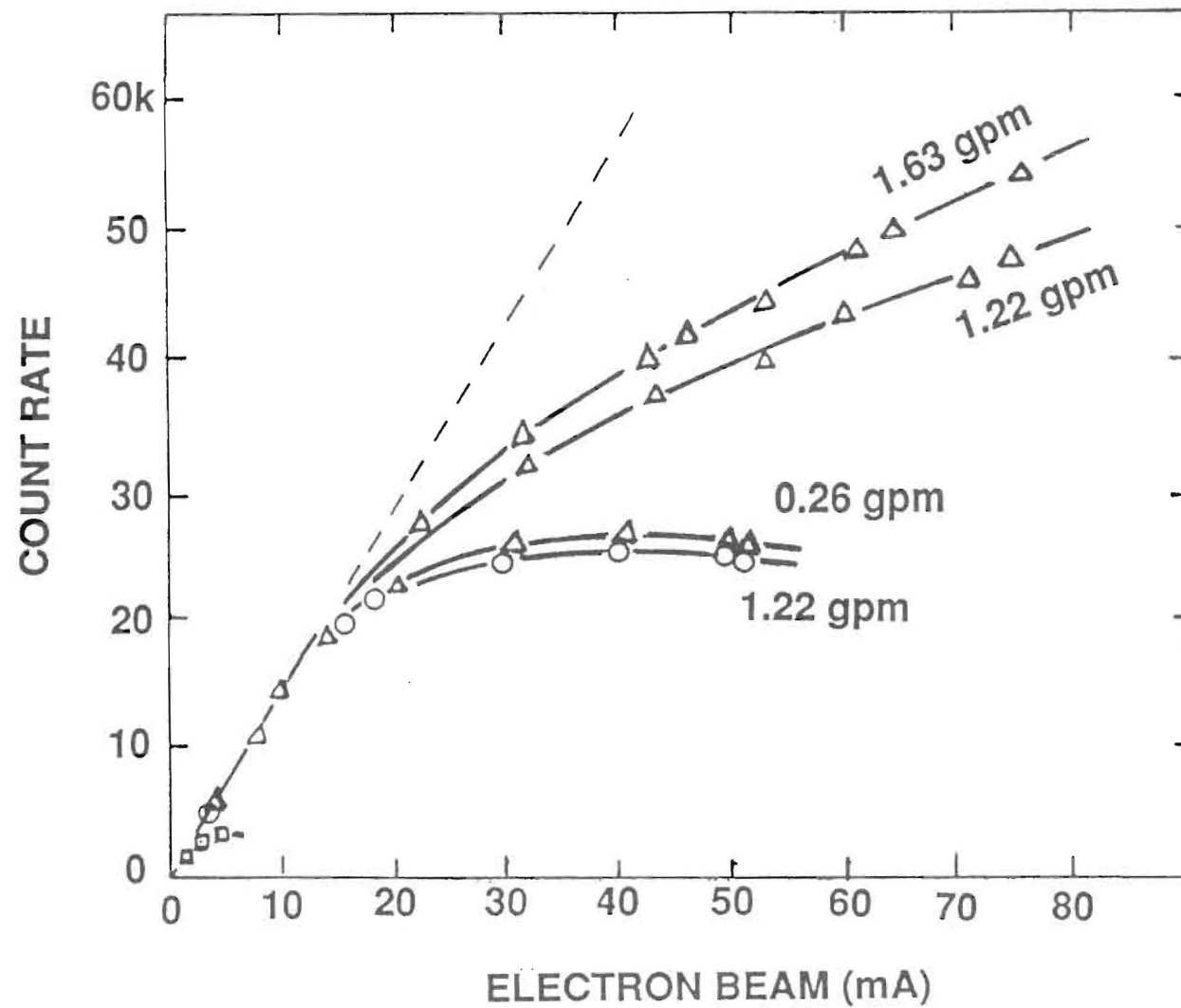


Fig. 14

Figure 14. Plot of the counting rate in the photon beam from the monochromator versus the electron beam current, for the slotted crystal (triangles), the 10-channel crystal (circles) and the standard CHESS side-cooled crystal (squares), withr different flow rates for the cooling fluid

VARIABLE FOCUS CRYSTAL DIFFRACTION LENS

R. K. Smither
Argonne National Laboratory, Argonne, IL 60439

ABSTRACT

A new method has been developed to control the shape of the surface of a diffracting crystal that will allow it to function as a variable focus crystal diffraction lens, for focusing photon beams from a synchrotron source. The new method uses thermal gradients in the crystal to control the shape of the surface of the crystal in two dimensions and allows one to generate both spherical and ellipsoidal surface shapes. In this work the thermal gradient was generated by core drilling two sets of cooling channels in a silicon crystal so that cooling or heating fluids could be circulated through the crystal at two different levels. The first set of channels is close to the surface of the crystal where the photon beam strikes it. The second set of channels is equal distant from the back surface. If a concave surface is desired, the fluid in the channels just below the surface exposed to the beam is cooler than the fluid circulating through the channels near the back surface. If a convex surface is desired then the cooling fluid in the upper channels near the surface exposed to the incident photon beam, is warmer than the fluid in the lower channels. The focal length of the crystal lens is varied by varying the thermal gradient in the crystal. This approach can also be applied to the first crystal in a high power synchrotron beam line to eliminate the bowing and other thermal distortions of the crystal caused by the high heat load.

INTRODUCTION

The most commonly used optical element for focusing photon beams at presently operating synchrotron facilities is a total reflecting curved mirror. Both cylindrical and ellipsoidal surfaces are used to obtain single and double focusing. This approach works well for energies below 10 keV and is useful for energies in the 10 to 20 keV range. Above this the total reflecting angles become small (less than 4 mrad.) with correspondingly smaller tolerances on the surfaces with longer lengths. Thus at energies above 20 keV, diffraction crystals become attractive as focusing elements because of their larger reflection angles. Presently, most bent crystals are bent with mechanical forces applied to the surfaces of the crystal and the bend is almost always only in one plane. Compound curves such as spherical and ellipsoidal surfaces are very difficult to obtain.

NEW METHOD USING THERMAL GRADIENTS

A new method has been developed to control the shape of the surface of a diffracting crystal that will allow it to function as a variable focus crystal diffraction lens. The new method uses thermal gradients in the crystal to control the shape of the surface of the crystal in two dimensions.¹ This allows one to generate both spherical and ellipsoidal surface shapes. Thus the photon beam can be focused in two dimensions. The method used in this work to apply thermal gradients to the

diffraction crystal is shown in figure 1.

Two sets of channels are drilled through the crystal so that fluids for cooling or heating can be circulated through them at two different levels in the crystal. The first set of channels is close to the surface of the crystal where the photon beam strikes it. These cooling channels serve the dual purpose of cooling the diffraction surface of the crystal as well as establishing one side of the thermal gradient. The second set of channels is in some cases a uniform distance from the back surface and in some cases at a variable distance from that surface. Surface shapes other than spherical can be generated by varying the distance between the two levels of channels and by varying the relative temperatures in different channels on the same level. If a concave surface is desired, the fluid in the channels just below the surface exposed to the beam is cooler than the fluid circulating through the channels near the back surface. Conversely, if a convex surface is desired then the cooling fluid in the upper channels near the surface exposed to the incident photon beam, is warmer than the fluid in the lower channels. The cooling fluid flows are usually counter to each other, with the cooler fluid in the upper channels flowing in the direction of the beam in the case of the concave surface. This generates a uniform thermal gradient between the two sets of channels and generates a spherical surface on the crystal. It also generates a gradual increase in the temperature of the surface in the direction of the beam that helps offset the decrease in incident angle of the photon beam. If this increase in temperature along the crystal surface is adjusted so that it exactly matches the change in incident angle, then a substantial increase in the photon flux per unit band width can be achieved.^{2,3} In order to realize this increase at the sample one must apply a similar temperature gradient to the second crystal of a two crystal monochromator. An alternate approach is to curve the surface of the first crystal so that the diffracted beam from the first crystal is parallel in the plane of diffraction (in the vertical direction). Then the maximum photons per unit band width can be diffracted by a flat second crystal.^{2,3} The thermal gradients needed in the crystal are typically 10° to 50°C per cm. Such gradients are easily attainable with working fluids of either liquid gallium or water using two sets of cooling channels. The crossed channels in the lower example in figure 1 can give complex surface shapes that compensate for second order aberrations if one can control the temperature in the individual channels. Liquid gallium works better as a cooling-heating fluid for the generation of thermal gradients because its heat transfer coefficient at the liquid/solid surface is much higher and varies more slowly with flow velocity than for the case of water.^{4,5} This allows one to use the cooling-fluid flow rate to adjust the temperature gradient along the surface of the crystal in the direction of the photon beam.

The radius of curvature, "R", of the surface for the case of a uniform thermal gradient applied to the crystal is given by equations (1-2)

$$R = \Delta R / \alpha \Delta T = k / \alpha Q \quad (1)$$

$$\Delta T = T_1 - T_2 = \Delta R Q / k \quad (2)$$

where ΔR is the separation between the two sets of cooling channels, α is the coefficient of thermal expansion, of the crystal, " ΔT ", is the temperature difference

between the two sets of cooling channels, " Q ", is the thermal heat flux per unit area and " k ", is the thermal conductivity of the crystal (see figure 2). The value of the radius is independent of the thickness of the crystal and depends only on the heat flux in the crystal, thus a thick crystal can be bent just as easily as a thin one given the same heat source. The ease of bending depends on the ratio of k / α for the crystalline material. Table I gives the values of " k ", " α ", and " k / α " for various materials. Thus a Ge crystal will bend easier than a Si crystal. A quartz crystal will bend easier than either the Si crystal or the Ge crystal and because of the asymmetry of its crystal constants will have different radii of curvature depending on the orientation of the crystal.

The radius of curvature of the crystal surface, " R_1 ", needed to refocus a synchrotron beam at a distance, " X ", equal to the distance from the source to the crystal, is given by equation (3)

$$R_1 = X / \sin \theta \quad (3)$$

where " $\sin \theta$ ", is the sine of the diffraction angle. Table II gives values of " R_1 " and the thermal gradient, " $\Delta T / \Delta R$ ", needed for different values " θ " and a value of " X " = 20 m. Table III gives similar values for a SiO_2 crystal for crystalline planes perpendicular to the c-axis. The relationship between these values and the focal circle is shown in figure 3. The fact that the radius of curvature needed for focusing changes with Bragg angle, requires that the focusing lens have a variable focal length, thus a variable radius of curvature, if it is to be used at more than one wave length.

THE USE OF SURFACE SHAPE CONTROL TO REDUCE THE EFFECTS OF HIGH HEAT LOADS

This method for controlling the shape of the surface of a diffraction crystal can be used to reduce the distortion effects of the heating of the diffraction crystal by the photon beam. The cooling fluid in the channels can be used to remove the heat from the photon beam and at the same time, it can be used to suppress bowing of the crystal and the thermal bulge generated by the thermal loading through control of the shape of the surface. One simply increases the thermal gradient in the crystal until the area in the center of the photon beam is flat.

In June of '88, photon beams from the newly installed ANL/CHES undulator at CHES⁶ were used to test the effectiveness of cooling diffraction crystals with liquid gallium flowing in channels just below the crystal surface.^{4,5} During this test period, some experiments on surface shape control were also performed using a silicon crystal with two sets of cooling channels.⁵ Figure 4 shows the cross section of this crystal and three views of the thermal profile of the beam on the crystal as measured with an infrared camera. The upper view shows the profile perpendicular to the beam direction, the side view shows the profile parallel to the beam direction and the center view shows the isothermal contours at the values indicated by the arrows on the upper and side profiles. The arrows indicate isothermal levels at 95%, 75%,

50%, 25%, and 5%. In these tests the crystal shown in figure 4 was used as the first crystal in a two crystal monochromator. The (111) planes of silicon were used to diffract an 8 keV photon beam. The experimental set up is shown in figure 5. The maximum flux from the monochromator obtained when the second crystal was rotated, was recorded as a function of electron beam current in the storage ring, first for the case when the temperature of the liquid gallium in the two sets of cooling channels was the same, and then when the temperature of the gallium in the lower channels was raised above that in the upper channels. The same gallium pump⁵ was used for both cooling fluid loops. The flow out of the pump was split into parts. The part that fed the upper set of channels was cooled with a heat exchanger and the part that fed the lower set of channels was passed through a heater to raise its temperature. The results of these two test cases is shown in figure 6. The flow rate of the gallium through the crystal was purposely kept low, 0.33 gpm in the upper channels and 0.20 gpm in the lower channels, to maximize the ΔT attainable for the two gallium flow loops. The slower the flow, the more efficient was the heater used to raise the temperature of the gallium in the lower channels. The improvement in beam intensity achieved with a ΔT applied (squares) to the case without a ΔT (triangles), at 20 mA of beam current, is about a factor of 1.5 to 1.0 and is almost full recovery of the photon beam. Figure 7 shows the expected dependence of the temperature inside the crystal as a function of position in the crystal perpendicular to the surface of the crystal. If one wishes to remove only the bowing of the crystal then the temperature difference between the two cooling channels needs to be only about one third of the temperature difference between the surface of the crystal and the upper set of cooling channels. If one wishes to compensate for the thermal bulge as well, then some additional ΔT is needed.

FUTURE EXPERIMENTS

Further experiments are planned to test the focusing properties of the crystal with dual levels of cooling shown in figure 4. If one neglects the effects of removing the heat of the photon beam from the crystal surface, then the temperature distribution in the crystal perpendicular to the surface is more symmetric as shown in figure 8. The regions of constant temperature at the two surfaces tend to reduce the curvature of the crystal. A more efficient design is will be tested in which the lower level of channels will be replaced thin film resistors on the lower surface to introduce the heat needed to maintain the thermal gradient. By using many small area resistors with individually controlled power supplies one can obtain much better control of the surface shape allowing second order corrections to be made in the focusing process. These procedures for controlling the shape of the crystal surface could also be used to control the shape of the surfaces of total reflection mirrors and multilayer structures.

ACKNOWLEDGMENTS

The author wishes to thank G. Forster for his assistance in preparing the experiment¹. The author wishes to thank the scientific staff at CHESS for their assistance in taking the experimental data. This work was supported by the U.S. Department of Energy under Contract No. W-31-109-ENG-38.

References:

- 1 Robert K. Smither, patent application No.ANL-S67,086.
- 2 R. K. Smither, Rev. Sci. Instrum. **53(2)**, 131 (1982).
- 3 G.S. Knapp and R.K. Smither, Nucl. Instr. and Meth. **A246**, 365 (1986).
- 4 R. K. Smither, G.A. Forster, C.A. Kot, T.M. Kuzay, Nucl. Instr. & Meth., **A266**, 517 (1988).
- 5 R. K. Smither, G.A. Forster, D. Bilderback, M. Bedzyk, K. Finkelstein, C. Henderson, J. White, L. Berman, P. Stephen, and T. Oversluizen, "Liquid Gallium Cooling of Silicon Crystals in High Intensity Photon Beams", Proceedings of the 3rd International Conference on Synchrotron Radiation Instrumentation, edited by M. Ando, Rev. Sci. Instrum. __, __, (1989).
- 6 B. Batterman, et al., "The performance of a Hard X-ray Undulator at CHESS", Proceedings of the 3rd International Conference on Synchrotron Radiation Instrumentation, edited by M. Ando, Rev. Sci. Instrum. __, __, (1989).

TABLE I. Comparison of the values of "k", the thermal conductivity, "α", the thermal expansion coefficient, and the ratio of "k / α", for varies crystals and materials (20°C).

MATERIAL	k (W / cm / °C)	α (ΔL / L per °C)	k / α (W / cm)
Si	1.5	3.0 x 10 ⁻⁶	2.0 x 10 ⁶
Ge	0.5	6.0 x 10 ⁻⁶	4.3 x 10 ⁵
SiO ₂ (a-axis)	0.066	7.53 x 10 ⁻⁶	8.8 x 10 ³
SiO ₂ (c-axis)	0.109	14.0 x 10 ⁻⁶	7.8 x 10 ³
Cu	3.85	16.6 x 10 ⁻⁶	1.6 x 10 ⁵
Al	2.01	24. x 10 ⁻⁶	8.4 x 10 ⁴
St. Steel	0.108	17. x 10 ⁻⁶	6.4 x 10 ³

TABLE II. A table of values for the radius of curvature, "R1", of the bent crystal needed to refocus the radiation from a point source a distance "X" from the crystal (column 2) and "R₁", when the distance "X" is 20m (column 3). Column 4 gives the thermal gradient, " $\Delta T / \Delta R$ " ($^{\circ}\text{C} / \text{cm}$), and column 5 gives the corresponding thermal flux, "Q", in W per cm^2 , needed if the crystal is Si, for different Bragg angles (column 1).

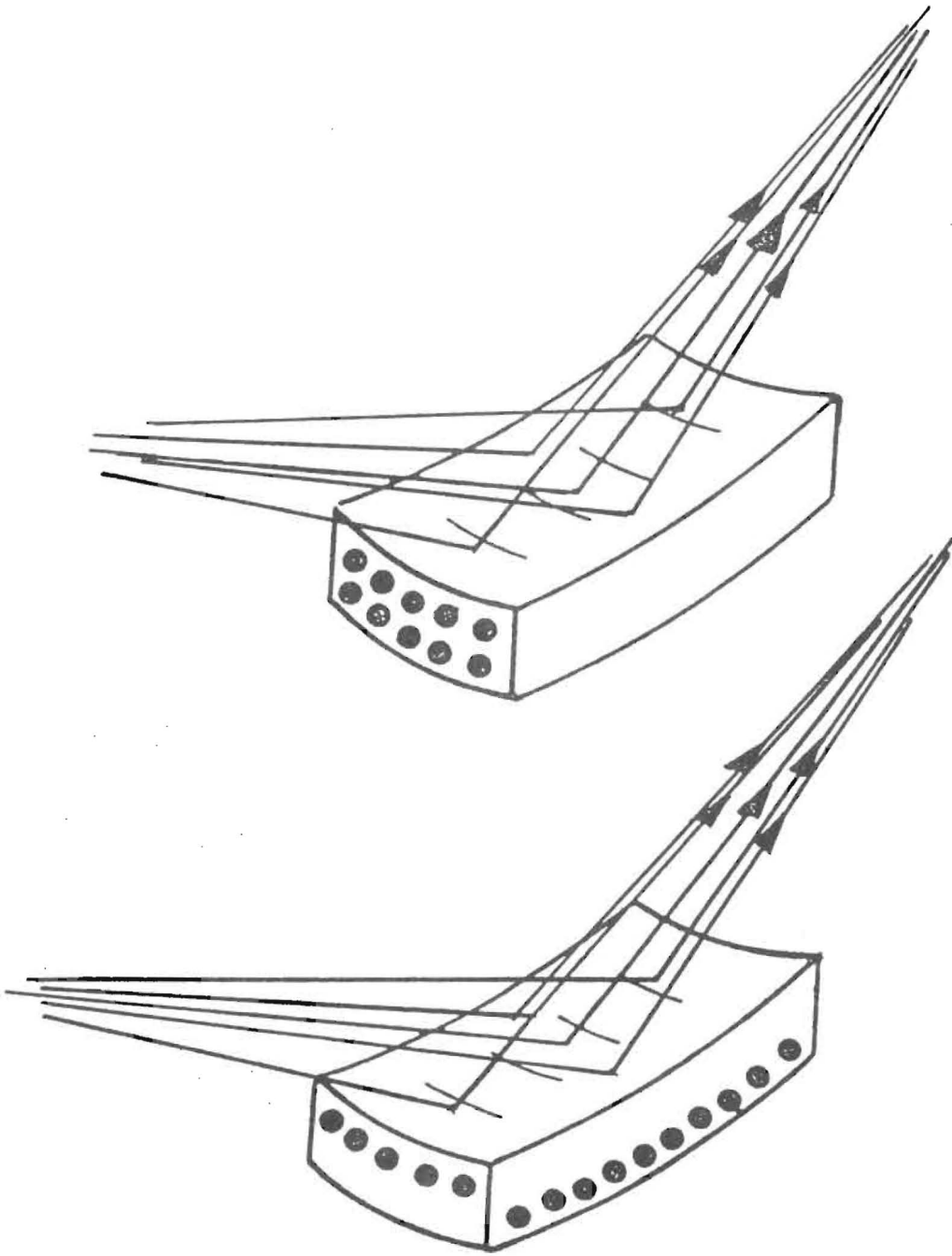
θ	R ₁	R ₁ (X = 20m)	ΔT ($^{\circ}\text{C} / \text{cm}$)	Q (W / cm^2)
6 $^{\circ}$	10. X	200. m	16.	24.
12 $^{\circ}$	5. X	100. m	32.	48.
30 $^{\circ}$	2. X	40. m	80.	120.
45 $^{\circ}$	1.4 X	28. m	114.	171.

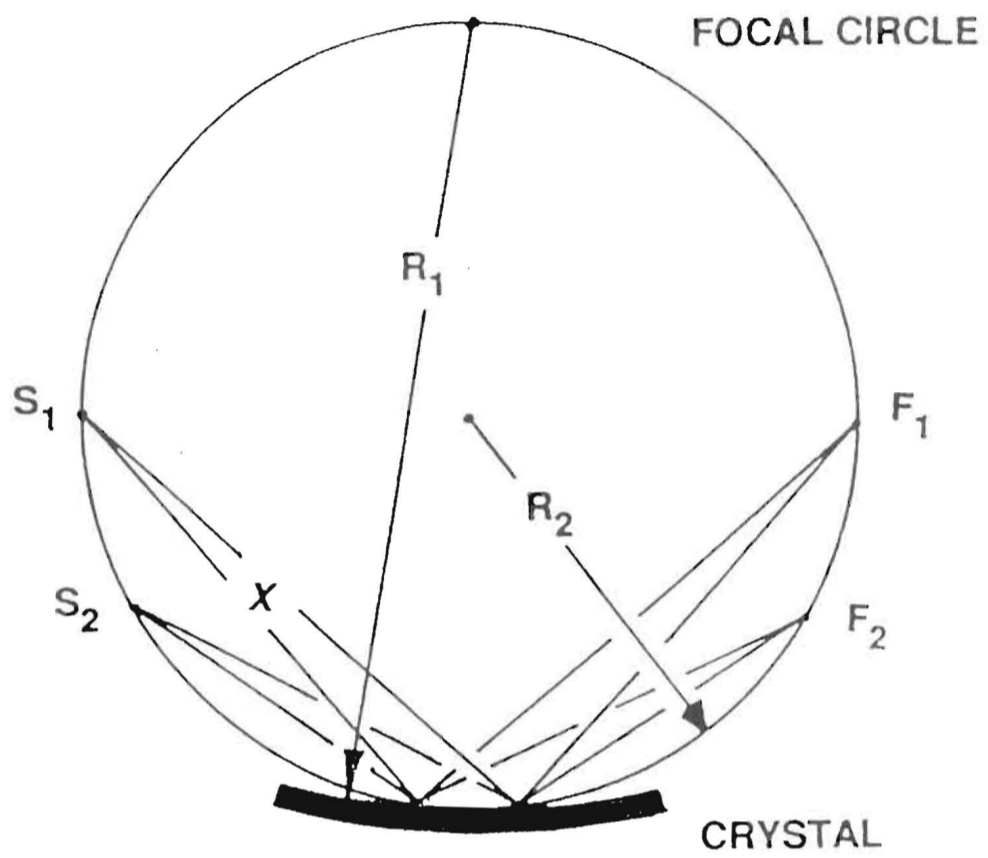
TABLE III. A table of values for the radius of curvature, "R1", of the bent crystal needed to refocus the radiation from a point source a distance "X" from the crystal (column 2) and "R₁", when the distance "X" is 20m (column 3). Column 4 gives the thermal gradient, " $\Delta T / \Delta R$ " ($^{\circ}\text{C} / \text{cm}$), and column 5 gives the corresponding thermal flux, "Q", in W per cm^2 , needed if the crystal is SiO₂, for different Bragg angles (column 1).

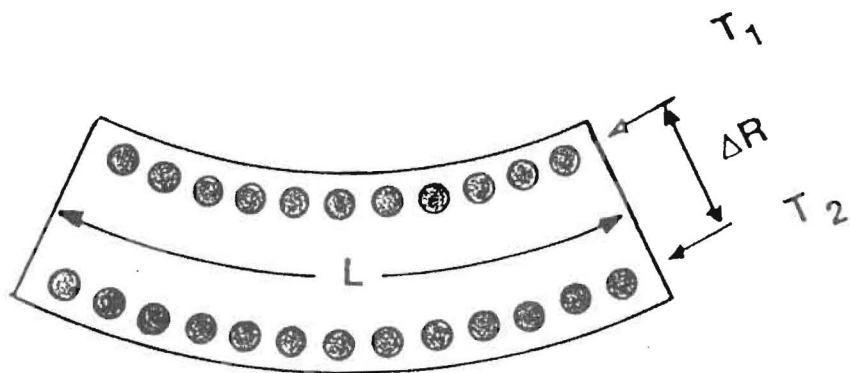
θ	R ₁	R ₁ (X = 20m)	ΔT ($^{\circ}\text{C} / \text{cm}$)	Q (W / cm^2)
6 $^{\circ}$	10. X	200. m	3.4	0.22
12 $^{\circ}$	5. X	100. m	6.8	0.45
30 $^{\circ}$	2. X	40. m	17.0	1.12
45 $^{\circ}$	1.4 X	28. m	24.0	1.58

Figure Captions

- Figure 1. Double focusing crystals using thermal gradients to control their shape. The thermal gradients are generated by controlling the temperature of the cooling fluids that flow through the two sets of cooling channels (upper and lower).
- Figure 2. Cross section of thermally bent crystal illustrating the use of equations (2,3) for calculating the radius of curvature, " R_1 ", obtained for a given temperature difference, " ΔT ", between the two sets of cooling channels, with a given spacing, " ΔR ".
- Figure 3. Geometric figure showing the relationship between the radius of curvature, " R_1 ", of the bent crystal needed to refocus the radiation from a point source located at a distance, " X ", from the crystal and the focal circle with radius, " R_2 ", equal to " $R_1 / 2$ ".
- Figure 4. Schematic drawing showing the cross section of the crystal with two levels of cooling-heating channels and three views of the thermal profile of the undulator beam on the crystal as measured with an infrared camera.
- Figure 5. Experimental set up for the experiments with the ANL/CHSS undulator.
- Figure 6. Plot of counting rate verses beam current for the case when there is no temperature difference, " ΔT ", between the two sets of cooling channels (triangles) and the case where a " ΔT " is applied to the crystal by raising the temperature of the cooling fluid in the lower channels above that of the upper channels (squares).
- Figure 7. Temperature profiles through the crystal when heat is added uniformly to the top surface and " T_3 ", the temperature of the cooling fluid in the lower channels is raised above " T_1 ", the temperature of the cooling fluid in the upper channels just enough to make the surface flat. The upper profile shows a cut through the channels and the lower profile shows a cut through the crystal in between the channels.
- Figure 8. Temperature profiles through the diffraction crystal with two levels of cooling channels where " T_3 " is higher than " T_1 ", and no appreciable heat is added to the top surface.







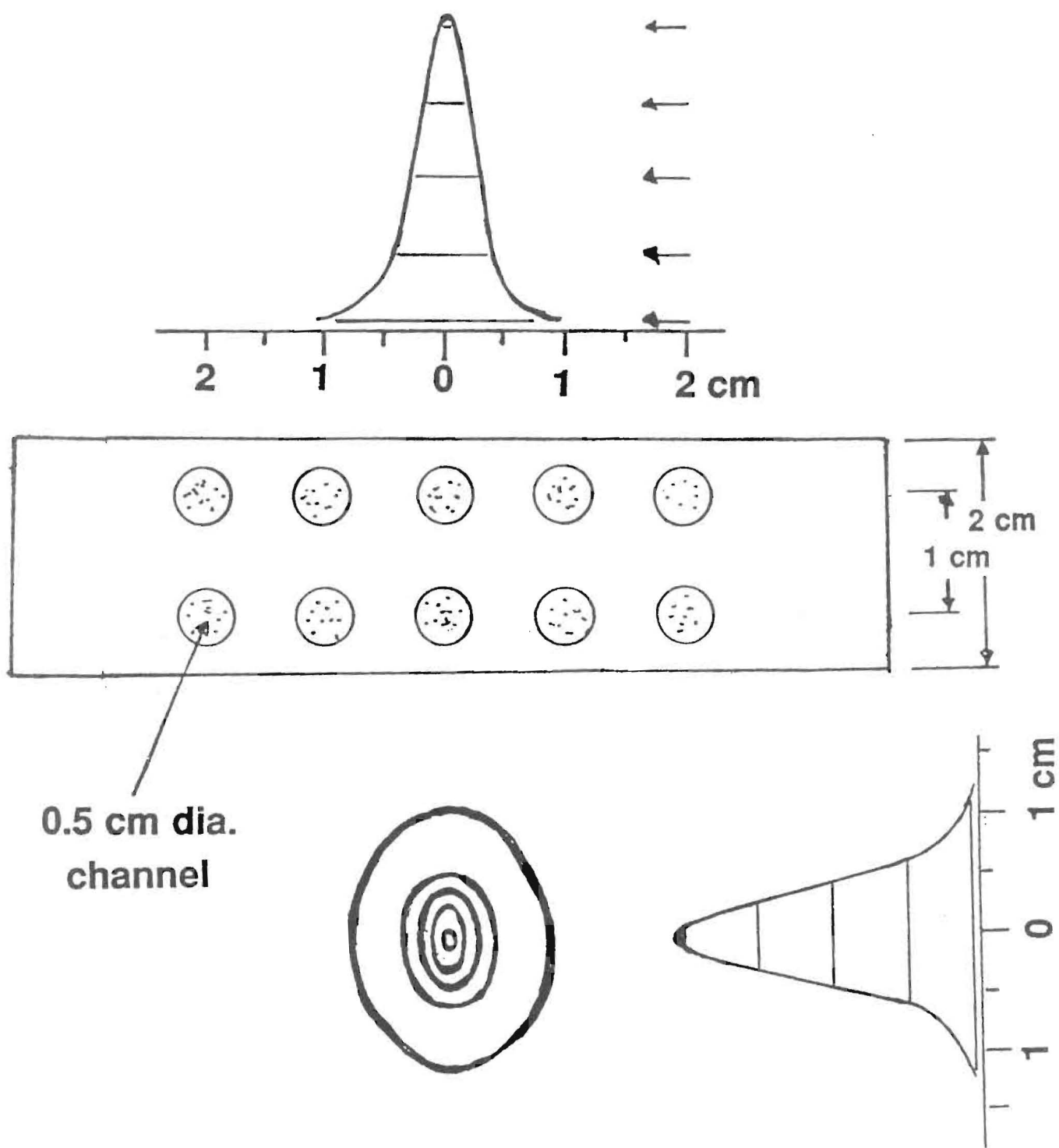
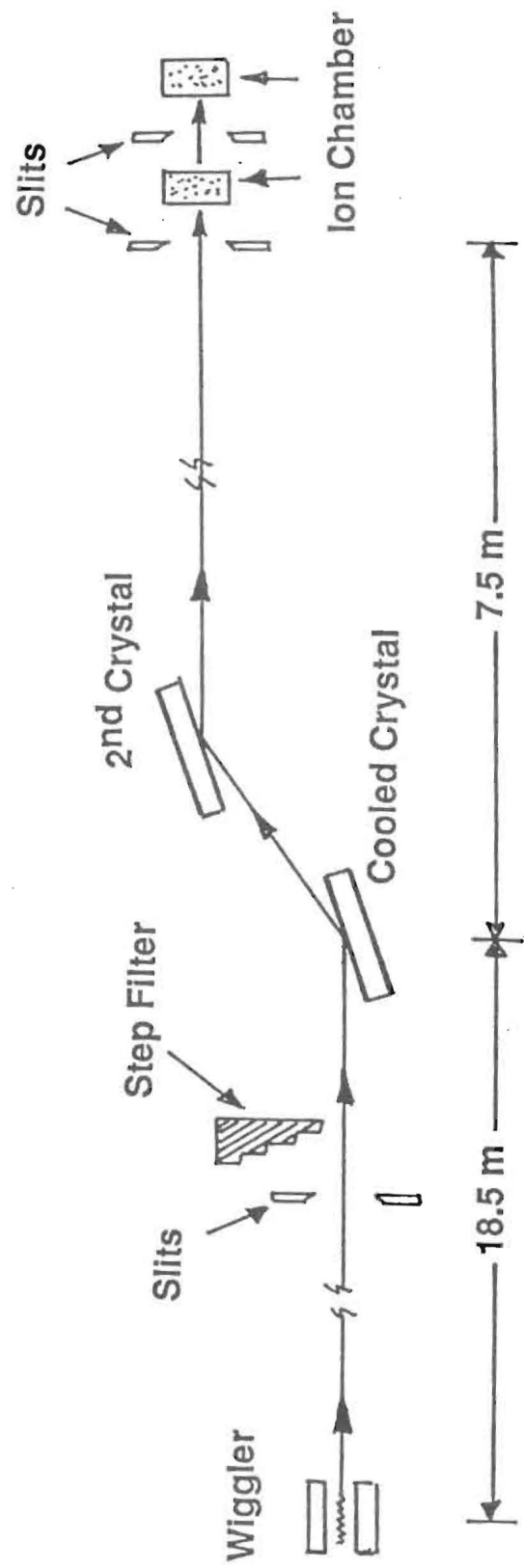


Fig. 4



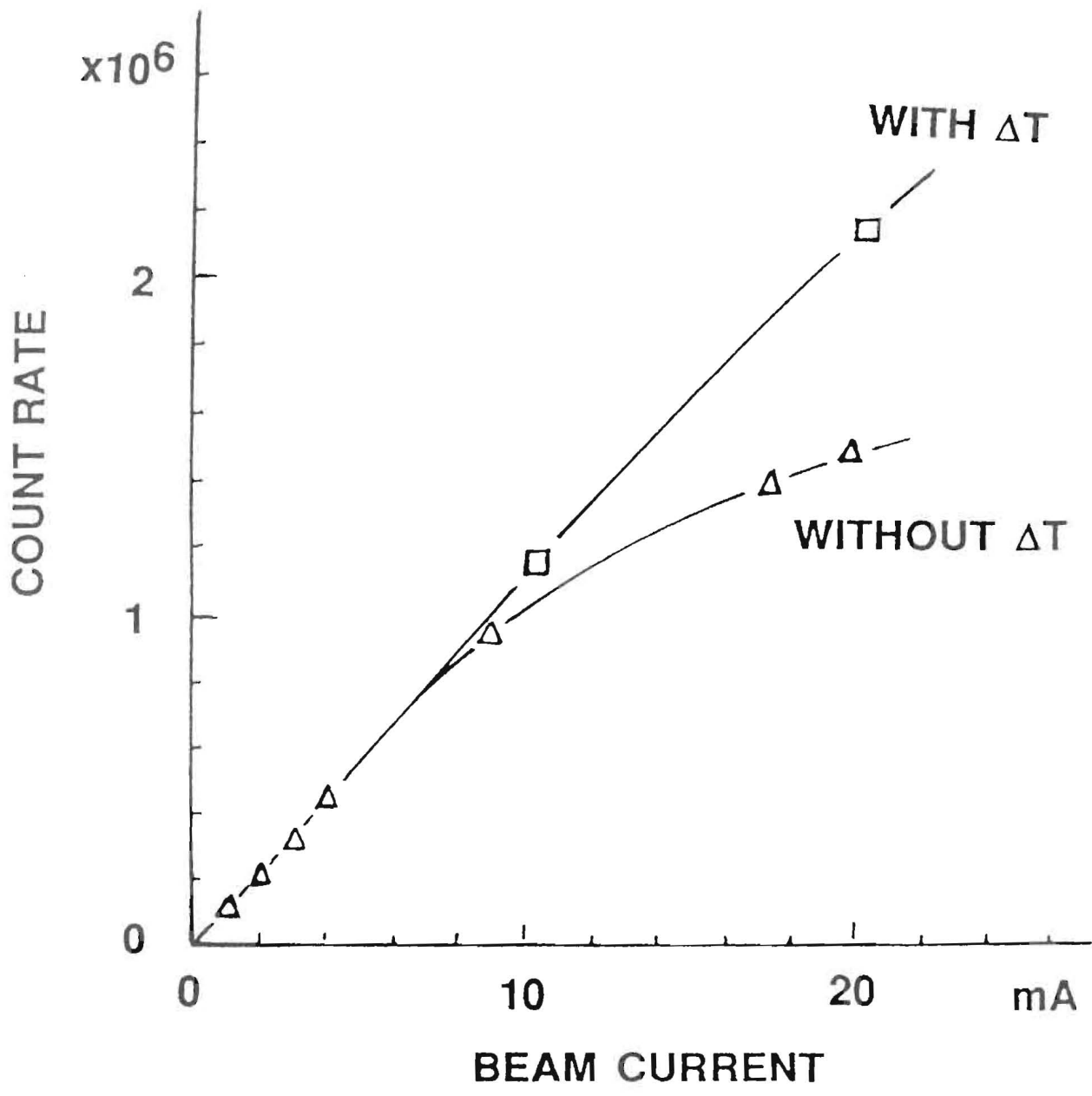


Fig. 6

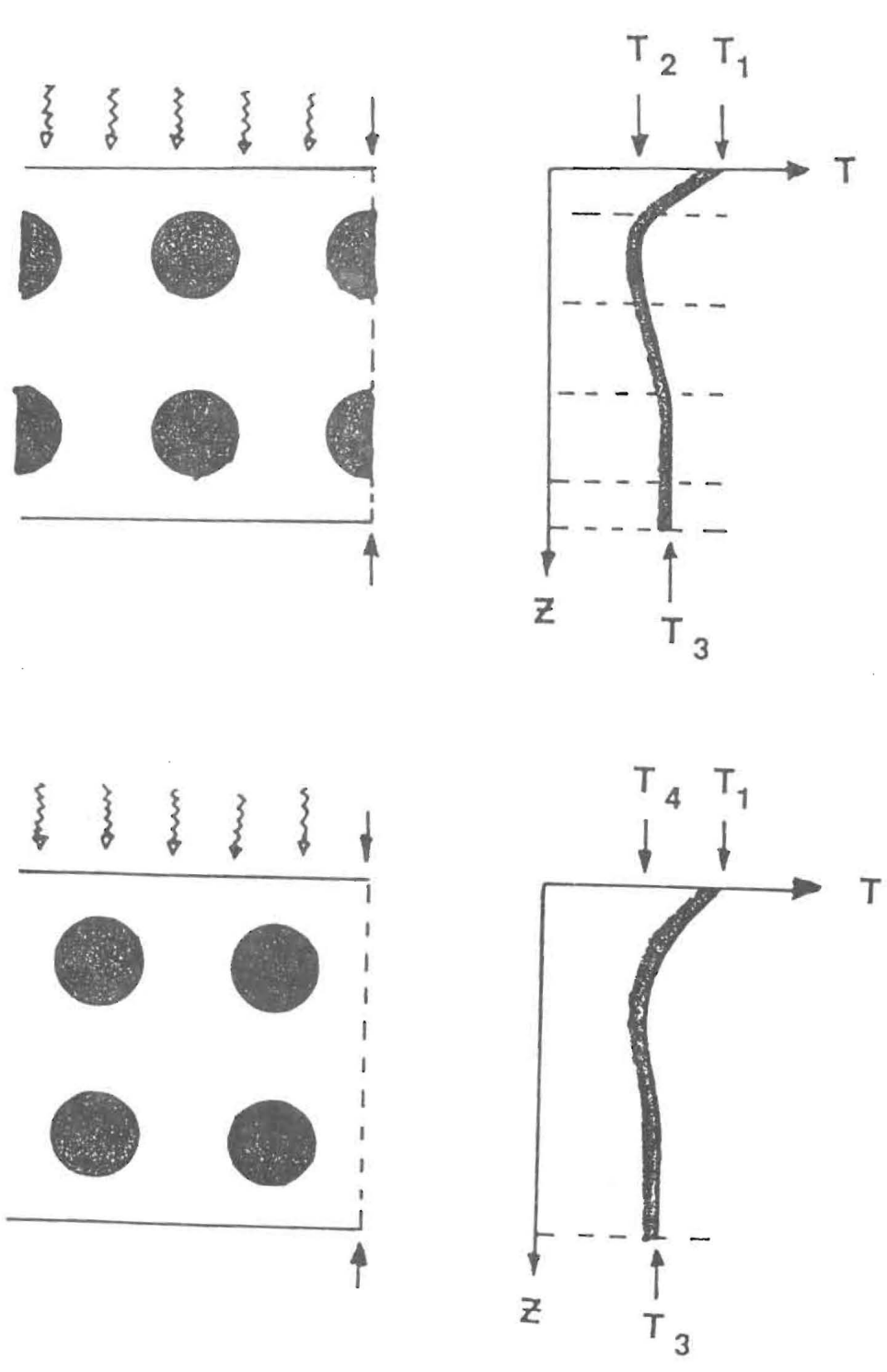


Fig 7

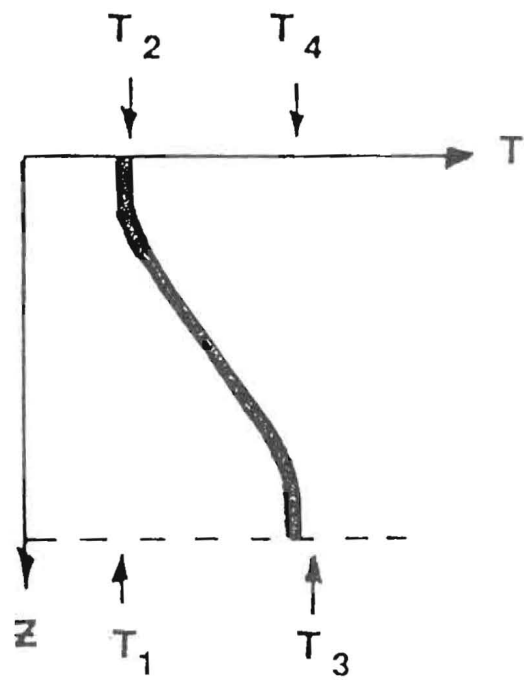
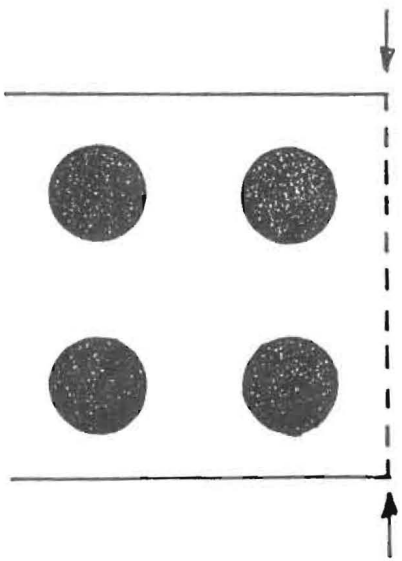
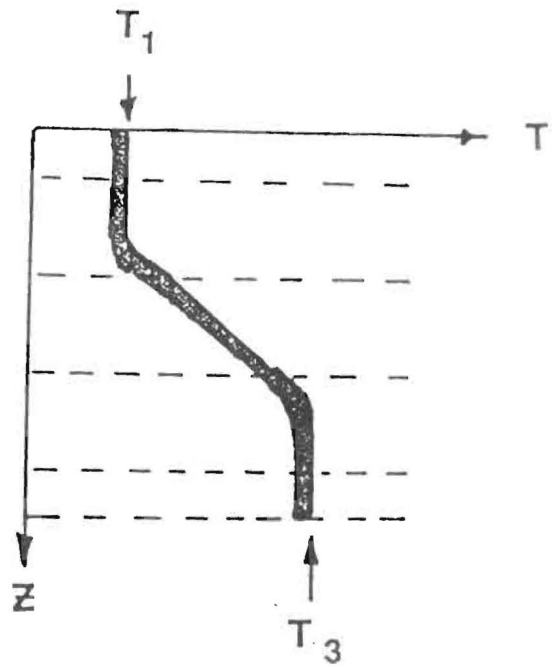
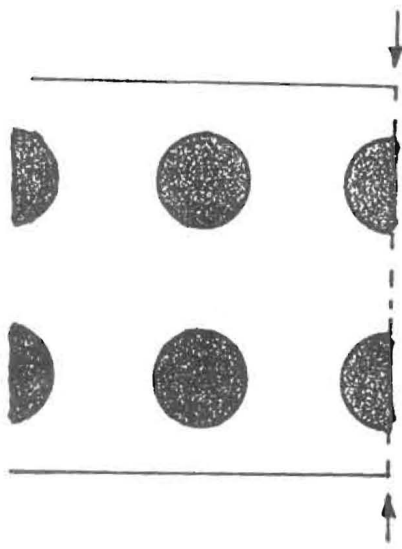


Fig 8

COOLING GEOMETRY FOR A CRYSTAL MONOCHROMATOR IN A HIGH POWER BEAMLINE

P. van Zuylen, A. D. Lemaire, A. Wijsman, and A. K. Freund*
TNO Institute of Applied Physics (TPD), Delft, Holland
*ESRF, Grenoble, France

The high power density and the high power gradient on the first optical elements in the next generation of beamlines, will cause large temperature gradients along the surface of these elements, which in many cases may be crystals. Due to the thermal expansion of the crystal bending may occur and an extra bump on the surface may appear.

Taking into account the width of the rocking curve of the crystal, as well as the possible imaging properties of the monochromator, one can define a maximum acceptable radius of curvature, or angular offset.

Taking an angular offset of 1 arcsec/mm, or a radius of 100 m, one finds for a crystal with a thickness of 1 mm a maximum allowable temperature gradient of 2 K/mm.

It can be shown that with an angle of incidence of a few degrees the temperature gradient as well as the maximum temperature on the crystal become tolerable. The maximum power in the spot will typically be 2 W/mm²; this power density can be cooled with water.

The small angle of incidence that is allowed has influence on the design of the monochromator. Our monochromator has a very asymmetric first crystal. The thickness of the crystal is of the order of 1 mm. It is cooled with water that is sprayed through many nozzles to the rear side. Scanning of the energy is around an axis perpendicular to the surface of the crystal. This means that the reflected beam is not only reflected in the vertical plane. By rotation around a spherical bearing with its centre of rotation on the centre of the crystal one can correct for this.



Cooling geometry for a crystal monochromator
in a high power beamline

P.van Zuylen, A.D. Lemaire, A. Wijsman
TNO Institute of Applied Physics (TPD),
Delft, Holland

A.K. Freund, ESRF, Grenoble, France



In this talk I want to present some results of a study that was carried out with the evolution of optical elements, especially crystal monochromators.

The study was carried out under a collaboration between TPD and ESRF.

You all know what ESRF is and has to become. TPD is our main partner the Institute of Applied Physics of the Netherlands Organization for Applied Scientific Research.

We are an institute that has a lot of expertise regarding the optical ^{design} group is involved in the design and development of optical instruments in the widest sense.

Our limiting experience on monochromators for synchrotron radiation lies in the monochromators that we built for the EXAFS station of the SRS.

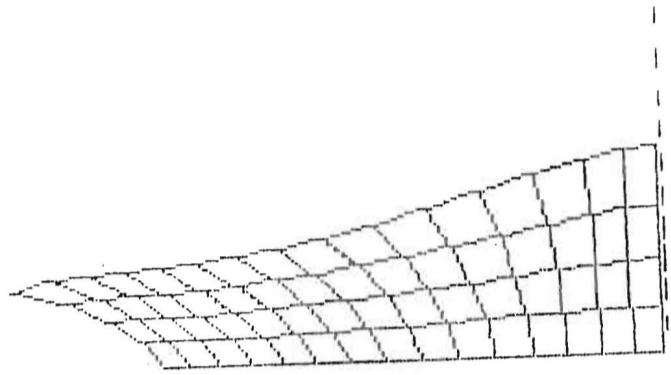


Plan

1. Introduction
2. Temperature gradient and shape
3. Temperature on crystal
4. Maximum temperature gradient
5. Thermal design
6. Mechanical design
7. Conclusion



TPD

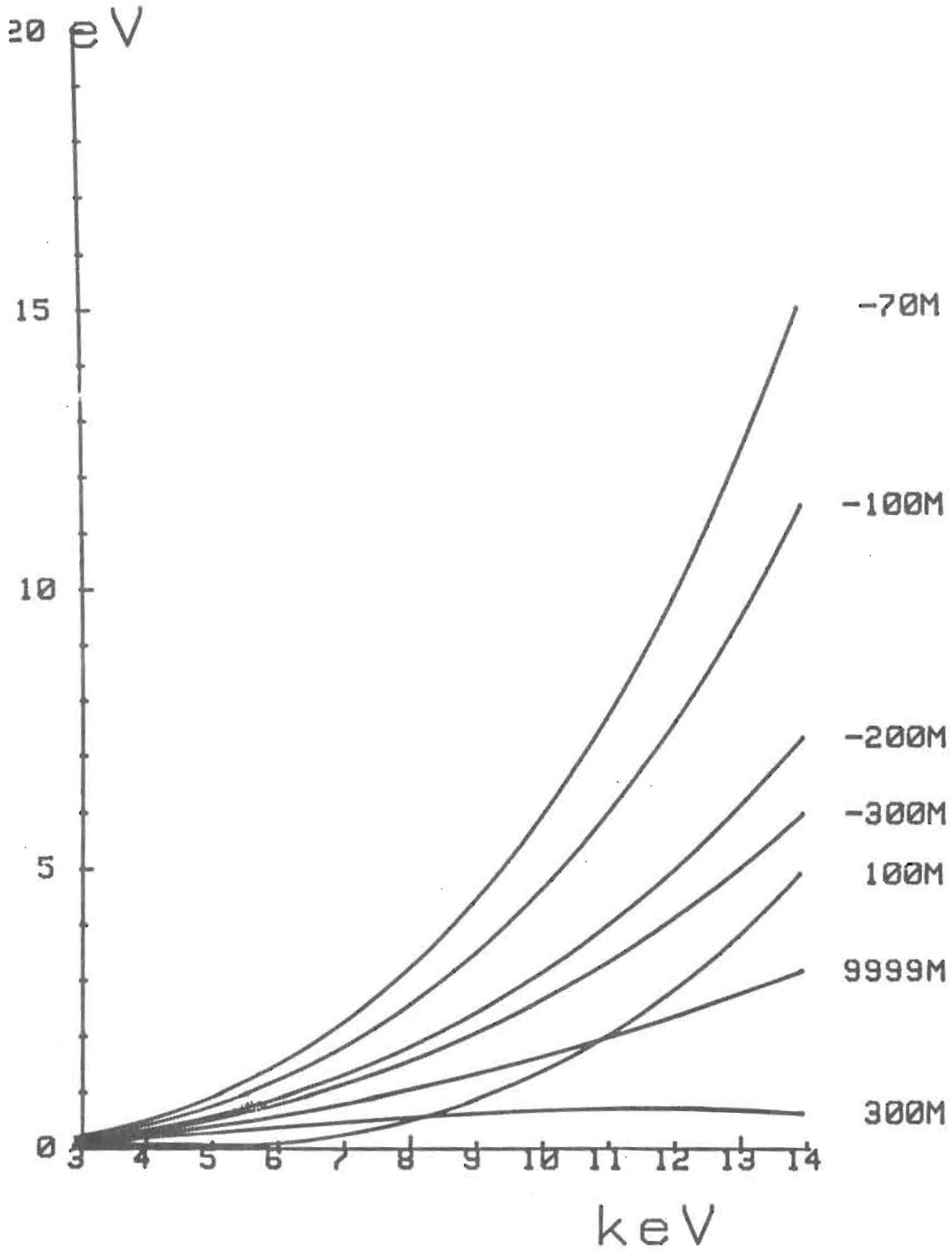


Deformation of a crystal due to a gaussian heat load. An extra bend due to mounting of the crystal may be superposed.

TPD

D. what I have said before is enough of an instruction I think and I like
to convey through the words of our poems, regarding.

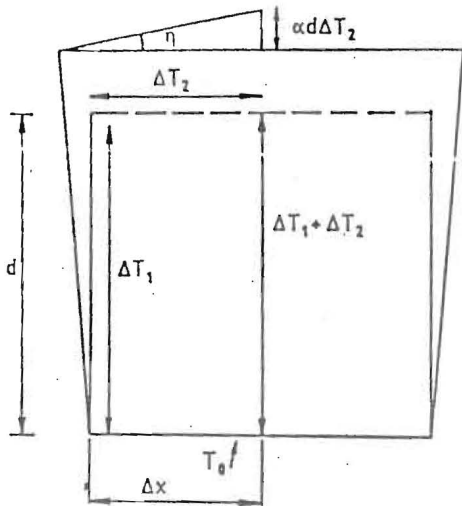
SOURCE SIZE .115 MM
BEAM APERTURE .033 MRAD
DISTANCE 35.0 M
Si 111



What happens if a gaussian beam hits a crystal.

- 1) The crystal gets a focusing effect.
- 2) Superposed may be an extra bending due to any the crystal is not flat.
- 3) One can define several radii of curvature.
How essential is a radius of curvature?

TPD



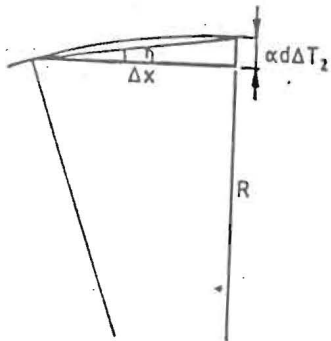
$$\eta = \frac{\alpha d \Delta T_2}{\Delta x}$$

$$\alpha = 2.5 \cdot 10^{-6}$$

$$d = 1 \text{ mm} = 10^{-3} \text{ m}$$

$$\eta \leq 1 \text{ arc sec} = 5 \cdot 10^{-6}$$

Longitudinal temp gradient $\frac{\Delta T_2}{\Delta x} \leq \underline{\underline{2 \text{ K/mm}}}$



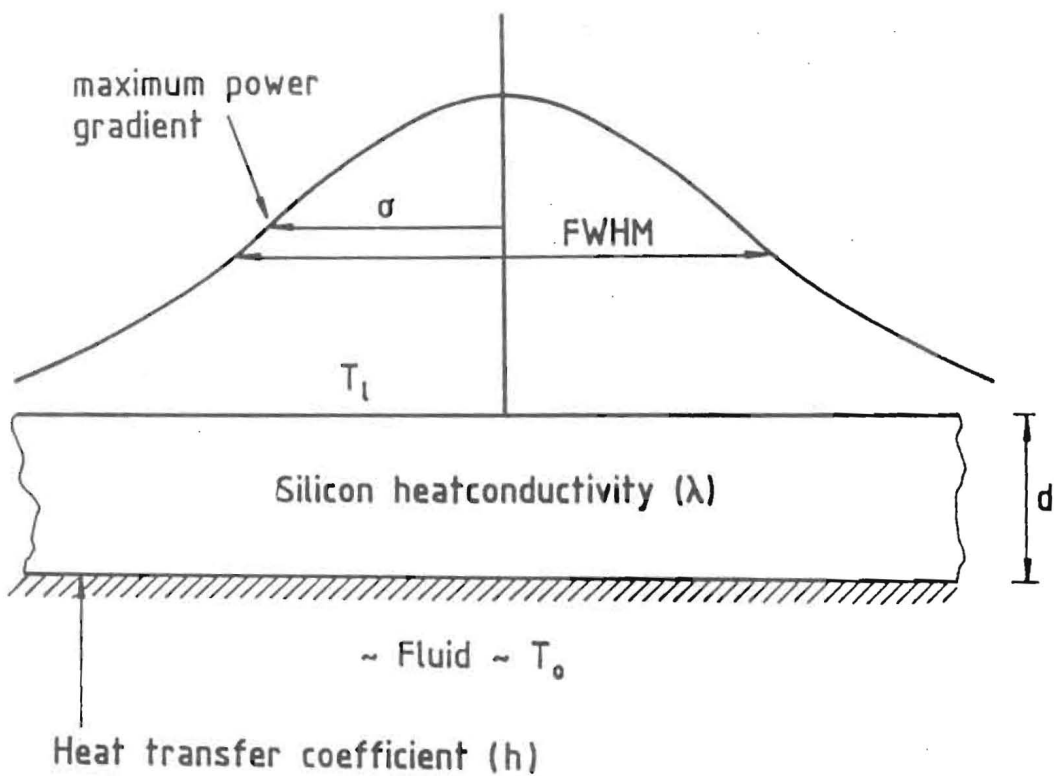
$$R = \frac{(\Delta x)^2}{2 \alpha d \Delta T_2}$$

$$2 \text{ K/mm} \rightarrow R = 100 \text{ m}$$

TPD

- Influence ^{etc.} of thermal effects.
- Only geometric effects.
 - Worst case.
 - One crystal
 - Loss of useful radiation.

TPD



$$\rightarrow T_l = T_0 + P_l \left(\frac{d}{\lambda} + \frac{1}{h} \right)$$

$$P_l = P_{\max} \exp\left(-\frac{1}{2} \left(\frac{x}{\sigma}\right)^2\right) = P_{\max}^{\perp} \sin\beta \exp\left(-\frac{1}{2} \left(\frac{x \sin\beta}{\sigma_{\perp}}\right)^2\right)$$

Lateral power gradient:

$$\Delta P_l = -P_{\max}^{\perp} \frac{\sin^3\beta}{\sigma_{\perp}^2} x \exp\left(-\frac{1}{2} \left(\frac{x \sin\beta}{\sigma_{\perp}}\right)^2\right)$$

Maximum lateral power gradient at $x = \frac{\sigma_{\perp}}{\sin\beta}$

$$\Delta P_{\max} : -P_{\max}^{\perp} \frac{\sin^2\beta}{\sigma_{\perp}}$$

TNO



Maximum temperature gradient:

$$\longrightarrow \left(\frac{\Delta T}{dx} \right)_{\max} = P_{\max} \frac{\sin^2 \beta}{\sigma_{\perp}} \left(\frac{d}{\lambda} + \frac{1}{h} \right) \quad \text{K/mm}$$

$$2 = 100 \cdot \frac{\sin^2 \beta}{\sigma_{\perp}} \left(\frac{1}{0.14} + \frac{1}{0.02} \right)$$

$$\sin^2 \beta = 4 \cdot 10^{-6} \quad \sin \beta = 0.02$$

$$\beta = 20 \text{ mrad} \quad \text{i.e. } \underline{1^\circ}$$

Very grazing incidence

$$\underline{P_{\max} = 2 \text{ W/mm}^2}$$



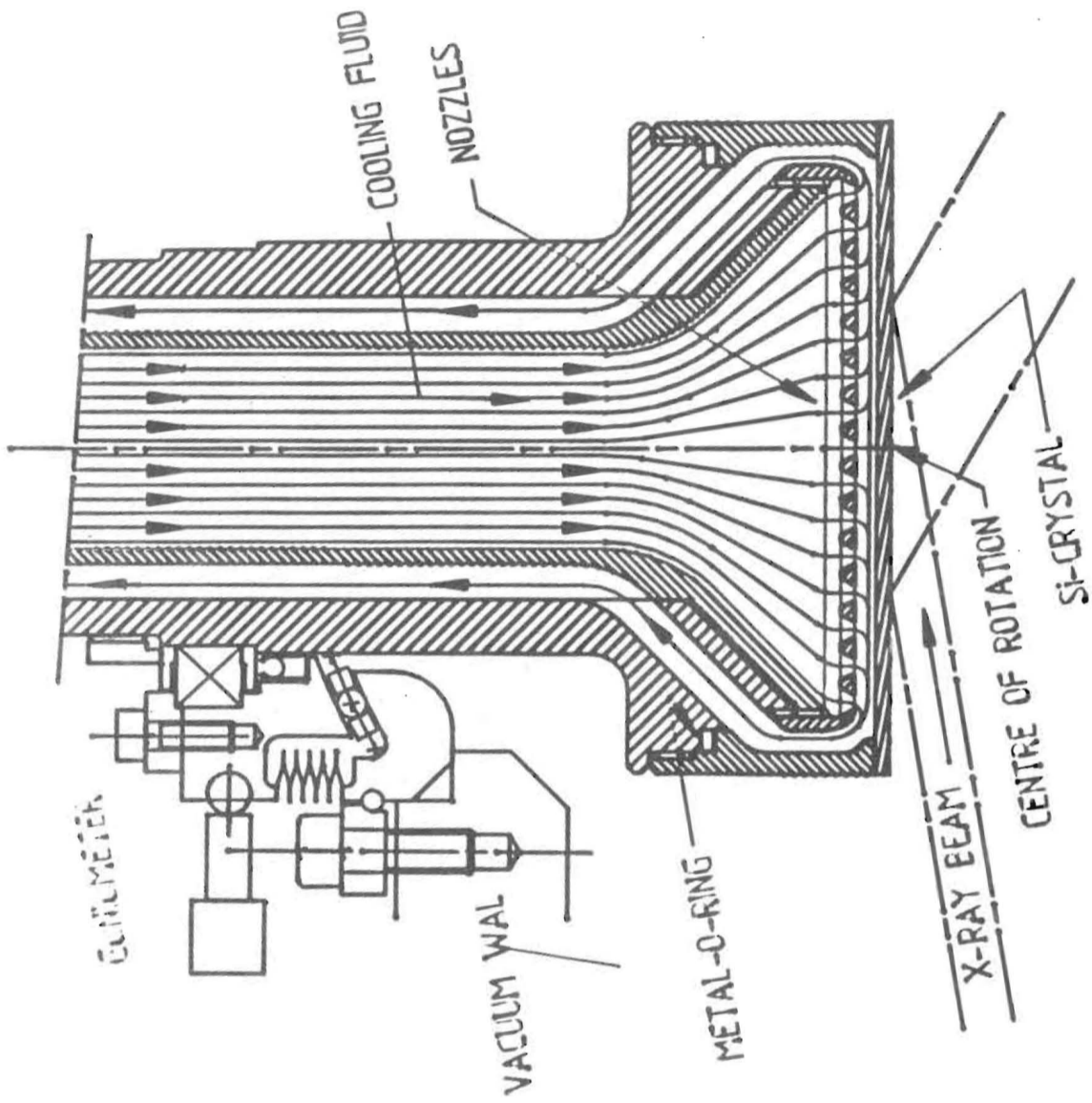
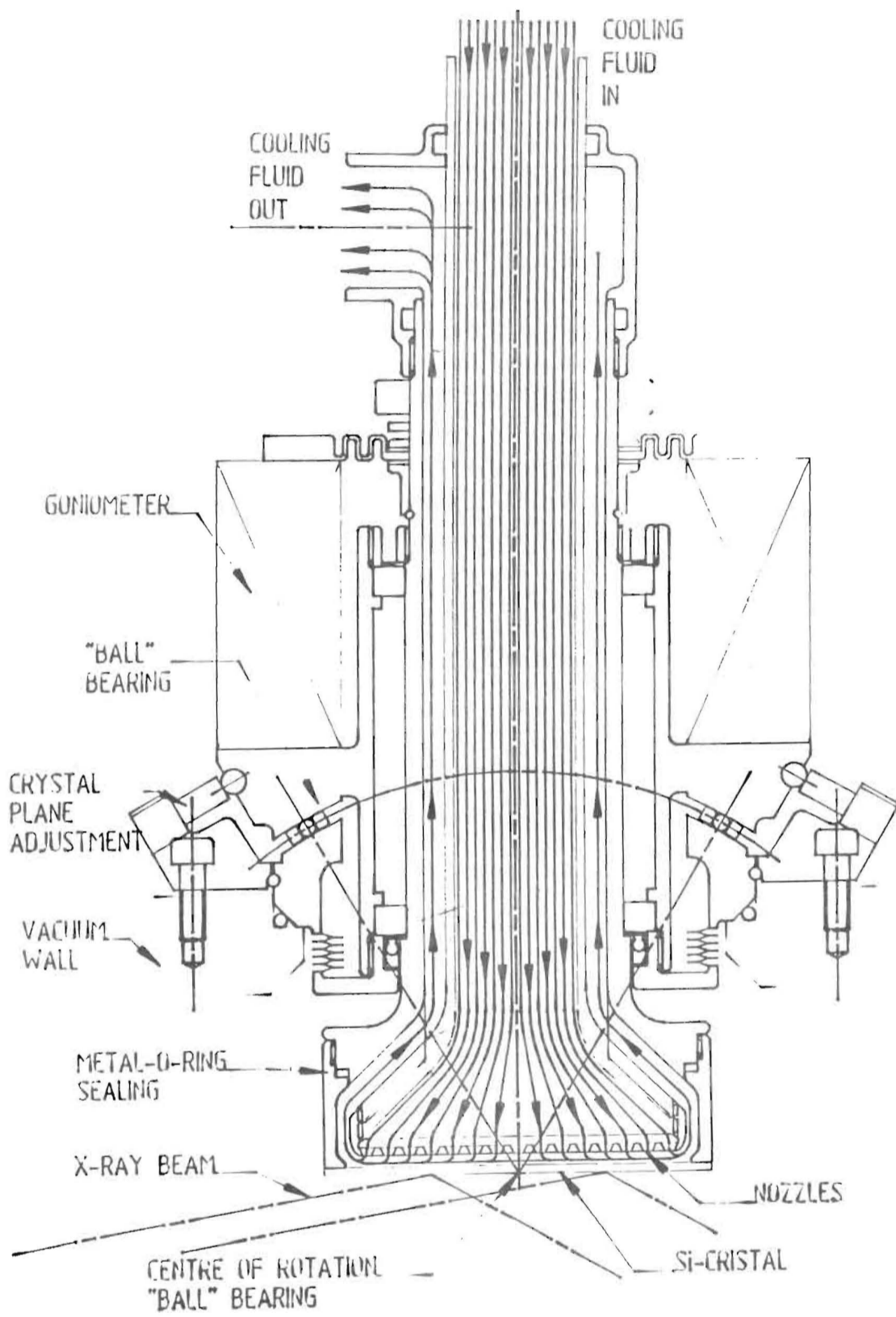


Fig. 10.1 Sketch of first crystal with cooling and goniometer.



- Anisotropic crystal → G. Gudenberg, A. Weichert
- Rotation & correction.
- constant angle of incidence → heat conduct constant.
- cooling through needles.
 - ↳ 100 needles, low water pressures compared with microchannels
 - ↳ little machining in silicon.
 - ↳ no channels
 - ↳ good heat transfer coefficient.
 - ↳ flexible design
- No bodily water evaporation in vacuum. (balloons, flexible tubes etc.)



Conclusion

1. The lateral temperature gradient is the limiting factor in thermo-optical design.
Typical value 2K/mm.
2. Only optical elements working at grazing incidence can handle the heatload.
Typical value 1 degree
3. We have presented a new design for an X-ray monochromator.



DESIGN AND TESTING OF WATER-COOLED MONOCHROMATORS ON THE SRS WIGGLER BEAM-LINE

P. Pattison

Daresbury Laboratory, Warrington WA4 4AD, England

The superconducting wiggler beam-line at the SRS Daresbury supplies radiation to seven experimental stations over a total opening angle of 64 mrad. The power density at a 20 m station for 300 mA operating current is about 0.5 W/mm^2 in the orbital plane. Two designs for water-cooled monochromators are presented, for use on a high resolution powder diffraction station and an EXAFS station. These monochromators were designed and fabricated in the Department of Physics at Manchester University. For the powder diffraction experiment, a channel-cut Si(111) monochromator accepts a beam cross section of $2.5 \times 8 \text{ mm}^2$ (corresponding to a heat load of about 10 W). The cooling of the first reflecting surface is achieved by forcing a jet of water at the underside of the crystal (in a similar way to the cooling of an X-ray tube). Preliminary tests have shown that the cooling system works well, but underlined the importance of good temperature stability for the cooling water. The EXAFS monochromator intercepts a beam with a maximum cross section of $2 \times 60 \text{ mm}^2$, resulting in a heat load of 54W. Here the design calls for two separate crystals, in which the first crystal has a cylindrical channel of 12 mm bore for the water cooling. The choice of Si(111) reflecting planes will allow the energy range 6 keV to 34 keV to be covered using one pair of crystals. Details of the monochromator design and assembly have been presented at the SRI-88 Conference.

Water-cooled, channel-cut monochromator

Wiggler beam-line

5T wiggler 2 GeV 300mA

→ 6kW into ca. 75 mrad \approx 80 W/mrad

Station 9.1 at 16m

Heat load \approx 1 W/mm² on axis at
centre of wiggler fan

Station 9.1 is 30 mrad from centre
and including absorption:

Heat load \approx 0.5 W/mm²

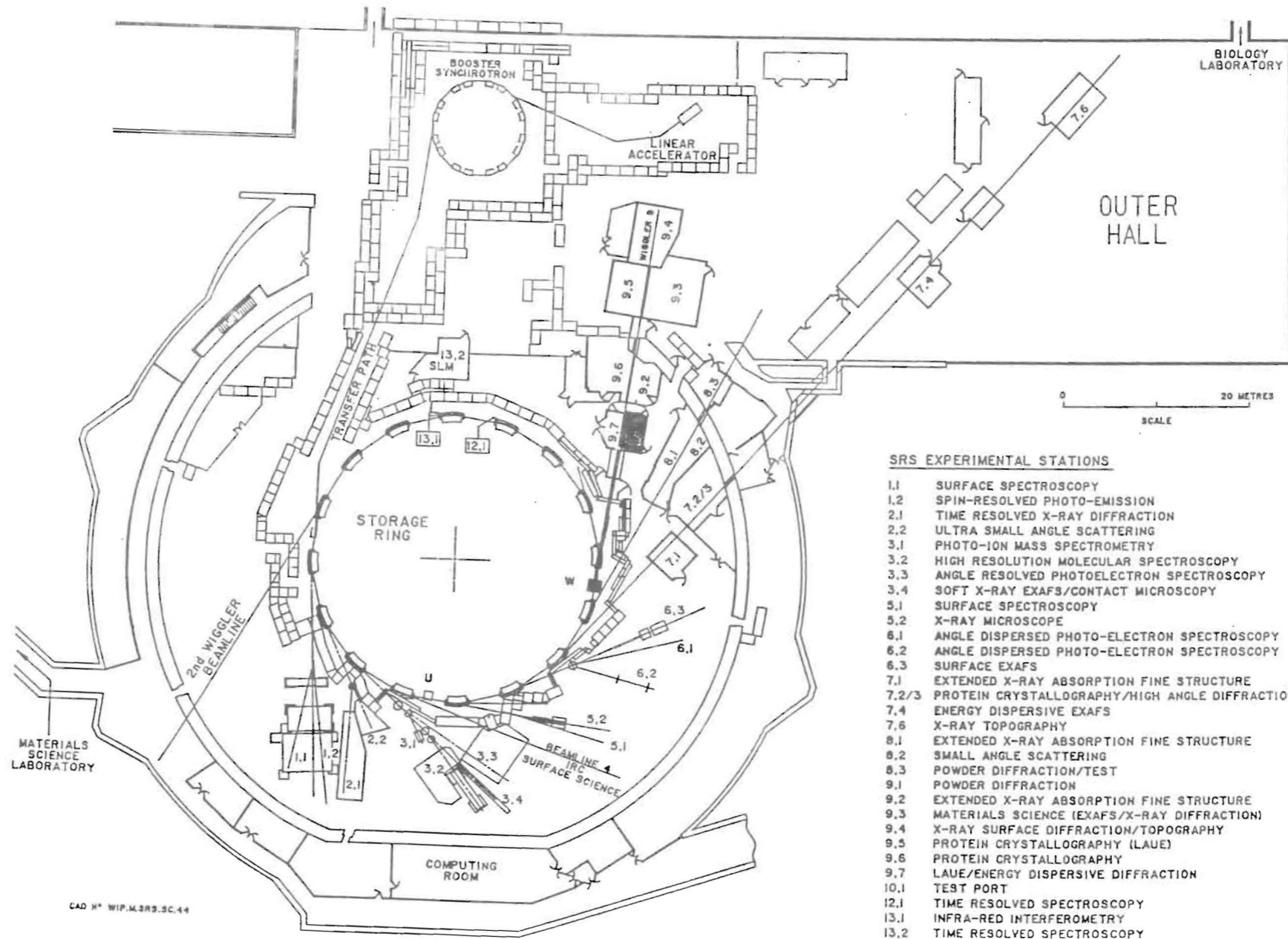
Monochromator

Si (111) channel cut

$\theta_{\text{Bragg}} \sim 4^\circ - 18^\circ$

Beam of 2.5mm x 8mm on monochromator

→ 10 W

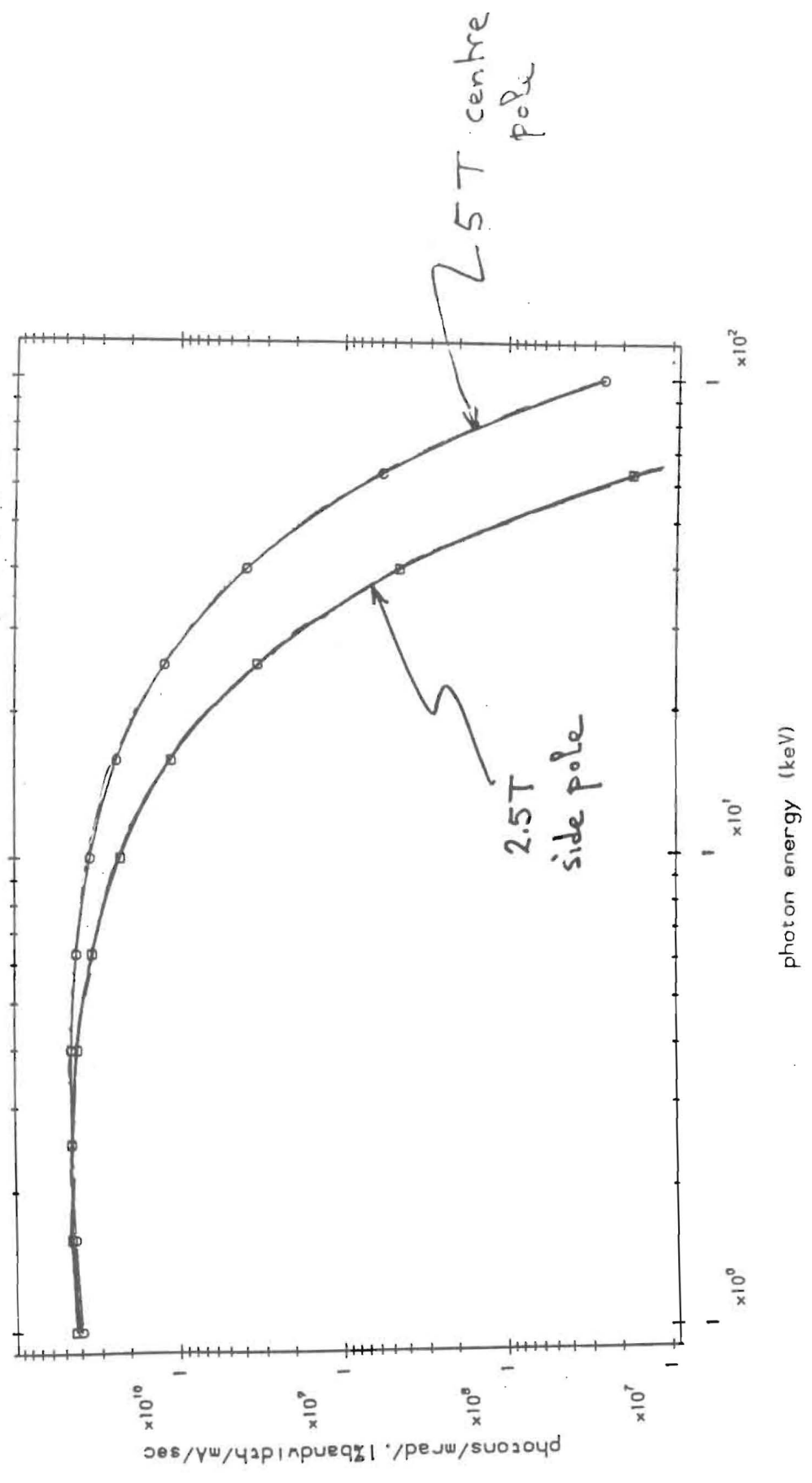


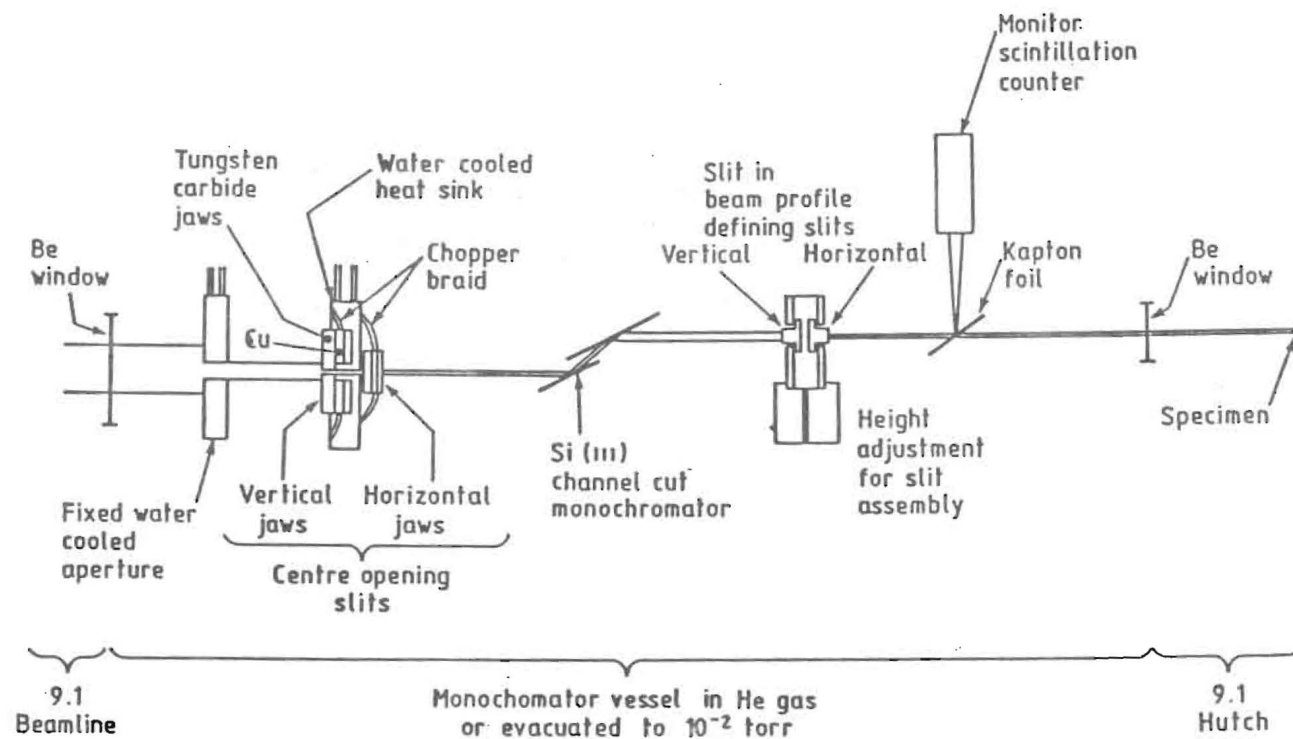
SRS EXPERIMENTAL STATIONS

- 1.1 SURFACE SPECTROSCOPY
- 1.2 SPIN-RESOLVED PHOTO-EMISSION
- 2.1 TIME RESOLVED X-RAY DIFFRACTION
- 2.2 ULTRA SMALL ANGLE SCATTERING
- 3.1 PHOTO-ION MASS SPECTROMETRY
- 3.2 HIGH RESOLUTION MOLECULAR SPECTROSCOPY
- 3.3 ANGLE RESOLVED PHOTOELECTRON SPECTROSCOPY
- 3.4 SOFT X-RAY EXAFS/CONTACT MICROSCOPY
- 5.1 SURFACE SPECTROSCOPY
- 5.2 X-RAY MICROSCOPE
- 6.1 ANGLE DISPERSED PHOTO-ELECTRON SPECTROSCOPY
- 6.2 ANGLE DISPERSED PHOTO-ELECTRON SPECTROSCOPY
- 6.3 SURFACE EXAFS
- 7.1 EXTENDED X-RAY ABSORPTION FINE STRUCTURE
- 7.2/3 PROTEIN CRYSTALLOGRAPHY/HIGH ANGLE DIFFRACTION
- 7.4 ENERGY DISPERSIVE EXAFS
- 7.6 X-RAY TOPOGRAPHY
- 8.1 EXTENDED X-RAY ABSORPTION FINE STRUCTURE
- 8.2 SMALL ANGLE SCATTERING
- 8.3 POWDER DIFFRACTION/TEST
- 9.1 POWDER DIFFRACTION
- 9.2 EXTENDED X-RAY ABSORPTION FINE STRUCTURE
- 9.3 MATERIALS SCIENCE (EXAFS/X-RAY DIFFRACTION)
- 9.4 X-RAY SURFACE DIFFRACTION/TOPOGRAPHY
- 9.5 PROTEIN CRYSTALLOGRAPHY (LAUE)
- 9.6 PROTEIN CRYSTALLOGRAPHY
- 9.7 LAUE/ENERGY DISPERSIVE DIFFRACTION
- 10.1 TEST PORT
- 12.1 TIME RESOLVED SPECTROSCOPY
- 13.1 INFRA-RED INTERFEROMETRY
- 13.2 TIME RESOLVED SPECTROSCOPY

CAD N° WIP.M.SRS.SC.44

5T Wiggler 30 mrad from centre of fan (station 9.1)





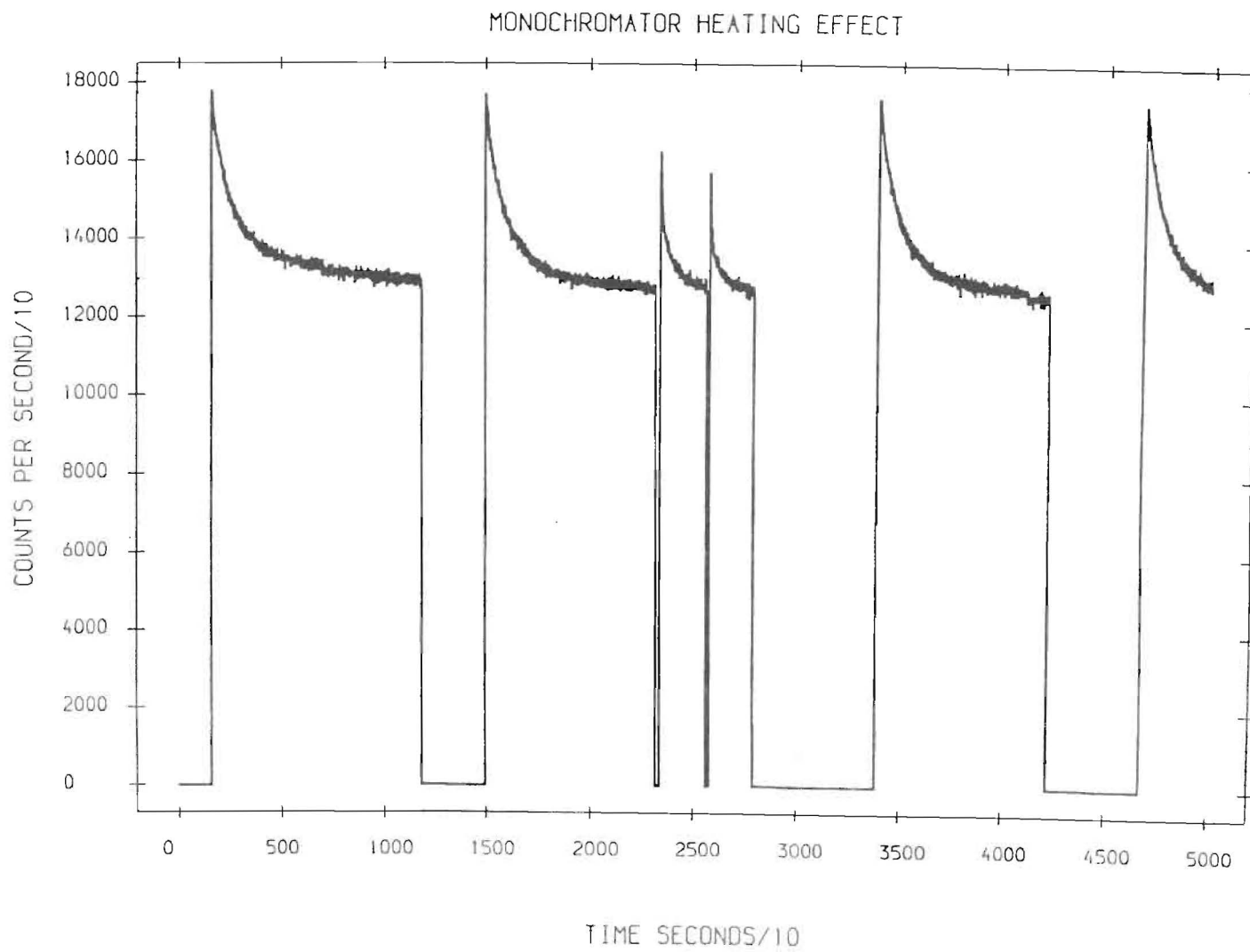
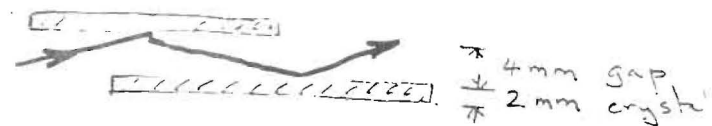
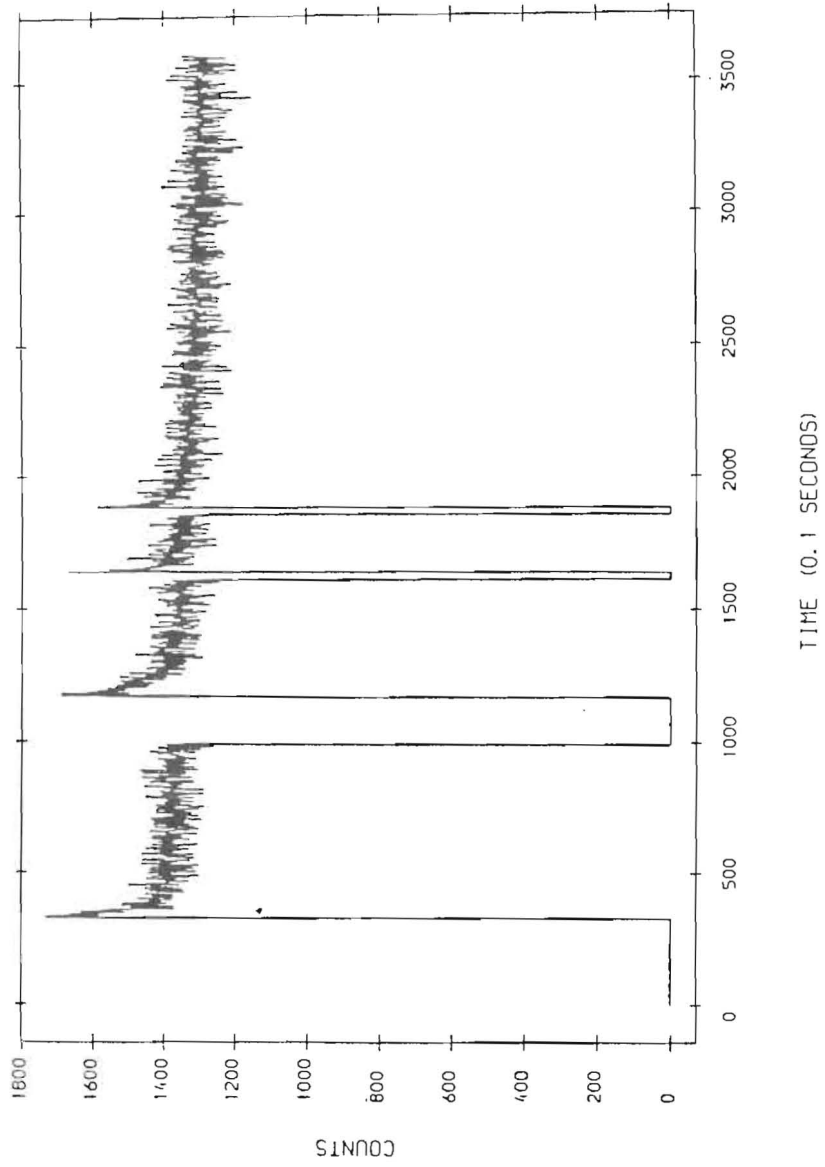


Fig 1

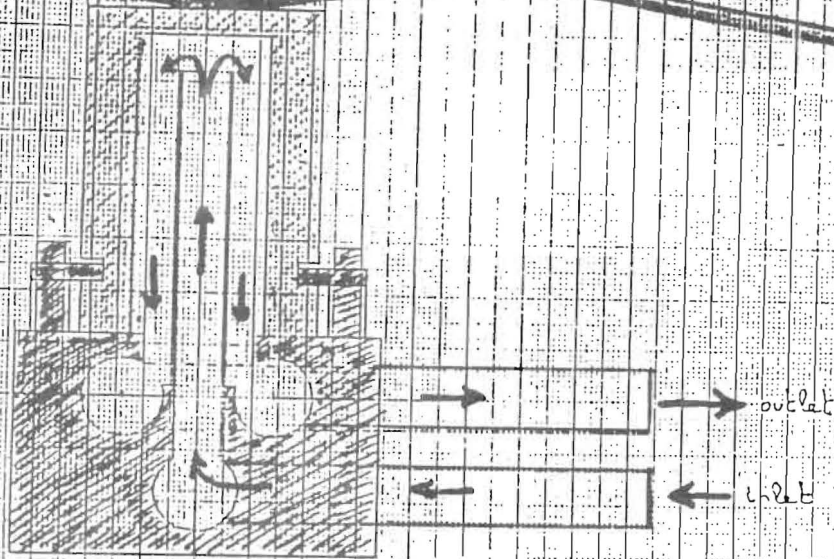


OLD CHANNEL CUT MONOCHROMATOR 5MM SLIT

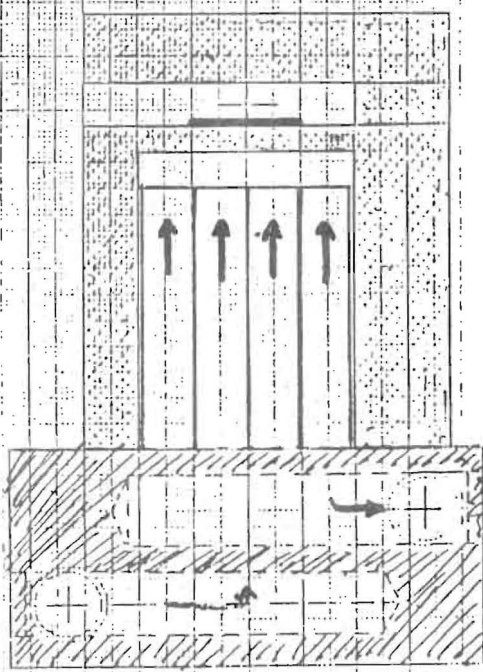
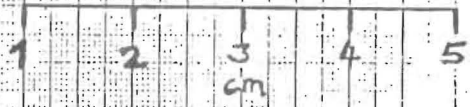


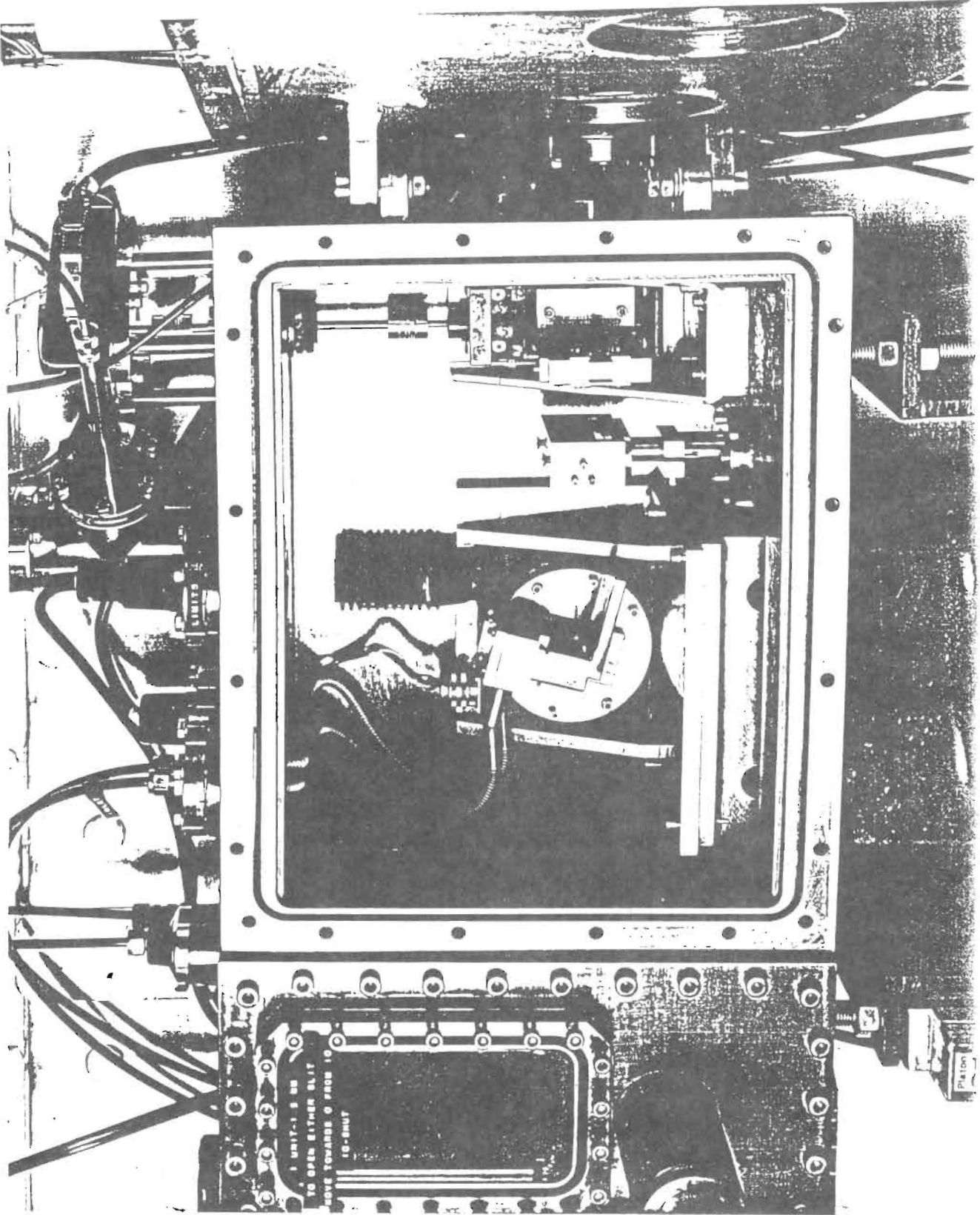
CHANNEL CUT Si (III) MONOCHROMATOR

WATER-FORCED MONOCHROMATOR

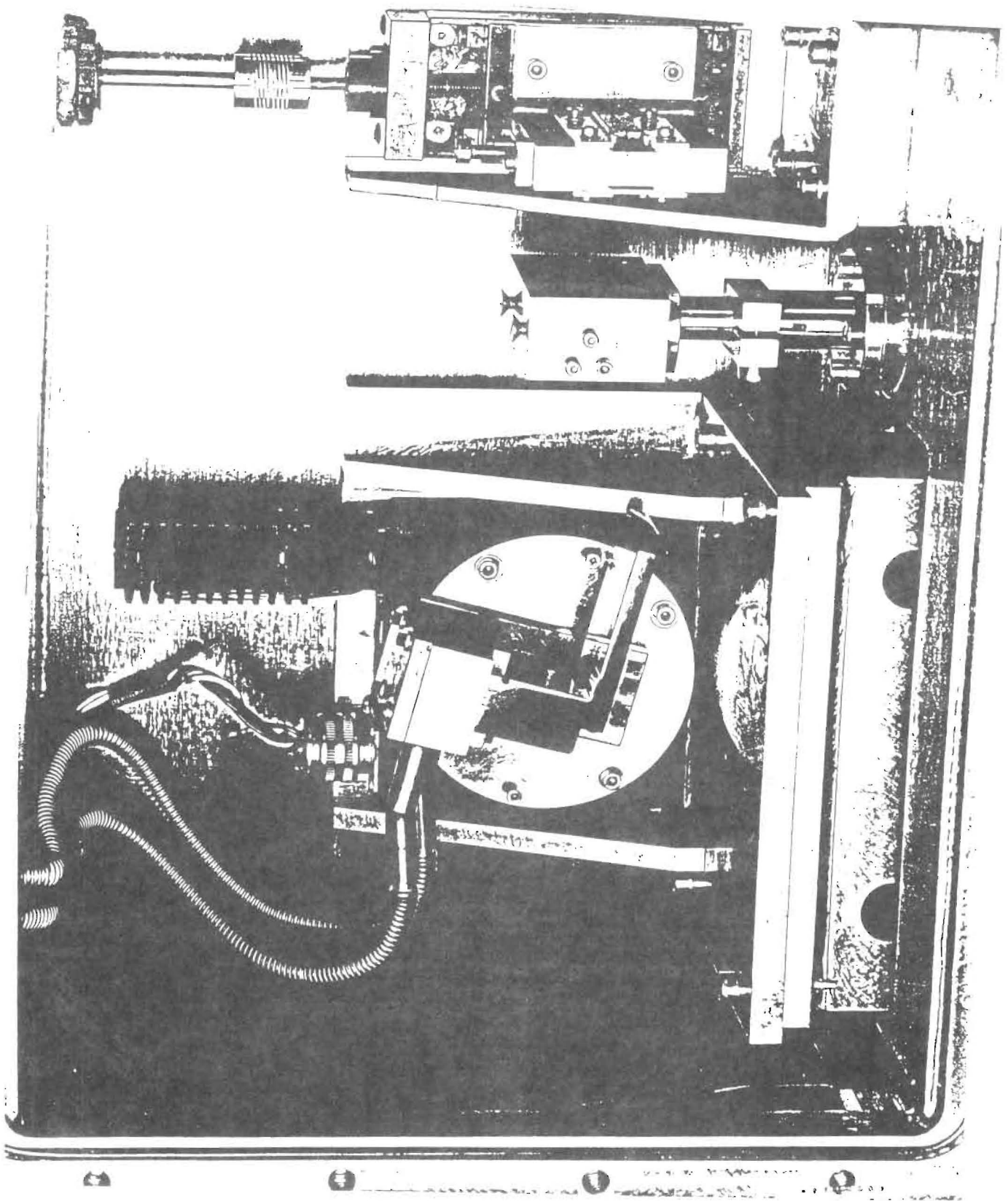


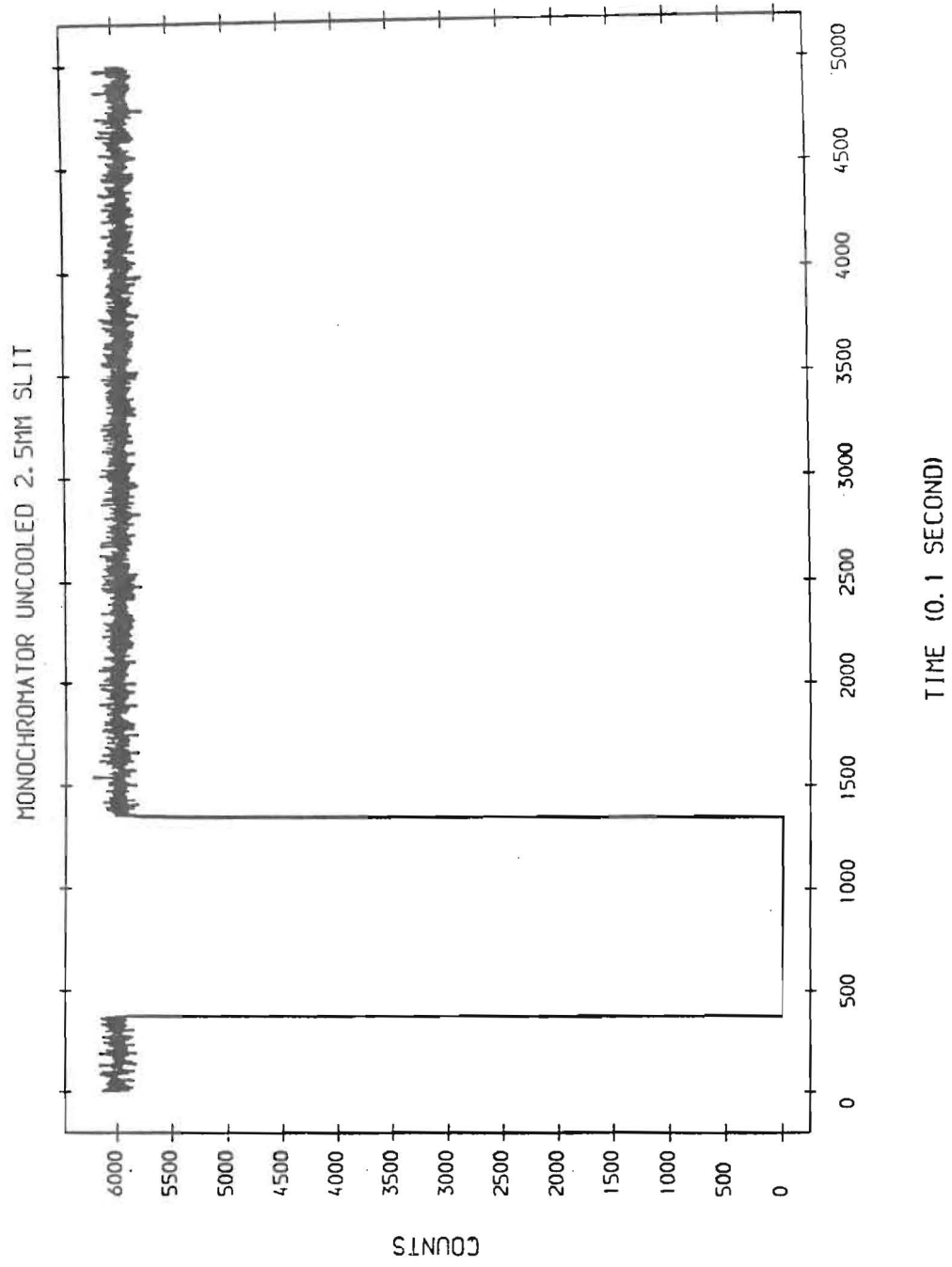
No strain is low
because of
distance of
refraction, and
from change

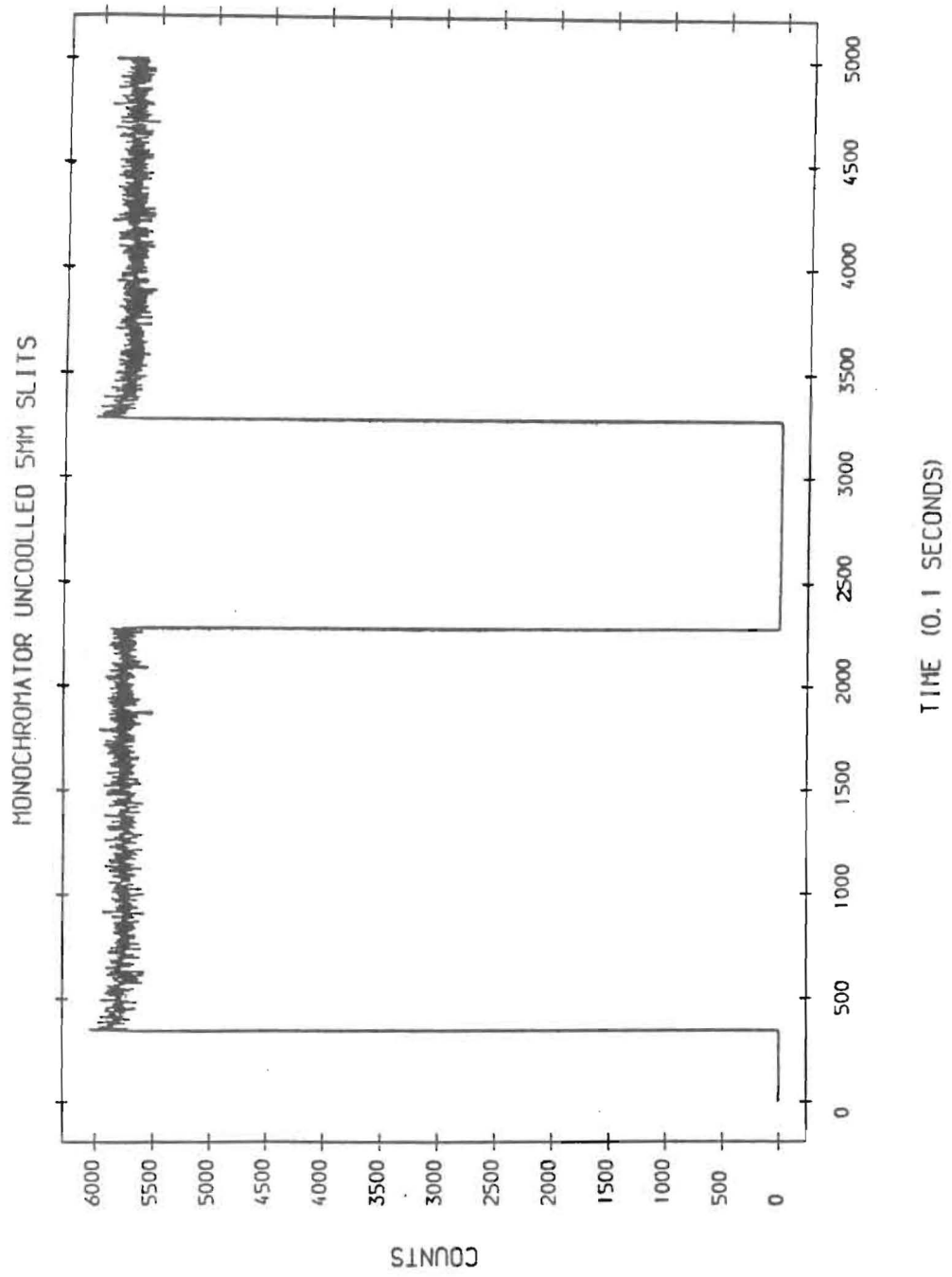


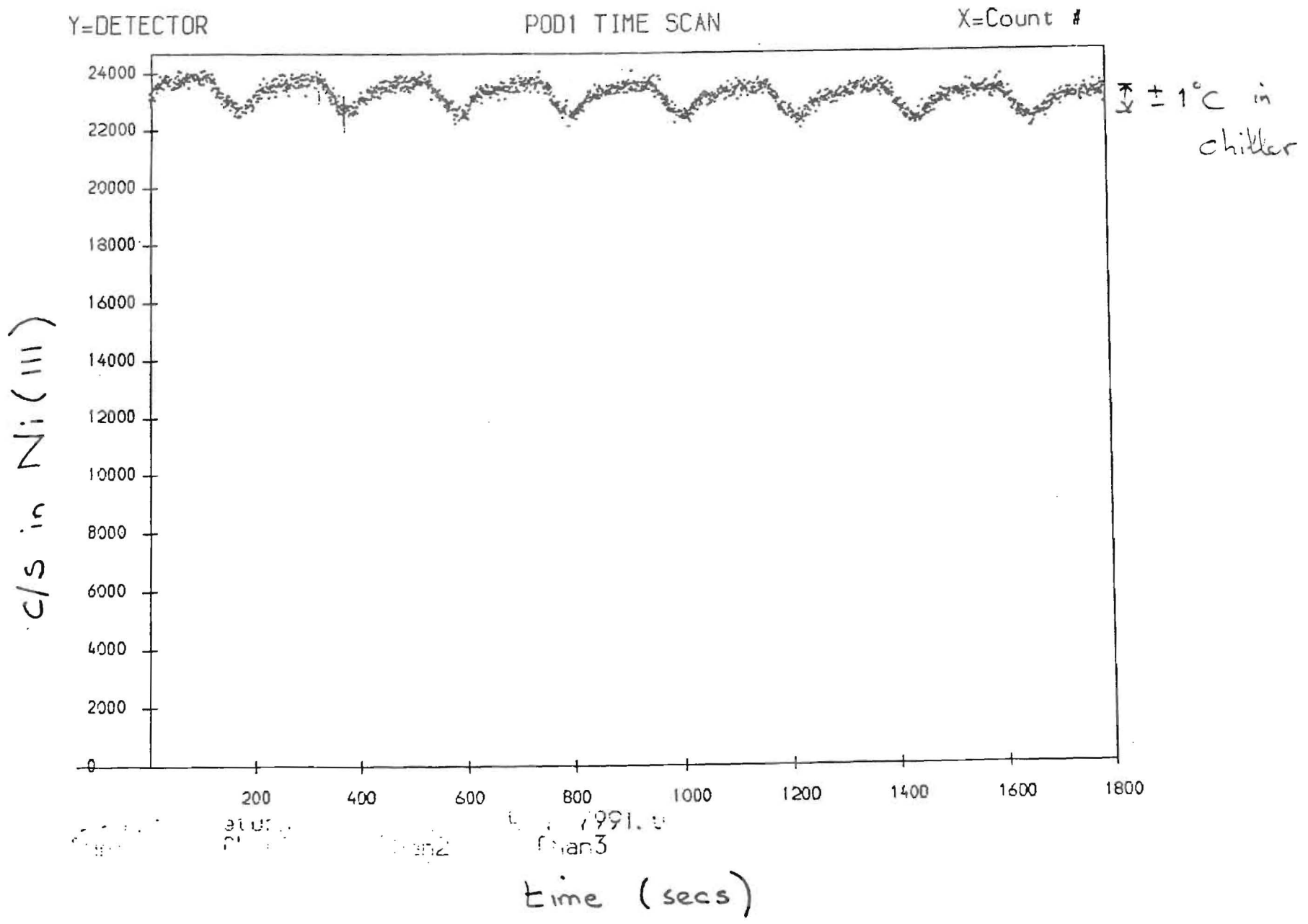


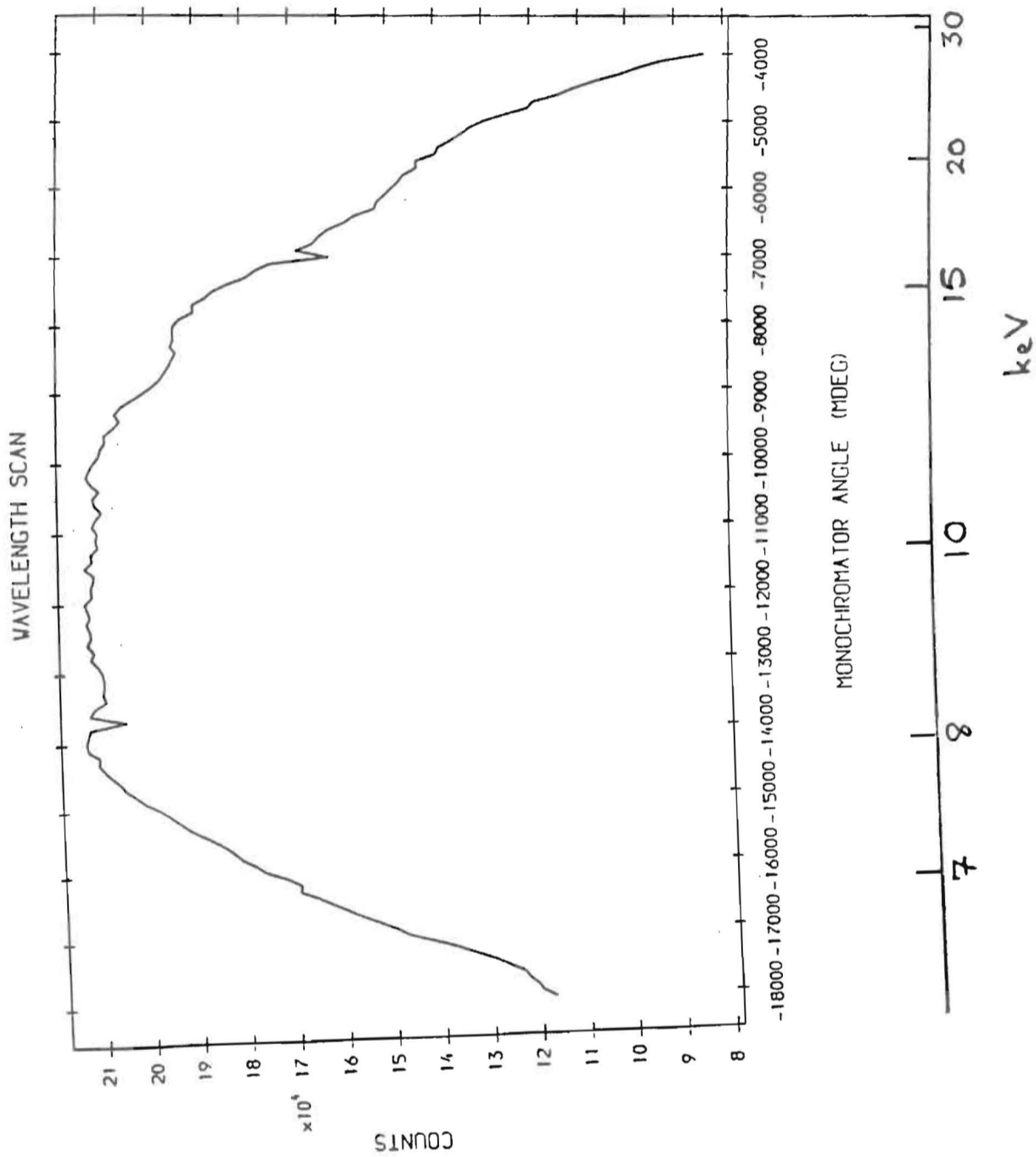
1 UNIT-3 IS SH
TO OPEN EITHER SLIT
MOVE TOWARDS 0 FROM 10
10-5000

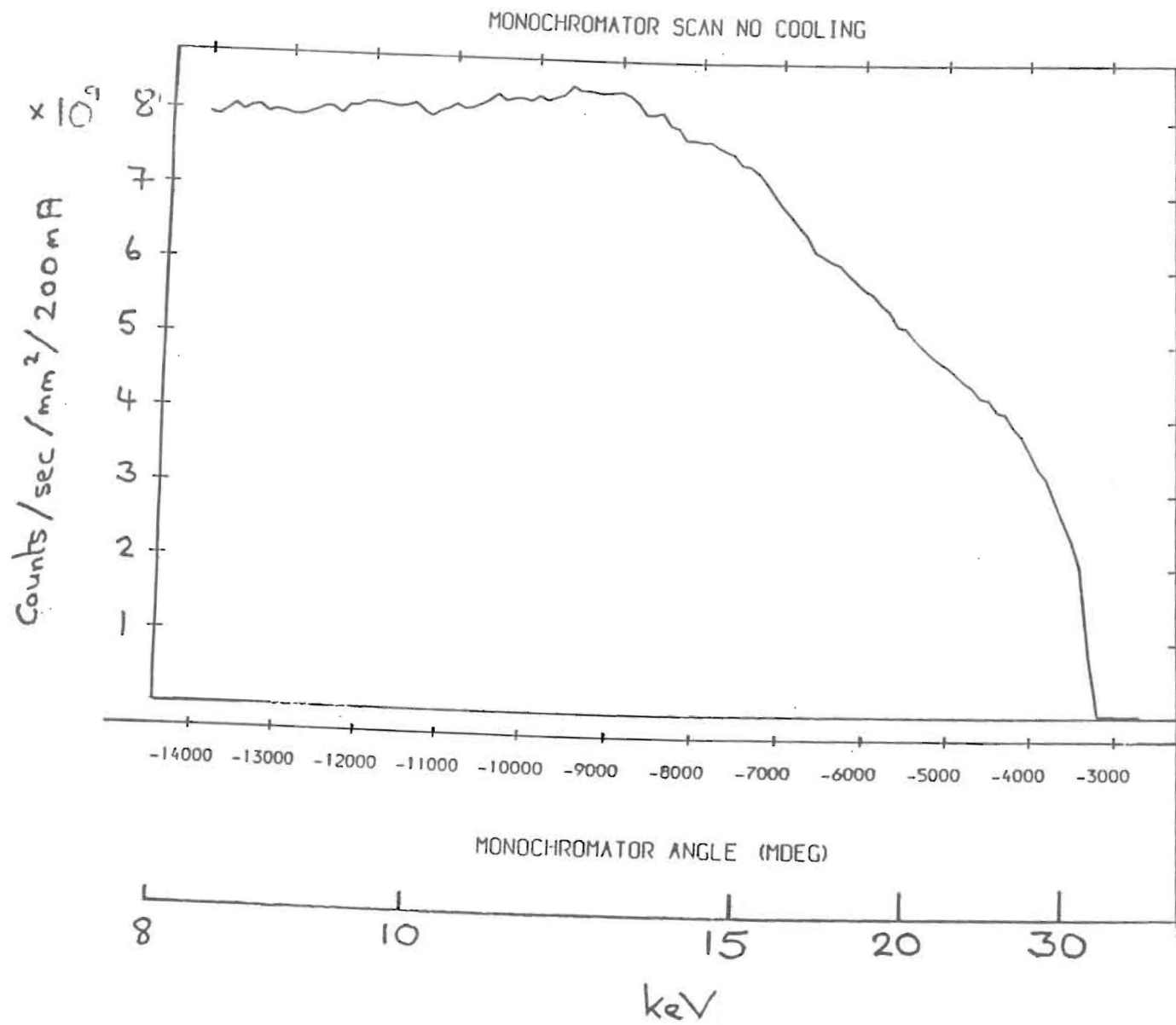












DIRECT-WATERCOOLED DOUBLE MONOCHROMATOR FOR QUANTITATIVE
MICROTOMOGRAPHY AT A SYNCHROTRON-RADIATION SOURCE

U. Bonse and R. Nußhardt

Institute of Physics, University of Dortmund, Federal Republic of
Germany

Abstract:

Double crystal monochromators when equipped with perfect crystals are capable of conditioning incident beams in a very well defined manner. This applies for example to the delivered wavelength and bandwidth, to beam divergence and beam cross section, to rejection or selection of harmonics, to suppression of Laue spots, and to the definition of polarization states¹⁻². Most of these properties are important parameters bearing on the performance of quantitative energy modulated microtomography³⁻⁶. In praxi however, because of the heat load imposed by the direct beam on the first crystal, cooling of this crystal is necessary in order to preserve its perfect crystal properties.

We describe⁷ the direct cooling with water of the first crystal of a double monochromator. Since the crystal is diffracting in the Bragg case solely the front layer with thickness of the order of 10 to 100 μm is engaged in the diffracting process. We therefore strive to cool this layer most directly by making the crystal less than 300 μ thick over the area where it is hit by the primary beam. At the same time, by this procedure, the total amount of radiation absorbed by the crystal itself is minimized. The thinned part is reinforced by ribs of crystal material in order to prevent bending under the impact of the coolant's flow pressure. Furthermore, special care is taken to avoid the imposing of mechanical stresses onto the crystal where it is connected to the water guiding rear cover. The perfect crystal qualities of the cooled crystal under applied radiation were tested by measuring rocking curves at the wavelenghts of the fundamental and the third harmonic.

¹U. Bonse, G. Materlik and W. Schröder, J.Appl. Crystallogr. 9 (1976) 223

²U. Bonse, K. Olthoff-Münter and A. Rumpf, J.Appl. Crystallogr. 16 (1983) 524

³U. Bonse, Q.C. Johnson, M. Nichols, R. Nußhardt, S. Krasnicki and J. Kinney, Nucl. Inst. Meth. A246 (1986) 644

⁴W. W.-R. Dix, K. Engelke, C.-C. Glüer, W. Graeff and K.H. Stellmaschek, HASYLAB Report, Hamburg 1986, 393

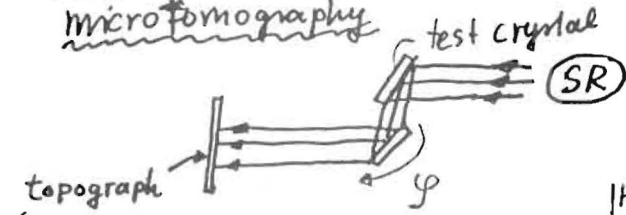
⁵Y. Suzuki, K. Usami, K. Sakamoto, H. Kozaka, T. Hirano, H. Shiono and H. Kohno, Jap.J.Appl.Phys. 27 (1988) L461

⁶B.P. Flannery, H. Deckman, W. Roberge, K. D'Amico, Science 237 (1987) 1439

⁷U. Bonse, R. Nußhardt, R. Pahl, Q. Johnson, J. Kinney, A. Saroyan and M. Nichols, HASYLAB Report, Hamburg 1986, 395

Direct-watercooled double monochromator for quantitative microtomography

Heat Load:

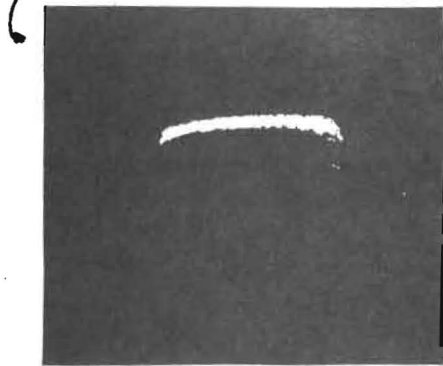


U. Bonse
R. Nussbaardt

Univ. Dortmund

[HASYLAB Report 1986]

DORIS: about 50 mA
3.7 GeV
bending magnet
 $\approx 1.4 \text{ \AA}$ wave length

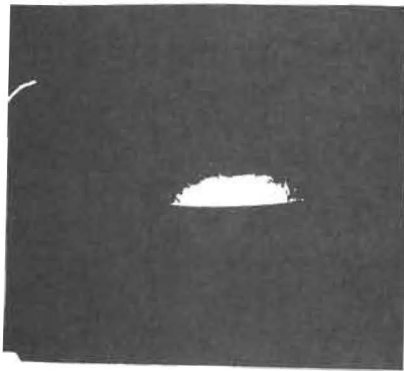


a)

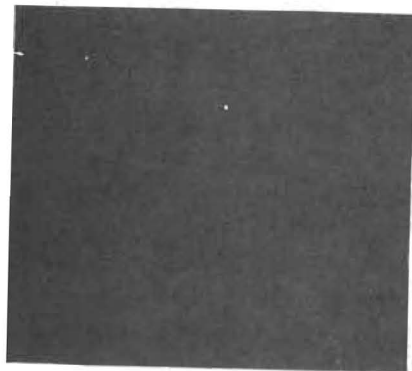
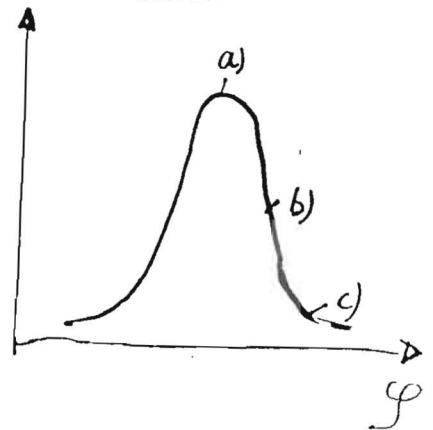
Intensitätsverteilung
im monochromatisierten
Strahl

Si 8 0 0 $\theta_B = 45^\circ$

- a) maximale Intensität
- b) und c) zwei Positionen auf der rechten Flanke der Rockingkurve



b)



c)

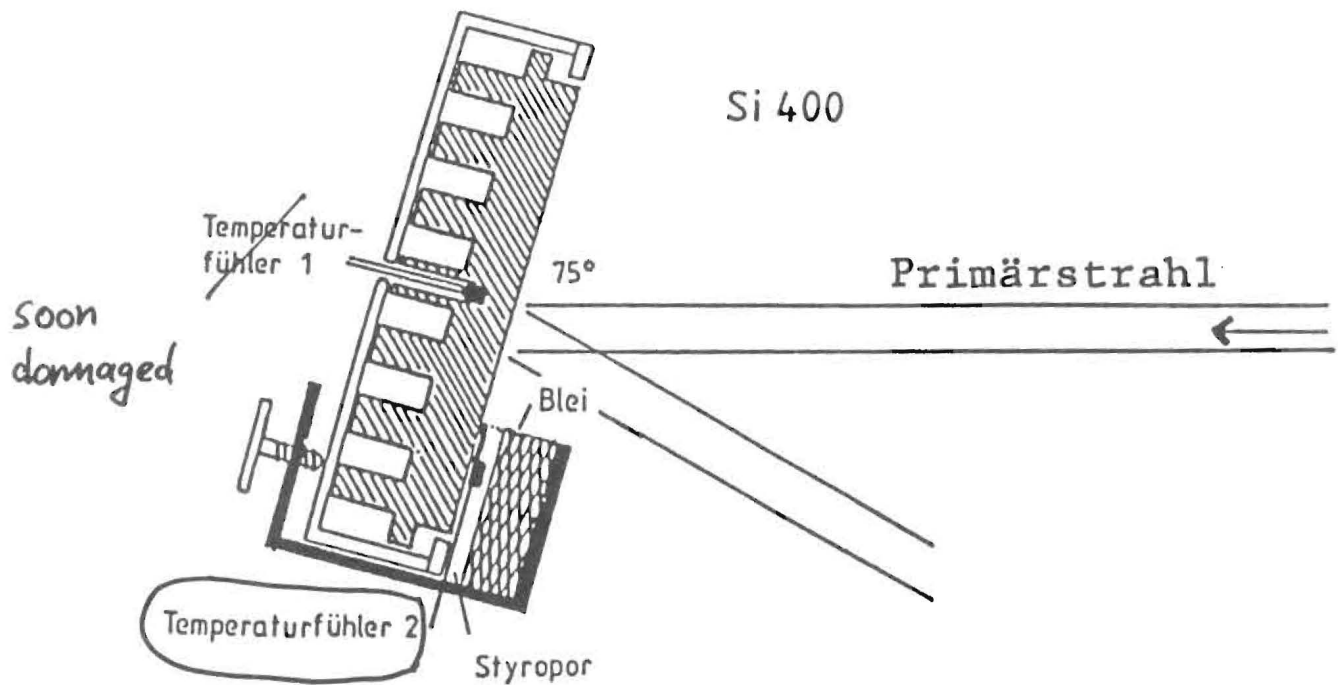


crystal is bent and has no longer properties of a

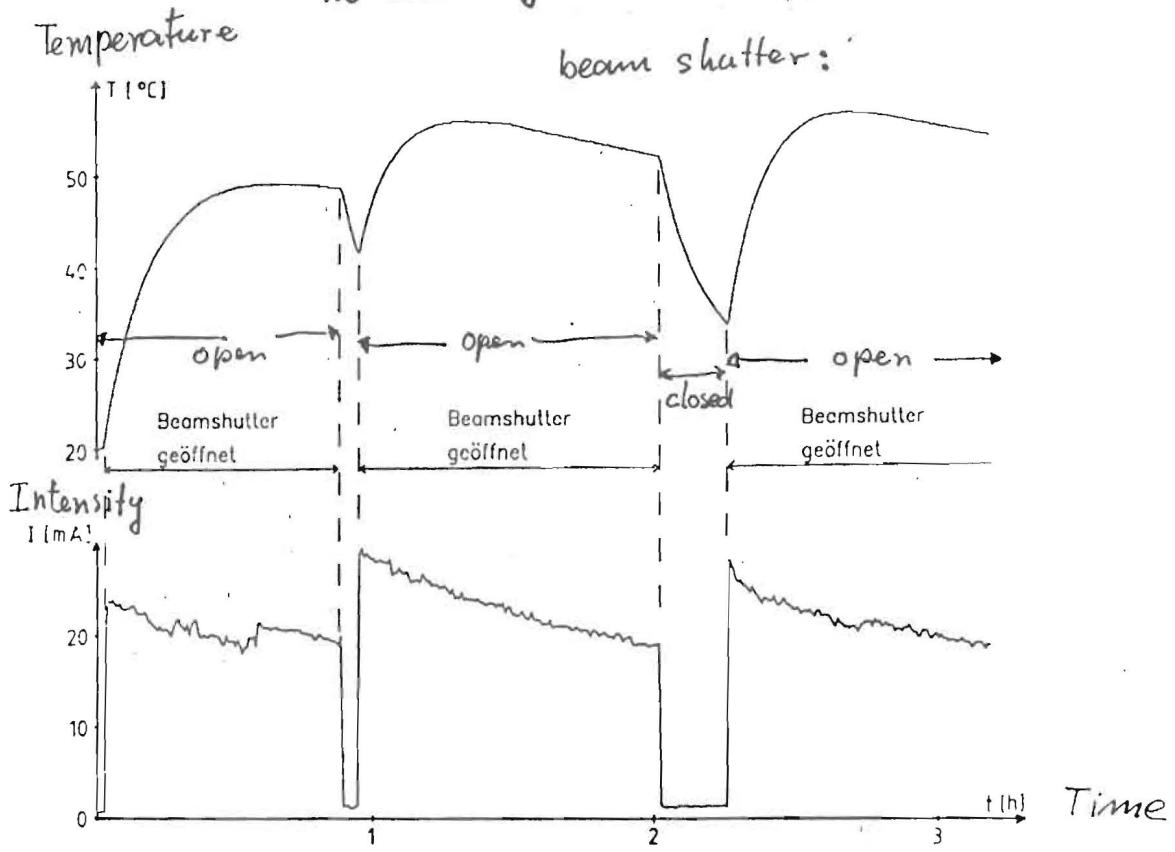
perfect crystal. Beam conditioning by making use of dynamical diffraction properties no longer possible

Der wassergekühlte Si400-Kristall

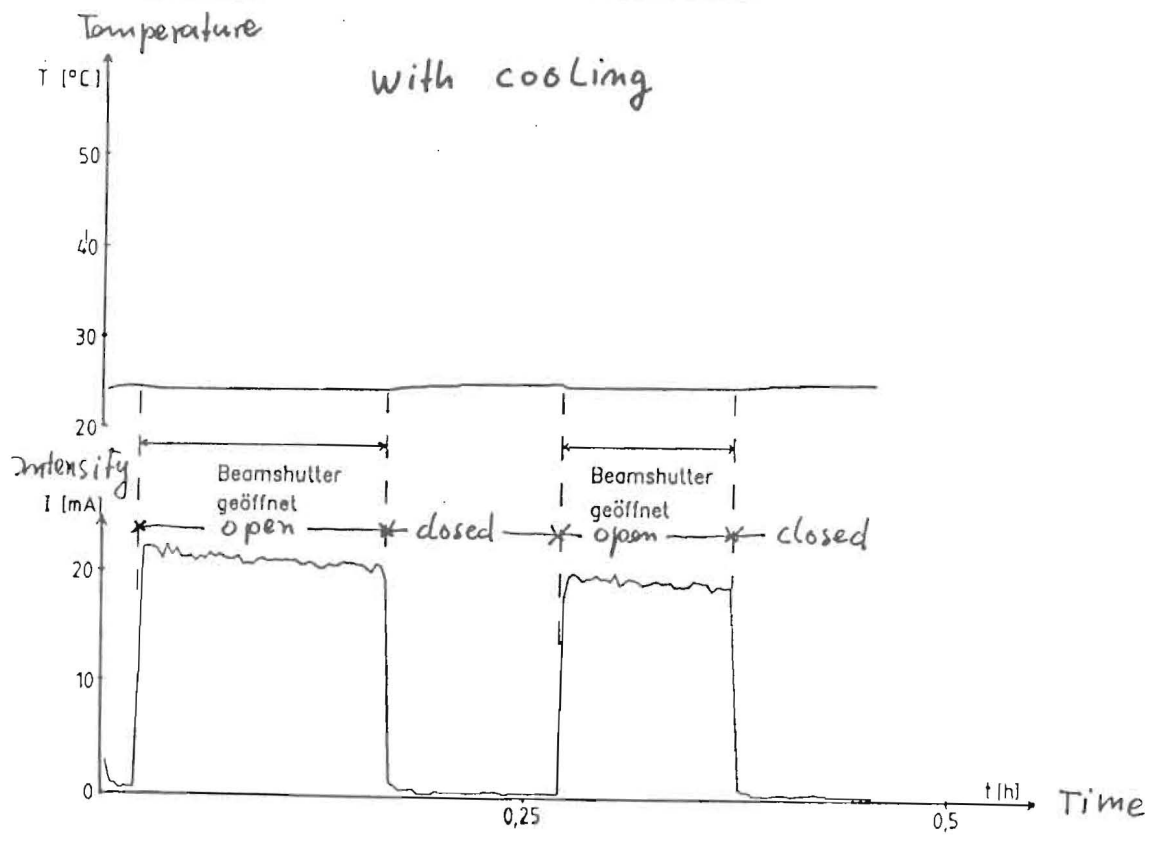
How the temperature is measured at the first crystal
Influence of cooling determined with test crystal



No Cooling (water stopped)

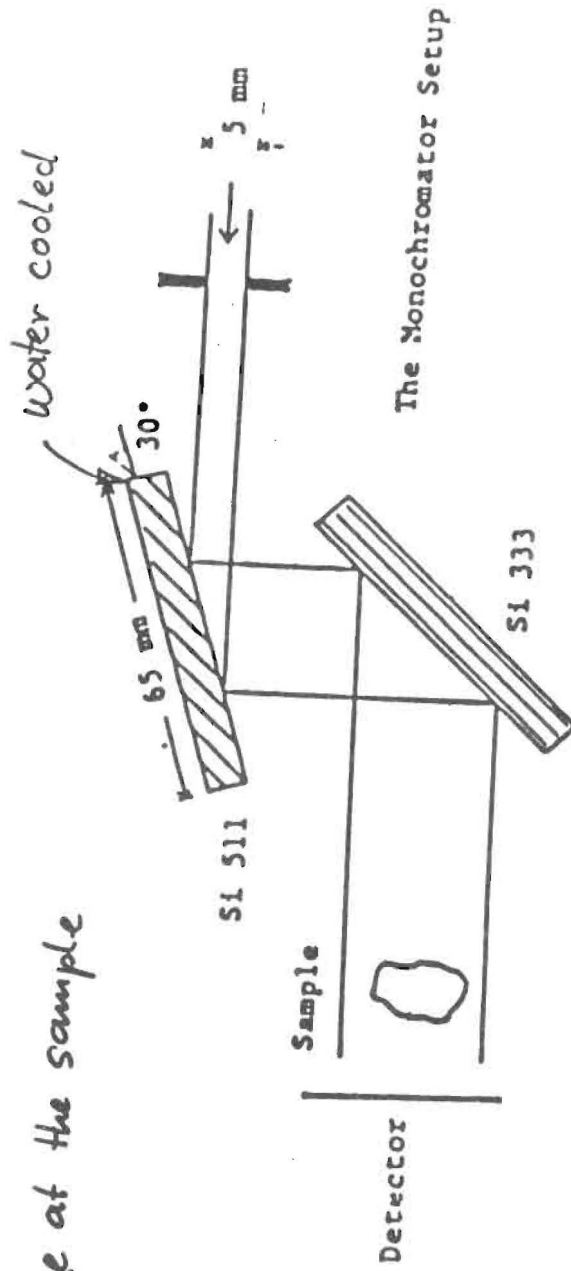


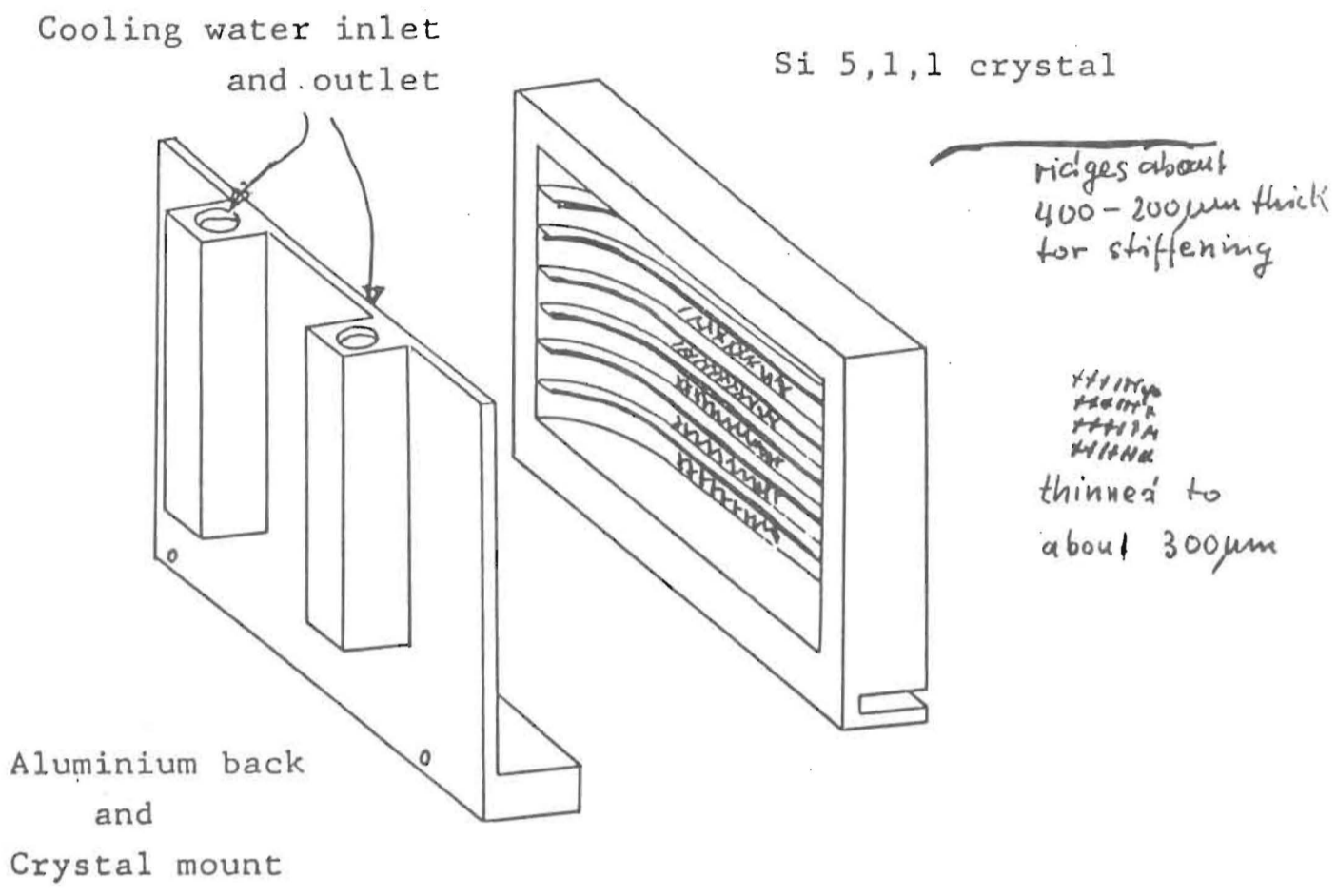
with cooling

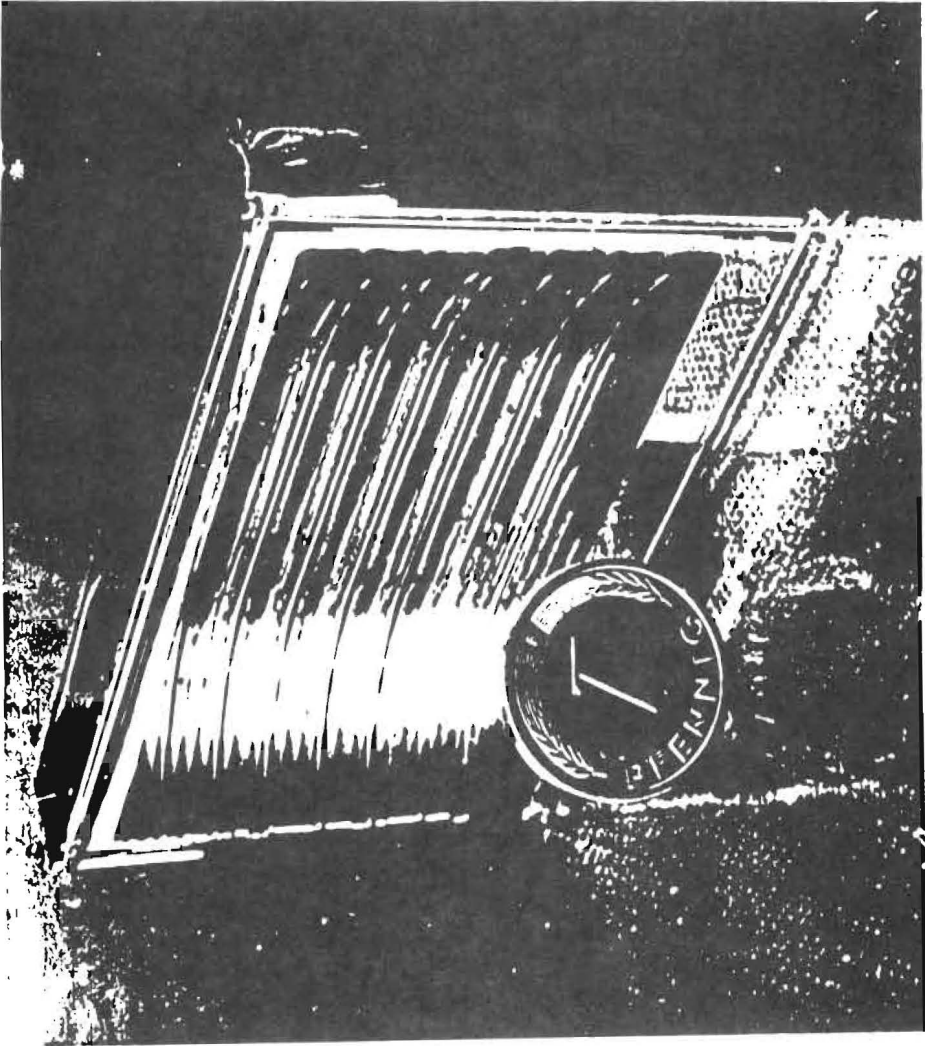


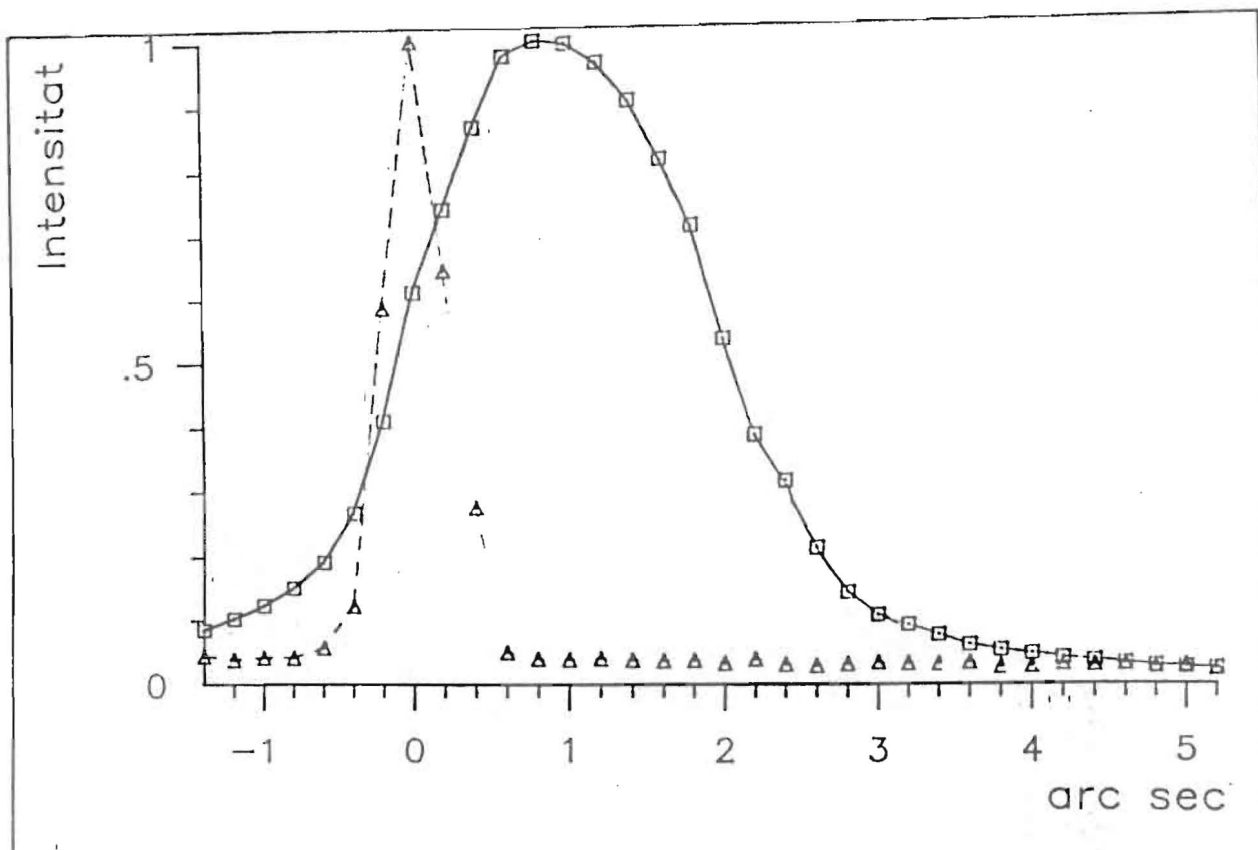
New monochromator optimized for

- ① rejection of Lorentz spots
- ② " " harmonics
- ③ maintaining dynamical reflection characteristics
- ④ widening the beam
- ⑤ reducing divergence at the sample







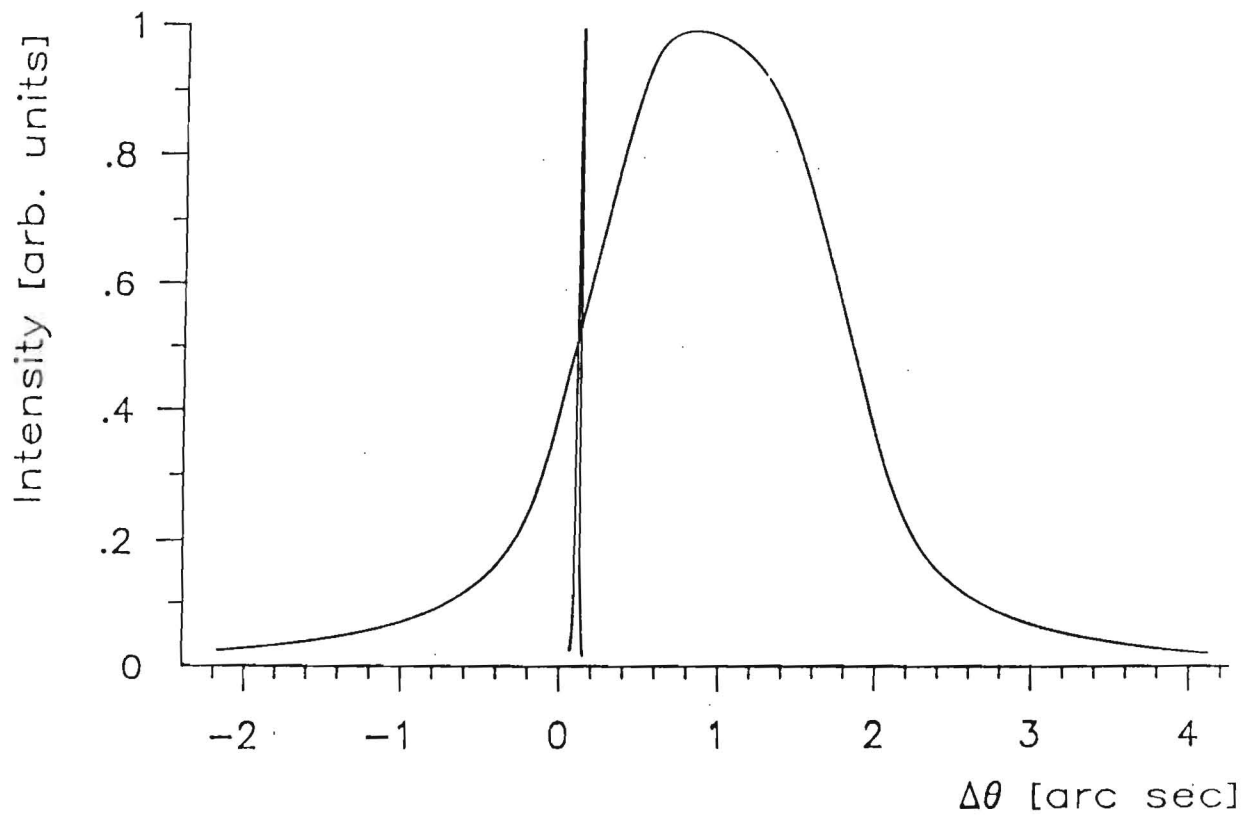


Measured Rockingkurves

a) Si 5,1,1 reflex at $\lambda=1.38 \text{ \AA}$

b) Si 15,3,3 reflex at $\lambda=0.46 \text{ \AA}$

maximum intensity normalized to 1.0
and back ground subtracted.



Calculated Rockingkurves

- a) Si 5,1,1 reflex at $\lambda=1.38 \text{ \AA}$
 - b) Si 15,3,3 reflex at $\lambda=0.46 \text{ \AA}$
- maximum intensity normalized to 1.0

MICRO-CHANNEL WATER COOLING OF SILICON MONOCHROMATOR CRYSTALS

J. Arthur, T. Troxel, H. Tompkins, and G. S. Brown
Stanford Synchrotron Radiation Laboratory, Stanford, CA USA
D. B. Tuckerman and E. Schmitt
Lawrence Livermore National Laboratory, Livermore, CA USA

We are attempting to improve the efficiency of cooling of silicon monochromator crystals at SSRL through the use of optimized water cooling channels cut into the crystals. The optimization analysis leads to a design involving very many channels with approximately 50 micrometer widths and similar spacing, located within 200 microns of the crystal surface. The pressure drop along the channels is 50 psi for this design, and the total water flow rate is slightly less than 1 liter/min. The channels are cut into a thin crystal plate using a small diamond saw; the crystal is then electrostatically bonded to a glass substrate and header assembly.

It has been found that such a construction is capable of removing power loads in excess of 20 W/mm^2 from a silicon crystal, with a surface temperature rise of about 10 deg/W/mm^2 . It remains to be seen whether or not it is possible to fabricate such a device without introducing excessive strain and curvature into the crystal plate. We hope to answer this question during the fall of 1988.

Microchannel Cooling Project

SSRL

Teresa Troxel
John Arthur
George Brown
Richard Boyce
Brad Youngman
Hans Przybylski

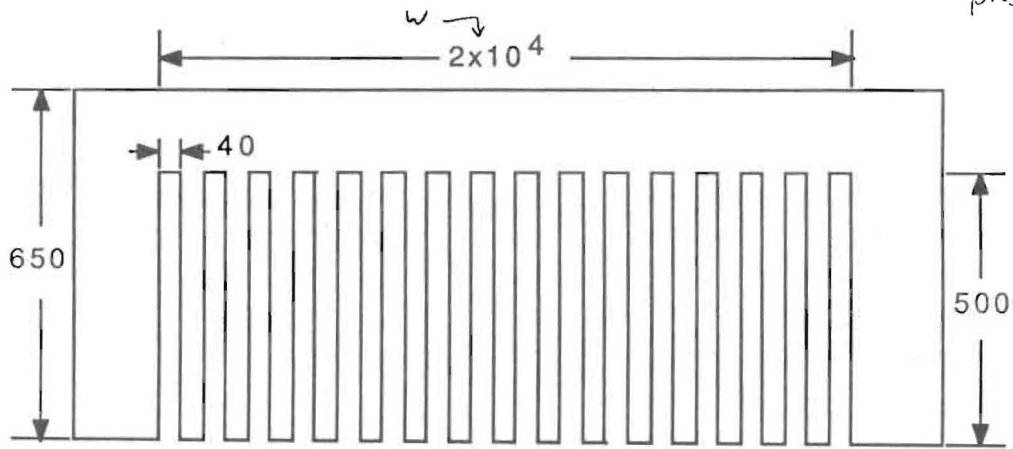
LLNL

David Tuckerman
Ed Schmidt
Gary Johnson
Bill Comfort

Object: To produce a working prototype of a silicon (111) monochromator system utilizing microchannel cooling by Sept 1, 1988 (to be tested during the PEP run).

Microchannels in silicon wafer

(Optimized for water cooling, 50psi pressure drop)



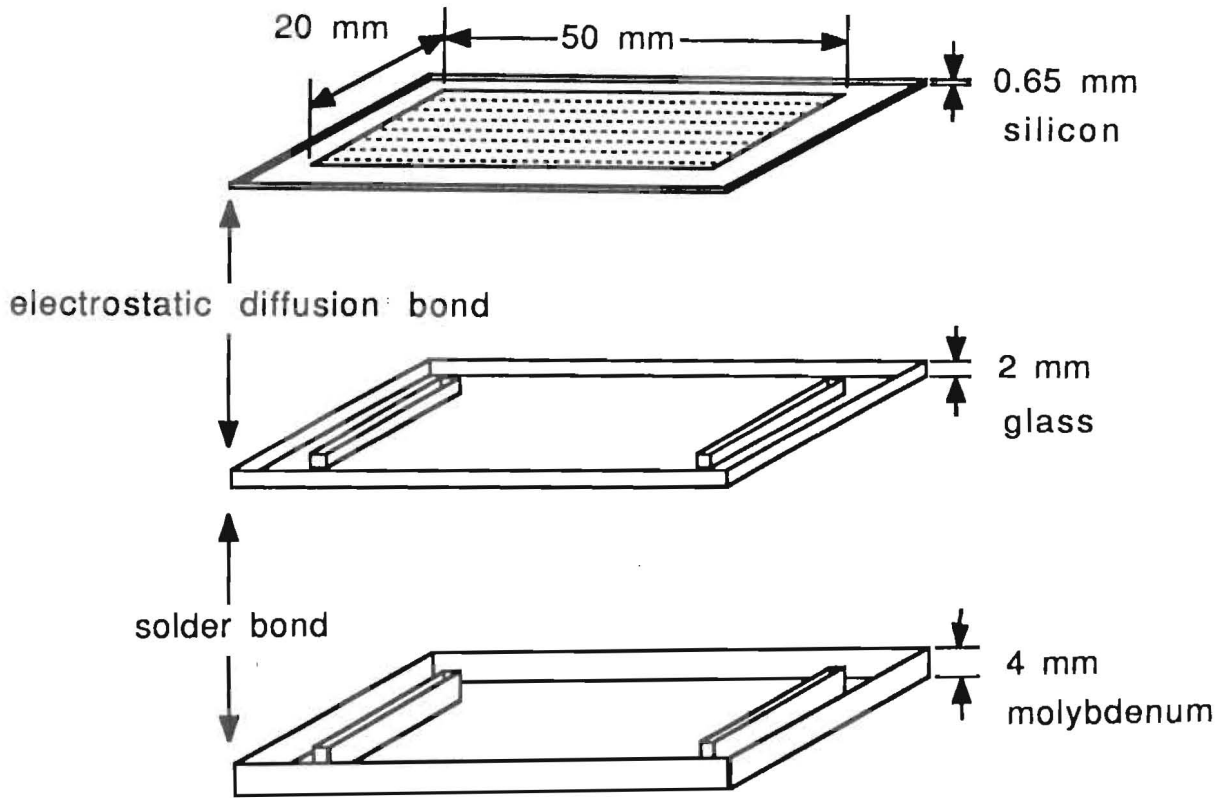
dimensions = micrometers

David Tuckerman thesis:

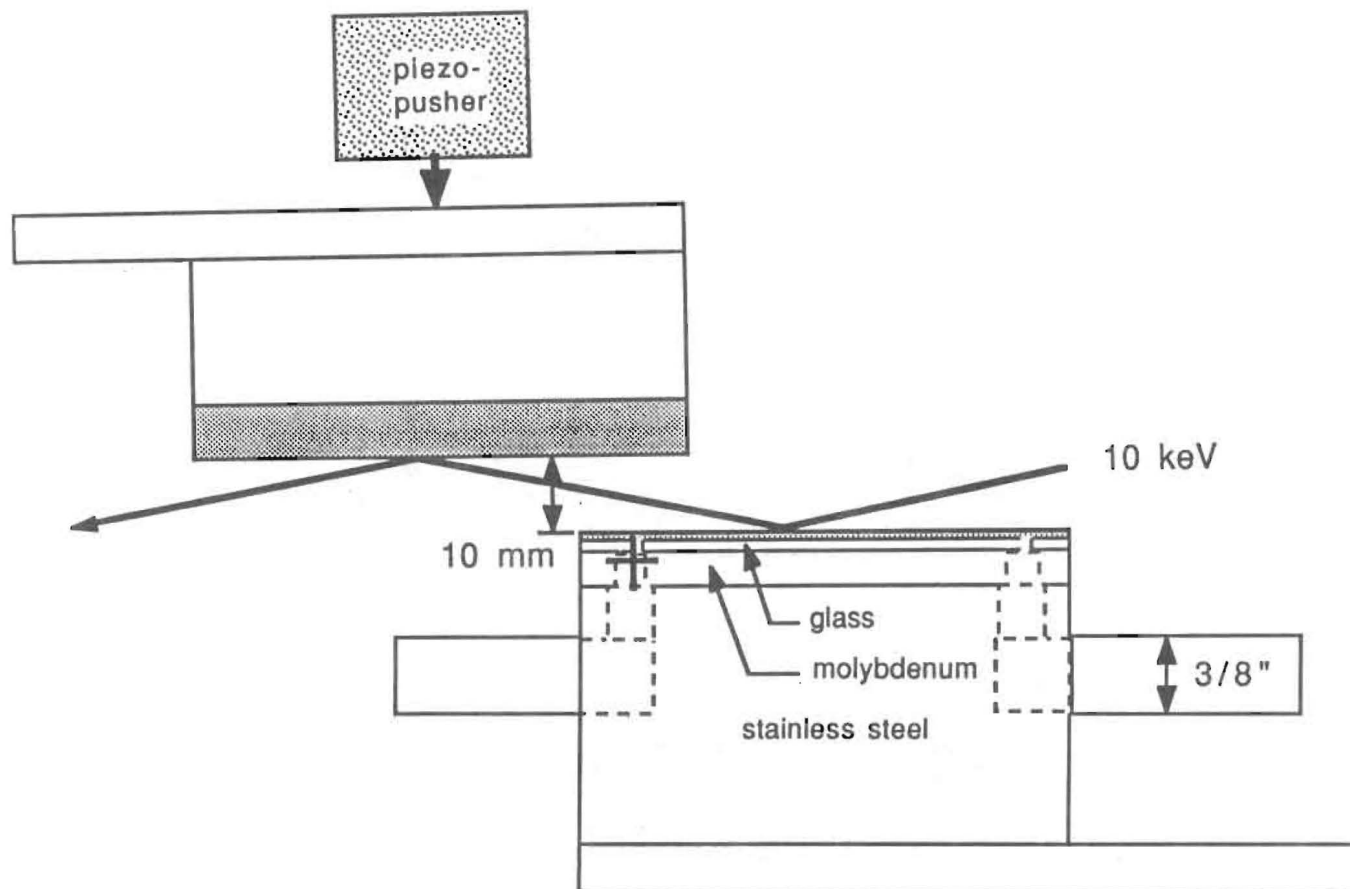
$$\text{optimized } \Theta \propto \left(\frac{\mu \Phi}{k_c Nu k_w^2 L^2 W^4 \rho C P} \right)^{1/4}$$

viscosity μ friction factor \times Reynolds number Φ
 coolant thermal conductivity k_c Si thermal conductivity k_w
 Nusselt number Nu length of heated area L
 width of heated area W
 coolant density ρ coolant heat capacity C pressure drop P
 thermal boundary resistance Θ ($^{\circ}\text{C}/\text{W}$)

Microchannel plate assembly



Double-crystal monochromator



Reference

D. B. Tuckerman and R. F. W. Pease: High-Performance Heat Sinking for VLSI, IEEE Electron Device Letters, Vol. EDL-2, 5, 126(1981).

COOLING OF SILICON MONOCHROMATOR OPTICS
-PRESENT TEST RESULTS AND FUTURE NEEDS-

Don Bilderback, CHESS (Cornell High Energy Synchrotron Source)
Cornell University, Ithaca, NY 14853, USA

We have tested the cooling of silicon monochromator blocks with high power wiggler and undulator beams with the help of CHESS, ANL, and BNL Staff. The performance was "Poor" for side and bottom cooling crystals with 1 to 2 cm heat paths. It was "good" for core-drilled holes placed within 2.5 mm of the diffracting surface of a second crystal and even "better" for slots 0.75 mm beneath the surface of a third crystal. At the highest beam currents, the slotted crystal was still somewhat distorted. Therefore, more work must go into optimizing flow rate and channel design to find the limits of this type of cooling. From these tests, it appears that the shorter the heat path, the better the X-ray performance.

Test were also made between two coolants, water and liquid Gallium. Ga was superior to water in all the cases we tried. We experienced problems with the seal between the silicon monochromator and the stainless steel cooling manifolds (rubber o-ring or silicon bathtub caulk). The seals could be made more radiation resistant by placing them further away from the source and/or shielding them better. It would be good to solve these seal problems and to finish the channel design of the next generation of better cooled monochromator and pump system. If the performance of the new system is superior, then we should install it as a regular component on a SR beamline.

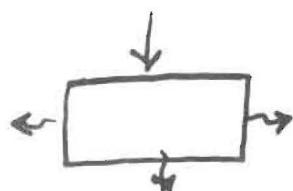
For the long range view, I think we need to continue to investigate cryogenic cooling where the thermal properties of silicon (and germanium) become more favorable than at room temperature. The engineering of the cryogenic design, although difficult, should start soon. We also need to develop better methods to cool germanium optics than we presently have, since liquid Ga attacks germanium. Another working fluid or better methods of water or helium cooling should be investigated. An important aspect in achieving these long range goals will be to continue to work together with other laboratory groups in collaborative effort and to continue to try out new ideas as they arise.

Cooling of silicon monochromator Optics

D. Bilderback - CHESS (8/31/88)

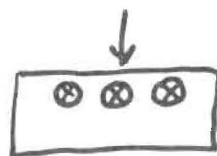
w/ ANL & BNL staff

Present Results: ① Geometry



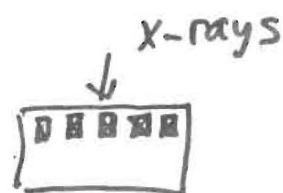
side cooling
1-2 cm heat path

Cooling ; Poor
Performance



core drilled
2.5mm path

Good



slotted
.75mm path

Better

② liquid gallium superior coolant to H_2O .

Future Plans :

Short range

- ① optimize cooling channel geometry
improve seals to pump lines
- ② develop a working silicon xtal,
Gallium pump combination and
regularly use it on a beamline

Long range

- ③ investigate cryogenic cooling,
make prototype tests
- ④ find better methods to cool
germanium optics (Gallium
attacks Ge).
- ⑤ continue to try new ideas, work
together in collaborative efforts.

D. Bilderback
8/31/88

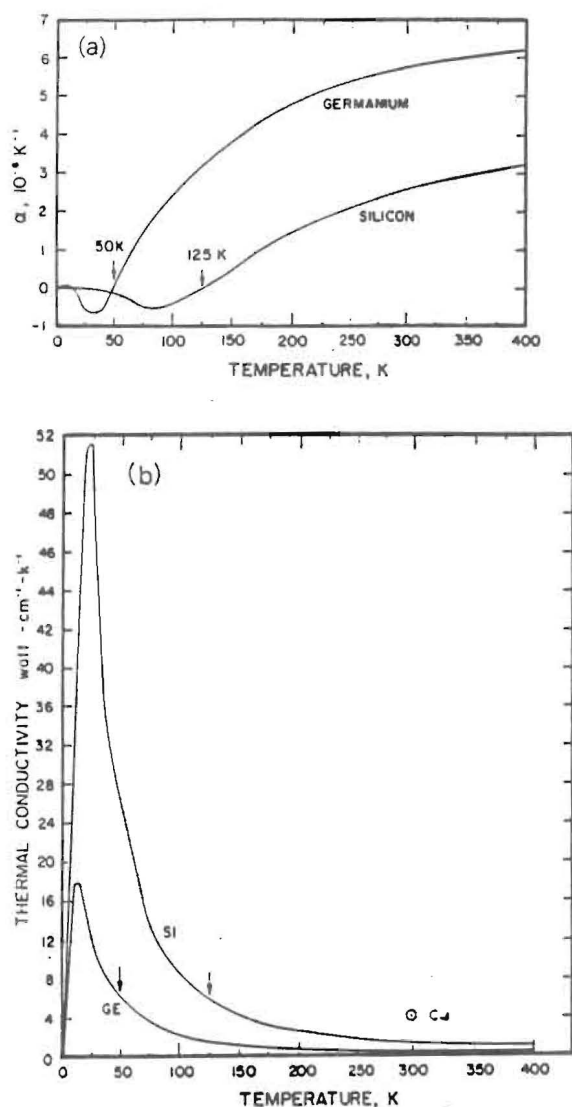


Fig. 1. (a) Thermal expansion coefficient for silicon and germanium as a function of temperature. (b) Thermal conductivity as a function of temperature. These curves are the composite curves from many measurements [3] and are for undoped materials.

where s is the fracture stress, E is Young's modulus and μ is Poisson's ratio [5]. The breaking or fracture stress for silicon has been measured in the range of 25 000–60 000 psi [6] (2×10^9 to 4×10^9 dynes/cm²) and 26 000 psi [7] (2×10^9 dynes/cm²). In the latter case the fracture stress was shown to be independent of temperature from -200°C to $+600^\circ\text{C}$. These values are an order of magnitude less than the theoretical yield strength of 330 000 psi (2.3×10^{10} dynes/cm²). It is most likely that small cracks on the surface are responsible for the low observed fracture stresses [7]. Poisson's ratio, and Young's modulus are almost constant below room temperature [3] and both are sensitive to crystallographic direction. [9]

We can now compare the heat loads at low temperature with those at room temperature that will just fracture a given crystal. For silicon whose temperature is 1 K away from the $\alpha = 0$ temperature (125 K), $\alpha = 0.02 \times 10^{-6} \text{ K}^{-1}$ and $k = 6.4 \text{ W cm}^{-1} \text{ K}^{-1}$. The corresponding room temperature values are $\alpha = 2.6 \times 10^{-6} \text{ K}^{-1}$ and $k = 1.5$.

$$\frac{q_{\max}^{\text{low temp}}}{q_{\max}^{\text{RT}}} = \frac{6.4 \times 2.6 \times 10^{-6}}{1.5 \times 0.02 \times 10^{-6}} = 550.$$

Therefore we estimate that silicon within a degree of 125 K can handle 550 times the heat load as it can at room temperature without fracture. It is assumed here that the only stresses present are induced by the thermal load. In practice, all other nonthermal stresses must be included to compute the net stress in the crystal.

In a practical monochromator design heat loads must be kept far below any fracture point. The stress and distortion of lattice planes for the cryogenic monochromator should be less by (of order $1/550 = 0.002$) than its equivalent room temperature monochromator under identical heat loads. Less distortion of lattice planes under large heat loads is clearly desirable since large thermally induced distortions can degrade monochromator performance [9].

4. Conclusion

THE POTENTIAL OF CRYOGENIC SILICON AND GERMANIUM X-RAY MONOCHROMATORS FOR USE WITH LARGE SYNCHROTRON HEAT LOADS

D.H. BILDERBACK

Cornell High Energy Synchrotron Source (CHESS) and the School of Applied and Engineering Physics,
Cornell University, Ithaca, New York 14853, USA

It appears feasible to construct cryogenic silicon and germanium monochromators which may withstand 100 to 1000 times more

A thin Laue crystal as a monochromator in a wiggler beam

W. Graeff

Hamburger Synchrotronstrahlungslabor HASYLAB at DESY,
Notkestr. 85, D-2000 Hamburg 52

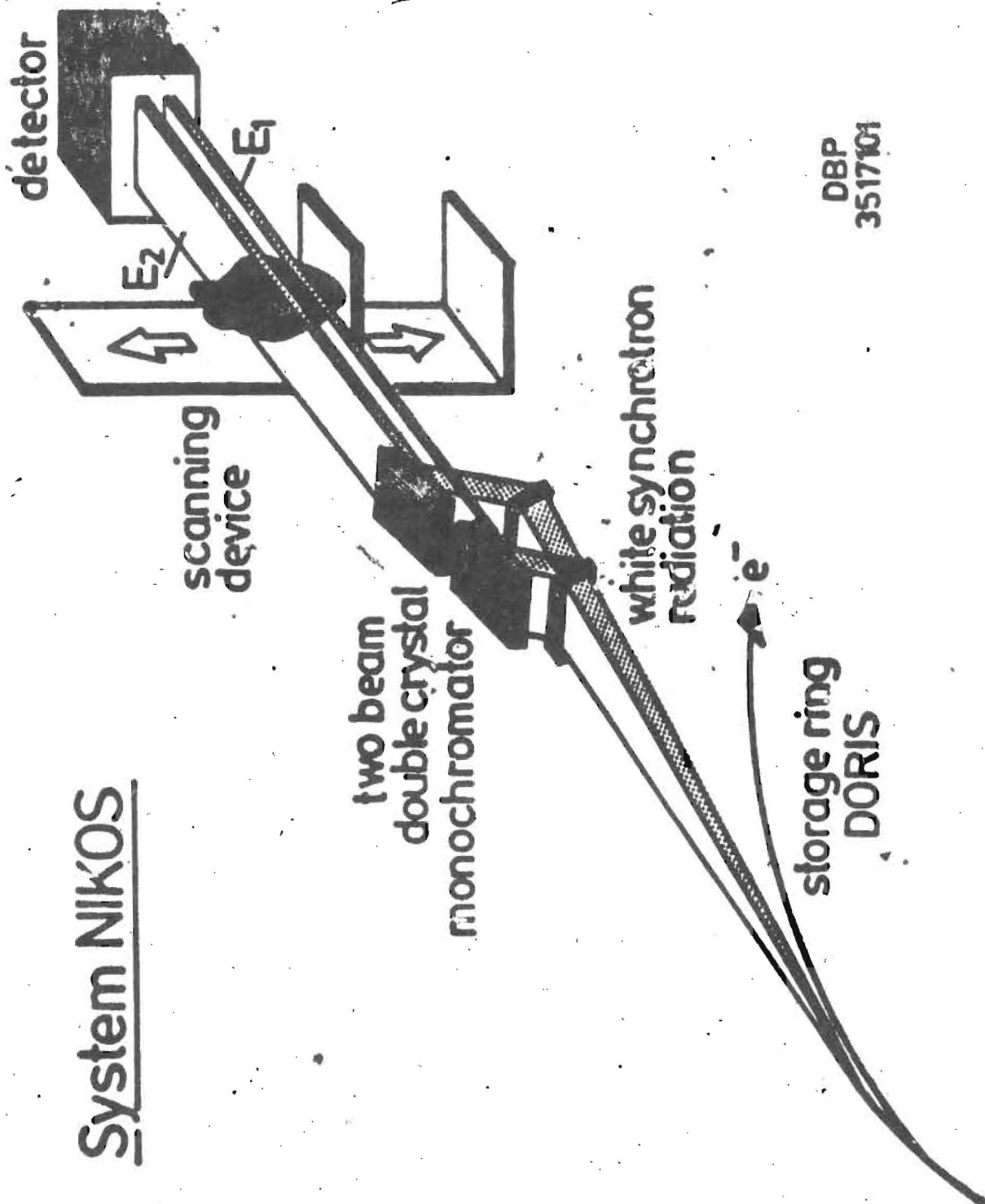
For coronary angiography with synchrotron radiation two monochromatic beams are necessary. The use of two Laue crystals as first crystals in the white beam has the advantage of using the full beam aperture twice. Other advantageous features of these thin Laue crystals are inherent focusing in the diffraction plane and little absorption of the intense wiggler beam.

The thickness of the Laue crystal can be optimized in reflectivity (Pendellösung effect of the Dynamical Theory) to yield about 80% of the integrated reflectivity of the corresponding Bragg case. In our case of Si 111 the thickness should be 30 μm . Such thin crystals with surface dimensions of 6 x 60 mm^2 can be realized by molecular beam epitaxy on a 0.5 mm thick Si substrate. On both sides of the epitaxial layer a thin layer of Si is doped with B and Ge where the boron acts as a stop layer for the etching agent which removes an appropriate part of the substrate and thereby yields a thin part of the desired thickness and a rigid frame around it for proper mounting of the crystal. The addition of Ge to the B-doped layers counteracts the contraction of the Si lattice due to the B-atoms.

In the case of the HARWI-wiggler beam line a filtration of 0.4 mm C, 1 mm Be and 1 mm Al reduces the total power load of 1.95 kW in the white beam to 0.8 kW. Out of this beam the silicon crystal absorbs 7 W. As the heat conduction through the thin part to the outer frame is much too small a gas cooling of either surface of the thin part is applied. Several hundred litres of He or N_2 per hour are sufficient to prevent a too strong deformation of the Laue crystal so that a second reflection from a Bragg crystal can be used to direct the beam back to the forward direction.

It is worth to note that even without a gas stream the Laue crystals were not destroyed as the maximum temperature stabilized somewhere around 120°C. Of course, at that temperature a double crystal setting was no longer possible due to a strong bending of the Laue crystal.

System NIKOS



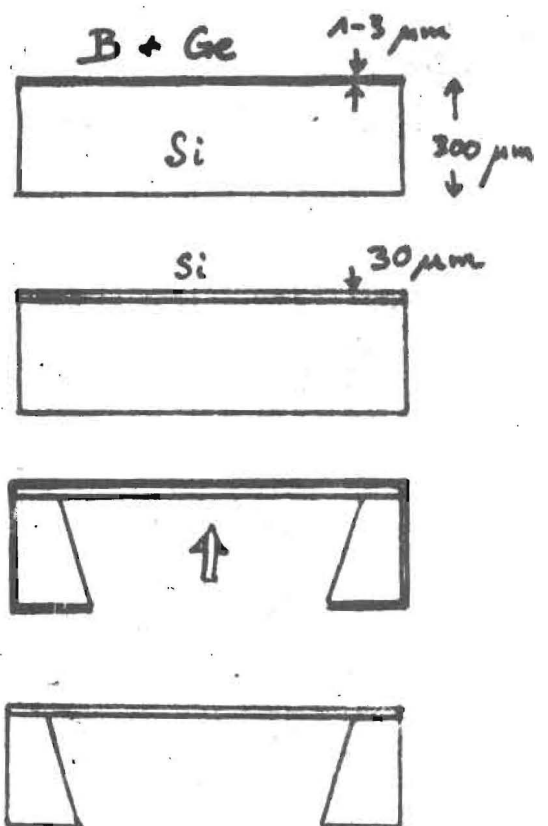
DBP
3517101

1. boron etch stop diffusion:

2. epitaxial growth of Si:

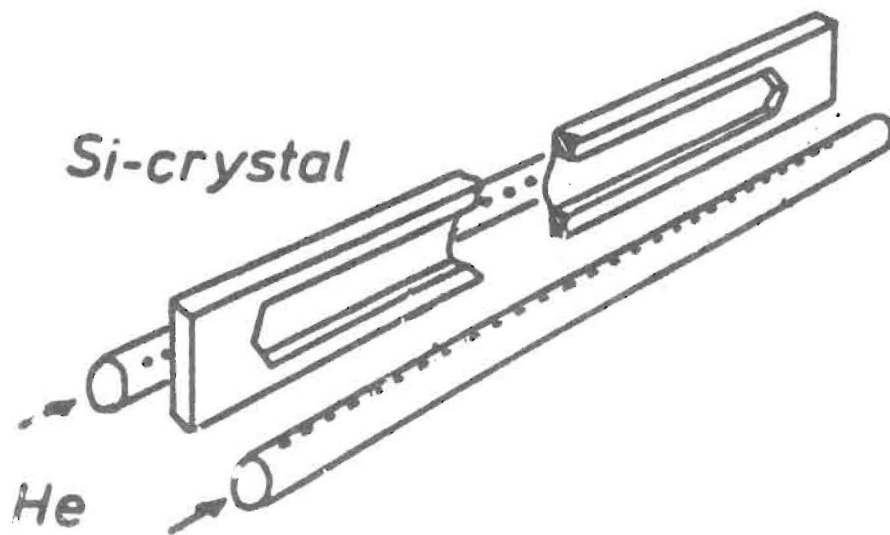
3. protective coating + etching:

4. removal of coating:



Csepregi, Inst. of Micromechanics
FHG Berlin

Thin Laue crystal



dimensions: frame: $100 \times 12 \times 0.5$ mm
thin part: $80 \times 8 \times 0.031$ mm

topographs revealed very few defects, if any.

Recent tests at W2-wiggler
cooling by gas stream

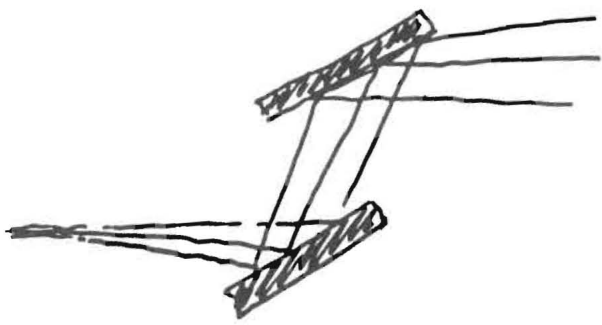
prefiltering: 0.4 mm C, 3 mm Be
 1 mm AL

→ $30 \mu\text{m}$ Si $5-10$ Watts
absorption

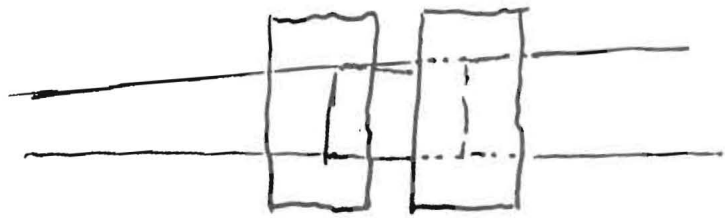
COOLING NOT SO PERFECT CRYSTALS

J. Hastings

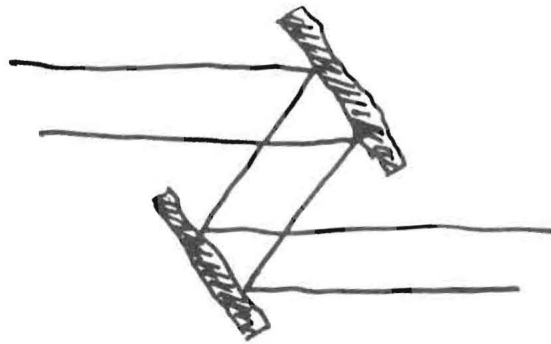
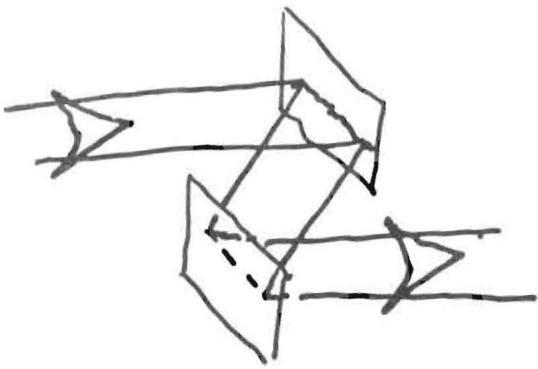
National Synchrotron Light Source
Brookhaven National Laboratory, Upton, NY 11973, USA



SIDE



TOP



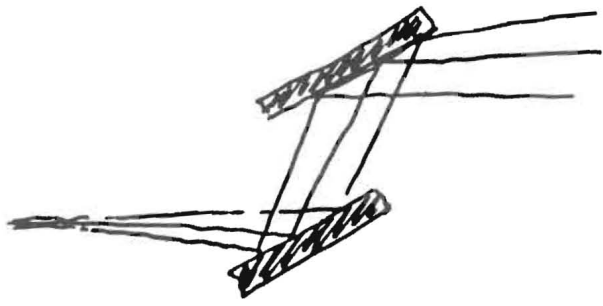
Workshop on Cooling of X-Ray Monochromators on High Power Beamlines
8/31/88 at Photon Factory

Heating Problems of Crystal Monochromators at the Photon Factory

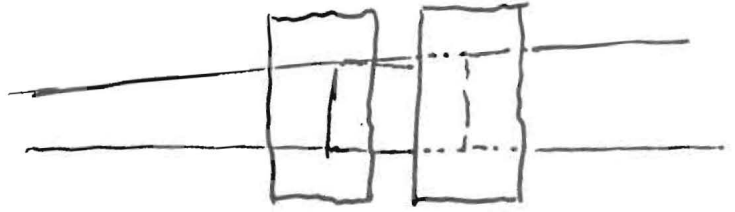
Tetsuya ISHIKAWA

Photon Factory, Japan

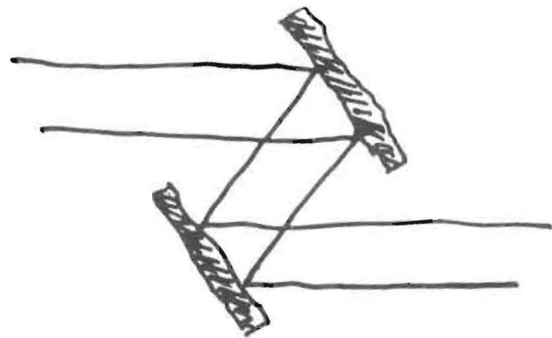
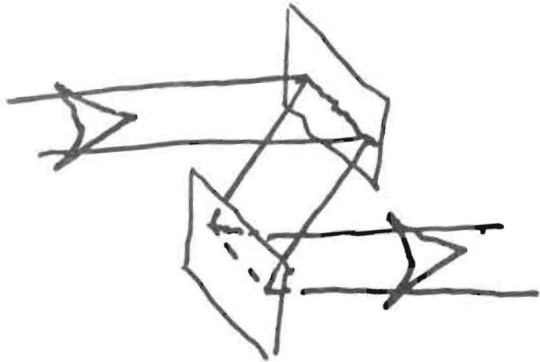
- 1) Insertion Device Beamlines at PF.
- 2) Crystal Cooling R&D Program at PF.



SIDE



TOP



High Resolution: Mosaic Crystals

- references: J.P. Woodruff et al. PRL 58, 1460 (1987)

"Simple X-Ray Standing-Wave Technique and Its Application to the Investigation of the $\text{Cu(III)} (\sqrt{5} \times \sqrt{5}) R30^\circ\text{-CP}$ Structure"

for example A. Freund BNL 38651

J.B. Hastings, D.P. Siddons to be published

- Peak Reflectivity (after Freund)

- kinematic approx. including only secondary extinction

$$r(\Delta) = a / [1 + a + \sqrt{1 + 2a} \coth(A\sqrt{1 + 2a})]$$

$$r_{pm} = r(\Delta) \Big|_{\substack{\Delta=0 \\ t \rightarrow \infty}} = a_0 / (1 + a_0 + \sqrt{1 + 2a_0})$$

where $a_0 = \frac{1}{\eta \sqrt{2\pi}} \cdot \left(\frac{F_x}{V_0} \right)^2 \frac{1}{\mu} \frac{\lambda^3}{\sin 2\theta}$

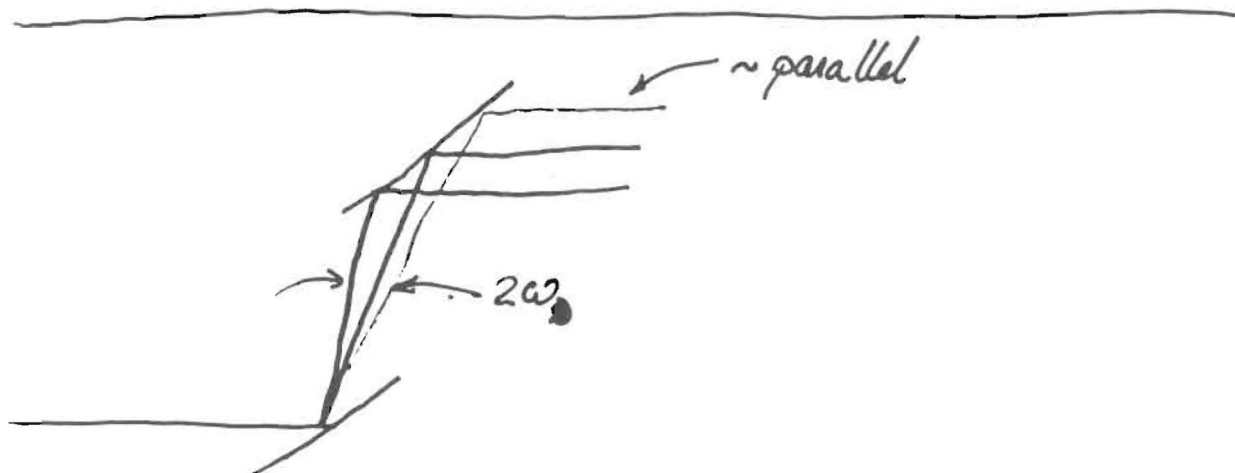
η of mosaic dist. structure factor wavelength
 V_0 unit cell volume linear abs. coeff. Bragg angle

- $\lim_{\theta \rightarrow \pi/2} r_{pm} = 1$

Mosaic Crystals:

Observed	<u>Peak Reflectivities</u>	ω_D	E
PG (00.2)	0.5	$\sim 0.4^\circ$	8 keV
Be (00.6)	0.2	$\sim 40 \text{ sec}$	17 keV
Be (11.0)	0.25	$\sim 100 \text{ sec}$	$\sim 8 \text{ keV}$

(Laue geo.)



in fact as long as the slope error from heat bump $\Delta\theta \ll \omega$ then 'no effect'

Double Graphite: JAC to be published.

~~revised, revised, revised, etc.~~

Heating Problems of Crystal Monochromators at the Photon Factory

Tetsuya ISHIKAWA

Photon Factory, Japan

- 1) Insertion Device Beamlines at PF.
- 2) Crystal Cooling R&D Program at PF.

Insertion Device Beamlines at PF.

PF Ring (2.5 GeV, max 300 mA max.)

**BL-2 121-pole SmCo undulator (SX)
Double-Crystal
Monochromator(SX)
Grating Monochromator**

BL-5 in designing

**BL-13 27-pole NdFe MPW/undulator
(HX/VUV) 1.5T max
Double-Crystal
Monochromators (HX)
Grating Monochromator**

**BL-14 3-pole Superconducting Vertical
Wiggler (HX) 6T max, Vertically
Polarized.
Double-Crystal
Monochromators (HX)**

- BL-16 53-pole NdFe MPW/undulator
(HX/VUV)
Double-Crystal Monochromator
(HX)
Grating Monochromator(VUV)**
- BL-19 NdFe Multi-Undulator
Grating Monochromators (VUV)**
- BL-28 25-pole NdFe MPW/undulator
(HX/VUV) Elliptically Polarized
Grating Monochromator (VUV)**

TRISTAN AR (6.5 GeV, 20 mA max.)

**AR-BL-1 41-pole NdFe MPW/undulator
(HX/SX) Elliptically Polarized
Quasi-Spherically Bent Crystal
Monochromator (HX)
Double-Crystal Monochromator
(HX)
Grating Monochromator (SX)**

**AR-BL-2 Hard X-Ray Undulator
in designing**

Crystal Cooling R&D Program

Direct Crystal Cooling R&D at BL-16, PF
Max. Total Power
(PF-NSLS collaboration)

Presented by T. Oversluizen (NSLS) in the
morning session.

Necessary Improvement
Thicker Crystal to avoid Thermal
Bending
Liquid Ga Cooling

Test at AR MPW
Max. Power Density

RESEARCH AND DEVELOPMENT OF X-RAY OPTICS AT THE ESRF

Present and Planned Activities

Andreas K. Freund
European Synchrotron Radiation Facility
B.P. 220
F-38043 Grenoble Cedex

INTRODUCTION

During the recent years it has become more and more evident that the effort in the development of powerful dedicated storage rings has to be accompanied by more systematical and ample research and development in the field of instrumentation in order to achieve an adequate use of the modern sources. This need has been taken into account when setting up the ESRF project and the resulting activities and facilities are described in Chapter V, Section 3 (pp. 500-525) of the ESRF's Foundation Phase Report issued in February 1987. In the following a brief account will be given on what has been achieved since then and on what are the present and planned activities in the field of X-Ray Optics.

The task of beam defining devices is to match source and experiment in terms of resolution (energy, angle, direct space, time) and intensity (final count rate in the detector). There is a wide variety of experimental conditions leading to quite different ways of beam conditioning for the various beamlines. Common to all is the need for strategic approaches to achieve optimum conditions for which phase-space and reciprocal space diagrams and ray-tracing programs are used. In addition, the performances and efficiencies of the optical elements (single crystal and layered monochromators, mirrors, gratings and multiple reflection devices) must be known in the whole energy range of interest. Because optical elements are not aberration-free and can be manufactured only to finite tolerances there is always some loss of emittance between source and sample. This is schematically shown in Fig. 1 where the emittance at the sample is plotted against the emittance produced by the source. The ideal optics would give a 1:1 ratio whereas the real optics fixes the lower bound of the emittance at a value which may be above the diffraction limit of the source.

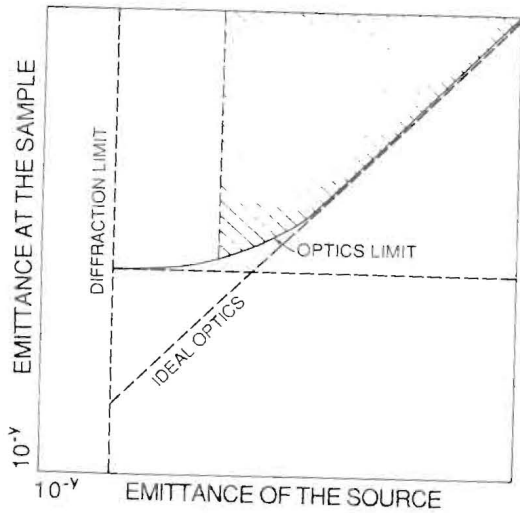


Figure 1

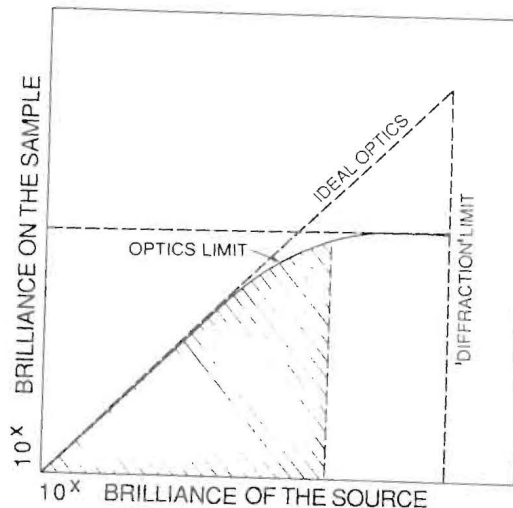


Figure 2

A similar diagram can be drawn for the brilliance which fills the phase-space volume defined by the emittance with a certain number of photons (Fig. 2). Again brilliance can never be increased by the optics (Liouville's theorem) but it will be decreased by absorption, diffuse and incoherent scattering which do not only remove the photons from the phase-space window of interest but also decrease the quality of the experimental data in terms of signal-to-noise ratio. Synchrotron radiation experiments are very inefficient in the sense that the experiments only use a very small fraction of the photons offered by the source. The huge amount of the absorbed "waste" gives rise to severe thermal problems which degrade the beam quality after reflection from the first optical element. Thus efficient cooling is not needed just to prevent melting or fracture of this element but to preserve the "high fidelity" of the optics for the reproduction of the source emittance at the sample, and this turns out to be the major problem at new generation storage ring facilities.

In the past many efforts have been made at the various operating synchrotron radiation facilities to solve problems with X-ray optics as they occurred in the course of experimental progress. The R&D activities at the ESRF will be based on this pioneering work and collaborative projects will help starting these activities and progressing faster in the improvement of the experimental conditions. To this aim an international workshop was organized at the ESRF in September 1987 (see Synchrotron Radiation News Vol. 1, n° 2, 10-12, 1988) where a complete review of the present state of the art was assessed thanks to the contributions of many experts in the field which is gratefully acknowledged.

TASKS OF THE ESRF OPTICS GROUP

Phase 1 : years 1 to 3 (1988-1990).

The ESRF-specific needs have to be assessed. The ESRF Optics Laboratory must be defined and built up and collaborative projects initiated and carried out in order to meet these requirements and to prepare phase 2.

Phase 2 : after year 3 (1990).

There will be essentially four major tasks :

- i) Advice and assistance have to be provided, implying active participation already from the beginning of the planning of a beam line until the final hardware production. In general, there should be a continuous emphasis on close collaboration with all instrument responsables, also to maintain and to improve existing instrumentation.
- ii) Once all the details are defined together with the beam line responsables the optical devices will be produced by the Optics Group or, depending on the in-house capabilities, either partly or entirely be ordered externally. There must be test facilities for the control of these devices before and regularly during their use.
- iii) There should be adequate R&D capacities (personnel, budget) to work on improvements of existing equipment and on novel designs of beam-optical components.
- iv) Experience has shown that experimentalists often need assistance on a short-term notice for sample preparation and characterization (e.g. crystal orientation) which can be provided by the optics laboratory in a most efficient way. This service activity, however, has lower priority than the first three activities.

After the ESRF workshop a programme of in-house activities and collaborations with research institutes and industry was set up. Two other workshops, namely on high energy X-ray scattering and on microfocusing organized by ESRF were also useful to determine the needs for optics. In the following several projects are described which fall into several categories of research and development work and which aim at solving ESRF-specific problems. Finally, the means available or to be provided at the ESRF will be outlined.

1. Subject : SINGLE CRYSTALS

Fig. 3 shows the opening angle (FWHM) of the beams produced by several ESRF sources and the Darwin widths of Si and Ge perfect crystals as a function of photon energy. From these curves it is clear that the matching between both is only fulfilled for undulator radiation at energies higher than a few keV. For all the other sources and in particular at high energies the mismatch could be reduced by using Ge instead of Si and by using slightly imperfect crystals. Thus for all experiments where the matching condition applies, intensity could be gained without loss in resolution.

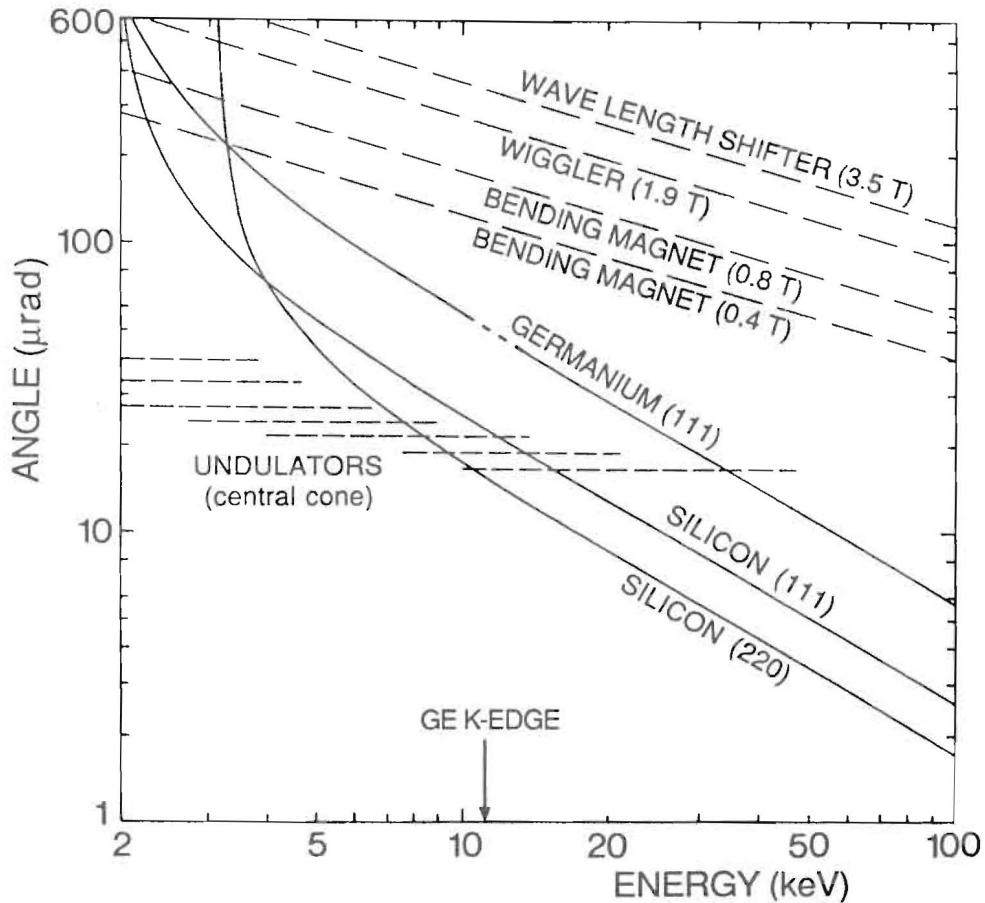


Figure 3

- 1.1 - Problem : Supply of ultraperfect silicon crystals.
- Action : Collaboration with NBS (R.D. Deslattes) searching for the best quality. Contact with firms : Wacker Chemitronic (Germany), Topsil (Denmark)....
 - Status : Several crystals ordered by ESRF, will be tested at NBS until ESRF laboratory will be ready.

- 1.2 - **Problem** : Supply of highly perfect germanium crystals.
- **Action** : Collaboration with ILL (A. Magerl) and LBL (E. Haller). Contact with Kristall-Labor of the KFA Jülich (H. Wenzl) and several firms : Hoboken (Belgium), Crismatec (Grenoble), Cristaltec (Grenoble), Eagle-Picher (Quapaw, U.S.), Wako-Bussan (Tokyo), Tsukuba Asgal Company (Tsukuba).
 - **Status** : An ILL technician (A. Escoffier) is presently working for a period of three months at the LBL to grow crystals of bigger diameter (8 cm) than presently available at LBL, i.e. 4 cm diameter (dislocation-free). Crystals of several firms will be ordered and tested at the ESRF.
- 1.3 - **Problem** : Search for other perfect crystals.
- **Action** : Systematic studies of high quality crystals other than Si and Ge (e.g. AsGa, InSb) will be carried out and a list of suppliers established.
 - **Status** : Some crystals are ordered and will be tested early in 1989.
- 1.4 - **Problem** : Not so perfect crystals.
- **Action** : **Be** : Collaboration with MPI Stuttgart.
Al : Collaboration with CNRS Marseille.
Cu : Collaboration with KFA Jülich and ILL.
Si : Collaboration with HMI and Wacker.
GGG : Contact with Crismatec (Grenoble).
 - **Status** : **Be** single crystals with a mosaic spread $\geq 40''$ can presently be grown at MPI Stuttgart. Some are already in use for Moessbauer experiments, magnetic and Compton scattering at NSLS and CHESS.
Al crystals can be grown nearly perfect at Marseille and studies are under way to increase the size.
Cu can be obtained even dislocation-free from the KFA Jülich but nearly-perfect crystals are of bigger diameter and can be handled with less problems. Big Bridgman crystals of about 50'' mosaic spread are grown at the ILL.
Si crystals with a mosaic spread of up to 10'' were developed by J. Schneider in collaboration with Wacker and can presently be obtained from the firm Wacker Chemitronic (W. Zulehner).
GGG crystals are grown dislocation-free by the firm Crismatec but they contain other defects giving rise to strains. Their suitability for high energy X-ray monochromatization is being studied at ESRF.

General : Systematic studies of the performances and applications of low-mosaic crystals are performed at ESRF. Experimental data are expected during 1989.

For theoretical performance, see : A.K. Freund, Nucl. Instr. & Methods A 266 (1988) 461-466.

2. Subject : MIRRORS

2.1 - Problem : Supply of high quality mirrors.

- Action : Collaboration with HASYLAB (V. Saile). Contact with several firms : Astron-Ferranti, Cranfield (UK), Zeiss (Germany), Bertin (France).

- Status : The firms above are informed about the specific performances of mirrors for the ESRF :

- Surface roughness better than 2 Å rms,

- Slope (figure) error less than 5 µrad,

- Si C substrate (cooled, power density : 100 W/mm²)

They are invited to tender for a test mirror being specified for the ESRF/CEA/LURE beamline. Performance under heat load will be tested at Hasylab, specifications will be checked at ESRF (see 2.2).

2.2 - Problem : Surface evaluation.

- Action : Setting up a laboratory for surface metrology at the ESRF.

- Status : Two optical interferometers will be purchased soon, one for testing figure, the other for measuring roughness, down to the Å level. In addition, the tunneling microscope of the ESRF's surface group permits still higher resolution. Finally, X-ray reflectivity studies can be carried out on a high resolution diffractometer (see subject 7.1) in early 1989.

3. Subject : MULTILAYERS

3.1 - Problem : Fabrication of layered synthetic microstructures.

- Action : During a first period, multilayers of different compositions are prepared at Argonne National Laboratory and at the University Aix-Marseille, also in order to design the most appropriate apparatus to be set up at the ESRF during 1989.

- Status : Theoretical and experimental studies are carried out in parallel with the aim to find out the best compromise between high contrast (reflectivity), resistance to intense wiggler beams, chemical compatibility, etc. First results are published by E. Ziegler et al. in the proceedings of the SRI'88 Conference, Tsukuba, 1988.
- 3.2 - Problem : Characterization of multilayer performance.
- Action : Surface evaluation facilities will be provided according to 2.2 in the laboratory while synchrotron radiation studies are carried out at LURE and Hasylab.
 - Status : Laboratory facilities for X-ray tests at the ESRF will be available in early 1989. Tests at LURE are planned for 1989 while studies of resistance to wiggler beams have been and will be carried out at Hamburg (see the reference under 3.1).
4. Subject : FOCUSING
- 4.1 - Problem : Geometrical optimization.
- Action : Collaboration with University of Helsinki (P. Suortti) on phase-space descriptions. Ray-tracing studies at ESRF (A. Boeuf, Euratom).
 - Status : First work has started on focusing for small-angle scattering (C. Riekel, ESRF, P. Suortti) and on parallel representations in phase-space and reciprocal space taking into account crystal thickness and/or penetration depth (P. Suortti and A. Freund, Proceedings SRI'88 Conference, Tsukuba, 1988). The ray-tracing program "Shadow" already installed at the ESRF is presently used by A. Boeuf to optimize the CEA/ESRF/LURE beamline. Further work will be carried out as needs will appear.
- 4.2 - Problem : Fundamental limits of focusing by crystals.
- Action : Collaboration with University of Dortmund (U. Bonse) and NSLS (P. Siddons). PhD student at the ESRF.
 - Status : A PhD thesis is starting on the theoretical and experimental limitations of microfocusing by curved crystals. This involves the calculation of reflection properties of curved crystals including penetration depth and their experimental verification in the laboratory and at existing synchrotron radiation laboratories.

- 4.3 - **Problem** : Accurate devices for curving optical elements.
- **Action** : Collaboration with NBS Washington (R. Deslattes, E. Kessler, A. Henins) and ILL (H. Boerner) on benders based on web structures. Finite element analysis of bending structures and optical element deformation.
 - **Status** : With the help of NBS and during a three months stay at NBS R. Hustache (ESRF, formerly ILL) built a new type of very precise crystal bender for gamma-ray spectroscopy at ILL designed by H. Boerner (ILL). This device will be tested soon. Ongoing studies try to improve the system and to optimize various parameters such as compactness, anticlastic bending and other elastic deformation effects (R. Hustache, G. Marot, ESRF). These devices will be useful also for the experimental work of the PhD thesis (see 4.2). They can be equally applied for bending mirrors and multilayered structures.

5. **Subject : RADIATION DAMAGE AND HEAT LOAD**

- 5.1 - **Problem** : Radiation damage.
- **Action** : Collaboration with Hasylab (V. Saile).
 - **Status** : The special test chamber on a wiggler beam at Hasylab is used for studying the stability of materials under intense X-ray irradiation. First results indicate that in addition to the heat problem, some multilayers suffer from radiation damage (see the reference given under 3.1).
- 5.2 - **Problem** : Cooling optical elements.
- **Action** : Coordination with work presently performed at several synchrotron radiation laboratories through regular workshops. Specific studies simulating the X-ray beam by a laser beam and investigations of deformation by topography and rocking curves. Development of cooling schemes using finite element calculations.
 - **Status** : Quite different approaches are presently tried at several laboratories to solve the cooling problem. One proposal was to cool Si down to 125 K where thermal expansion vanishes and thermal conductivity is much higher than at room temperature. In order to know whether this idea is feasible a collaboration study was carried out with TNO-TPD Delft (P. van Zuylen) which showed that

unrealistically high cooling power is needed when using cryogenic liquids. Another cooling scheme was proposed using asymmetric reflection geometry (see report n° 832.020 by P. van Zuylen, A.D. Lemaire and A.J.Th.M.A. Wijsman, July 1988). In collaboration with Daresbury Laboratory (P. Pattison) topographic and rocking curve studies will be carried out soon at the topography station there. Silicon and other materials will be heated by a laser beam and the cooling efficiency of various devices will be examined. Finite element analysis of the schemes used in these devices is carried out at ESRF (G. Marot).

- 5.3 - Problem : Thin crystals and total reflection foils.
- Action : Preparation, mounting and testing of thin crystals in conjunction with Hasylab (W. Graeff). Development of thin foil beam splitters following an idea of D. Bilderback (CHESS).
 - Status : The work already done in this field by W. Graeff for the angiography monochromator at Hasylab will be followed up for other energies and also in Bragg geometry. The feasibility of making very thin and straight foils is presently studied. Experimental work will start in the ESRF laboratory in the beginning of 1989.

6. Subject : "EXOTIC" DEVICES

- 6.1 - Problem : Development of three-dimensional Bragg Optics.
- Action : Collaboration with Chernogolovka (V. Aristov and collaborators) and with Lawrence Livermore Laboratory (T. Barbee), maybe other laboratories providing facilities for microstructure preparation.
 - Status : It has been shown that three-dimensional Bragg optics can open new opportunities in X-ray techniques, e.g. Bragg-Fresnel-Optics, Multilayer Gratings based on both single crystal and multilayer diffraction. Very accurate preparation of the corresponding microstructures is a by-product of microcircuit fabrication which has been developed in the above laboratories with special application to X-ray optics. It is planned to start further developments in conjunction with both laboratories starting 1989 and involving regular exchange of

scientists and both hardware and software during a three years program, with the main application to microfocusing and high energy resolution.

- 6.2 - Problem : Other novel techniques in X-ray optics.
- Action : Regular exchange of ideas during ad-hoc meetings and collaborative projects with other laboratories.
 - Status : There are several ideas which merit to be developed in more detail : upper energy limit for the use of gratings taking low emittance of new sources into account; the so-called "X-ray whispering gallery" (M. Howells); X-ray microguides, (flat or curved, parallel or tapered), combined optics-detector devices, e.g. for beam-position monitoring; special optics for very high/low energy. These studies are suited for PhD thesis and must be promoted adequately in order to discover and invent new methods and techniques, to use new materials and thus to innovate X-ray optics. Some projects in this field have already started, e.g. optical devices for very high energy.

7. Subject : ESRF OPTICS LABORATORY

- 7.1 - Problem : Laboratory space and equipment
- Action : Definition of optimum laboratory space and environment, search and purchase and/or building of laboratory facilities.
 - Status : *i) Laboratory space.* About 200 m² in an existing building on the CENG site (LMA) is presently allocated to the Optics Group, half of this space is in the basement where a very stable thermal and vibrational environment is provided. After about three years from now a total of approximately 500 m² most of which are located in ESRF Experimental Hall will be available. In this space two bending magnet beamports will be dedicated to test beamlines. All equipment requiring stable conditions will be in this space, all the other machines will be housed in laboratories adjacent to the Hall (PLUO space).
 - ii) Laboratory equipment.* Surface metrology (see 2.2). Multilayer preparation apparatus (see 3.1). Clean room facility. Various machines for crystal cutting

(Meyer-Burger TS 121, small diamond wheel and wire saws, acid saws, EDM), grinding and polishing (abrasive, chemical and electrochemical; jig grinder; EDM). Precise devices for X-ray crystal orientation and transfer to cutting and grinding machines. Ultra-high resolution X-ray triple axis diffractometer (0.3 arcsec encoded; 0.01 arcsec controlled with electronic autocollimator; positioning and parallelism of translations with 1 μm resolution over distances of up to 110 cm) equipped with three sources : high-stability 3 kW sealed-tube generator, high energy generator (420 keV), rotating anode generator), and several detectors (NaI; intrinsic Ge, position-sensitive). Double-crystal diffractometer with topographic equipment and fine rocking curve (0.1 arcsec) possibility, also for crystal orientation. Some of these items are already purchased, designed and built. The laboratory will become operational during 1989. It is not yet decided whether growth of single crystals will be envisaged, too.

7.2 - Problem : Staff of the Optics Group

- Action : Building up the group, teaching and learning.
- Status : Presently there 4 people in the group : 2 scientists (E. Ziegler and A. Freund), 1 technician (R. Hustache) and 1 student (M. Krisch). In 1989 there will be 2 more people : 1 engineer and 1 technician. Finally, for 1993 a total of about 10 persons is planned. During phases 1 and 2 (see introduction) stays at existing synchrotron laboratories or other research institutes took already place or are envisaged on a regular basis, mostly in the framework of technical/scientific collaborations, but also in order to learn special techniques required at the ESRF. On the other hand, the ESRF invites guest scientists for short periods to work on common projects.

List of Participants

Name	Institute & Address	<Bitnet> or FAX
J. Arthur	SSRL Stanford University Bin 69, PO Box 4349 Stanford, CA 94305, USA	<Arthur@SSRL750> 415-926-4100
T. Barbee	Lawrence Livermore National Laboratory L-350, PO Box 808 Livermore, CA 94550, USA	415-422-1370
M. Bedzyk	CHESS Cornell University Ithaca, Ny 14853, USA	<BEDZYK@CRNLCHES> 607-255-8062
D. Bilderback	CHESS Cornell University Ithaca, NY 14853, USA	<BILDERBACK@CRNLCHES> 607-255-8062
U. Bonse	Universität Dortmund Lehrstuhl für Experimentelle Physik 1 Postfach 500 500 46 Dortmund 50, FRG	<UPH038@DDOHRZ11> 231-7553504
G. Brown	SSRL Stanford University Bin 69, PO Box 4349 Stanford, CA 94305, USA	<BROWN@SSRL750> 415-926-4100
P. L. Cowan	National Bureau of Standards Gaithersburg, MD 20899 USA	<COWAN@NBSENH> 301-869-7761
K. D'Amico	EXXON Research & Engineering Co. Clinton Township, RTE 22E Annandele, NJ 08801, USA	516-282-5239

B. Dobson	Daresbury Laboratory Daresbury Warrington, WA4 4AD, UK	<HLD@DLVA DARESBUY.AC.UK>
A. K. Freund	ESRF BP 220 F-38043 Grenoble Cedex France	<FREUND@FRILL51> 76-88-20-20
W. Graeff	HASYLAB at DESY Notkestr. 85 D-2000 Hamburg 52, FRG	<F41GRA@DHHDESY3> (040)8998-3282
J. B. Hastings	Brookhaven National Laboratory Upton, NY 11973, USA	<HASTINGS@BNLCL1> 516-282-4745
T. Ishikawa	PF, KEK 1-1 Oho, Tsukuba Ibaraki 305, Japan	298-64-2801
H. Kawata	PF, KEK 1-1 Oho, Tsukuba Ibaraki 305, Japan	298-64-2801
M. Knotek	NLS Brookhaven National Laboratory Upton, NY 11973, USA	<KNOTEK@BNLUX0.BNL>
J. B. Kortright	Lawrence Berkeley Laboratory University of California Berkeley, CA 94720, USA	<JBKORTRIGHT@LBL>
G. Materlik	HASYLAB at DESY Notkestr. 85 D-2000 Hamburg 52, FRG	<F41MAT@DHHDESY3>
M. Matsuoka	RIKEN 2-1 Hirosawa, Wako Saitama 351-01, Japan	484-62-9097
T. Matsushita	PF, KEK 1-1 Oho, Tsukuba Ibaraki 305, Japan	<MATSUS@JPNKEKVM>
D. Mills	Advanced Photon Source	<DMM@ANLHEP>

D. Mills	Advanced Photon Source Argonne National Laboratory Argonne, IL 60439, USA	<DMM@ANLHEP>
D. Moncton	Advanced Photon Source Argonne National Laboratory Argonne, IL 60439, USA	<DEM@ANLHEP> 312-972-7819
T. Oversluizen	NSLS Brookhaven National Laboratory Upton, NY 11973, USA	<OVER@BNLUX> 516-282-4745
P. Pattison	Daresbury Laboratory Daresbury Warrington, WA4 4AD, UK	<PN@DLVA.DARESBUY.AC.UK>
J. Phillips	NSLS Brookhaven National Laboratory Upton, NY 11973, USA	415-282-4745
R. Redaelli	Italian Council of Research Via Dalmazia 2 20138 Milano, Italy	
V. Saile	HASYLAB at DESY Notkestr. 85 D-2000 Hamburg 52, FRG	<F41SAI@DHHDESY3> (040)8998-3282
S. Sharma	NSLS Brookhaven National Laboratory Upton, NY 11973, USA	<SHARMA@BNLCL1> 516-282-4745
P. Siddons	NSLS Brookhaven National Laboratory Upton, NY 11973, USA	<SIDDONS@BNLCL1> 516-282-4745
R. K. Smither	Advanced Photon Source Argonne National Laboratory Argonne, IL 60439, USA	<RKS@ANLHEP> 312-972-3308
P. Suorti	Department of Physics University of Helsinki Siltavuorenpenger 20D SF-00170 Helsinki 17, Finland	<SUORTTI@FINUHCB> 358-0-174072

A. Thompson	Lawrence Berkeley Laboratory University of California Berkeley, CA 94720, USA	<THOMPSON@LBL>
T. Watanabe	RIKEN 2-1 Hirosawa, Wako Saitama 351-01, Japan	484-62-1449
P. Zuylen	Institute of Applied Physics TPD, Delft The Netherlands	31-15-78-2811